Durham E-Theses

Preclinical Evaluation of Cardiotoxicity Associated with Vascular Disrupting Agents Used for the Treatment of Cancer

ASMA K I MOHAMED

How to cite:

Use policy

Preclinical Evaluation of Cardiotoxicity Associated with Vascular Disrupting Agents Used for the Treatment of Cancer

Asma K. I. Mohamed

Submitted for the Degree of

Doctor of Philosophy

Faculty of Social Sciences and Health

Durham University

2021

Abstract

The therapeutic value of vascular disrupting agents (VDAs) as cancer therapeutics is compromised by cardiovascular toxicity, a major limiting factor for clinical progression. In addition to causing vascular damage and subsequent indirect cardiotoxicity, there is now evidence to support an effect of VDAs upon cardiomyocyte pathophysiology and consequent direct cardiotoxicity. The aim of this project was to investigate effects of VDAs upon cardiac cells *in vitro* and thereby ascertain a molecular basis of VDA-induced cardiotoxicity, to drive strategies for clinical mitigation of this toxicity.

Using the human adult ventricular cell line (AC10) and the beating murine stem-cell derived cardiomyocytes (Cor.AT®), the VDAs Colchicine and Combretastatin-A4 both caused the expected growth inhibition in proliferative cells, due to their effect on microtubular dynamics. However, VDAs were also shown to affect survival and function of quiescent cardiomyocytes, representative of the non-proliferative nature of the adult heart. Furthermore, VDAs at non-toxic concentrations, also perturbed the contractile functionality of cardiac cells, as determined by impedance-based real-time cell analysis of stem-cell derived cardiomyocytes Cor.AT®. In terms of a mechanism, the preliminary investigations show that treatment with VDAs caused a concentration-dependent change in gene expression of several genes involved in apoptosis and cell death, a pro-inflammatory response, vascular tonicity, extracellular-signal-regulated kinase (ERK) pathways, platelet activation and aggregation and ultimately vascular damage and cardiac remodelling. Taken together, these findings imply alternative toxicity mechanisms to mitotic arrest and cell cycle inhibition, involving induction of both a structural toxicity and interruption of the contractile response of cardiomyocytes. The observation show that pre-treatment with agents targeting disruption of angiotensin-signaling may reduce VDA-mediated toxicity, analogous to that observed with anthracycline-induced cardiotoxicity, also suggests pharmacological strategies for clinical mitigation of VDA-induced toxicity may be possible.

Key words: Cardiovascular toxicity, cardiotoxicity, Colchicine, combretastatin A 4 Phosphate, tubulin, vascular disrupting agents, preclinical cardiac models.

Acknowledgment

Firstly, I would like to express my sincere gratitude to my advisor Dr Jason Gill for the continuous support of my PhD study and related research, for his patience, motivation, and immense knowledge. His guidance helped me in all the time of research and writing of this thesis.

Besides my advisor, I am deeply grateful to my husband and soulmate Osama Abushafa for supporting me throughout my journey of PhD, throughout writing this thesis and my life in general.

My sincere thanks also go to Omar Al mukhtar University and the Libyan Government. Without their generous financial support, it would not be possible to conduct this research.

Additionally, I would like to express gratitude to my friends Kimberly Rockley, Carol De Santis and Farah Elfakhri for Their treasured support.

I thank my fellow lab mates at Durham University for the stimulating discussions, for their assistance at every stage of the research project, and for all the fun and nice experience we have throughout this journey. Also, I thank my colleagues at the Medical School, Newcastle University.

Last but not the least, I would like to thank my family: my parents, my children and to my brothers and sisters and all members of my family in-law for their tremendous understanding and encouragement in the past few years.

Table of contents

List of Figures

List of Tables

List of Abbreviations

ACE	Angiotensin Converting Enzyme
ANF	Atrial Natriuretic Factor
ARB	Angiotensin Receptor Blocker
ATCC	American Tissue Culture Collection
ATP	Adenosine 5'-Triphosphate
BSA	Bovine Serum Albumin
CA4/CA4P/CA4DP	Combretastatin-A4 / Phosphate / Disodium Phosphate
CI	Cell Index
CICR	Calcium Induced Calcium Release
CiPA	Comprehensive *In Vitro* Proarrhythmia Assay
DAPI	4',6-Diamidino-2-Phenylindole
DMEM	Dulbecco's Modified Eagle Medium
ECL	Enhanced Chemiluminescence
ERK	Extracellular-Signal-Regulated Kinase
ES cell	Embryonic Stem Cell
FBS	Foetal Bovine Serum
GAPDH	Glyceraldehyde-3-Phosphate Dehydrogenase
GPCR	G-Protein Coupled Receptor
HBSS	Hanks Balanced Salt Solution
hERG	Human Ether-À-Go-Go Related Gene
hiPSC/ -CM	Human Induced Pluripotent Stem Cells / Derived Cardiomyocytes
hSC-CM	Human Cardiac Stem Cell Derived Cardiomyocyte

ICH	International Conference on Harmonisation
MEA	Multielectrode Array
mESC / -CM	Mouse ES Cells / Cardiomyocytes
MTT	3-(4,5-Dimethylthiazol-2-Yl)-2,5-Diphenyltetrazolium Bromide
NSCLC	Non-Small Cell Lung Cancer
PVDF	Polyvinylidene Difluoride
RPMI	Roswell Park Memorial Institute
RTCA / RTCA DP	Real-Time Cell Analyser / Dual purpose
RTK	Receptor Tyrosine Kinase
RT-PCR	Reverse Transcriptase Polymerase Chain Reaction
SV40	Simian Virus 40
TdP	Torsades de pointe
VDAs	Vascular Disrupting Agents
VEGF / VEGFR	Vascular Endothelial Growth Factor / Receptor

Chapter 1. Introduction

1.1 The cardiovascular system and cardiac myocardium

Survival of all organs and tissues is dependent upon their receipt of adequate nutrients and oxygenation in conjunction with the removal of waste products, facilitated by the cardiovascular system. Within this system, the heart receives blood and pumps it around the body at a defined rate and pressure through a series of blood vessels, principally arteries, veins and capillaries. Consequently, the heart and vasculature system form a closed circulatory system and maintenance of the correct function of this system is paramount to life itself.

The heart fulfils its role in the circulation of blood and transport of chemicals and gases through its ability to continuously pump without interruption, cycling between relaxing (diastole) and contracting (systole). The four chambers of the heart either receiving (atria) or distributing (ventricles), with the right-side of the heart concentrated on passage of blood through the pulmonary system, and the left-side of the heart responsible for transport of the blood around the body.

Cardiac tissue is heterogeneously composed of a number of cell types, with cardiomyocytes being the primary contractile cells of the cardiac muscle (termed myocardium) responsible for the generation of contractile force (Sinnatamby, 2011, Stivens and Lowe, 1997). Within the heart, cardiomyocytes constitute 30% of the cell distribution, with the other 70% is provided by a number of additional cell types, namely cardiac fibroblasts, endothelial cells, pericytes and immune cells (Raulf et al., 2015).

1.1.1 Cardiomyocytes

Despite only constituting 30% of cell types within the heart, cardiomyocytes are actually estimated to make up approximately 85% of the volume of the myocardium, due to their large size (Anversa et al., 1980). These cells are arranged into highly organised repeating structures of myofilaments termed sarcomeres, forming the contractile structure of the myocardium. From a mechanistic perspective, myocardial contraction is driven by the energy-dependent intercellular movement of thick myosin filaments against thin actin filaments resulting in the co-ordinated multi-sarcomere shortening and triggering of contraction of the cardiomyocyte, a process termed the sliding filament theory of muscle contraction. As the myocardium exists as a syncytium, co-ordinated cardiomyocyte contractions occur which culminate in ventricular contraction and the expulsion of blood around the body (Gordon et al., 2000, Sinnatamby, 2011, Stivens and Lowe, 1997).

Individual cardiomyocytes are electrophysiologically stimulated to contract via the highly regulated action of specific ion channels in their membrane, controlling entry of calcium into the cell which facilitates contraction of the myosin filaments. This leads to a progressive synchronised wave of myocardial contraction across the heart and efficient ejection of blood into the circulatory system. Interruption of these signalling pathways and subsequent uncoordinated contraction or alteration of cardiac structure, as can be caused by drugs or chemicals, therefore can have a detrimental effect upon cardiac efficiency and an individual's quality of life (Josephson, 2008, Eisner et al., 2017).

1.1.2 Cardiac fibroblasts

The efficient functioning of the heart is dependent upon the existence and cooperation of cardiomyocytes with other supporting cell types. Stereological analysis of human heart histological sections and flow cytometry of isolated cell nuclei estimated the frequency of mesenchymal populations at and 58% and 43%, respectively. Presuming the most mesenchymal cells are fibroblasts, research and report that fibroblasts are the predominant cardiac cell type. Until recently, fibroblasts were considered primarily as providing the collagenous extracellular matrix within the myocardium, being fairly inert in terms of cardiac function. However, it is now known that cardiac fibroblasts provide numerous structural and functional networks permissive of cardiac contraction, being a central contributor to cardiomyocyte differentiation, and cellular and tissue adaptive responses (Camelliti et al., 2005). Furthermore, communications between cardiomyocytes is now known to be reinforced by cardiac fibroblasts, with several homeostatic pathways facilitated by fibroblasts and factors secreted from these cells (Rohde et al., 2015). Consequently, cardiac fibroblasts are gaining increased attention for the study of cardiac functional and structural changes in the heart.

1.1.3 Cardiac microvascular endothelial cells

Endothelial cells are another cellular type present within the cardiac myocardium, present in the endocardium and lining of the heart as well as the numerous myocardial capillaries which provide myocardial nutrition and oxygenation to the highly metabolically active myocardial tissue (Minami and Aird, 2005). Additional to forming a lining in the heart for areas in direct contact with blood, these microvascular cells facilitate an environment permissive of immune surveillance and communication route from circulatory factors and the myocardium (Aird, 2007).

1.1.4 Cardiac Pericytes

The role of the contractile pericyte cell population within the myocardium is to provide structural integrity and regulation of permeability to the vascular network with which they associate (Armulik et al., 2005). It is also now accepted that these pericytes play a major role in maintaining blood flow and managing vascular responses to biological factors and their environment (Bergers and Song, 2005). Consequently, the importance of pericytes to the integrity of the cardiovascular system and more widely toxicological response is now being recognised (Lee and Chintalgattu, 2019, Kwon et al., 2008, Avolio et al., 2015).

1.2 Generation of contractile force: Excitation-contraction coupling of cardiomyocytes.

Cardiac contraction is initiated by the pacemaker cardiomyocytes present within the sinoatrial node of the heart, wherein an action potential is spontaneously generated. This impulse then propagates across the heart and sequentially depolarises cardiomyocytes, from atria to ventricle, passing from cardiomyocyte to cardiomyocyte via membrane located gap junctions. The overall effect being myocardial systole and ejection of blood from the heart, followed by myocardial relaxation and cardiac diastole.

Cardiac excitation-contraction coupling describes the series of events required to translate an electrical impulse (action potential) into mechanical contraction. Cardiomyocytes generate action potentials by regulated transfer of Ca^{2+}, K^+ and Na^+ ions across the cell membrane, creating an electrochemical gradient and subsequent electrical current. Although slight differences exist between cardiomyocytes from different areas of the heart (atria, sinoatrial node and ventricles.) in terms of specific ion channels and their activity, the principal of this

sequential process is relatively the same. Ultimately, at the level of the cardiomyocyte, the electrical impulse travels along the sarcolemma within the sarcomere, utilising deep transverse tubules (t-tubules) and specific ion channels within these structures to drive the action potential and depolarisation of the cardiomyocyte, culminating in entry of Ca2+ into the cardiomyocyte through the L-type Ca2+ channels. Inside the cell, Ca2+ bind to the ryanodine receptors (RyRs) of the sarcoplasmic reticulum, triggering the sarcoplasmic reticulum to open and increase intracellular Ca2+ levels, a process known as calcium induced calcium release (CICR). The Ca^{2+} binds to troponin C of the myofilaments, which uncovers myosin binding sites of the actin filaments and allows the energy-dependent formation of cross-bridges with myosin filaments, culminating in shortening of the sarcomere and a contraction (Figure 1). This represents the systole phase of cardiac contraction where blood is forced out of the heart. The subsequent dissociation of Ca^{2+} causes the cardiomyocyte to relax and initiation of the cardiac diastole phase allowing the heart to re-fill with blood (Flucher, 1992, Fabiato and Fabiato, 1975, Fabiato, 1983, Bers, 2002).
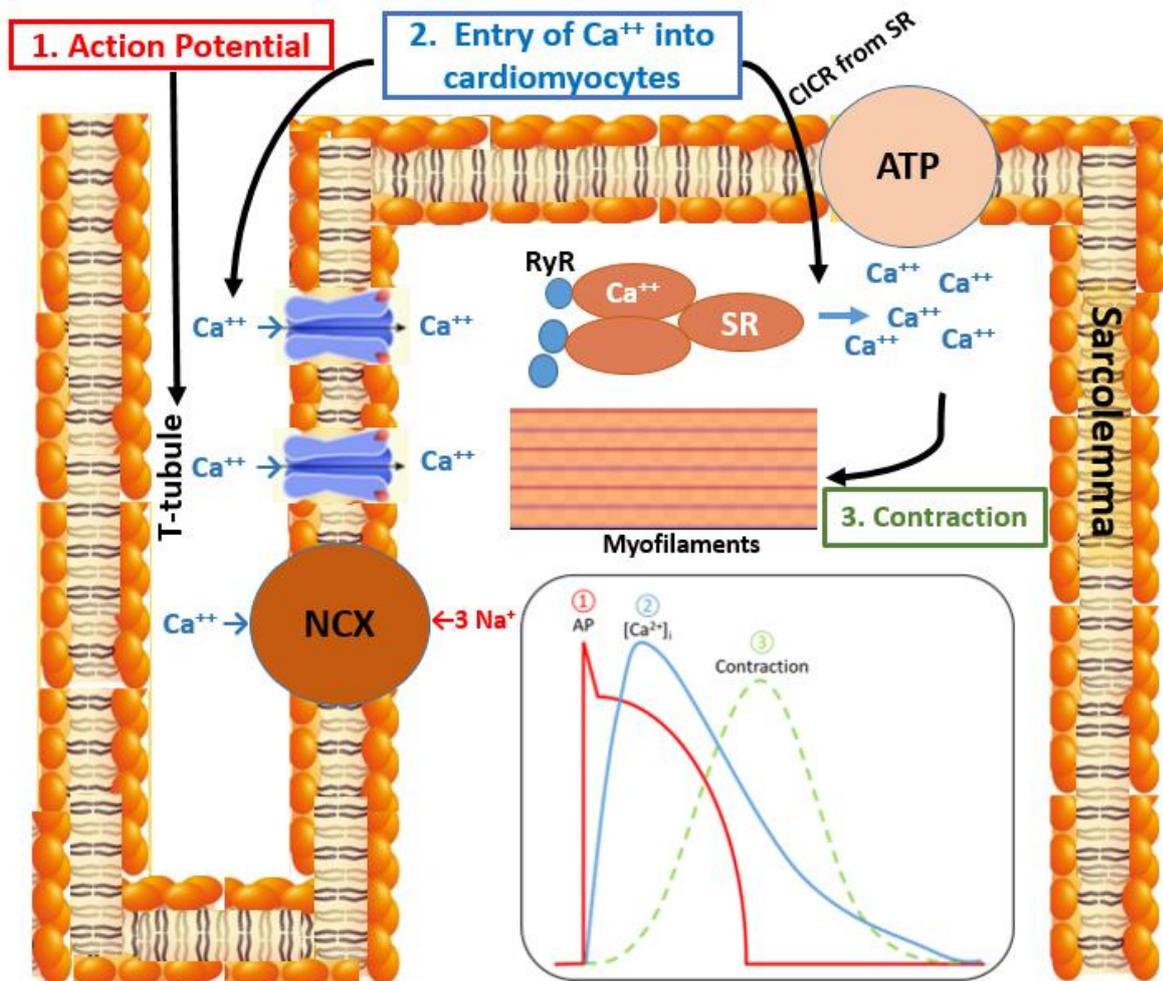
Figure 1-1: Cardiac excitation-contraction coupling.

 1. Action potentiel enter T-tubules and initiale membrane dépolarisation. 2. Depolarised membrane cause opening of L-type Ca^{2+} Channels (LTCC) and lead to accumulation of Ca^{++} in the cardiomyocytes. Ca^{2+} then bind to the sarcoplasmic reticulum (SR) via ryanodine receptors (RyR) resulting in Ca^{2+} release (Calcium induced calcium release - CICR). 3. The Ca^{2+} bind to the myofilaments and initiate cardiac cell contraction. Following repolarisation Ca^{2+} ions are loaded back into the SR then removed out of the cardiomyocytes causing dissociation of Ca^{2+} from the myofilament and consequently causing relaxation. Adapted from (Bers, 2002)

1.2.1 Generation of an action potential in cardiomyocytes.
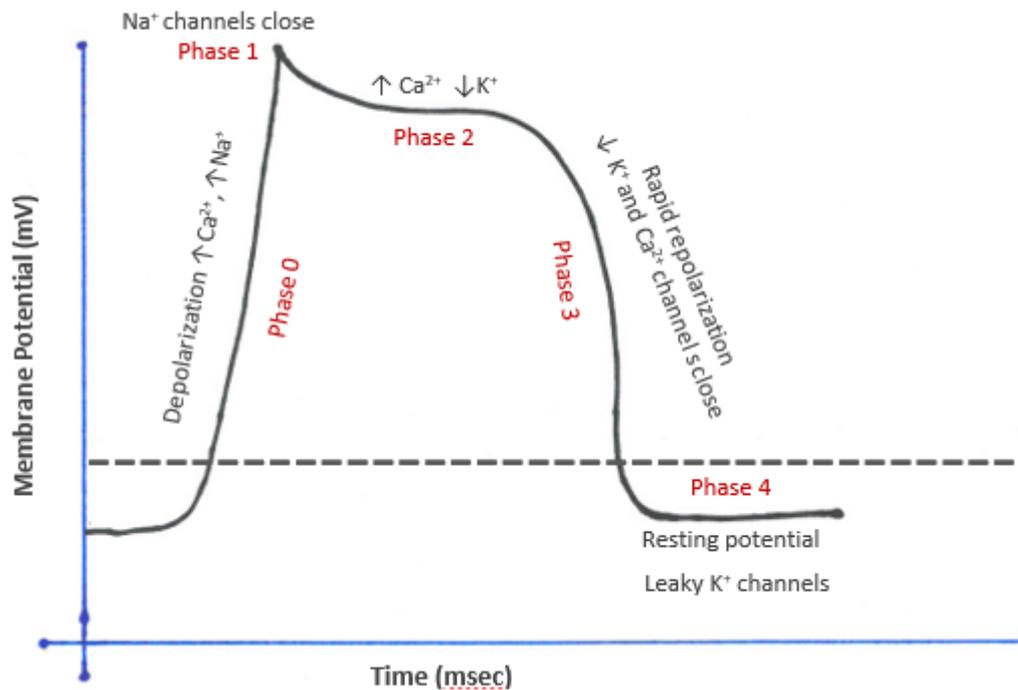
Figure 1-2: Cardiac action potential. Adapted from (Killeen, 2012)

The action potential of ventricular cardiomyocytes consists of five phases (Killeen, 2012).
Phase 0 - triggering of a threshold potential (approximately -90mV), following initiation of an action potential originating in the sinoatrial node, causes a rapid transient influx of Na^+ ions into the cardiomyocyte through fast Na^+ ion channels;
Phase 1 - resulting from inactivation of Na^+ channels and the transient efflux of K^+ through K^+ channels, and subsequent cardiomyocyte depolarisation;
Phase 2 - an equilibrium is reached, forming a plateau due to the balance between the influx of Ca^{2+} through Ca^{2+} channels and outward repolarizing K^+ currents, and resulting in Ca^{2+}-mediated cardiomyocyte contraction;
Phase 3 – following contraction and efflux of Ca^{2+} ions, repolarisation occurs, facilitated by efflux of K^+ ions through rectifier ion channels;
Phase 4 – cardiomyocyte electrophysiological polarisation is maintained at the resting potential through the inward K^+ currents (Killeen, 2012).

1.3 Drug-induced cardiovascular toxicity

Cardiotoxicity is a general term used to define toxicity that affects the heart, either through direct damage to the cellular components and structure of the cardiovascular system, or disturbances to cardiac electrophysiology and subsequent contractility (Killeen, 2012). This manifests itself as an inability of the heart to maintain sufficient cardiac output, cardiomyopathies and ultimately heart failure (Killeen, 2012).

Drug-induced cardiotoxicity and subsequent heart failure is a major clinical issue, associated with both non-prescribed and prescribed medications. However, unlike genetic conditions, drug-induced cardiotoxicity can be viewed as a potentially avoidable adverse effect of drug treatment.

1.3.1 Classification of drug-induced cardiotoxicity.

Clinically there are two types of drug-induced cardiotoxicity, classified as either irreversible or reversible toxicity and commonly termed type I and type II, respectively.

Type I drug-induced cardiotoxicity is associated with irreversible dose-dependent morphological damage to cardiomyocytes through cellular stress or injury, developing as a consequence of drug-induced oxidative stress, cellular remodelling and morphological change, or disengagement of calcium homeostasis. The outcome being a structural change to the heart and concomitant decrease in functionality of cells within the myocardium, affecting the efficiency of the heart as a pump and leading to development of heart failure. Although this type of toxicity maybe observable acutely, at any time from the beginning of drug administration up to a few weeks after the completion of therapeutic course, it may also not

be noticed until several weeks/months (early cardiotoxicity) or years (late cardiotoxicity) after drug-exposure exposure (Albini et al., 2010, Dolci et al., 2008, Pai and Nahata, 2000).

In contrast, type II drug-induced cardiotoxicity, rather than causing permanent structural damage to cells within the myocardium, manifests as a perturbation of signalling pathways important for normal myocardial function and survival, thereby causing acute alteration of myocardial function. Unlike type I, which is irreversible, this toxicity usually disappears upon, or shortly after, termination of treatment. Although this transient nature of cardiotoxicity poses less of a long-term threat, the development of treatment related arrhythmias and the possibility of drugs accentuating the cardiotoxic effects of type I therapies makes this type of cardiotoxicity a considerable problem (Albini et al., 2010, Dolci et al., 2008, Pai and Nahata, 2000).

1.3.2 Regulatory requirement for preclinical screening of drug-induced cardiotoxicity risk.

It is now well established that drug-induced cardiotoxicity is a major clinical problem associated with either off-target or secondary effects upon the cardiovascular system of many marketed drugs (Laverty et al., 2011, Killeen, 2012, Lasser et al., 2002, Shah, 2006, Redfern et al., 2010). This issue however does not stop there, as cardiotoxicity is also a significant issue for development of new drugs and therapeutics, being a primary cause of drug withdrawal during this process and a major burden for pharmaceutical companies (Figure 3)(Killeen, 2012).
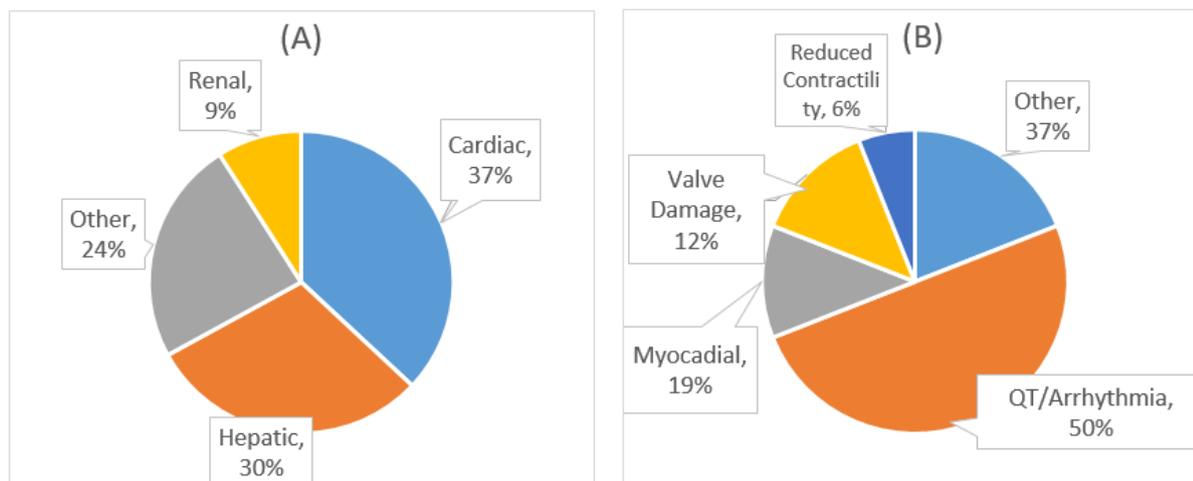
Figure 1-3: Adverse events causing drug withdrawals. Adapted from (Killeen, 2012).

(A) major adverse events that have evoked drug withdrawals. (B) The vast majority of drugs were withdrawn because of their ability to cause QT interval prolongation and arrhythmias

The impact of drug-induced cardiotoxicity is exemplified by the fact that several drugs for non-cardiovascular indications have been withdrawn from the market as a consequence of drug-induced sudden cardiac death, arrhythmias and QT-interval prolongation. As an exemplar, the non-steroidal anti-inflammatory drug (NSAID) rofecoxib was used worldwide by an estimated 80 million people to treat pain conditions such as arthritis and dysmenorrhea. It was withdrawn from the market in 2004 due to cardiac safety concerns and its long-term use has been consequently linked to between 88,000 and 140,000 reports of serious cardiac abnormalities (Sooriakumaran, 2006). Consequently, significant efforts are now made by pharmaceutical companies to identify putative medicines with cardiovascular risk liability as early as possible in the development cycle.

In this context, preclinical evaluation of the potential to cause adverse cardiovascular effects is now a regulatory requirement for all therapeutics before they enter the clinic. Accordingly, these regulatory studies are documented in the S7B guidelines of the International Conference on Harmonisation (ICH) of Technical Requirements for Registration of Pharmaceuticals for

Human use. The guidelines detail the preclinical safety pharmacology studies required to assess pro-arrhythmic risk of new pharmaceutical agents and their potential influence on ventricular repolarisation, specifically the evaluation of drug effects upon cardiac ion channels in vitro and cardiac assessments to be conducted *in vivo* (Friedrichs et al., 2005).

1.3.3 The Comprehensive In Vitro Proarrhythmia Assay (CiPA) initiative.

The ICH S7B guidelines detail the preclinical assessment of in vitro cardiac liabilities via determination of drug effects specifically upon a single K^+ channel, the Human Ether-À-Go-Go Related Gene (hERG) channel, as it is a known toxicity target with relationships to clinical effects. This assay utilises a non-cardiac cell line engineered to artificially express a functional hERG channel (Friedrichs et al., 2005). However, although successful in the identification of several drugs with cardiac liabilities, the complexity of the cardiac system and involvement of several ion channels in cardiomyocyte contractility was such that many drugs with defined cardiac liabilities have occasionally progressed into clinical trials, unnecessarily (Gintant, 2011, Ferri et al., 2013). Conversely, many drugs with effects on hERG have now been shown to induce little actual proarrhythmia and have been unnecessarily excluded from further development or, if approved, seen their clinical use limited by inappropriate warnings in product labelling (Vicente et al., 2018). Consequently, it is now accepted that whilst blockade of the hERG channel is central to proarrhythmia risk, activation of other channels, such as those controlling Na^+ and/or Ca^{2+} currents are needed to trigger a proarrhythmic response. Similarly, drugs affecting both inward and outward cardiac currents (e.g. Ca^{2+} inhibition) may have effects on repolarization but subsequently not induce proarrhythmia, due to effects upon other ion channels (Zhang et al., 1999, Sager, 2008).

The Comprehensive *in vitro* Proarrhythmia Assay (CiPA) initiative aims to develop a new paradigm for assessing drug-induced proarrhythmic risk, which is not measured exclusively by potency of hERG block and delayed repolarisation (Cavero and Holzgrefe, 2014). The CiPA initiative is driven by a suite of mechanistically based *in vitro* assays coupled to *in silico* reconstructions of cellular cardiac electrophysiologic activity. The three main principles of CiPA are thus: estimation of drug effect on multiple cardiac ion channel currents, use of *in silico* approaches to aid understanding of drug effect on cardiac action potential, and finally the comparison of predicted and observed responses in human-derived cardiac myocytes (Gintant et al., 2016).

1.4 Drug-induced vascular toxicity

Drug-induced cardiovascular toxicity, although commonly manifesting as an effect upon the cardiac system, also poses a risk to the coronary and peripheral vascular systems, through exacerbation of hypertension, perturbations in vascular tone, or direct vascular damage (Herrmann et al., 2016, Gill et al., 2019). Alongside cardiac toxicity, this obviously has an effect upon the circulatory cardiovascular system and indirectly upon the heart itself.

New onset or worsening of already persistent systemic hypertension is observed with many drugs (Herrmann et al., 2016, Touyz et al., 2018, Zambelli et al., 2011, Todaro et al., 2013, Poprach et al., 2008, Curigliano et al., 2016, Berardi et al., 2013). For example drugs that alter signalling of vascular endothelial growth factor (VEGF), with adverse vascular effects ranging from hypertension to direct cardiotoxicity. For example, patients treated with Bevacizumab are known to show elevation in the overall rate of systemic hypertension (Hurwitz et al., 2004, Rosiak and Sadowski, 2005, Touyz et al., 2018). Similarly, several cytotoxic chemotherapies also exhibit direct vascular toxicities. For instance, 5-fluorouracil (5-FU) modifies molecular

signalling pathways controlling vascular smooth muscle cell tone, thereby promoting vasoconstriction (Polk et al., 2014, Anand, 1994, Labianca et al., 1982, Villani et al., 1979). The topoisomerase II poison etoposide has been associated with development of vasospastic angina, hypotension and myocardial infarction, implying a vascular toxicity risk for this drug (Brana and Tabernero, 2010, Cappetta et al., 2017, Lipshultz et al., 2013, Lotrionte et al., 2013, Airey et al., 1995, Escoto et al., 2010, Schwarzer et al., 1991, Gill et al., 2019, Herrmann, 2016) (Yano and Shimada, 1996).

Similarly, toxicity caused by vinca alkaloids is primarily vaso-restrictive in nature, including angina, hypertension and myocardial ischaemia (Csapo and Lazar, 2014, Mandel et al., 2010, Yeh and Bickford, 2009, Yeh et al., 2004, Floyd et al., 2005). In this context, vinca-induced coronary spasm and subsequent cardiac ischaemia (Mandel et al., 2010)are rationalised as the driver for cardiovascular toxicities of this class of cancer chemotherapeutic (Herrmann et al., 2016). Such a theory is reinforced by a reported increased risk of ischaemic complications with vinca alkaloid administration in patients with established coronary artery disease (Herrmann et al., 2016).

1.5 Preclinical *in vitro* models for evaluation of cardiotoxicity

Screening for risk of drug-induced cardiotoxicity during preclinical drug development is a regulatory requirement (section 1.3.2). The progression from evaluation of putative drug effects upon the hERG ion channel in a non-cardiac cell to more translational cardiac cell models outlined by the CiPA initiative (section 1.3.3) has significant scope for improvement of the ability to detect drug-induced proarrhythmias However, the ability to detect other types of cardiotoxicity, interrogation of molecular mechanisms underpinning cardiotoxicity, evaluation of longer-term cardiotoxic effects, and the clinical relatability of the outcomes is still very much

in its infancy. Therefore, there is a need for characterisation, qualification, validation and application of further cell-based models to support and enhance the CiPA initiatives and wider studies for understanding drug-induced cardiotoxicity.

1.5.1 Human Primary Cardiomyocytes in vitro

The most appropriate model for understanding drug-induced cardiotoxicity in humans would be to use of primary cardiomyocytes. However, this is not feasible because of the terminal differentiated state of cardiomyocytes during the perinatal period *in vivo* (Tam et al., 1995). Cardiomyocytes in cell culture tend to have a very limited life span *in vitro*, and this is due the lack of satellite cell within the myocardium cable to proliferate in reaction to muscle injury (Murry et al., 1996, Chiu et al., 1995). These cultures are not proliferative, have a poor survival rate, limited number of cells per experiment and over time both structural and functional alteration are likely to occur.

Different to skeletal muscle, the myocardium does not have satellite cells capable of proliferating in response to muscle injury (Murry et al., 1996, Chiu et al., 1995). Consequently, cultures of cardiac tissue appear to have a finite lifespan *in vitro*. In addition to a lack of proliferative state, limited availability, and thus a limited number of cells for study, these cultures also undergo morphological and functional changes over time (Claycomb and Palazzo, 1980, Welser, 2015). Furthermore, the heterogeneous population of cells obtained during cellular isolations and disaggregation of cardiac tissues introduces complications for assessment of effects upon pure cell populations. Taken together, this significantly hinders and limits the utility of these cells for *in vitro* cardiotoxicity studies. Therefore, a readily available and stable line of proliferating cardiomyocytes that expresses specific markers of cardiac tissues

and capable of differentiating under appropriate culture conditions would be a valuable tool for cardiovascular research.

1.5.2 Rodent Adult and Neonatal Primary Cardiomyocytes in vitro

Analogous to human primary cardiomyocytes, those derived from rodents are also terminally differentiated and have a limited lifespan *in vitro*. However, the ability to source larger numbers of these cells and undertake parallel toxicological studies *in vivo*, with access to *ex vivo* tissue provides an advantage over human primary cardiomyocytes. Several in vitro studies have been undertaken using rodent cardiomyocytes, primarily short-term assays or those using cells derived from genetically modified animals. Although indicative of mechanisms and informative for developmental aspects of cardiac tissue, differences in ion channel expression and morphology, alongside the heterogenous nature of cardiac tissue isolates, impact upon the clinical translation of study outcomes and utility for predicting drug-induced cardiotoxicity in humans.

The use of neonatal rodent cardiomyocytes has also been appraised as a cellular model for investigation of drug-induced cardiac effects and associated cardiac functional perturbations (Estevez et al., 2000, Burton, 1994, du Pré et al., 2017). An advantage over adult cardiomyocytes for these is their retention of a limited ability to proliferate, allowing a degree of manipulation for *in vitro* cellular studies and scope for larger scale studies. A caveat is that these cells are immature relative to adult cardiomyocytes and thus exhibit differences in electrophysiological response and behaviour, factors which can affect comparative studies for clinical translation. Furthermore, the heterogenous nature of cardiac cell isolations, temporal changes in cellular morphology *in vitro*, smaller tissue size and lower cell numbers, coupled with differences in

rodent versus human cells, impacts upon their utility for assessment of drug-induced cardiotoxicity studies (du Pré et al., 2017, Nuss and Marban, 1994, Gomez et al., 1994).

1.5.3 Immortalised rodent cardiomyocyte cell lines

The limited ability and scope for the use of primary cardiomyocytes for pharmacology and toxicological analyses, in particular their limited lifespan, restrictions on expansion for use in larger scale studies, and their unstable phenotype in vitro, identified a need for a readily available and stable proliferative cardiac cell line model exhibiting a cardiac phenotype and capability for mechanistic and investigative studies (Steinhelper et al., 1990, Jahn et al., 1996, Sen et al., 1988, Jaffredo et al., 1991).

Important criteria for a cardiac cell line model are that it retains a cardiac phenotype and 'behaves' like a cardiomyocyte, whilst having the ability to proliferate *in vitro* to provide a continuous source of the cells. Many approaches have been evaluated over the years including differentiation of precardiac splanchnic mesoderm (Baldwin et al., 1991), simian virus 40 large T antigen (SV40) mediated immortalisation of cardiac cells under the control of cardiac promoters in transgenic animals (Katz et al., 1992, Negishi et al., 2000, Brunskill et al., 2001), retroviral transfection of primary rodent cardiomyocytes (Louch et al., 2011), and transformation of cardiac myoblasts using Myc and Ras protooncogenes (Land et al., 1986). In the majority of these approaches the gain of continuous growth in *in vitro* culture has been offset by the gradual loss of either the cardiac phenotype or the ability to proliferate, much like the situation with primary cells. Despite these difficulties, three models used commonly in the laboratory for cardiac studies are the H9c2, AT-1 and HL-1 cell lines.

The H9c2 cell line is derived from rat cardiomyoblasts and despite being proliferative and exhibiting immortality, it is immature and morphologically distinct from cardiomyocytes.

Although expressing some cardiac ion channels, these are poorly aligned to human cardiomyocytes and development of action potentials. The cell line has been shown to fuse to form multinucleated myotubes but remains non-contractile (Kimes and Brandt, 1976, Branco et al., 2015). This cell line has however been utilised in studies of cardiac biology and electrophysiology, with the caveat of its immaturity and weaker representation of human cardiomyocytes (L'Ecuyer et al., 2001, Spallarossa et al., 2004, Abas et al., 2000, Filigheddu et al., 2001, Turner et al., 1998).

Approaches to develop a contractile cardiac cell model, which maintained a differentiated phenotype, led to the production of the murine AT-1 atrial cell line. Targeting of SV40 using the atrial natriuretic factor (ANF) promoter in a transgenic mouse model resulted in development of atrial tumours, from which the AT-1 cell was derived (Field, 1988). Although this cardiomyocyte cell line exhibits a high degree of differentiation and can be cultured *in vitro*, wherein it maintains a cardiac phenotype, it unfortunately cannot be passaged or successfully cryopreserved. Its propagation requires its growth *in vivo* as an ectopic graft in syngeneic mice (Steinhelper et al., 1990, Delcarpio et al., 1991, Borisov and Claycomb, 1995).

Although demonstrating the ideal characteristics for an *in vitro* cardiac cell line model, the inability for *in vitro* passage and continuous use significantly limits the utility of the AT-1 cell line for preclinical studies. Subsequently, significant efforts were undertaken to identify parameters to facilitate the *in vitro* maintenance and sustainability of this cell line and overcome these limitations. Through improvement of methodologies for dissociation of the AT-1 tumour and isolation of viable cells and optimisation of the culture media and environment, success was achieved in this objective and the HL-1 cell line was isolated (Claycomb et al., 1998). The HL-1 cell line retains a differentiated phenotype during continuous passage *in vitro*, a gene

expression profile characteristic of normal mouse cardiomyocytes, and maintenance of an ability to contract (Claycomb et al., 1998). However, in relation to AT-1 cells, the HL-1 cell line contains fewer arrays of myofibrils and thereby morphologically is more like a proliferative embryonic cardiomyocyte than a mature adult one (Claycomb et al., 1998). Despite behaving like an embryonic cardiomyocyte, the cell line does not revert to an embryonic phenotype or express embryonic cardiac markers during passage. These factors together have led to this cell line being used for *in vitro* studies of cardiomyocyte function, for assessment of chemical modulators of cardiac ion channels, and as a cultured source for production of cardiac proteins (Collier et al., 2002, McWhinney et al., 2000, Suzuki, 2003). The limitations of this cell line are its murine origin in conjunction with its atrial derivation, restricting its utility for translational clinical studies and interrogation of effects upon ventricular cardiomyocytes, the predominant type within the heart.

1.5.4 Immortalised human cardiomyocyte cell lines

As with rodent cell lines, several attempts have been made to develop an immortalised human cardiomyocyte cell line, with considerably less success. In the absence of experimental models and comparative tissue to animal studies, the focus has been exclusively upon transformation of primary human cardiomyocytes using the SV40 oncogene (Wang et al., 1991, Li et al., 1996). The lack of success has been attributed to the post-mitotic and terminally differentiated nature of primary cardiomyocytes.

An approach which has delivered success in this area is the fusion of SV40-transformed fibroblasts with differentiated adult cardiomyocytes, creating the AC cell line models (AC1, AC10, AC12, AC16)(Davidson et al., 2005). Utilisation of uridine auxotroph human fibroblasts, devoid of mitochondrial deoxyribonucleic acid (DNA), permitted selection of fused cells by their

survival and growth in uridine-free medium (Davidson et al., 2005).The resulting AC cell line clones all show the expression of characteristic cardiomyocyte markers and capacity for continuous *in vitro* growth and passaging (Davidson et al., 2005). Their growth in mitogen-free media reportedly drives the differentiation of these cells, associated with cessation of proliferation and formation of multinucleated syncytium, representative of primary cardiomyocytes (Figure 1-4)(Davidson et al., 2005). However, despite expressing many cardiac specific transcription factors, contractile proteins and possessing functional gap junctions, these cells remain in a pre-contractile state. As such, these cell lines have potential utility for the *in vitro* study of structural cardiomyocyte changes and associated molecular signalling pathways but have limited validity for evaluation of functional contractility of cardiomyocytes (Davidson et al., 2005).

1.5.5 Induced pluripotent stem cell derived cardiomyocytes.

The capability of stem cells for self-renewal and differentiation into a panoply of cell types (Takahashi and Yamanaka, 2006), in conjunction with improved methodologies for their isolation and generation into different cell types under laboratory conditions has revolutionised medicine and tissue-specific studies (Laflamme et al., 2007). According to their plasticity, stem cells can be classified into four different types: totipotent, pluripotent, multipotent and adult stem cells. Totipotent stem cells are the most flexible type of stem cells, with potential to form any and all human cells or organs. Similar to totipotent stem cells, pluripotent stem cells can
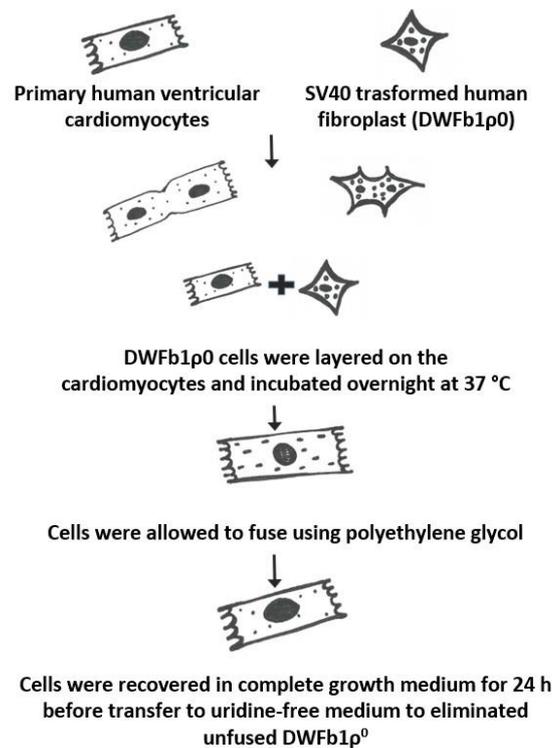
Figure 1-4: Creation of AC cardiomyocytes.

Primary cardiomyocytes from adult ventricular tissue were fused with SV40 transformed mtDNA-less fibroblasts and selected in -Ur medium, sub-cloned and screened to generate the AC human cardiomyocyte cell lines. Adapted from Davidson et al., 2005.

differentiate into all cell types; however, they are not able to give rise to human organs. The least plastic ones are multipotent stem cells, which differentiate into only a limited number of cell types (Kalra and Tomar, 2014).

The discovery that somatic cells can be reprogrammed into human induced pluripotent stem cells (hiPSC) (Takahashi and Yamanaka, 2006) and the subsequent development of the processes required to differentiate these cells into functional human cardiomyocytes (Yang et al., 2008, Laflamme et al., 2007) instigated a new dimension for preclinical *in vitro* studies of cardiomyocytes and their responses to exogenous factors, such as drugs. Comparisons of these human induced pluripotent stem cell derived cardiomyocytes (hiPSC-CM) and primary

cardiomyocytes indicated a vast number of similarities, with very few anomalies (Table 1-1) (Ma et al., 2011). Whereas action potential values, resting membrane potentials and ionic currents in hiPSC-CM were found to be similar to primary human ventricular cardiomyocytes, unlike healthy human ventricular cardiomyocytes, the membrane of hiPSC-CM was shown to be spontaneously depolarised (Ma et al., 2011).

Although hiPSC-CMs possess many favourable features such as the ability to spontaneously contract, responsiveness to cardioactive drugs and expression of important cardiac ion channels and receptors (Braam et al., 2010); many studies have reported that these cells are more aligned to embryonic cardiomyocytes and exhibit an immature phenotype (Claire Robertson, 2013). However, the level of maturity and adoption of a more adult phenotype appears to improve following more time in culture, offering scope for advancement of the utility of these cell types for a more diverse array of studies (Lundy et al., 2013).

Despite the immature phenotype of hiPSC-CMs, this cell type is considered clinically and physiologically relevant than other *in vitro* models, such as the rat H9c2 cell line, the contractile murine AT-1 and HL-1 cell lines, and potentially human AC cell lines. As such, there is a growing preference for the use of hiPSC-CMs for pre-clinical cardiotoxicity assessment of new drugs, as indicated in the CiPA initiative (section 1.3.3). In this context, hiPSC-CMs have become fundamental to many *in vitro* cardiotoxicity assays and have shown considerable promise to accurately detect cardiac liabilities in drugs with known cardiac effects on a number of these platforms (Tang et al., 2016)

Similarity	Difference
- Presence of all major cardiac ion channel, calcium handling and sarcomeric proteins. - There are robust I_{Na}, I_{Ca}. I_{Kr}, I_{Ks} and I_{t0}. - Calcium-induced Calcium release is present. - Functional Sarcoplasmic reticulum calcium stores present. - Atrial or ventricular-like action potential >80% of cells.	- Immature phenotype. - Large cell-to-cell variation. - Small cell size. - Spontaneously beating - Depolarized diastolic membrane potential. - Large pacemaker current (I_f) - Small I_{K1} current - Relatively weak contractility - Lack of t-tubules - Large IP3-sensitive calcium stores - Confounding effects of trophic factors in culture

Table 1-1: Comparison between iPSC cardiomyocytes and human adult cardiomyocytes. (Ma et al., 2011).

1.6 Preclinical in vitro assays for determination of functional and structural drug-induced cardiotoxicity effects

The increased requirement of *in vitro* cardiac cell assays and the identification of improved cardiac cell models has caused a surge in the development of new high-throughput assays that allow the functional activity, and increasingly the structural changes, of cardiomyocytes to be assessed. These assays are increasingly pertinent for the sensitive and specific assessment of drug-induced cardiotoxicity.

1.6.1 In vitro determination of cell survival and drug-induced toxicity

Many screening tests have been developed for *in vitro* evaluation of cytotoxicity over the years, ranging from dye exclusion techniques of vital stains such as trypan blue or neutral red (Cavanaugh et al., 1990), to bioluminescent detection of released intracellular proteases following loss of membrane integrity (Cho et al., 2008) or quantitation of cellular adenosine triphosphate (ATP) levels (Crouch et al., 1993, Shukla et al., 2010), to common methodologies

involving metabolism of tetrazolium salts by intracellular organelles of viable cells (Mosmann, 1983). In this latter method, succinate dehydrogenase present in mitochondria of metabolically active cells converts the tetrazolium salt, such as the yellow MTT tetrazolium salt (3-(4,5-Dimethylthiazol-2-yl)-2,5-diphenyltetrazolium bromide), to dark purple formazan. This product is detected spectrophotometrically, with the amount of formazan created being directly proportional to the viable cell number (Mosmann, 1983).

1.6.2 In vitro impedance-based measurement of cellular adherence, proliferation, morphology, viability and contractility.

In recent years technological advances and improved understanding of cellular behaviour have also allowed new screening approaches to be developed, which expand upon the established cellular and biochemical assays, and use biophysical properties such as cellular impedance to be exploited for evaluation of cell viability and post-treatment survival (Khoshmanesh et al., 2011, Limame et al., 2012, Park et al., 2009, Moniri et al., 2015). Such methodologies, such as the xCELLigence analytical system, permit real-time and label-free evaluation of these effects and extend the level and depth of information that can be gained from these *in vitro* studies.

The xCELLigence technology is a non-invasive, real time, label free *in vitro* biosensor technique utilising plates impregnated with high density gold electrodes and associated impedance of current as a measure of cellular adherence and morphology (Ke et al., 2011). In the absence of cells, or limited attachment to the culture plate, a low impedance of current is detected. Conversely, an increase in cell number or attachment is associated with a high degree of electrical impedance across the electrodes of the plate (Figure 1-5). Cellular changes and perturbations, such as morphological changes (size, shape, and volume), variances in

adherence, cell proliferation, motility, or cellular hypertrophy are thus all measured in real-time and non-invasively (Ke et al., 2011).

In addition to evaluation of cellular viability and morphological changes, such as hypertrophy, impedance-based methodologies have functionality for label-free real-time monitoring of cardiomyocyte contractility (Kho et al., 2015, Knollmann, 2013, Abassi et al., 2012, Yokoo et al., 2009, Nguemo et al., 2012). This is facilitated by the fact that the formation of a complete cellular monolayer results in the formation of a contractile syncytium within the culture plate (Figure 1-6). The resultant cardiomyocyte contractility causes transient changes in cellular attachment and morphology and thus impedance across the plate, resulting in a record of this contractile movement. This is in addition to the 'standard' detection of cellular viability and cell loss. Together this is permissive for the sensitive and continuous monitoring of the effects of compounds on both cardiomyocyte structure and functional capacity (Himmel, 2013, Scott et al., 2014, Zhang et al., 2016).

As cardiomyocyte contraction is downstream of the cardiac action potential and calcium-mediated excitation-contraction coupling (Section 1.2), any changes in impedance may be indicative of drug-induced disturbances to the action potential, calcium flux and/or mechanical contraction. In support of this technology for identification of drug-induced cardiotoxicity, in a comparative evaluation of similar methodologies and their ability to detect drug-induced functional cardiac effects, the xCELLigence (Cardio) system detected 16/18 known cardiotoxicants as cardiotoxic and attained greater detection capability than other multielectrode systems (Doherty et al., 2015)
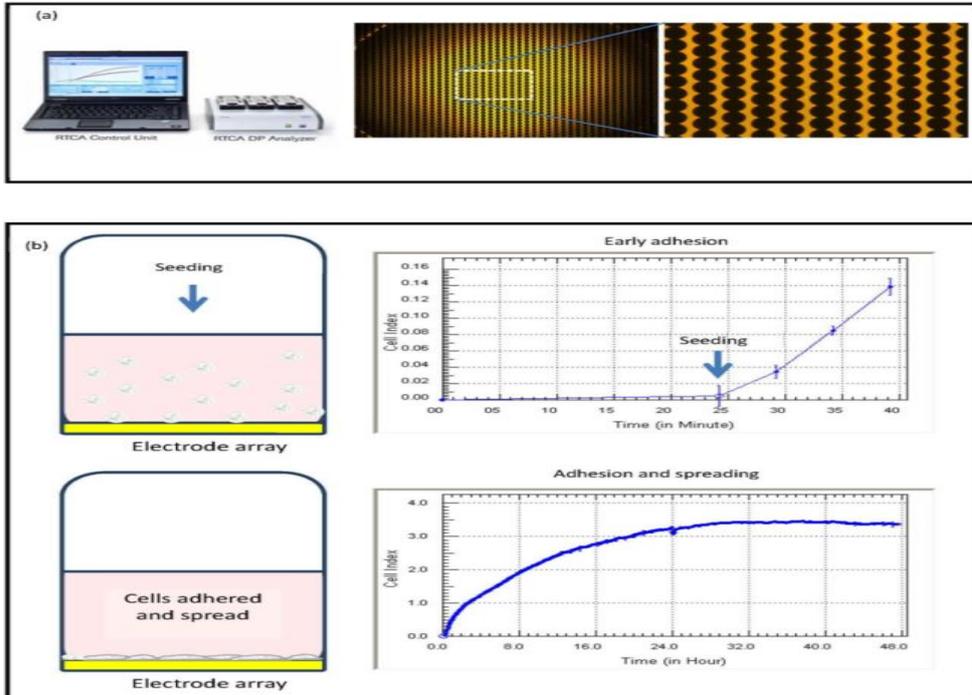
Figure 1-5: Summary of xCELLigence system technology and impedance.
The figure shows: (a) The high density gold array on the E-plates; and (b) The initial phases of seeding and adhesion, which is recorded by the biosensor and represented as the Cell Index (adhesion) (Kho et al., 2015). Image courtesy of ACEA Biosciences.
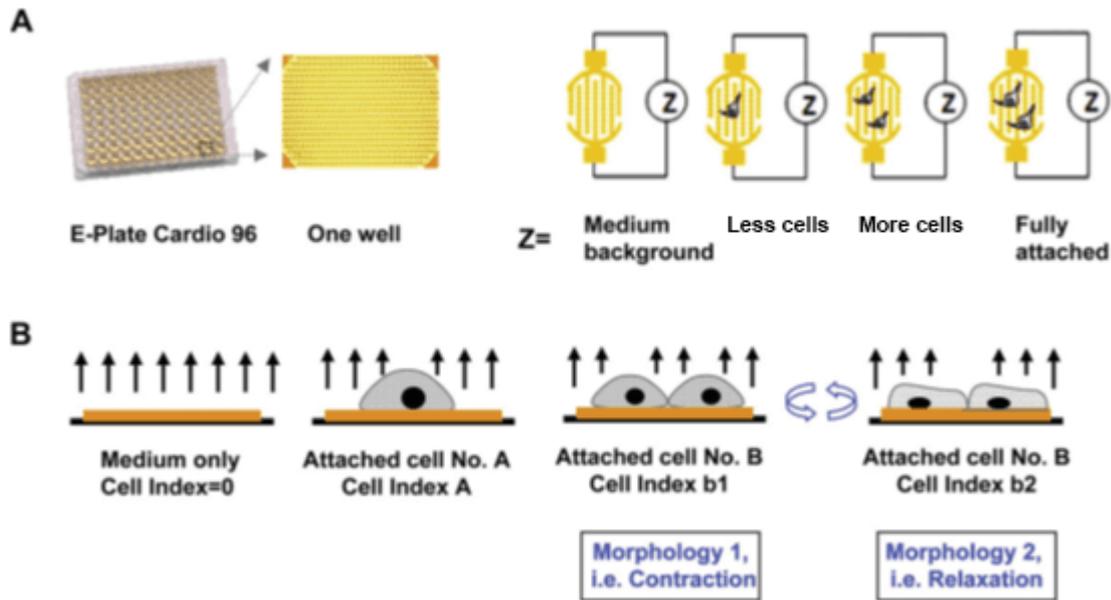
Figure 1-6: Quantitative analysis of cardiomyocytes conditions and functions via impedance measurement in real time.
(A) An electrode coated 96 well plate (E-Plate Cardio 96). Low voltage between electrodes creates current. The more the cell adhere to the electrodes the more impedance increased. Impedance (Z) is directly proportional to the cell number, morphologic and adhesive properties of the cells. The measurements recorded called cell index which is the ratio of impedance value in presence of cells to value of impedance without cells. (B)This technology is capable of monitoring the functional changes in beating cardiac cell line, this as a result of the ability of the electrode to sense changes in size/shape and attachment strength of beating CM that show phases of relaxation and contraction. Image courtesy of ACEA Biosciences.

1.6.3 In vitro determination of cardiac cell electrophysiology: Patch clamping

The conventional methodology utilised for evaluating cellular electrophysiology is patch clamping. This involves the evaluation of ion channel activity on the cell surface of a single cell, wherein an area has been isolated by the 'patch clamp'. The movement of ions is then determined by the change in charge and current across the membrane. However, it is labour intensive and limited to isolated cardiomyocytes, making this technique unsuitable for high-throughput screening (Ogden and Stanfield, 1994).

1.6.4 In vitro determination of cardiac cell electrophysiology: Calcium flux.

As Ca^{2+} is intrinsically involved in cardiomyocyte contraction, measurement of intracellular Ca^{2+} transients can be used as a surrogate measure of contraction. Calcium specific fluorescent dyes are added to monolayers of cells in a plate based format, as the iPSC-CMs spontaneously beat and their intracellular Ca^{2+} levels fluctuate, the peaks and troughs in fluorescence intensity are recorded. (Daily et al., 2017). This technique allows changes in contraction force and frequency to be quantified, however it should be noted that compounds which affect the contractile machinery, such as the myosin II inhibitor blebbistatin will not be detected (Guo et al., 2011).

1.6.5 In vitro determination of cardiac cell electrophysiology: Microelectrode arrays (MEAs)

Microelectrode arrays (MEAs) are plate-based assays whereby electrically active cells such as hiPSC-CMs are seeded into the wells of specialised plates that have a series of electrodes on the bottom of the wells. Once the cells form a cohesive monolayer and begin to spontaneously contract, their electrophysiological profile is captured by the electrodes in real-time allowing parameters such as beat rate, field potential duration, amplitude and conduction velocity to be assessed. In contrast to the traditional patch-clamp approach, MEAs measure the total extracellular change of ions and therefore assess changes in all major ion channels implicated in the action potential. One advantage of MEAs over traditional patch-clamp methodology is the ability to measure total extracellular ionic changes and thus display alterations in all major ion channels involved in the action potential. Another advantage is the capability to recognise drugs that block potassium and calcium channels (Blinova et al., 2017).

1.7 Cancer

Cancer is a broad and complex family of diseases that can affect all tissues of the body, with greater than 100 distinct types. Despite having multiple causes and histological features, cancer is defined as a set of diseases characterised by upregulated cell growth leading to invasion of surrounding tissues and metastasis to different parts of the body (Hanahan and Weinberg, 2011, Pecorino, 2016).

In the UK, and in many parts of the developed world, cancer incidence and survival have both shown a considerable increase in the past decade, with today's cancer patients benefitting from life expectancies ten times longer than their counterparts 40 years ago (Quaresma et al., 2015). This improvement is attributed mainly to increase the average survival age due to enhanced treatment for life shortening conditions and more importantly is due to the improvement in cancer screening, diagnosis and treatments(Miller et al., 2016). Future mortality rates are predicted to decrease by 15.3% from 2014-2035 (Smittenaar et al., 2016), thereby further increasing the size of the cancer survivor group. Furthermore, the total number of cancer survivors is also anticipated to increase by one million per decade from 2010 – 2040 (Maddams et al., 2012). Therefore, long-term health problems which would otherwise not have surfaced are likely to become an issue in this unique population, including cardiotoxicity and cardiac failure caused by treatment with chemotherapy (Maddams et al., 2012).

1.7.1 Cancer development and hallmarks

Despite the wide range of 'causes' and 'types' of cancer, and diversity amongst individuals, cancer fundamentally develops from non-lethal genetic damage causing modifications to key

molecular pathways inside the cell, which confer a survival advantage to the affected cells, and ultimately the progressive ability to invade tissues and spread to other parts of the body.

In order for a cancer to develop there are key pathways and processes that need to be activated or perturbed, termed the 'Hallmarks of Cancer' (Hanahan and Weinberg, 2011). There are eight essential hallmarks identified, which are essential for cancer development, and two enabling characteristics, which provide the correct physical environment for the cancer to establish and grow (Figure 1-7) (Hanahan and Weinberg, 2011). These distinctive biological 'hallmark' capabilities are defined as:

- Limitless replicative potential;

- Self-sufficiency in growth signals;

- Insensitivity to anti-growth signals;

- Evasion of cell death;

- De-regulation of cellular energetics;

- Ability to avoid immune destruction;

- Development of sustained angiogenesis

- The ability to invade and metastasise.

The enabling characteristics being genome instability and tumour-promoting inflammation (Hanahan and Weinberg, 2011).

Figure 1-7: Hallmarks of cancer and enabling characteristics. Adapted from (Hanahan and Weinberg, 2011)

The vast majority of the hallmarks are concerned with gain of a selective growth advantage relative to neighbouring cells coupled with diminished ability to be destroyed either by factors intrinsic or extrinsic to the affected tumour cells, ultimately culminating in the development of a tumour. Subsequent gain of malignant potential is a consequence of development of a viable blood supply to the tumour, through angiogenesis, and further molecular aberrations providing the tumour with the tools and capacity to invade and metastasise. As such, targeting of a tumour blood supply is now postulated as a viable opportunity for therapeutic intervention in cancer (Hanahan and Weinberg, 2011).

1.7.2 Tumour angiogenesis

In order for cancer cells to survive they must be within close proximity of a blood (or lymphatic) vessel, to allow maximal diffusional delivery or clearance of these factors (Folkman, 1971). Like normal cells, this concept is also applicable to cancer, as tumours cannot grow to a diameter larger than 1-2mm unless they have a vascular supply (Muthukkaruppan et al., 1982, Brooks, 1996). The difference that exists with cancer is that the ever-increasing tumour mass subsequently needs a larger blood supply to support this rapidly expanding tumour mass.

Angiogenesis, as opposed to vasculogenesis, is responsible for establishment of a blood supply to the tumour, through formation of blood vessels from surrounding pre-existing blood vessels (Baluk et al., 2005, Barlow et al., 2013, Siemann et al., 2017, van Dijk et al., 2015). Until the tumour mass reaches a critical size (approximately 1mm^3) associated with 'supply and demand' there is no requirement for further blood vessels (Fang et al., 2000). However, once exceeded the 'Angiogenic Switch' is triggered, allowing the balance of pro-angiogenic factors to exceed anti-angiogenic factors and the establishment of a vascular system supporting the tumour mass. The resulting vasculature initiated in the tumour, due to rapidity of tumour growth, is, however, abnormal, poorly organised, chaotic, and leaky (Baluk et al., 2005, Barlow et al., 2013, Siemann et al., 2017, van Dijk et al., 2015). Furthermore, in addition to facilitating and supporting tumour growth and expansion, the newly developed neovasculature increases the 'escape routes' for tumour cells and, by default, increases tumour malignancy and the spread of tumour cells to other parts of the body (metastasis).

Angiogenesis is a potential good therapeutic target for cancer treatment because tumour progression is dependent upon angiogenesis (Cross and Claesson-Welsh, 2001); therefore, if

this stage could be halted the cancer would not be able to survive due to the lack of essential nutrients.

1.7.3 Tumour invasion and metastasis

Uncontrolled cell growth is not necessarily hazardous to the wellbeing of the patient, especially when the cells have not yet established a capacity to invade neighbouring tissues or relocate from their resident location to another site within the body. However, by definition, malignant cancer cells exhibit the ability to spread, show invasive potential and, ultimately, metastasise to distant regions of the body. Metastasis is the most important cause of cancer mortality and, if present, dramatically worsens the prognosis for the patient, compared to if the cancer was diagnosed prior to metastatic spread. However, it is often the case that metastasis has already begun to occur by the time the primary cancer has been diagnosed (Fang et al., 2000, Chambers et al., 2002, Tarin, 2008, Bacac and Stamenkovic, 2008, Chaffer and Weinberg, 2011).

The process of metastasis is a series of rate-limiting steps that must occur in order for cancer to disseminate to sites other than the primary tumour. Tumour metastasis follows a set pattern of processes: i) Activation of the angiogenic switch and the resultant tumour vascularisation increases scope for tumour expansion and, ultimately, malignancy; ii) Gain of further genetic aberrations provide molecular tools to increase tumour cell motility and invasiveness; iii) Acquisition of an ability to invade through tissues eventually results in the tumour cell(s) breaching the local basement membrane and transiting towards blood and lymphatic vessels; iv) Tumour cells then intravasate from the 'invaded tissue' into the circulation (or lymphatic system), transit through the vasculature until becoming 'trapped' or 'deposited' in capillaries of another tissue, whereby they extravasate out of the blood vessel and into the new host tissue

forming a metastatic deposit (Martin TA, 2000, Fares et al., 2020, Welch and Hurst, 2019, Valastyan and Weinberg, 2011). Consequently, therapeutic strategies are focused on prevention or interruption of the metastatic process and retention of the tumour to as few locations as possible.

1.7.4 Cancer chemotherapy

The mainstay of the vast majority of clinical treatment regimens for cancer include exposure of the cancer cells to a cytotoxic chemotherapeutic. Principally these "conventional" drugs interfere with cancer proliferation through interference with DNA replication and associated processes. These include the anthracyclines, alkylating agents, antimetabolites, and microtubule inhibitors amongst others (Delgado et al., 2018, Nitiss, 2009, Pommier, 2013, Thurston and Pysz, 2021, Jordan, 2002, Wang et al., 2000, Peters et al., 2000, Oronsky et al., 2012). However, despite demonstrating significant activity against a large number of tumours, their efficacy is significantly diminished due to dose-limiting toxicities (notably neurotoxicity and cardiotoxicity) and development of drug-resistance (Lindenfeld and Kelly, 2010).

Over the past decade or so, through increased understanding of the molecular basis of cancer, a revolutionary step change has developed in cancer therapy. This is associated with a move from classical cytotoxic drugs to target-led, rationally designed agents. These therapeutics are designed to expand beyond being purely DNA interactive and exploit defined abnormalities responsible for the causation, maintenance or progression of human tumours such as genetic instability, aberrant cell cycle control, invasion, angiogenesis and the ability to metastasise (Aggarwal, 2010, Stegmeier et al., 2010, Bhullar et al., 2018). The identification of aberrant signalling pathways in cancer has led to the development of therapies that target specific oncogenic processes, such as aberrant intracellular signalling pathways and receptor tyrosine

kinases associated with cancer hallmarks, cellular invasion mechanisms, and the processes of angiogenesis and metastasis (Aggarwal, 2010, Stegmeier et al., 2010, Bhullar et al., 2018). These approaches have changed treatment outcomes and improved the diversity of treatable cancers. The use of these "targeted molecular therapeutics" alongside "conventional cytotoxic agents" have been shown to positively impact patient survival (Ma and Waxman, 2008, Gotwals et al., 2017, Galluzzi et al., 2015).

1.7.5 Targeting the tumour vasculature as a therapeutic approach for cancer

Tumour growth and expansion, invasive capacity and ultimately metastasis and dissemination to other parts of the body, are all hugely dependent upon a functioning vascular network, as described previously (Weis and Cheresh, 2011, Tozer et al., 2005). The absence or failure of a tumour to sustain a viable blood flow causes a restriction in growth and cessation of progression due to lack of nutrition and oxygen, and build-up of metabolic waste products and carbon dioxide (Tozer et al., 2005). Similarly, the inability or prevention of a tumour to develop new blood and lymphatic vessels (angiogenesis and lymphangiogenesis) causes a restriction in growth volume to a few millimetres and concomitant tumour dormancy (Weis and Cheresh, 2011). Consequently, targeting of the vasculature within tumours has significant potential for therapeutic intervention (Ji et al., 2015, Weis and Cheresh, 2011, Tozer et al., 2005), with strategies broadly categorised into two areas; i) inhibition or interference in the development and recruitment of a new vascular supply to the tumour with consequent stasis of tumour expansion, through perturbation of the angiogenic process (Weis and Cheresh, 2011), and ii) disruption and collapse of the existing tumour vasculature, resulting in 'tumour starvation', and consequent tumour necrosis and death (Ji et al., 2015, Tozer et al., 2005) (Figure 1-8 & Figure 1-9).

There are now several strategies proposed for the targeting and interference of the angiogenesis process and thus prevention of tumour expansion and dissemination. Anti-angiogenesis therapeutics have seen an explosion of interest over the past 'molecular therapeutic' decade and has resulted in advancement of agents within this class into the clinic with significant success (Khosravi Shahi and Fernández Pineda, 2008, Weis and Cheresh, 2011). The majority of these anti-angiogenic therapeutics are concerned with blockade of vascular endothelial growth factor (VEGF) activity within the tumour, through either sequestering circulating VEGF and prevention of its binding to the cell-surface receptor VEGFR (e.g. the monoclonal antibody bevacizumab), and inhibition of downstream signalling from VEGFR and other similar receptors (e.g. the tyrosine kinase inhibitors such as axitinib, pazopanib, sorafenib, and sunitinib) (Weis and Cheresh, 2011).

1.7.6 Vascular Disrupting agents (VDAs) for treatment of cancer

In contrast to anti-angiogenic approaches which prevent neo-vasculature development, the vascular-disrupting strategy for cancer treatment is focused on affecting the 'established' vasculature within the tumour (Figure 1-8 & Figure 1-9). In 'normal' non-tumorous tissue, the vasculature architecture is organised into regular structures, with mature endothelial cells forming a defined lumen supported by a well-established network of pericytes and smooth muscle cells (Barlow et al., 2013, Siemann et al., 2017, van Dijk et al., 2015, Baluk et al., 2005). In contrast, as a consequence of the rapid and relatively uncoordinated nature of their development, tumour vascular networks are particularly unorganised and formless, with random irrational vessel connections and chaotic blood flow (Barlow et al., 2013, Siemann et al., 2017, van Dijk et al., 2015, Baluk et al., 2005). Furthermore, tumour vasculature is actively growing and lacks control mechanisms that are protective to blood flow normalcy (Barlow et

al., 2013, Deryugina and Quigley, 2015, Baluk et al., 2005). The differential in vasculature structure and blood flow across the tumour, the rapid growth and concomitant dependency on a supportive blood supply, and the immaturity of the endothelial cells within the tumour therefore exposes the validity of targeting vascular supply to limit and inhibit tumour growth, survival, and dissemination. Consequently, selectively disrupting the established blood supply to tumours is now known to be an effective therapeutic strategy.

VDAs offer several positive therapeutic attributes relative to the majority of cancer therapeutics. Firstly, they are not required to extravasate from the blood vessel and penetrate across several cell layers for their activity and thus are not hindered by intra-tumoral pharmacokinetic dilution. Secondly, they target a fundamental process for survival of all solid tumours and therefore have widespread potential, through affecting 'non-tumorigenic cells' within the tumour microenvironment avoiding undesirable acquired drug resistance associated with genomic instability of malignant cells (Kanthou and Tozer, 2007, Mita et al., 2013, Lippert, 2007, Tozer et al., 2005).

VDAs are classified into two subgroups: the tubulin-binding agents which target the Colchicine-binding domain of β-tubulin and thus act on the dynamic tubulin heterodimers (Hill et al., 1993) and the flavonoids (Bibby et al., 1989) which enhance cytokine activity within the tumour by increasing the production of local cytokines such as TNF-alpha (Baguley et al., 1996, Cai, 2007). Both ultimately lead to the destruction of vascular cytoskeleton. Subsequently, causing cessation of blood flow and increase in tumour hypoxia.
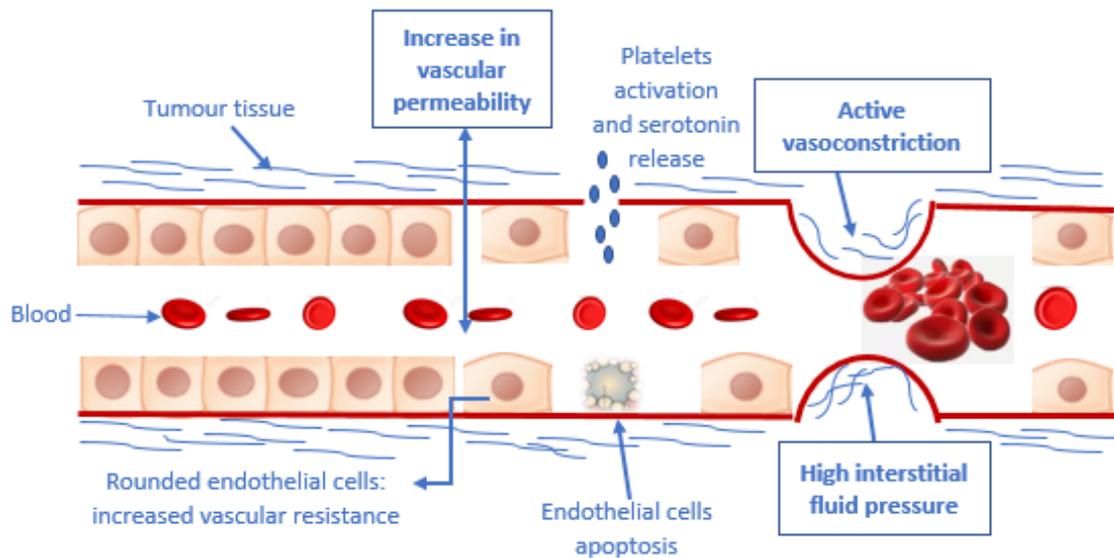
Figure 1-8: Mechanism of action of VDAs.

Exposure of endothelial cells to VDAs cause cellular changes, therefore, number of cells rounded up and some show signs of membrane blebbing and increase in the cell membrane permeability. Resulting in rising the vascular resistance to blood flow within the tumour. The very rapid apoptotic effect could play a role in the quick VDAs-induced shutdown of blood vessels. The vasoconstriction effect might be exacerbated by platelets stimulation, the discharge of serotonin and the active vasoconstriction caused by interfering with vessel dilatation. In addition, the increase in vascular permeability of tumour cells could cause increase in the interstitial fluid pressure thus inducing vascular stenosis. The water loss in tumour microcirculation cause increase in blood viscosity leading to blood clotting 'rouleaux'. Adapted from Tozer et al., 2005.

and subsequent haemorrhagic necrosis of the malignant tumour (Figure 1-10). Despite flavonoids showing initial preclinical promise, these have not yet progressed to the clinic and their exact mechanism is yet to be elucidated. In contrast, several VDAs focused against disruption of β-tubulin have now progressed into preclinical development or late-stage clinical trial (Ji et al., 2015, Mason et al., 2011)(Table 1-2: Tubulin-targeted VDAs in clinical development. 1-2). Henceforth, when describing VDAs, it is specifically those targeting the Colchicine-binding domain of β-tubulin which are being referred to herein.

The underlying mechanism as to why these tubulin interactive VDAs have such a profound effect on tumour over "normal" blood vessels has yet to be conclusively proven clinically. However, there is compelling preclinical information to suggest that the demands of the tumour and its environment presents the tumour endothelial cells with an abnormal cellular physiology, such that their immaturity results in their rigidity and shape being dependent upon an intracellular tubulin cytoskeleton rather than the largely actin cytoskeleton present in mature established endothelial cells and blood vessels (Fürst and Vollmar, 2013, Kanthou and Tozer, 2007, Mahal et al., 2015, Schwartz, 2009). Consequently, agents which disrupt tubulin dynamics would have a profound effect on tumour endothelial cell structure, with minimal effects to endothelial cells in mature blood vessels. Furthermore, it is now well established that the disruption of a single tumour blood vessel results in death of the large number of tumour cells it supports (Kanthou and Tozer, 2007, Mita et al., 2013)(Figure 1-9).

Drug	Company	Stage of development	Combination therapies
ABT-751*	Abbvie	Phase II	Pemetrexed (NSCLC); Carboplatin (NSCLC); Docetaxel (Prostate)
BNC105 / BNC105P	Bionomics	Phase I ; Phase I (CLL); Phase II (Colorectal); Phase II (Mesothelioma)	Everolimus (Renal); Carboplatin/Gemcitabine (Ovarian); Ibrutinib (CLL); Nivolumab (Colorectal)
CKD-516	Chong Kun Dang Pharma	Phase I; Phase I/II (Colorectal)	Irinotecan (Colorectal)
Crolibulin (EPC2407)	Cytovia/Immune Pharma	Phase II (Thyroid)	Cisplatin (Thyroid)
Denibulin (MN-029)	Medicinova	Phase I	None reported to date
CA4P	Mateon Therapeutics (Oxigene)	Phase I; Phase III (Ovarian); Phase II (Glioblastoma); Phase II (Thyroid); Phase II (Neuroendocrine); Phase II (Melanoma)	Carboplatin & paclitaxel (Ovarian); Bevacizumab; Pazopanib (Ovarian); Carboplatin, paclitaxel, & bevacizumab (NSCLC); Carboplatin & paclitaxel (Thyroid); Everolimus (Neuroendocrine); Nivolumab (Melanoma)
Lexibulin (CYT997)	Cytopia / YM Biosciences /Gilead Sciences	Phase I; Phase Ib (Glioblastoma); Phase II (Myeloma)	Carboplatin (Glioblastoma)
Ombrabulin (AVE8062)*	Sanofi-Aventis	Phase I; Phase II (NSCLC) Phase III (Sarcoma)	Taxane/Platinum; Cisplatin; Docetaxel; Bevacizumab.
Oxi4503 (CA41P)	Mateon Therapeutics (Oxigene)	Phase I; Phase II (Hepatic); Phase II (Leukaemia)	Cytarabine (Leukaemia)
Plinabulin (NPI-2358)	BeyondSpring Pharma	Phase I/II; Phase II (NSCLC) Phase II (SCLC)	Docetaxel (NSCLC); Nivolumab (Melanoma) Nivolumab & ipilimumab (SCLC)
Soblidotin (TZT-1027)	Daiichi Sankyo	Phase I; Phase II (Sarcoma) Phase II (NSCLC)	Carboplatin
Verubulin (MPC-6827)	Myrexis / Cytovia	Phase I; Phase I/II (Glioblastoma)	Carboplatin (Glioblastoma) Temozolomide (Glioblastoma)
ZD6126*	Angiogene Pharma	Phase II	Oxaliplatin & 5-Fluorouracil (Colorectal)

*Development discontinued.

Table 1-2: Tubulin-targeted VDAs in clinical development. (Gill et al., 2019)
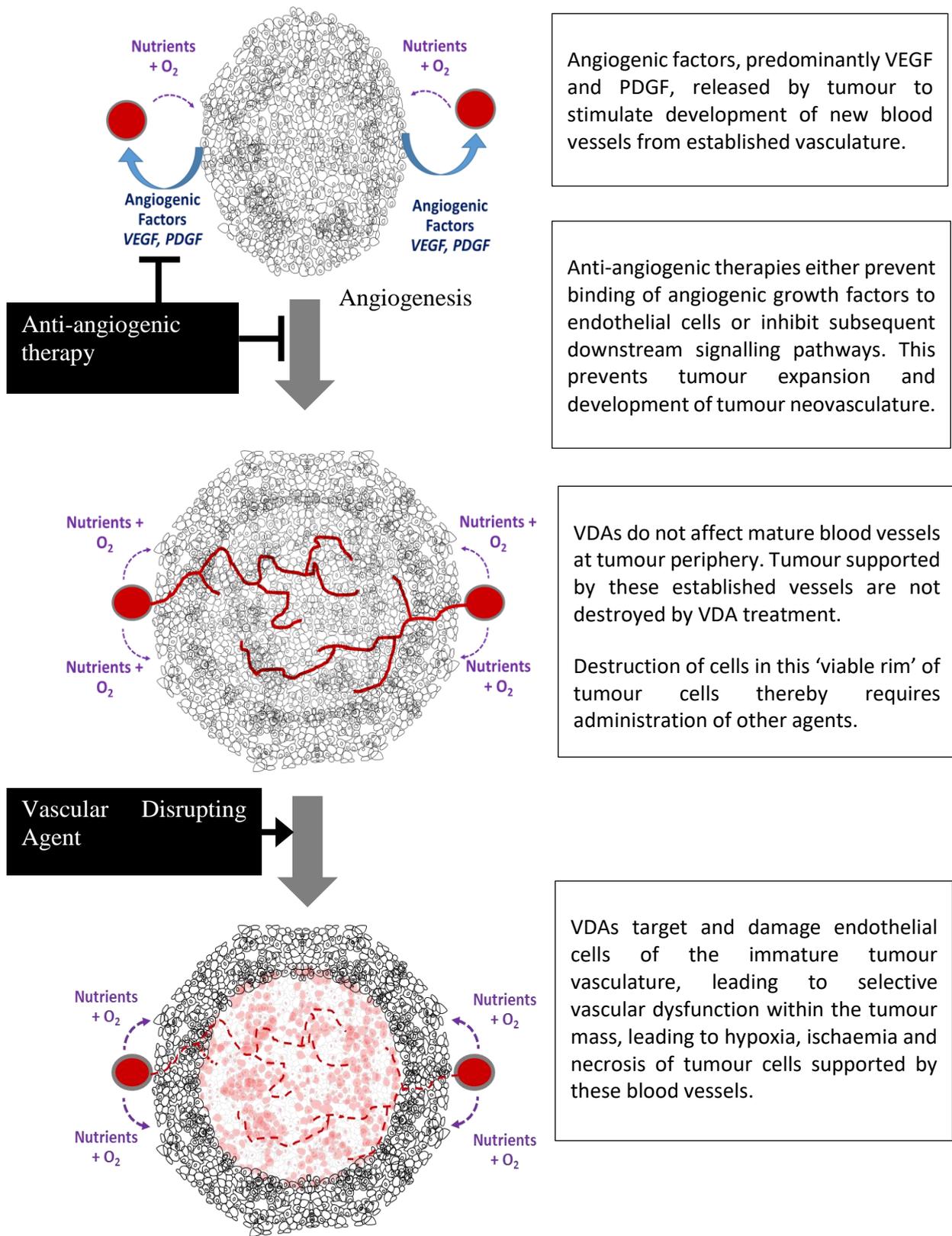
Figure 1-9: The effect of tubulin-interactive VDAs on tumour. (Gill et al., 2019)

1.7.7 Necessity for use of VDAs in combination with other chemotherapeutics

A major limitation to the use of VDAs for management of solid cancer is their apparent lack of ability to affect the whole tumour, with cells at the periphery of the tumour mass showing a lesser therapeutic response. This area of the tumour being referred to commonly as the "viable tumour rim" (see Figure 1-9) (Tozer et al., 2005, Blakey et al., 2002). Although not conclusively proven, it is hypothesised that tumour cells at the periphery are supported by the existing established vasculature rather than that produced as a consequence of tumour angiogenesis. This established vasculature, unlike the tumour neovasculature, does not purely rely on tubulin for its cytoskeletal architecture but rather a more well-established cytoskeletal structure underpinned by actin and other such fibres. Additionally, these blood vessels also have a higher density of supporting pericytes, contributory to vascular stabilisation and structural integrity of the blood vessel. Consequently, the tubulin-disruptive capacity of VDAs has a significantly lower effect on established vasculature (Chen et al., 2017, Tozer et al., 2008).

To address this deficiency of VDA therapeutics, it is highly likely that their clinical use will need to be partnered with a cytotoxic therapeutic to target the tumour cells of the viable rim (Table 1-2)(Gill et al., 2019). However, in contrast to this being perceived negatively, it is probable that this approach will be significantly beneficial and efficacious than either therapeutic strategy alone. This is because it is well known that a major limitation to current cancer treatment is the limited activity of 'standard' chemotherapeutics against those tumour cells towards the centre of the mass because of diffusional limitations (Minchinton and Tannock, 2006). By linking the VDA with this cytotoxic approach, it is probable that this would deliver a "cannon" and "pawn" strategy (Song et al., 2016), with the VDA "cannon" destroying the 'hard-to-reach' cancer cells from mid-tumour towards periphery (via shutdown of tumour blood vessels), and the cytotoxic chemotherapeutic "pawn" destroying the VDA-resistant cells

of the tumour viable rim. Further benefits are also proposed to be a reduction in drug doses due to a lack of necessity to inherently compensate for difficulties in drug penetration, and entrapment of drugs within the tumour mass because of VDA-mediated vascular collapse with subsequent reduced systemic toxicities. Such an approach has been exemplified by the recently identified tumour-activated VDA, ICT2588 (Gill et al., 2014, Atkinson et al., 2010).

A co-administration approach does however introduce several confounding factors to their putative success, not least an elevated risk of additive or synergistic deleterious effects upon normal body systems, particularly upon the cardiovascular system. This could be due to direct cytotoxicity to cells of the myocardium, drug-induced perturbations of cardiac excitation-contraction coupling, induction of structural hypertrophic responses, or wider effects upon the cardiovascular system, as discussed later. Conversely, a co-administration approach could improve success and be associated with an improved response and reduced deleterious effects. Removal of the requirement for the cytotoxic chemotherapy to penetrate throughout the tumour, due to therapeutic action of the VDA, could equate to systemic delivery of lower but highly efficacious concentrations of toxic chemotherapeutic, thereby reducing systemic toxicities (Atkinson et al., 2010, Martinelli et al., 2007, Siemann et al., 2017).

With regards combination therapy with VDAs, there are several chemotherapeutic classes which could be used, each with their advantages and disadvantages in terms of cardiovascular toxicities.

1.8 Cancer chemotherapy and cardiotoxicity

Despite many cancer chemotherapies significantly improving cancer treatment and patient survival, it is now clear that their benefit is counterbalanced by adverse toxic effects,

particularly upon the cardiovascular system (Lindenfeld and Kelly, 2010). The improved success of cancer treatment has in itself created issues regarding cardiovascular toxicity, as the prolonged patient survival allows the patient to live long enough to encounter the long-term detrimental effects of the particular therapeutic. A situation then arises in which cardiovascular toxicity can be the main determinant of quality of life and potentially be responsible for premature death, as opposed to cancer (Oeffinger et al., 2006). This is shown by the fact that a patient diagnosed with breast cancer at early stage has a high possibility of dying from drug induced cardiotoxicity rather than cancer (Hanrahan et al., 2007, Mann and Krone, 2010). Consequently, challenges exist with respect to identifying, managing or at least monitoring cancer-therapy related cardiovascular toxicity, to provide the most beneficial cancer treatment, and ultimately improve patient outcomes and longer-term healthcare (Albini et al., 2010, Curigliano et al., 2012, Force et al., 2007, Schmidinger et al., 2008). Therefore, in order to administer safer yet still effective cancer treatments, a much greater appreciation of the underlying molecular mechanisms by which current therapies cause adverse effects upon the cardiovascular system and how to predict these toxicities before they arise in the clinic is essential.

Due to the often-asymptomatic nature of acute cardiotoxicity, which presents as rhythm disturbances, transient reductions in myocardial contractility, and/or hypotension, and the fact that it is reversible by discontinuation of treatment, this adverse effect is commonly under recognised. The infrequency of this cardiotoxicity subtype does not equate to it being inconsequential or irrelevant; as sub-clinical adverse effects may contribute to cumulative cardiac damage or asymptomatic loss of cardiac function. In the case of early- and late-onset chronic progressive cardiotoxicities, these are associated with electrophysiological changes and

left ventricular dysfunction, which presents clinically as irreversible cardiomyopathy (Curigliano et al., 2012). With late-onset chronic progressive cardiotoxicity, the deterioration in cardiac function is progressive over many years and can be as long as one to two decades after completion of cancer therapy.

Chemotherapy-induced toxicity, although commonly manifesting as an effect upon the cardiac system, also poses a risk to the coronary and peripheral vascular systems, through exacerbation of hypertension, perturbations in vascular tone, or direct vascular damage (Herrmann et al., 2016). Alongside cardiac toxicity, this obviously has an effect upon the circulatory cardiovascular system and indirectly upon the heart itself. Several chemotherapeutic drugs, most notably the molecular targeted kinase inhibitors, have been shown to induce vascular toxicity in the clinic (Herrmann et al., 2016, Touyz et al., 2018). However, unlike the recent cross-disciplinary awareness of chemotherapy-induced cardiotoxicity, vascular toxicity per se is still largely under-appreciated in the clinic and strategies targeted towards its mitigation and management are not fully defined. Nevertheless, chemotherapy-induced effects upon the vascular system remain important and directly pertinent to cancer management and cardio-oncology.

Cardiovascular toxicity is without doubt a long-term complicating factor in cancer treatment, from asymptomatic electrocardiographic perturbations through to symptomatic life-threatening events such as heart failure, appearing both acutely and taking several years to manifest (Cardinale et al., 2016, Salvatorelli et al., 2015, Todaro et al., 2013). Despite this, the severity and life-threatening nature of cancer in conjunction with the improvement in overall survival associated with treatment often outweighs these toxicological safety risks (Cardinale et al., 2016, Salvatorelli et al., 2015, Todaro et al., 2013).

1.8.1 Cardio-oncology

Increases in the survival rate of cancer patients and those with cardiovascular disease have been observed during the past three decades, which can be attributed to improved treatments and greater awareness of risk factors (Mensah et al., 2017, Arnold, 2019, Miller et al., 2019, Wang et al., 2016). However, alongside this is the observation of an increased incidence and prevalence of both cardiovascular disease and cancer, with the number of patients presenting with both conditions increasing (Lindenfeld and Kelly, 2010, Yeh, 2006, Chu et al., 2007, Mulrooney et al., 2009). Concomitant is the existence of overlapping risk factors for both conditions (such as obesity and smoking) resulting in patients with heart disease possessing an increased cancer risk (Koene et al., 2016, Duong et al., 2017, Formica et al., 2020). Therefore, closer scrutiny and studies are now focused on addressing this issue (Anderson and Sawyer, 2008, Maitland et al., 2010, Abraham et al., 2009). In addition to this relationship between cardiovascular disease and cancer, a pivotal concern is the increased appearance of chemotherapy-induced cardiovascular disease. This is due to the visible progress in terms of early diagnosis, the advanced oncological care, the usage of targeted drugs and use combinations of two or three different drugs which all leads to long life span of cancer patients. This has a significant bearing on a patient's quality of life, such that a patient diagnosed with early-stage breast cancer now has a high possibility of dying from drug induced cardiotoxicity rather than cancer (Hanrahan et al., 2007, Mann and Krone, 2010).

Consequently, cardio-oncology is an evolving discipline covering the area of antineoplastic induced cardiotoxicity in preclinical stage, clinical stage, treatment and observation of those who were given cancer therapy (Ewer et al., 2011). The ultimate aim being to develop interdisciplinary expertise to effectively treat a patient's cancer whilst minimising any collateral damage to the cardiovascular system (Lenihan et al., 2016, Cardinale et al., 2016).

1.8.2 Cardiotoxicity of 'conventional' cytotoxic chemotherapy

The majority of 'conventional' cancer chemotherapeutics in the clinic interfere with DNA replication and subsequently cellular proliferation. These mechanisms of action are central players in the detrimental cardiac effects of this family of drug, often associated with dose-related and cumulative toxicity and considerable morbidity and mortality (Gill et al., 2019). Effects include arrhythmias, left ventricular dysfunction and repolarisation, depressed contractility, myocarditis, congestive heart failure and thromboembolic events. In the majority of cases, the toxic effects are acute with no late-stage chronic cardiotoxicity reported (Gill et al., 2019).

However, an exception is observed with drugs targeting topoisomerase II (TOPII), the commonest cytotoxic treatment used in the clinic for the management of a wide-range of adult and paediatric malignancies, specifically the anthracyclines (e.g., doxorubicin, epirubicin and daunorubicin) (Delgado et al., 2018, Nitiss, 2009, Pommier, 2013). Despite these therapeutics being potent and widely used cancer therapeutics, their use is undeniably associated with detrimental effects upon the cardiac system, both acutely and longer-term (Gill et al., 2019). The major risk factor for development of anthracycline-induced cardiac dysfunction is cumulative drug exposure. However, several other contributory factors are now known to be involved, including dosing rate and schedule, patient age, female gender, hypertension, previous cardiovascular disease, and genetic predisposition (Brana and Tabernero, 2010, Cappetta et al., 2017, Lipshultz et al., 2013, Lotrionte et al., 2013). Although there are several hypotheses proposed to explain the mechanistic basis for anthracycline-induced cardiotoxicity, including iron-mediated generation of reactive free radicals, specific interactions with TOPIIβ, drug-induced mitochondrial dysfunction, and perturbation of mitochondrial topoisomerase (mTOP) activity, no definitive exclusive mechanism has been confirmed (Cappetta et al., 2017,

Cappetta et al., 2018, Khiati et al., 2014, Octavia et al., 2012, Piegari et al., 2013, Renu et al., 2018, Vejpongsa and Yeh, 2014).

1.8.3 Cardiotoxicity of therapeutics targeting tumour angiogenesis.

As previously defined, the vast majority of anti-angiogenic therapies are concerned with perturbation of the VEGF-signalling pathway in endothelial cells (Weis and Cheresh, 2011). VEGFR signalling is important in the normal vasculature and plays a role in vascular density and generation of the vasodilatory mediator nitric oxide (NO). Consequently, many of the anti-angiogenic drugs have reported close relationships to cardiovascular toxicity, both asymptomatically and symptomatically, with hypertension being a major issue with both VEGF-sequestering and kinase inhibitor classes of these agents (Faruque et al., 2014, Alameddine et al., 2015, Cameron et al., 2016, Ky et al., 2013, Tocchetti et al., 2013). The fact that hypertension occurs so frequently with these agents, it is now commonly considered a biomarker of therapeutic efficacy (Ewer and Yeh, 2013).

Although not yet conclusively proven, it is highly likely that these cardiovascular toxicities are a result of direct effects upon the vasculature and subsequent hypertension, supported by the fact that Inhibition of VEGF signalling by angiogenesis inhibitors results in decreased NO which both contribute to hypertension by increased peripheral resistance and vasoconstriction. These effects further complicated by cardiac strain and heart failure, in conjunction with effects upon the renal system (Cosmai et al., 2015, Di Lorenzo et al., 2009). Such a hypothesis is supported by the fact that cardiovascular toxicity induced by these agents is higher in patients with pre-existing cardiovascular risk factors (Chu et al., 2007, Di Lorenzo et al., 2009, Grisham et al., 2018, Rhea and Oliveira, 2018)

1.8.4 Cardiotoxicity of vascular disrupting agents (VDAs)

Several preclinical *in vivo* laboratory investigations and clinical trials have been performed to evaluate toxicity of the tubulin-interactive VDAs (Beerepoot et al., 2006, Hinnen and Eskens, 2007, Ho et al., 2017, Sessa and Pagani, 2001, Subbiah et al., 2011, Tozer et al., 2005)

In several cases VDAs have been shown to cause a wide range of detrimental effects upon the cardiovascular system (Table 1-3)(Hinnen and Eskens, 2007, Ho et al., 2017, Siemann et al., 2009, Subbiah et al., 2011).

VDA-induced cardiac ischaemia
Myocardial infarction
Asymptomatic elevation in circulating troponin I levels
VDA-induced haemodynamic changes
Hypertension
Hypotension
VDA-induced perturbations in cardiac
Transient QT prolongation
Delayed ventricular repolarisation.
Tachycardia
Bradycardia
Atrial fibrillation

Table 1-3: VDAs-induced cardiac effects reported in preclinical and clinic studies.

Preclinical studies of cardiac effects of the tubulin-binding VDAs, ZD6126 and the combretastatin family of anticancer drug, were performed in rats, involving continuous monitoring of both heart rate and blood pressure alongside histopathological and biochemical (Anderson et al., 2003, Gould et al., 2007, Grosios et al., 1999, Jaroch et al., 2016, LoRusso et al., 2007, Rustin et al., 2010, Subbiah et al., 2011, Tochinai et al., 2016, Zweifel et al., 2011).

Administration of ZD6126 was associated with high levels of circulating troponin T (clinical biomarker of cardiac toxicity) in the blood and drug-induced delayed tachycardia and hypertension (Gould et al., 2007). In the case of combretastatin-A4-phosphate (CA4P) and its analogue combretastatin-A4-disodium-phosphate (CA4DP), drug-induced increases in mean arterial blood pressure were also observed. However, no detectable increases in troponin were observed (Ke et al., 2009). Interestingly, pre-administration of calcium channel blockers prevented hypertension induced by both ZD6126 and combretastatins in these rat models (Gould et al., 2007, Ke et al., 2015) offering the notion that VDA-related elevated blood pressures may be linked to increased peripheral vessel resistance (Grisham et al., 2018, Anderson et al., 2003).

In clinical trials, several cardiotoxic effects were detected within a few hrs of administration of ZD6126, including abnormal cardiac function, pain or pressure in the mid-chest region or left arm, and increased systemic levels of the biomarker of cardiotoxicity troponin (Beerepoot et al., 2006). Although CA4P is tolerated better than ZD6126 and other VDAs, its use is still accompanied by a range of cardiac adverse effects. The most common adverse effect of CA4P is an acute transient increase in baseline blood pressure, wherein a 10-15% increase above baseline is observed within one hr of administration, with normal state returning within 3-4 hrs post-infusion (Grisham et al., 2018). Drug-induced tachycardia and contradictory bradycardia are both evident with CA4P therapy; patients who received CA4P show biphasic response as they were typically characterised by a decrease in heart rate (bradycardia) within the first hr post-infusion followed by an increase (tachycardia) around 3-4 hrs later, and a return to baseline by 24 hrs (Grisham et al., 2018, Rustin et al., 2003, Zweifel et al., 2011). Several patients receiving CA4P have also experienced myocardial ischaemia, although in the

majority of cases an underlying confounding issue was identified, such as coronary artery disease (Garon et al., 2016, Grisham et al., 2018, Rustin et al., 2003, Sosa et al., 2011)

In terms of clinical management of CA4P-induced cardiac effects, a treatment algorithm was devised for use in the phase II FOCUS trial (CA4P in combination with the anti-angiogenic agent bevacizumab and cytotoxic chemotherapy) involving differential strategies for patients presenting with hypertension and those normotensive (Monk et al., 2016). Patients with hypertension were managed through optimisation of their current medication, and in those patients without established hypertension an evaluation of cardiovascular risk factors was undertaken prior to receiving CA4P (Monk et al., 2016, Grisham et al., 2018). High-risk patients were those with any previous CA4P-induced blood pressure effect or with baseline blood pressure >130 mmHg, and the presence of cardiovascular risk factors (diabetes, previous myocardial infarction, prior uncontrolled hypertension etc.). A major risk factor of pertinence for cancer therapy was also receipt of prior anthracyclines. However, in all cases, frequent monitoring of blood pressure after CA4P administration was deemed essential to mitigate the acute CA4P-induced cardiac complications (Monk et al., 2016, Grisham et al., 2018).

1.9 Aims and Objectives

Vascular disrupting agents exhibit significant scope and potential for the improved management of solid cancers in the clinic. The inhibitory factor retarding their clinical progression is however the expected adverse effects of these agents upon the cardiovascular system, a hypothesis supported by preclinical *in vivo* evaluation studies. In order to fully appraise the risk-benefit ratio for the use of VDAs as cancer therapeutics and identify strategies toward mitigation of any adverse effects upon the cardiovascular system, an understanding of the mechanistic basis of their cardiotoxicity is necessitated.

The overall aim of this thesis is the assessment of drug-induced structural and functional cardiotoxicity of VDAs and identification of potential toxicological mechanisms. These studies will evaluate the structural and functional cardiotoxicities caused by the agents using the AC10 (non-contractile) human ventricular cardiomyocyte cell line and stem-cell derived cardiomyocytes and a number of molecular and cellular analytical methodologies, especially impedance-based non-invasive measurement of drug-induced cellular effects and excitation-coupling of cardiomyocyte contractility of cellular monolayers, using the xCELLigence real-time analyser (RTCA) systems. Furthermore, mitigation of any cardiotoxicological effects of VDAs through concomitant administration of cardioprotective agents will be app

Chapter 2. Material and methods

2.1 Materials

All reagents were obtained from Sigma-Aldrich Company Ltd (Gillingham, Dorset, UK) unless otherwise stated. Plastic tissue culture materials were supplied by Sarstedt (Leicester, UK).

2.2 Cell lines

The human cardiomyocyte cell line AC10 was originally derived by fusion of adult ventricular cardiac cells with SV40 transformed fibroblasts, as described by Davidson et al (Davidson et al., 2005). These cells were kindly donated by Dr Barbara Savoldo from Texas Children's Hospital, Texas, USA. The NCI-H460 immortalised human non-small cell lung cancer (NSCLC) cell line was originally obtained from the American Tissue Culture Collection (ATCC).

2.2.1 Maintenance of cell lines

AC10 cells were maintained in Dulbecco's modified Eagle's medium (DMEM) supplemented with 12.5% foetal bovine serum (FBS), 2mM L-Glutamine and 50-100 units/mL penicillin/streptomycin. The H460 cell line was maintained in Roswell Pak Memorial Institute (RPMI) 1640 medium supplemented with 10% FBS, 2mM L-Glutamine and 50-100 units/mL penicillin/streptomycin. Both cell lines were grown as monolayers *in vitro* and maintained in a humidified incubator at 37°C in 5% CO_2. Cells were passaged when flasks were ~75-80% confluent by washing the monolayer with Hanks Balanced Salt Solution (HBSS) and subsequent addition of 0.25% trypsin-EDTA followed by cell detachment. A cell pellet was then obtained by centrifugation at 300 x g (1000 rpm) for 5 mins and the resulting cells were either re-suspended in fresh medium and passaged into a new flask, fixed in ethanol at 4°C for flow cytometry, or cell pellets were stored at -20°C for molecular analysis.

2.3 Determination of cell number by manual counting

To accurately calculate cell number, a 20μL volume of cell suspension was loaded beneath the coverslip and into the chamber of a Neubauer haemocytometer. Cells were counted under 10 x magnification using an inverted microscope, with the number of cells counted in five 1mm^2 areas. The average number of cells (N) in the five areas equating to N x 10^4 cells/mL. To calculate the total cell number present = (N x 10^4 cells/mL) x (total volume of cell suspension).

2.4 Determination of cell viability by Trypan blue exclusion

A 10μL volume of cell suspension was mixed with an equal volume of Trypan blue dye and mixed by gentle pipetting. The resultant solution was loaded beneath the coverslip and into the chamber of a Neubauer haemocytometer, as per methodology (section 1.1.2) for manual cell counting. The number of clear (viable) and blue (membrane compromised & non-viable) cells were counted across five 1mm^2 sections of the haemocytometer chamber. The mean number of dead or non-viable cells (D), viable cells (V), and total cell counts were recorded and total numbers calculated (Section2.3), with the final value adjusted by 2-fold to address the dilution factor introduced via Trypan blue inclusion.

2.5 Cryopreservation of cells

Cell stocks were produced from confluent flasks for each cell line (passaged less than five times) and stored under liquid nitrogen. Cells were collected as per routine cell passage, the resulting pellets suspended in 1 mL of fresh cell culture medium and transferred to 1.8 mL cryovials. To each cryovial 100 μl dimethyl sulfoxide (DMSO) was added (final concentration 10% DMSO) and the vials placed in a cryogenic freezing at a -80°C. The following day cells were transferred to a liquid nitrogen storage drawer for long term storage.

2.6 Routine screening for cells for mycoplasma contamination

All cell lines in culture were monitored on a monthly basis for evidence of mycoplasma contamination. Cell media was submitted for in-house screening, using the MycoAlert® kit (MycoAlert Mycoplasma Detection Kit, Lonza, UK). Any cell lines found to be contaminated were immediately disposed of and new growing cultures developed from cryopreserved cell stocks.

2.7 Characterisation of cardiac phenotype of AC10 cells by immunostaining

AC10 cardiomyocytes (AC10-CMs) were immunostained to verify the expression of a variety of cardiac specific proteins including contractile proteins and transcription factors. The immunostaining was performed in conjunction with Kimberly Rockley (PhD student, Durham University) utilising a protocol developed by Dr Gavin Richardson (Newcastle University) who kindly provided reagents and antibodies.

A suspension of AC10-CMs was created and cell number determined using a haemocytometer (section 2.3). The cell number was adjusted and cells were seeded in 2-chambers cell culture slides (NUNC, USA) at a density of 1×10^5 cells per chamber. The cells were left overnight to adhere to the slide surface. Cells were washed with PBS and then incubated with 1ml 4% paraformaldehyde (PFA; diluted in PBS) at room temperature for 20 minutes, PFA preparation is described in appendix 1. Following this the cells were washed once with PBS and incubated in PBS at 4°C until commencing staining. Slides were then incubated in 0.4% Triton-X-100 for 20 minutes and then blocked with 20% FBS for 30 minutes. Following addition of primary antibody (1:200 dilution in PBS) or no antibody control (PBS alone) the slides were incubated overnight at 4°C. Slides were washed (3 x 5 minutes) in PBS and then incubated at room

temperature for one hr with the relevant secondary antibody (1:500 dilution in PBS, see Table 2-1 below for antibody details) and the nuclear stain 4',6-diamidino-2-phenylindole (DAPI; 1:500 dilution in PBS).

SN	Primary Antibody	Secondary Antibody	Fluorescent Tag	Emitted Colour
1	Troponin I/Goat Polyclonal	Anti-goat	Alexa 594	Red
2	Troponin C/Goat Polyclonal	Anti-goat	Alexa 488	Green
3	Tropomyosin/Rabbit Polyclonal	Anti-rabbit	Alexa 488	Green
4	Alpha Actinin/Rabbit Polyclonal	Anti-rabbit	Alexa 488	Green
5	NKX2.5/Rabbit Polyclonal	Anti-rabbit	Alexa 488	Green
6	BMP-2/Goat Polyclonal	Anti-goat	Alexa 488	Green
7	PCM1/Rabbit Polyclonal	Anti-rabbit	Alexa 488	Green
8	Ki-67/Murine Monoclonal	Anti-mouse	Alexa 594	Red
9	Vimentin/Chicken Monoclonal	Anti-chicken	Alexa 594	Red
10	Alpha Smooth Muscle Actin/Rabbit Polyclonal	Anti-rabbit	Alexa 488	Green

Table 2-1: Antibodies used for AC10 cardiac phenotyping by immunostaining. All antibodies were purchased from Invitrogen.

For no secondary antibody control chambers, PBS and DAPI were used. Slides were then washed in PBS (3x 5 minutes), and antifade solution and the coverslips added. Slides were subsequently visualised on a Nikon Eclipse Ti confocal fluorescence microscope and images captured using NIS elements software V4.2.

2.8 Determination of cell proliferation and survival using the MTT Assay

The MTT (3-(4,5-Dimethylthiazol-2-yl)-2,5-Diphenyltetrazolium Bromide) assay is a colorimetric assay which harnesses mitochondrial activity as a surrogate indicator of cell viability and proliferative activity. In viable cells, a soluble tetrazolium dye is converted by mitochondrial

enzymes into insoluble purple formazan crystals, whereby the amount of purple crystals created reflects the number of viable cells (Mosmann, 1983).

The optimal cell seeding density (in a 96-well cell culture plate) to facilitate assessment of the effects of compounds upon cells in their proliferative (exponential) growth phase was determined as 2×10^3 cells/well and 5×10^2 cells/well for AC10 and H460, respectively. For evaluation of the effect of compounds upon quiescent cardiac cells, representative of the adult heart, a higher seeding density for AC10 cells of 4×10^4 cells/well is required, to facilitate residence in the plateau phase of cell growth.

Cells were seeded in flat-bottomed 96 well plates at the identified cell density, apart from one column which served as a cell-blank (medium only) control. Plates were placed in a humidified incubator at 37°C in 5% CO_2 to adhere overnight. Media was then removed from all wells and replaced with media containing the required compound or drug. Controls on the plate include the drug vehicle (≤1% dimethyl sulphoxide; DMSO), and no drug or vehicle (cells and media only) to ensure any observed effects were due only to the compounds/drugs added. All plates were then placed in a humidified incubator at 37°C in 5% CO_2 for the required incubation period, up to a maximum of 96-hrs post-compound addition. For compound/drug exposures of less than 96-hrs, compounds and media were removed at the appropriate timepoint and fresh media were added to the entire plate, with the plates returned to the incubator for the remaining exposure period. At the end of the required incubation period, media was removed from all wells of the plate and replaced with medium containing a 1:10 dilution of MTT (5mg/mL diluted in PBS). Plates were then incubated at 37°C for an additional 4-hrs to allow the formation of formazan crystals. Following careful removal of the MTT and media solution from the plate, the formazan crystals (settled at base of well) were dissolved in DMSO and the

absorbance of each well measured at 550nm using a UV-Vis spectrophotometer plate reader (MultiSkan GO, Thermos Scientific, USA).

The relative cell viability (%) related to vehicle control was measured as follows, following correction for background absorbance (Medium only control wells): Relative cell viability (%) = $[A]_{test}$/ $[A]_{control}$ × 100; where $[A]_{test}$ is the absorbance of the treated cells and $[A]_{control}$ is the absorbance of the vehicle control treated cells. All experiments were performed in triplicate on at least three separate occasions. IC_{50} values (concentration of drug resulting in 50% reduction in cell survival) were determined using dose-response curves, obtained by implementing curve fitting by nonlinear regression. Results are presented as mean ± SEM. Statistical analyses were performed using Student's paired t test, with a value of $P < 0.05$ considered to be significant.

2.9 Analysis of cell growth, attachment and morphology using the xCELLigence real-time cell analyser (RTCA) dual-purpose (DP16) system

The xCELLigence[®] DP16 real-time cell analyser (RTCA) instrument monitors cell proliferation, structural changes and the quality of cell adherence using non-invasive electrical impedance in real-time, with the operating unit housed in the incubator at 37 °C in 5% CO_2. This technology relies on detecting and measuring net cell adhesion, as determined by changes in cellular impedance using multiwell plates impregnated with high density gold microelectrodes, termed E-plates (Ke et al., 2011). In the case of the DP16 the system can simultaneously analyse 3 x 16-well E-plates. During studies, impedance readings alter in relation to cellular attachment, detachment and changes in cellular size. In blank wells containing only media the circuit between electrodes in the base of each well is completed and therefore impedance is equal to zero. In wells containing media and live adherent cells, the impedance increases. The impedance values are converted by the xCELLigence software to a value termed cell Index (CI).

In absence of cells or lack of cell attachment, the value of CI is zero. As cells attach and more electrodes are impeded, the CI value rises. Accordingly, CI is a quantitative indicator of mean cell number, attachment and cell size in a well (Figure 2-1).

Prior to cell seeding into E-plates, 100 µL DMEM-F12 media is added to all wells of the E-plate and the plate allowed to reach equilibrium in a sterile cell culture cabinet for at least 30 mins. The E-plate is then inserted into the cradle of the RTCA instrument and the background impedance reading measured.

AC10 cells were detached from stock flasks, the cell concentration calculated and the final concentration adjusted to 2×10^4 cells/mL for experiments examining cells in the exponential growth phase or to 1×10^5 cells/mL for experiments requiring cells to be in the plateau phase of growth. The E-plate was disengaged from the RTCA instrument and 100µL of cell suspension was added to the media present in 14 wells of the E-plate, with a further 100µL media (no cells) added to the remaining two wells of the plate as a control. Final cell concentrations within the plate are thus 2×10^3 cells/well or 1×10^4 cells/well for exponential and plateau growth, respectively. The E-plate was then incubated in a sterile cell culture cabinet at room temperature for 30 min to allow the cells to settle in an evenly distributed manner at the bottom of the wells. The E-plate was then transferred to the cradle of the RTCA instrument in the incubator, with the experiment started and readings collected at least every 30 min.

For experiments evaluating effects during exponential cell growth, cells were incubated on the DP16 RTCA for at least 24hrs prior to drug addition, to allow for cellular attachment and equilibrium of culture conditions. However, for investigations of effects upon quiescent cells, treatment was initiated when a steady plateau growth phase was observed, approximately 96 hrs post-seeding. Media was replaced upon compound addition, containing the

compound/drug at the relevant concentration. Experiments were performed in triplicate. Cell index values were normalised to the point of drug loading and statistical analysis was performed by one-way analysis of variance (ANOVA) test.
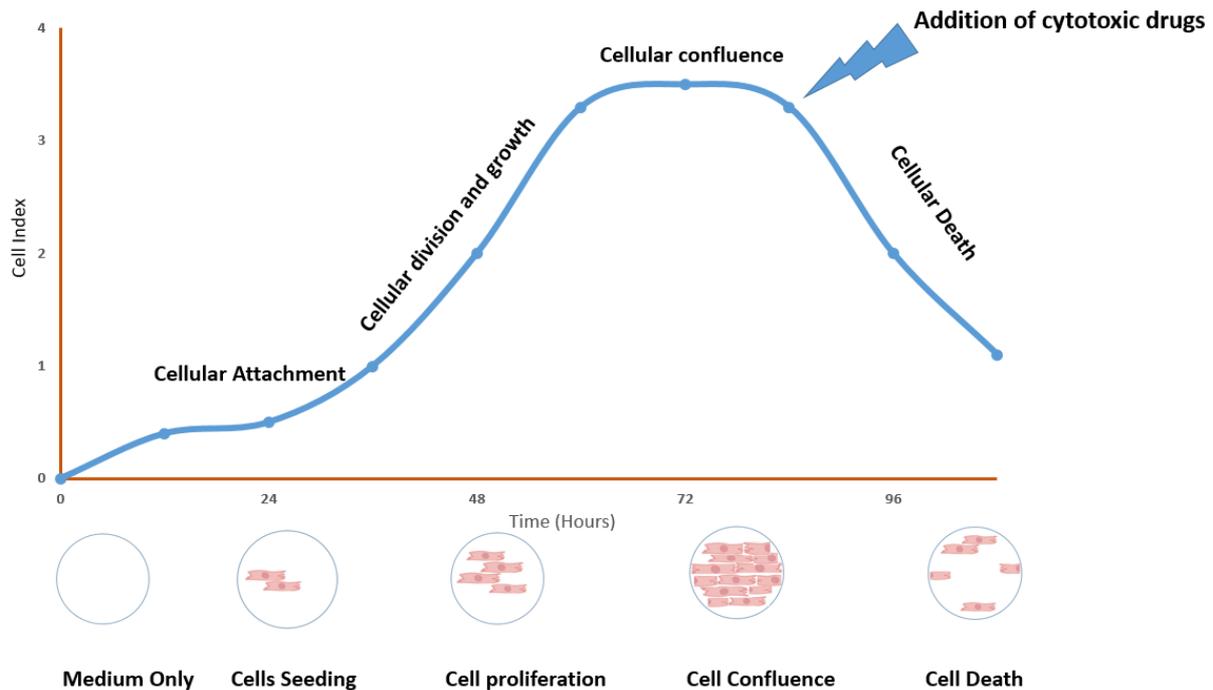
Figure 2-1: Cell growth monitoring using the xCELLigence impedance-based system.

Schematic showing the output on the cell growth monitoring using the xCELLigence impedance-based system when monitoring cellular growth and response to cytotoxic drugs, whereby cell index (measurement of impedance) is related to the phase of cellular growth and the cell density in the wells. xCELLigence impedance-based system when monitoring cellular growth and response to cytotoxic drugs, whereby cell index (measurement of impedance) is related to the phase of cellular growth and the cell density in the wells.

2.10 Evaluation of cellular cytotoxicity of VDAs using the MTT assay.

Cytotoxicity is one of the essential assessments for evaluation of cellular biological activity *in vitro*. Due to various mechanisms, drugs can result in cellular death induced by cytotoxicity. The colorimetric MTT assay provides a cheap, easy to apply, reliable, safe and reproducible cytotoxicity/ cell viability assay.

2.10.1 Evaluation of viability of AC10 cardiac cell line in the exponential phase of growth following exposure to VDAs, using the MTT assay.

The doses used in this study represent clinical doses, between 1-2 µM (Rustin et al., 2003, Jung et al., 2003). The drug concentration that causes a 50% inhibition of cell proliferation (IC_{50}) values were calculated for all drugs. AC10 cells were seeded into 96 well plates (as described in Section 2.8) in exponential phase at a density of 2000 cell/well in a total volume of 200 µL DMEM media. Cells were allowed to adhere to the plate by incubation overnight at 37°C and 5% CO_2. The next day, media were removed and fresh media containing specific concentrations of the compound of choice (Colchicine and CA4 dissolved in DMSO) over a selected a range of various concentration for exposure time either 24hrs or 96hrs. Concentration ranged from 1 µM to 0.01 nM. Each plate has three controls, a lane with no cells served as blank, a lane with no treatment and a vehicle control lane where wells were loaded with (0.1%) DMSO solution, which is the same concentration used to prepare the highest drug concentration. After 24 hrs exposure time, the drug containing media were removed and fresh media were loaded. The cardiomyocytes were cultured further in DMEM media until 96 hrs post treatment. After 96 hrs media were removed from all plates (24 and 96 hrs drug exposure) and cell viability was determined using MTT assay (section 2.8).

2.10.2 Evaluation of viability of AC10 cardiac cell line in the plateau growth phase following exposure to VDAs at clinically relevant concentrations, using the MTT assay.

AC10 cells were seeded into 96 well plates in plateau phase at a density of 40,000 cell/well in a total volume of 200 µL DMEM media and allowed to adhere to the plate overnight. The next day, media were removed and fresh media containing specific concentrations of the compound of choice (Colchicine and CA4 dissolved in DMSO) over a selected range of various concentration for exposure time either 24hrs or 96hrs. Concentration ranged from 1µM to 0.01nM. Each plate has three controls, a lane of wells with no cells served as blank, a lane with cell but no treatment and a vehicle control lane where seeded wells were loaded with (0.1%) DMSO solution, which is the same concentration used to prepare the highest drug concentration. After 24 hrs exposure time, the drug containing media were removed and fresh media were loaded. The cardiomyocytes were cultured further in DMEM media until 96 hrs post treatment. After 96 hrs media were removed from all plates (24 and 96 hrs drug exposure) and cell viability was determined using MTT assay (section 2.8).

2.10.3 Evaluation of viability of cancer cell line in the exponential phase of growth following exposure to VDAs, using the MTT assay.

In order to identify the therapeutic index of these drugs between cancer cells and cardiac cells, it is important to evaluate the IC$_{50}$ values in cancer cells. A similar experiment of assessing IC$_{50}$ using MTT assay was conducted on H460 cell line. The H460 cell line was originally derived from the lung pleural effusion of a patient with large cell lung cancer (Banks-Schlegel et al., 1985). Lung cancer H460 cells were seeded in exponential phase at density of 500 cells/well. the cell lines were allowed to adhere to the plate by incubation overnight at 37°C and 5% CO$_2$. The next day, media were removed and fresh media containing specific concentrations of the compound

of choice (Colchicine and CA4 dissolved in DMSO) over a selected a range of various concentration for exposure time either 24hrs or 96hrs. Concentration ranged from 1μM to 0.01nM. Each plate has three controls, a lane with no cells served as blank, a lane with no treatment and a vehicle control lane where wells were loaded with (0.1%) DMSO solution, which is the same concentration used to prepare the highest drug concentration. After 24 hrs exposure time, the drug containing media were removed and fresh media were loaded. The cardiomyocytes were cultured further in DMEM media until 96 hrs post treatment. After 96 hrs media were removed from all plates (24 and 96 hrs drug exposure) and cell viability was determined using MTT assay (Section 2.8).

2.11 Investigations of changes in cellular morphology and viability of the AC10 cell line following VDA exposure using the xCELLigence DP16 RTCA.

The overarching methodology for this technique is described in section 2.9. AC10 cells were seeded at 2×10^4 cell/mL into the wells of the DP16 xCELLigence E-plate and incubated at 37°C 5% CO_2 for 24 hrs. Cells were then treated with Colchicine or CA4 at concentrations of 3, 30 or 300nM or solvent control (0.1% DMSO), in duplicate, for either 24 or 96 hrs. At the end of the exposure period, all drug-containing media was removed and replaced with fresh media, and cell monitoring continued for a further 7 days. All experiments were conducted in triplicate and data normalised to the point of drug-addition. Student t-test statistical analyses were conducted to evaluate significance of drug exposures.

2.12 Analysis of drug effects upon contractile function of stem-cell derived murine cardiomyocytes (Cor.AT) using the xCELLigence Cardio RTCA system.

The xCELLigence cardio RTCA system (ACEA Biosciences, Agilent, USA) is similar to the xCELLigence DP16 system permits real-time monitoring and label-free measurement of changes in cell attachment, growth and morphology, although on a 96-well rather than a 16-well format. However, due to higher sensitivity and read times the xCELLigence Cardio system can also measure physiological changes of spontaneously contractile cardiomyocytes, providing non-invasive and real-time monitoring of drug effects upon cardiomyocyte contractility parameters (Li et al., 2016, Lamore SD, 2015).

Prior to cell seeding the E-plate was coated with fibronectin to facilitate cellular adhesion. Each well of the 96-well Cardio E-plate was coated with 50 µL of 10 µg/mL fibronectin, diluted in PBS (inclusive of Ca^{2+} and Mg^{2+}), and the plate incubated overnight at 4°C. Excess coating solution was removed from the wells and 180 µL of Cor.AT culture medium (containing 10µg/mL puromycin) (Axiogenesis, Cologne, Germany) was added to each well. The E-plate was transferred into the cradle of the RTCA instrument inside the incubator, the plate allowed to reach equilibrium for at least 30 min, and the background impedance measured.

Murine stem-cell derived cardiomyocytes, Cor.AT (purchased from Axiogenesis, Cologne, Germany) were thawed rapidly from cryostorage on ice, the contents of the cryovial reconstituted in 5 mL of warm Cor.AT media (without puromycin), centrifuged at 300 x g for 5 min and the resultant cell pellet resuspended in 5 mL Cor.AT media (without puromycin). The concentration of Cor.AT cells and their viability were ascertained by manual counting (section 2.3) and Trypan blue exclusion (section 2.4), respectively. The resulting cell suspension of viable Cor.AT cells was adjusted to a final concentration of 2.2 x 10^5 cells/mL in Cor.AT media

(containing puromycin), permitting a seeding density of 4 x10^4 viable cells per well across the Cardio E-plate.

The E-plate was disengaged from the Cardio RTCA instrument and the media aspirated from all wells. To each well (except two cell-free control wells) 180 µL of Cor.AT cell suspension was added, to give 4 x 10^4 viable cells per well, and the plate placed in the incubator at 37°C for 30 mins to allow even cell distribution in the well. Following this, the E-plate was returned to the cradle of the Cardio RTCA and the recording of impedance measurements initiated.

The following day the culture medium was exchanged twice; Once in the morning approximately 18 hrs after seeding and then again in the evening approximately 26 hrs after seeding. For each medium change a 100% medium replacement was performed in four steps – Whereby 90 µL of medium was removed from all wells, without disturbing the cell monolayer, and the same amount of fresh warmed medium added to those wells, with this process repeated four times to achieve a complete media change. Subsequently, a media change was performed twice daily with Cor.At media, using the same methodology, until the addition of compounds.

Compounds were added to the Cor.At cells once the cell growth had plateaued and stable baseline beating was observed. The following criteria were checked before commencing with compound addition: An absolute cell index >3, beat rate of 40 – 100 bpm and a beat amplitude of >0.02.

Approximately 2 hrs prior to compound addition a full media change was performed, as described in section 2.12. The compounds to be added were prepared at double the concentration required in Cor.At growth medium (absent of puromycin), with at least 110 µL of compound solution in each well of a parallel 96-well loading plate, mirroring the defined

required E-plate layout. The compound containing 96-well plate was placed at 37°C to allow temperature equilibration. The E-plate was disengaged from the RTCA and compounds were added by removal of 90 μL medium from the respective well of the E-plate and replacement with 90 μL of the appropriate double concentrated compound. Once all compounds were added the E-plate was returned to the cradle of the Cardio RTCA and the impedance measurements resumed.

On subsequent days, compounds were added again by removing 90 μL media from each well followed by addition of 90 μL of the appropriate single concentrated compound solution. For drug washout studies, the four-step medium change method was utilised, as described above.

Parameters relating to cellular contractility such as beat frequency and beat amplitude were analysed using the data analysis function of the RTCA Cardio software V1.0. Statistical analysis on normalised cell index. Where only two data groups were compared, a paired T-test was used.

2.13 Analysis of cell cycle by propidium iodide incorporation and flow cytometric analyses.

The stage of cell cycle distribution of individual cell populations was determined by flow cytometric analyses of cells following staining with propidium iodide (PI), with the degree of PI staining being proportional to cellular DNA content and thus cell cycle stage. PI is a dye which binds to the cellular DNA. To allow entry of PI dye, the membranes of AC10 cardiomyocytes were first permeabilized by ethanol fixation at 4 C. Ribonuclease H was added to the staining mixture and this to ensure only DNA, not RNA, is stained. Binding to PI determine the cell cycle. In the G_0/G_1 interphase, cells are diploid (2N DNA content); in G_2/Mitotic phase, cells are

tetraploid (4N DNA content); whilst undergoing DNA synthesis (S phase) the DNA content of cells are between 2N and 4N.

Control and treated samples of cells were harvested by trypsinsation (section 2.3). Cell pellets were suspended in 1 mL cold PBS, centrifuged at 300 xg (1000 rpm) and the resulting cell pellet fixed in 70% ethanol at 4°C for 30 min. Cell pellets were collected by centrifugation and the pellet re-suspended in DNA staining solution (PBS containing 1mg/mL RNase H and 40 mg/mL propidium iodide). Cells were incubated in the dark at 37°C for 30 min to facilitate DNA staining. Samples were either analysed immediately or stored at 4°C for up to 72 hrs prior to analysis.

Fluorescence emission of PI was determined using a FACS Calibur flow cytometer (Becton Dickinson, San Jose, CA, USA) on FL2-Channel. When bound to nucleic acid, PI has maximum emission wavelength of   617 nm. To exclude cell debris and cell aggregation, collected data were gated with at least 10,000 cells analysed per each sample. Obtained data were recorded and analysed with Cell Quest software (Becton Dickinson BD Biosciences).

 In addition to the cell cycle, flow cytometric forward scattered (FSC) and side scatter (SSC) parameters were determined, to determine changes in cell size and cellular granularity, respectively (Leif, 1989).

2.13.1 Analysis of effects of VDAs upon cell morphology and cell cycle distribution of AC10-CMs   phase of proliferative growth by flow cytometry.

AC10-CMs were seeded into T25 flasks at a density of 1×10^6 cells/flask and the flasks incubated at 37°C, 5% CO_2 for 24 hrs to facilitate cell adhesion and stability. Cells were then exposed to Colchicine or CA4 at a final concentration of 3, 30 or 300 nM or vehicle control (0.1% DMSO) and incubated at 37°C, 5% CO2. After a 24 hr or 96 hr incubation period, cells were detached

(section 2.3) and analysed for their cell cycle profile by staining with propidium iodide and flow cytometric analyses (section2.13).

2.13.2 Analysis of effects of VDAs upon cell morphology and cell cycle distribution of AC10-CMs whilst in plateau phase of growth by flow cytometry.

AC10-CMs were seeded into T25 flasks at a density of 1×10^6 cells/flask and the flasks incubated at 37°C, 5% CO_2 for 72 hrs to allow the cells to enter the plateau growth phase. Cells were then exposed to Colchicine or CA4 at a final concentration of 3, 30 or 300 nM or vehicle control (0.1% DMSO) and incubated at 37°C, 5% CO2. After a 24 hr or 96 hr incubation period, cells were detached (section 2.3) and analysed for their cell cycle profile by staining with propidium iodide and flow cytometric analyses (section 2-13).

2.14 Fluorescent imaging of cellular microtubules in AC10 cardiomyocyte cells.

Polymerised tubulin in live cells was visualised using Tubulin Tracker^{TM} Green (Invitrogen by Thermos Scientific, USA), analysed by confocal microscopy (Leica SPE point scanning confocal microscope,). All image acquisition is controlled via LasX software installed to the microscope. The reagent was prepared as per the manufacturer's instructions (Appendix 2). AC10 cells were seeded at a density 1×10^4 cell/well into each chamber of 4-chamber microscopy slides (Nunc, USA). Cell-loaded slides were incubated overnight at 37°C, 5% CO_2 to facilitate cell adhesion and stability. Cells were then exposed to Colchicine or CA4 at a final concentration of 3, 30 or 300 nM or vehicle control (0.1% DMSO) and incubated at 37°C, 5% CO_2. After a 24- hr incubation period, 0.5 mL Tubulin Tracker Green was added to each chamber of the microscope slide. Slides were incubated for 30 mins at 37°C, 5% CO_2, all media removed, and chambers washed three times with warm (37°C) PBS solution. To each chamber a 1 mL mounting medium was

applied and a coverslip added, reagents and reagents preparations are indicated in appendix 2. Slides were viewed immediately as staining intensity diminishes with time, with tubulin labelled by green fluorescence. .

2.15 Determination of VDA-induced changes in cell size of AC10 cardiomyocytes by manual measurement.

Paraformaldehyde (PFA) fixation method was used to measure changes in AC10 cell size following exposure to CA4. AC10 cells were seeded into wells of 6-well plates at a density of $4x10^3$ cells/well. Plates were incubated overnight at 37°C and 5% CO_2. The following day CA4 was added into the cell media at a final concentration of 0, 3, 30 or 300nM (final DMSO ≤0.1%) and the plates incubated at 37°C and 5% CO_2 for 24 hrs. All media was aspirated and each well of the plate washed with PBS then fixed using 0.5 ml of 4% Paraformaldehyde (PFA, diluted in PBS) at room temperature for 20 min, see appendix 1 for full details of PFA preparation. Cells were washed twice in PBS, then suspended in fresh PBS before visualising under an inverted microscope (Leica DIC DMI6000-B). Images were collected from at least five random fields and cell size determined using Image J software (Version 1.51d, National institute of Health, USA), counting a minimum of 50 cells per field. The experiment was performed in triplicate.

2.16 Evaluation of cardioprotective drugs to mitigate VDA-induced cardiotoxicity.

To identify whether co-administration of cardio-protecting agents would alleviate VDA-induced cardiotoxicity *in vitro*, the effects of the β-blocker (Carvedilol) or angiotensin targeting agents (Enalapril, Enalaprilat and Telmisartan) on viability of cardiac cell treated with VDAs was evaluated.

2.16.1 Evaluation of cytotoxicity of cardioprotective drugs.

AC10 cardiac cells or H460 NSCLC cell lines were plated in exponential phase at density of 2000 or 500 cells/well, respectively. Following incubation overnight at 37°C and 5% CO_2, media were removed and fresh media containing 10 µM to 0.01nM concentrations of the cardioprotective agents Carvedilol, Enalapril, Enalaprilat, Telmisartan or the drug vehicle (DMSO). In all cases, DMSO concentrations ≤0.1%. Compounds were left in contact with the cells for 96 hrs and cell viability determined using MTT assay (Section 2.8).

2.16.2 Evaluation of cardioprotective drugs to mitigate VDA-induced cardiotoxicity in AC10 cardiac cells.

AC10 Cardiomyocytes were seeded into 96-well plates for analyses of cells in exponential or plateau growth phases (as defined in section 2.10).

For pre-exposure studies, cells were exposed to either 1µM Enalapril, 1µM Enalaprilat, 200 nM Telmisartan or 200nM Carvedilol. Following incubation for 24 hrs at 37°C and 5% CO_2, media was removed and replaced with that containing the respective cardioprotective agent and either 0, 3, 30 or 300nM Colchicine, CA4 or drug vehicle (0.1% DMSO, final). For 24 hr exposure studies, all media was removed and replaced with fresh media after a further 24 hr incubation, whereas for 96 hr studies no media change was undertaken. Meanwhile drug dilutions were left in wells designated for investigation of 96hrs exposure. Cell viability was measured at 96 hrs post-addition of cardioprotective agents by MTT assay (Section 2.8).

To evaluate the ability of cardioprotective drugs to retard or reverse effects of VDAs, cells were exposed to 0, 3, 30 or 300nM Colchicine, CA4 or drug vehicle (0.1% DMSO, final) for 24 hrs at 37°C and 5% CO_2. For 24 hr exposure studies, all media was removed and replaced with fresh media containing either 1µM Enalapril, 1µM Enalaprilat, 200 nM Telmisartan or 200nM

Carvedilol. For 96 hr exposure studies, all media was removed and replaced with fresh media containing the respective VDA and either 1µM Enalapril, 1µM Enalaprilat, 200 nM Telmisartan or 200nM Carvedilol. Cell viability was measured at 96 hrs post-addition of VDAs by MTT assay (Section 2.8).

2.17 Analysis of Colchicine-induced gene changes related to cardiotoxicity in murine cardiac tissue

Changes in gene expression in response to drug treatment were assessed using quantitative real-time PCR (qRT-PCR) arrays targeted to a panel of toxicity pathway specific genes. These arrays provide both quantitative measurements of gene expression and multiple-gene profiling targeted to specific pathways. The PCR array used for this study was the RT^2 profiler™ mouse cardiotoxicity array (PAMM-095Z; SABiosciences, Qiagen, Germany), which contains analysis of 84 genes selected as being relevant to cardiotoxicity, 5 standard reference (housekeeping) genes, a genomic DNA negative control to detect non-transcribed genomic DNA contaminants, 3 reverse transcriptase gene positive control genes, and 3 internal gene-expression controls (Figure 2-2 and Table 2-2).

2.17.1 In vivo treatment protocol and collection of cardiac tissue.

Mice (Female Balb/c immunodeficient) (Harlan, Loughborough, UK), between the ages of 6 and 8 weeks, were injected intraperitoneally with either high-dose Colchicine (1.5 mg/kg), or solvent control (10% DMSO/saline). At 24 hrs post-treatment mice were sacrificed and whole hearts removed, snap frozen on liquid nitrogen and then stored at -80°C until RNA extraction.

Throughout the study, all mice were housed in air-conditioned rooms in facilities approved by the Home Office to meet all current regulations and standards of the United Kingdom. All

procedures were carried out under a United Kingdom Home Office Project License, following

UK National Cancer Research Institute Guidelines for the Welfare of Animals (UKCCCR)

guidelines.
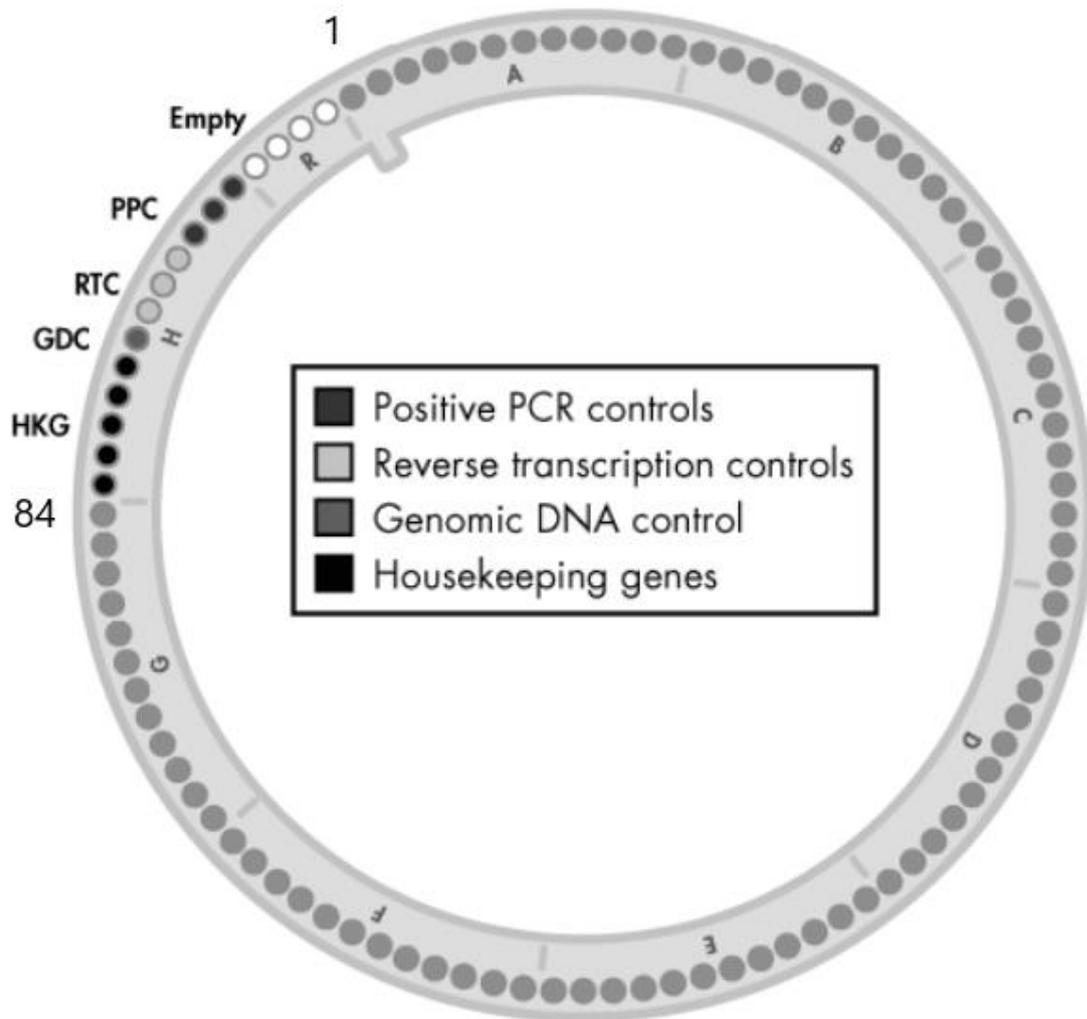
Figure 2-2: Image of RT² Profiler PCR Array.

Wells 1-84 contain genes for analysis, wells 85-89 contain the housekeeping gene panel (HKG) to normalize array data, well 90 contains a genomic DNA control (GDC), wells 91-93 contain replicate reverse-transcription controls (RTC), wells 94-96 contain replicate positive PCR controls (PPC) and wells 97 to 100 are empty.

Position	GenBank	Symbol	Description
A01	NM_018811	Abhd2	Abhydrolase domain containing 2
A02	NM_175456	Abra	Actin-binding Rho activating protein
A03	NM_009606	Acta1	Actin, alpha 1, skeletal muscle
A04	NM_007417	Adra2a	Adrenergic receptor, alpha 2a
A05	NM_012019	Aifm1	Apoptosis-inducing factor, mitochondrion-associated 1
A06	NM_021299	Ak3	Adenylate kinase 3
A07	NM_138679	Ash1l	Ash1 (absent, small, or homeotic)-like (Drosophila)
A08	NM_016755	Atp5j	ATP synthase, H+ transporting, mitochondrial F0 complex, subunit F
A09	NM_007532	Bcat1	Branched chain aminotransferase 1, cytosolic
A10	NM_007542	Bgn	Biglycan
A11	NM_007567	Bsn	Bassoon
A12	NM_007570	Btg2	B-cell translocation gene 2, anti-proliferative
B01	NM_013654	Ccl7	Chemokine (C-C motif) ligand 7
B02	NM_009912	Ccr1	Chemokine (C-C motif) receptor 1
B03	NM_009841	Cd14	CD14 antigen
B04	NM_013459	Cfd	Complement factor D (adipsin)
B05	NM_009890	Ch25h	Cholesterol 25-hydroxylase
B06	NM_007710	Ckm	Creatine kinase, muscle
B07	NM_009928	Col15a1	Collagen, type XV, alpha 1
B08	NM_009930	Col3a1	Collagen, type III, alpha 1
B09	NM_013498	Crem	CAMP responsive element modulator
B10	NM_009974	Csnk2a2	Casein kinase 2, alpha prime polypeptide
B11	NM_008748	Dusp8	Dual specificity phosphatase 8
B12	NM_007913	Egr1	Early growth response 1
C01	NM_010187	Fcgr2b	Fc receptor, IgG, low affinity IIb
C02	NM_010211	Fhl1	Four and a half LIM domains 1
C03	NM_010235	Fosl1	Fos-like antigen 1
C04	NM_010288	Gja1	Gap junction protein, alpha 1
C05	NM_153581	Gpm6a	Glycoprotein m6a
C06	NM_032541	Hamp	Hepcidin antimicrobial peptide
C07	NM_008301	Hspa2	Heat shock protein 2
C08	NM_013559	Hsph1	Heat shock 105kDa/110kDa protein 1
C09	NM_018854	Ift20	Intraflagellar transport 20 homolog
C10	NM_010518	Igfbp5	Insulin-like growth factor binding protein 5
C11	NM_031168	Il6	Interleukin 6

C12	NM_019923	Itpr2	Inositol 1,4,5-triphosphate receptor 2
D01	NM_001081087	Kbtbd10	Kelch repeat and BTB (POZ) domain containing 10
D02	NM_028202	Kbtbd5	Kelch repeat and BTB (POZ) domain containing 5
D03	NM_010603	Kcnj12	Potassium inwardly-rectifying channel, subfamily J, member 12
D04	NM_008567	Mcm6	Minichromosome maintenance deficient 6 (S.cerevisiae)
D05	NM_013602	Mt1	Metallothionein 1
D06	NM_199465	Nexn	Nexilin
D07	NM_008687	Nfib	Nuclear factor I/B
D08	NM_013743	Pdk4	Pyruvate dehydrogenase kinase, isoenzyme 4
D09	NM_178654	Pkn2	Protein kinase N2
D10	NM_008869	Pla2g4a	Phospholipase A2, group IVA (cytosolic, calcium-dependent)
D11	NM_008873	Plau	Plasminogen activator, urokinase
D12	NM_023129	Pln	Phospholamban
E01	NM_011126	Plunc	Palate, lung, and nasal epithelium associated
E02	NM_015784	Postn	Periostin, osteoblast specific factor
E03	NM_023785	Ppbp	Pro-platelet basic protein
E04	NM_133485	Ppp1r14c	Protein phosphatase 1, regulatory (inhibitor) subunit 14c
E05	NM_182997	Prkab2	Protein kinase, AMP-activated, beta 2 non-catalytic subunit
E06	NM_008944	Psma2	Proteasome (prosome, macropain) subunit, alpha type 2
E07	NM_010817	Psmd7	Proteasome (prosome, macropain) 26S subunit, non-ATPase, 7
E08	NM_030723	Pum2	Pumilio 2 (Drosophila)
E09	NM_027514	Pvr	Poliovirus receptor
E10	NM_016809	Rbm3	RNA binding motif protein 3
E11	NM_011036	Reg3b	Regenerating islet-derived 3 beta
E12	NM_172612	Rnd1	Rho family GTPase 1
F01	NM_028259	Rps6kb1	Ribosomal protein S6 kinase, polypeptide 1
F02	NM_010333	S1pr2	Sphingosine-1-phosphate receptor 2
F03	NM_008871	Serpine1	Serine (or cysteine) peptidase inhibitor, clade E, member 1
F04	NM_010831	Sik1	Salt inducible kinase 1
F05	NM_009208	Slc4a3	Solute carrier family 4 (anion exchanger), member 3
F06	NM_009238	Sox4	SRY-box containing gene 4
F07	NM_009263	Spp1	Secreted phosphoprotein 1
F08	NM_013685	Tcf4	Transcription factor 4
F09	NM_009367	Tgfb2	Transforming growth factor, beta 2
F10	NM_146153	Thrap3	Thyroid hormone receptor associated protein 3
F11	NM_009384	Tiam1	T-cell lymphoma invasion and metastasis 1

F12	NM_011593	Timp1	Tissue inhibitor of metalloproteinase 1
G01	NM_026473	Tubb6	Tubulin, beta 6
G02	NM_023719	Txnip	Thioredoxin interacting protein
G03	NM_025692	Uba5	Ubiquitin-like modifier activating enzyme 5
G04	NM_145441	Ubxn2a	UBX domain protein 2A
G05	NM_030724	Uck2	Uridine-cytidine kinase 2
G06	NM_009463	Ucp1	Uncoupling protein 1 (mitochondrial, proton carrier)
G07	NM_001081249	Can	Versican
G08	NM_009505	Vegfa	Vascular endothelial growth factor A
G09	NM_011701	Vim	Vimentin
G10	NM_145940	Wipi1	WD repeat domain, phosphoinositide interacting 1
G11	NM_011749	Zfp148	Zinc finger protein 148
G12	NM_175480	Zfp612	Zinc finger protein 612
H01	NM_007393	Actb	Actin, beta
H02	NM_009735	B2m	Beta-2 microglobulin
H03	NM_008084	Gapdh	Glyceraldehyde-3-phosphate dehydrogenase
H04	NM_010368	Gusb	Glucuronidase, beta
H05	NM_008302	Hsp90ab1	Heat shock protein 90 alpha (cytosolic), class B member 1
H06	SA_00106	MGDC	Mouse Genomic DNA Contamination
H07	SA_00104	RTC	Reverse Transcription Control
H08	SA_00104	RTC	Reverse Transcription Control
H09	SA_00104	RTC	Reverse Transcription Control
H10	SA_00103	PPC	Positive PCR Control
H11	SA_00103	PPC	Positive PCR Control
H12	SA_00103	PPC	Positive PCR Control

Table 2-2: Genes included on RT^2 profiler™ mouse cardiotoxicity array.

2.17.2 Isolation of RNA from murine cardiac tissue

Mouse hearts exposed to either Colchicine or drug vehicle were previously rinsed in PBS, snap frozen in liquid nitrogen and stored at -80°C. Heart tissue (circa 30 g) was roughly chopped and then ground to a powder under liquid nitrogen. RNA was extracted using the RNeasy mini kit, following the manufacturer's instructions (Qiagen, Germany). Briefly, ground cardiac tissue was resuspended in 600μL RLT buffer and homogenized using a QIAshredder spin column. RNA was precipitated from the lysate by addition of 350μL 70% ethanol. The RNA was isolated from the sample using a RNeasy spin column and then on column DNA digestion performed using an RNase-Free DNase set, by washing in RW1 buffer, digestion of DNA using RDD buffer and DNase I for 15 mins, and a final wash in RW1 and RPE buffers to remove unwanted biomolecules and salts. RNA was eluted by addition of RNase free water and centrifugation of the column. RNA was stored at -80 °C.

The quality and concentration of RNA in the samples was determined using the NanoDrop 2000c (Thermo Scientific, USA), analysing 1μL RNA sample relative to an RNase free water blank. Concentration of RNA in the samples was recorded, with a 260:280 absorbance ratio of greater than 1.8 confirming RNA quality. To prevent degradation, purified RNA was stored at -80°C.

2.17.3 Synthesis and amplification of cDNA

First strand cDNA was produced from total RNA using the RT^2 PreAMP cDNA synthesis kit, according to manufacturer's instructions (Qiagen, Germany)(Qiagen., 2014). Briefly, 100ng RNA was combined with genomic elimination (GE) buffer and RNase-free water to a volume of 10μL and incubated at 42°C for 5 minutes before immediate transfer to wet ice. To this solution, 4μL Buffer BC3, 1μL Control P2, 1μL cDNA Synthesis Enzyme Mix, 1μL RNase inhibitor and 3μL

RNase-free water were added before incubation at 42°C for 30 minutes. The reaction was halted by incubation at 95°C for 5 minutes.

Pre-amplification of cDNA was conducted using the RT^2 PreAMP cDNA Synthesis Kit (Qiagen), as per manufacturer's instructions. To 5 µL of cDNA synthesis reaction product, 12.5 µL of RT^2 PreAMP PCR master mix and 7.5 µL RT^2 PreAMP pathway primer mix were added. The pre-amplification reactions were carried out using a thermocycler (Prime, Fischer Scientific, UK) using the following cycling conditions (Table 2-3):

Step	Temperature	Duration	Cycles
Initial denaturation	95˚C	10 minutes	One cycle
Denaturation	95˚C	15 seconds	12 cycles
Extension	60˚C	2 minutes	
Hold	4˚ C	-	-

Table 2-3: Cycling conditions for the PCR required for cDNA pre-amplification.

After completion of the pre-amplification reaction, 2 µL of side reaction reducer (Qiagen) was added, incubated at 37˚C for 15 minutes and then heat inactivated at 95˚C for 5 minutes. The volume of reaction was then adjusted to a final amount of 111 µL through addition of RNase-free water and the cDNA stored at -20°C until required.

2.17.4 Verification of cDNA quality prior to the RT² Profiler™ PCR Array

Quality of the cDNA was ascertained by investigating the expression of the GAPDH house-keeping gene using semi-quantitative reverse-transcriptase PCR (RT-PCR). A PCR amplification mixture was created containing 10µL Taq MM (x2; New England Biolabs) 0.2µL GAPDH forward primer (5'-CCACCCATGGCAAATTCCATGGCA-3'), 0.2µL GAPDH reverse primer (5'-

TCTAGACGGCAGGTCAGGTCCACC-3') (Invitrogen, UK), 2µL cDNA and 7.6µL RNase-free water. RT- PCR was then carried out using a thermocycler (Prime, Fischer Scientific, UK) on the samples using the following cycling conditions (Table 2-4).

The PCR products were analysed by separation through a 1% (w/v) agarose gel, containing 0.01% ethidium bromide. Samples were combined with 10% loading dye (30% glycerol, 0.25% bromophenol blue) to allow sample visualisation and loaded into the gel alongside a DNA ladder (QuickLoad 100bp DNA ladder, New England Biolabs). Electrophoresis was performed in Tris-Acetate EDTA buffer (TAE; 40mM Tris, 20mM acetic acid and 1mM EDTA) at 100V for approximately 1 hr. The gel was viewed using a ChemiDoc MP System (BioRad, UK) and ImageLab software (BioRad, UK). The expected PCR product size was 598bp, cDNA quality was deemed suitable if discrete bands of comparable intensity were observed.

Step	Temperature	Duration	Cycles
DNA denaturation and polymerase activation	94 ˚C	5 minutes	One cycle
Denaturation	94 ˚C	30 seconds	30 cycles
Primer annealing	60 ˚C	30 seconds	
Extension	68 ˚C	90 seconds	
Final Extension	68 ˚C	10 min	One cycle

Table 2-4: Cycling conditions for the PCR required for verification of cDNA quality.

2.17.5 Real-time PCR of gene expression arrays

The qRT-PCR protocol and methodology was as per the manufacturer's protocol (Qiagen., 2011). A reaction mixture was produced by combination of the following: 102µL test cDNA, 1048µL RNase-free water and 1150µL SYBR Green ROX FAST 2x mastermix (Qiagen, Germany).

To each well within the array of the gene array, 20µL of the PCR component mix was added. The RT^2 Profiler PCR Array plate was sealed and inserted into the Rotor-Gene instrument (Qiagen, Germany). The template for the RT^2 Rotor-Gene mouse cardiotoxicity array was loaded into the Rotor-Gene Q software (V2.0) and the programme initiated. After the qRT-PCR run, the baseline was automatically defined and the threshold cycle value (CT) determined for each well. Changes in gene expression for drug vehicle and Colchicine treated cDNA samples were analysed using the SABiosciences data analysis web software. Data was normalised against the reference (housekeeping) gene panel on the qRT-PCR array, with the resulting CT values used to calculate normalized gene expression ($\Delta\Delta$CT) expressed as fold change. A fold change value >1 indicates an up regulation and fold change values <1 indicate down regulation.

Chapter 3. Characterisation and qualification of in vitro models for evaluation of drug-induced cardiotoxicity of Vascular Disrupting Agents (VDAs)

3.1 Preclinical Assessment of cardiac liabilities during drug development

Cardiotoxicity is a leading cause of drug attrition and withdrawal, responsible for more than a third of safety related drug withdrawals (Siramshetty et al., 2016). The current method of preclinical assessment of drug-induced cardiac liabilities is outlined by the ICH-S7B guidelines (ICH, 2005b). These guidelines focus predominantly on drug-induced functional cardiac disturbances by assessment of the ability of compounds to block cardiac potassium currents, disregulate ventricular repolarisation, prolong the QT-interval and induce cardiac proarrhythmias (ICH, 2005b). It is estimated that up to 60% of drugs during development were deemed positive using the initial in vitro screening approach defined in these guidelines, resulting in cessation of their further development (Gintant et al., 2016, Poluzzi et al., 2017). However, in many cases, despite being identified as exhibiting cardiac liabilities it is now believed that the risk of many of these drugs in the clinic exhibiting cardiac liabilities is significantly lower due to simplicity of the initial screen compared to the relative complexity of the cardiac system *in vivo*. Additionally, blockade of non-potassium channels, which do not lead to QT prolongation, but still induce proarrhythmias further complicates this screening paradigm (Gintant et al., 2016). Similarly, the effect of drugs upon other mechanisms known to cause cardiac functional disturbances including perturbation of signalling pathways relating to cardiac homeostasis, function and survival is a further complexity (Killeen, 2012). Consequently, these factors alongside concern regarding impacts of species differences in screening for drug-induced functional cardiac disturbances have now led to the development of a new screening paradigm, the Comprehensive in vitro Proarrhythmia Assay (CiPA)(Sager et al., 2014). The CiPA defines proarrhythmic risk based on an integrated assessment of drug effects on multiple ion channels, involving in silico predictions of electrophysiological

disturbances, alongside evaluation in human stem-cell derived cardiomyocytes (hSC-CMs) *in vitro* (Sager et al., 2014, Colatsky et al., 2016). Ultimately this approach provides a more robust assessment of drug-induced cardiac functional liabilities, thereby improving predictability of cardiac liabilities.

In parallel with drugs perturbing cardiac functional regulation and causing proarrhythmias, drug effects upon cardiac structure and subsequent drug-induced cardiomyopathies are also now known to be a major driver of drug-induced cardiotoxicity (Higgins et al., 2015, Zamorano et al., 2016, Michel et al., 2019). These effects can manifest as a change in cardiac cellular composition through induction of cardiac loss or damage, with consequent cardiac remodelling, or modification of subcellular architecture and composition leading to changes in cellular morphology and contractility (Pointon et al., 2013, Doherty et al., 2015). However, unlike drug-induced functional cardiotoxicity, preclinical evaluation of drug-induced structural cardiac liabilities is currently not evaluated *in vitro* and is only identified upon specific interrogation of *ex vivo* tissues or *in vivo* animal studies.

Despite several advances being made in the preclinical prediction of drug-induced cardiotoxicity, specifically functional effects, issues still persist in this regard. The use of human stem-cell derived cardiomyocytes (hSC-CMs) for functional studies are costly and restricted by limited longevity of cultures *in vitro*. In terms of evaluation of drug-induced structural cardiac effects, no standardised methodology is currently applied and the use of *ex vivo* and *in vivo* approaches often have limited translation to humans due to differences in electrophysiology and cardiac composition. As such, there is an urgent need for better preclinical models that are able to accurately capture information on a compound's ability to cause both functional and structural cardiotoxicity.

3.1.1 Preclinical evaluation of cardiac effects during development of oncology drugs

In contrast to development of 'conventional' drugs, a degree of toxicity risk is generally accepted during the development of cytotoxic and cytostatic oncology drugs. By definition these agents do not have a safety margin and therefore must be screened using a paradigm focused on mechanism of action and monitorability, as defined in the ICHS9 guidelines (ICH, 2009). Such a strategy aims to identify cardiovascular side effects during discovery and identify and mitigate the occurrence of undesirable cardiovascular toxicities in oncology drug development.

Furthermore, in addition to measurement of drug-induced proarrhythmia induced during and directly after initiation of oncology treatment, many of these drugs are now known to also cause latter chronic forms of toxicity including pathological cardiac changes (Curigliano et al., 2016, Ewer and Ewer, 2010). Moreover, since chronic progressive cardiomyopathies are now a major concern for clinical use of cancer drugs, there is a need to build upon our improved understanding of mechanisms of drug-induced cardiotoxicity to explore and predict long-term effects of many anticancer therapeutics(Laverty et al., 2011).

In light of the inherent cardiac risks of treatment with cancer therapeutics and the increasingly sensitive patient population, as with other drug classes, improved screening paradigms are also required for the development of oncology drugs. Consequently, cardiac liabilities need to be addressed concurrently with risk-benefit analyses, considering the specifics of the indication and the drug. By identifying cardiovascular toxicities and their mechanistic basis the objective is to therefore be able to better manage or prevent these adverse effects in the clinic, increasing the chance of success for much-needed novel therapeutics to address unmet clinical needs.

One class of cancer therapeutic with potential impact for improving cancer outcomes of solid cancers are the vascular disrupting agents (VDAs). These therapeutics target tubulin within immature endothelial cells associated with tumour vasculature resulting in their collapse and induction of subsequent tumour cell death (Gill et al., 2019). However, despite exhibiting significant potential, it is becoming increasingly apparent that the therapeutic value for these Colchicine-related VDAs is compromised by their intrinsic toxicity, including cardiac toxicities (Hinnen and Eskens, 2007, Ho et al., 2017, Siemann et al., 2009, Subbiah et al., 2011, Chase et al., 2017). Consequently, studies are required to identify and qualify both the extent of toxicity and responsible molecular mechanisms for this class of drug.

3.2 Preclinical *in vitro* models for evaluation of drug-induced cardiac effects

The identification of potential for drug-induced proarrhythmia s, as outlined in the ICH S7B guidelines, currently still involves assessment against a non-cardiac cell line expressing a specific potassium ion channel (hERG channel), although this is likely to be superseded by the guidelines outlined by the CiPA initiative. However, these guidelines focus specifically upon perturbations in cardiac electrophysiology and function and do not as yet encompass evaluation of wider drug-induced functional or structural effects (Colatsky et al., 2016, Sager et al., 2014, ICH, 2005a). For this purpose, models representative of cardiac cells, that are both clinically and physiologically relevant are required.

The preclinical identification of potential for drug-induced cardiac liabilities has historically been limited by a lack of these *in vitro* cardiac models *i.e.*, human derived cells that exhibit a cardiac phenotype. The immortalised rat cardiomyoblast H9c2 cell line has been used assess cardiac biology studies but is hampered by the fact it is non-human, morphologically distinct

from cardiomyocytes, without relevant contractile proteins and ion channels, and has no contractile capacity. Similarly, the HL-1 murine atrial cardiomyocyte cell line, despite expressing relevant ion channels, organised sarcomeric structure and exhibiting transient contractile ability, is also non-human and is beset by differences in structure and biochemical activity (Claycomb et al., 1998, Watkins et al., 2011). Consequently, human-derived cardiac models with applicable molecular and physiological profiles are required to better address human drug safety and facilitate clearer translation between preclinical and clinical studies. Such models are essential for detection of drug effects upon cardiac cells, including both structural and functional changes. For this purpose, primary human cardiomyocytes were initially investigated as a 'gold-standard' to address these requirements. However, the use of these cells was shown to be unfeasible for regular and routine preclinical cardiac assessments, including a requirement for special growth conditions, an extremely short culture period before de-differentiation or loss of function, relative lack of cellular purity, and ultimately lack of clonal homogeneity and limitations in sufficient supply (Li et al., 1996). Therefore, more practical, reliable, reproducible, and cost-effective models with the ability to monitor drug effects in a cardiac and physiological relevant manner, and with capability for longer-term assessment are required.

3.2.1 The AC10 human ventricular cardiomyocyte cell line

The AC10 cell line is a proliferative human cardiomyocyte cell line derived from non-proliferative primary adult ventricular cardiac tissue (Davidson et al. 2005). This cell line was created by fusing adult human ventricular cardiomyocytes with fibroblasts transformed with SV40 and devoid of mitochondrial DNA, which also created the similar AC1, AC12 and AC16 cell lines (Davidson et al., 2005). Induction of differentiation in these cell lines results in a loss

of cellular proliferation and formation of a multinucleated syncytium (Davidson et al., 2005). The development of this differentiated cell state in the AC10 and analogous cell lines is facilitated by either growth in mitogen-depleted media, via inhibition of DNA synthesis by exposure to 5-aza cytidine and cytosine arabinoside, or via silencing of the SV40 transformation factor (Davidson et al., 2005). The AC10 cardiomyocyte cell line, as well as the other sibling AC cell lines, has the distinct advantage over both Hc92 and HL-1 cell lines in that it is human derived, and despite being in a pre-contractile state, expresses many cardiac specific transcription factors, contractile proteins and possesses functional gap junctions (Davidson et al., 2005). Although immortalised and thus useful for longer-term and comparative studies of human drug-induced toxicities, the major limitation in the use of this cell line is its lack of contractility, supporting its applicability for structural but not functional contractile studies.

3.2.2 Human stem cell derived cardiomyocytes.

In 2006, Takahashi and Yamanaka demonstrated that somatic cells could be reprogrammed into pluripotent stem cells (Takahashi and Yamanaka, 2006). Following this, a process to differentiate these pluripotent cells into functional human cardiomyocytes was developed (Laflamme et al., 2007). This revolutionised the *in vitro* assessment of cardiomyocyte physiology and functional activity.

Many advances have now been made and the field has now progressed from embryonic stem cells (ESC-CMs) to human induced pluripotent stem cell derived cardiomyocytes (hiPSC-CMs). This has opened the field and many technologies have now been aligned to these cells, providing a resolution to assessment of drug-induced functional changes in cardiomyocytes, as they spontaneously contract *in vitro*, and are human in nature. These cells exhibit the

complex nature of cardiomyocyte electrophysiology and cardiac cell function and therefore have significant advances over previous cardiac cell models, particularly in assessment of drug-induced proarrhythmia s detection (Braam et al., 2010, Laflamme et al., 2007). Based on this, hiPSC-CMs are integrated into the CiPA screening paradigm (Gintant et al., 2016).

Although iPSC-CMs possess many favourable features, a number of limitations associated with this model persist, particularly in relation to their immature phenotype, electrophysiological differences and suitability for assessment of drug-induced structural cardiotoxicities. Despite these issues, this cell model is still considered more functionally relevant than other *in vitro* cardiac cell models, such as the rodent cell lines Hc92 and HL-1, and the non-contractile human AC10 or AC16 cell lines (Garg et al., 2018, Magdy et al., 2018). However, despite hiPSC-CMS showing worth for functional studies *in vitro*, their utility for longer-term and molecular studies are limited by their lack of immortality, inhibitive costs, and complex culture methods.

In the context of limitations of hiPSC-CMs, there is thus an advantage to the use of cell lines, such as AC10 and AC16, due to their scalability, relatively low maintenance costs, and improved capacity for analyses of molecular and subcellular changes, particularly detection of sub-acute and structural cardiotoxicities.

3.3 Aims and Objectives.

In order to qualify their use for *in vitro* screening, this chapter aims to determine the suitability of AC10 cardiomyocyte cell line for detection of structural cardiotoxicity, specifically in the assessment of vascular disrupting agents (VDAs).

The objectives are as follows:

1) Characterise *in vitro* growth characteristics and parameters of the AC10 cell line for utility as a model for structural cardiotoxicities.

2) Evaluate the responses of AC10 cells to the VDA class of chemotherapeutic agent, specifically Colchicine and combretastatin A4, *in vitro*

3) Evaluation of the differential effects of VDAs on viability of H460 lung cancer cells. In order to identify the therapeutic index of these drugs between cancer cells and cardiac cells, it is important to evaluate the IC_{50} values in cancer cells and compare it to IC_{50} values in cardiac cells.

3.4 Results.

The purpose of this phase of the project was to determine the suitability of the AC10 cardiomyocyte cell line for detection of structural and functional cardiotoxicity, specifically in the assessment of vascular disrupting agents (VDAs). Following characterisation of growth kinetics, cytotoxicity evaluations of VDAs were conducted to appraise concentration-response relationships.

3.4.1 Confirmation of cardiac phenotype of AC10 cardiomyocyte cell line.

To confirm the cardiac phenotype of the AC10 cell line and thus its suitability for characterisation of drug-induced cardiotoxicity, cells were characterised by immunostaining for expression of specific cardiac proteins (section 2.7).

The cell line was confirmed to express the cardiac contractile proteins troponin I, troponin C, tropomyosin and α actinin (Figure 3-1). Additionally, AC10 cells were also shown to express the cardiac specific transcription factor NKX2.5, the cardiac differentiation marker bone morphogenetic protein 2 (BMP-2) and the mesenchymal specific protein vimentin (Figure 3-1). The proliferative capacity of the cells was confirmed by their expression of both pericentriola material 1 (PCM1) and Ki-67, along with that and vascular protein was identified (Figure1-4). A lack of expression of α-smooth muscle actin, a predominant marker of vascular muscle as opposed to cardiac muscle, was also noted (Figure 3-1).
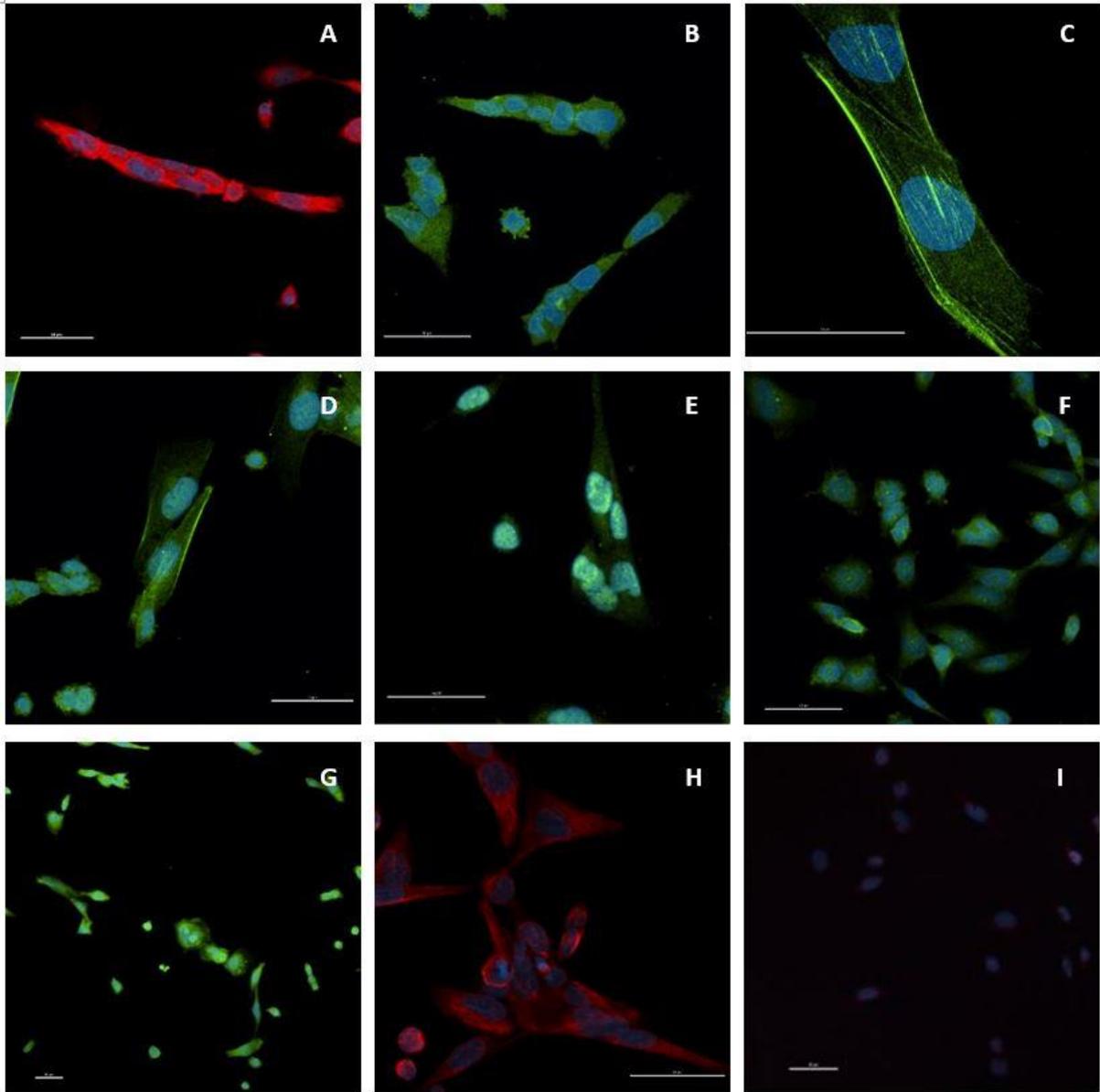
Figure 3-1: Immunostaining of AC10 cell line for cardiac proteins.

AC10 cells were shown to express cardiac cell markers: Troponin-I (A); Troponin-C (B); Tropomyosin (C and D); α actinin (E); BMP-2 (F); NKX2.5 (G) and Mesenchymal vimentin (H). AC10 does not express α smooth muscle actin (I). Images are at either x40 or x10 with a magnification bar representing 50µm. Proteins of interest are stained red or green, nuclei are stained blue with DAPI.
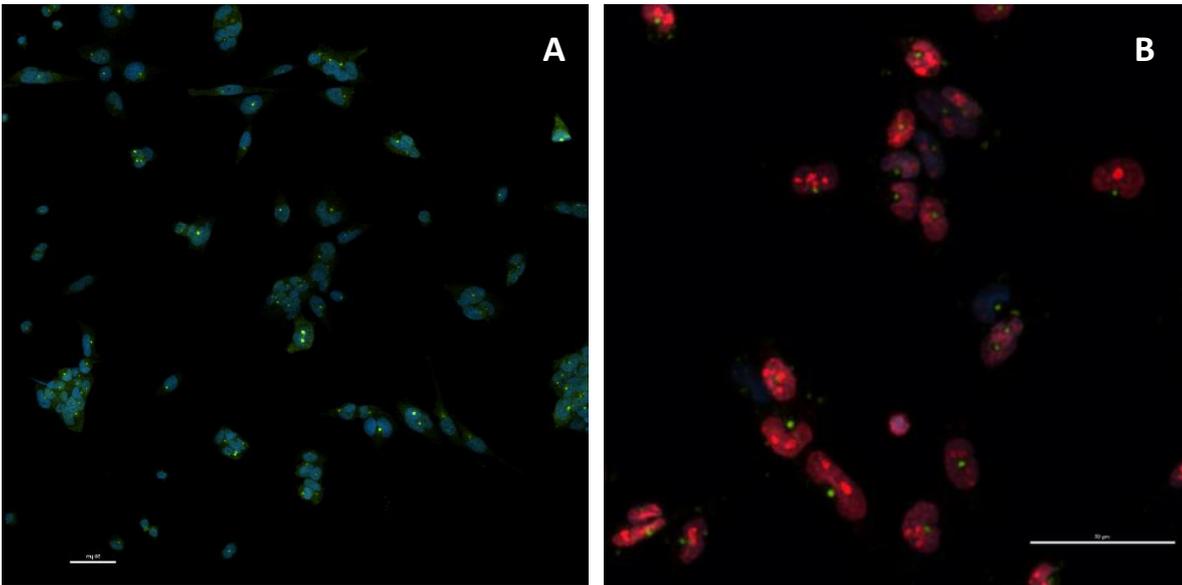
Figure 3-2: Positive immunostaining of AC10 cell line for proliferative markers.

(A) PCM1 and (B) Ki-67+ PCM1. Images are at either x10 with a magnification bar representing 50µm. Proteins of interest are stained red or green, nuclei are stained blue with DAPI.

3.4.2 Characterisation of in vitro AC10 cell growth kinetics.

AC10 cells were plated at a density of 2×10^5 cells/flask (8×10^3 cells/cm^2) into 25cm^2 flasks and the number of cells per day over a 10-day period determined by trypsinisation of attached cells and haemocytometer counting (section 2.3). Cell growth curves were constructed (Figure 3-3) with the lag phase of growth between 0- 24 hrs, exponential growth phase from 24-120 hrs and plateau growth phase > 120 hrs post-seeding. Cell doubling time during exponential growth was calculated as 25 hrs (Figure 3-4). For studies to evaluate drug effects during exponential cell growth, in culture flasks, a seeding density of 50 $\times 10^4$ cells/25cm^2 flask (equating to 2×10^4 cells/ cm^2).
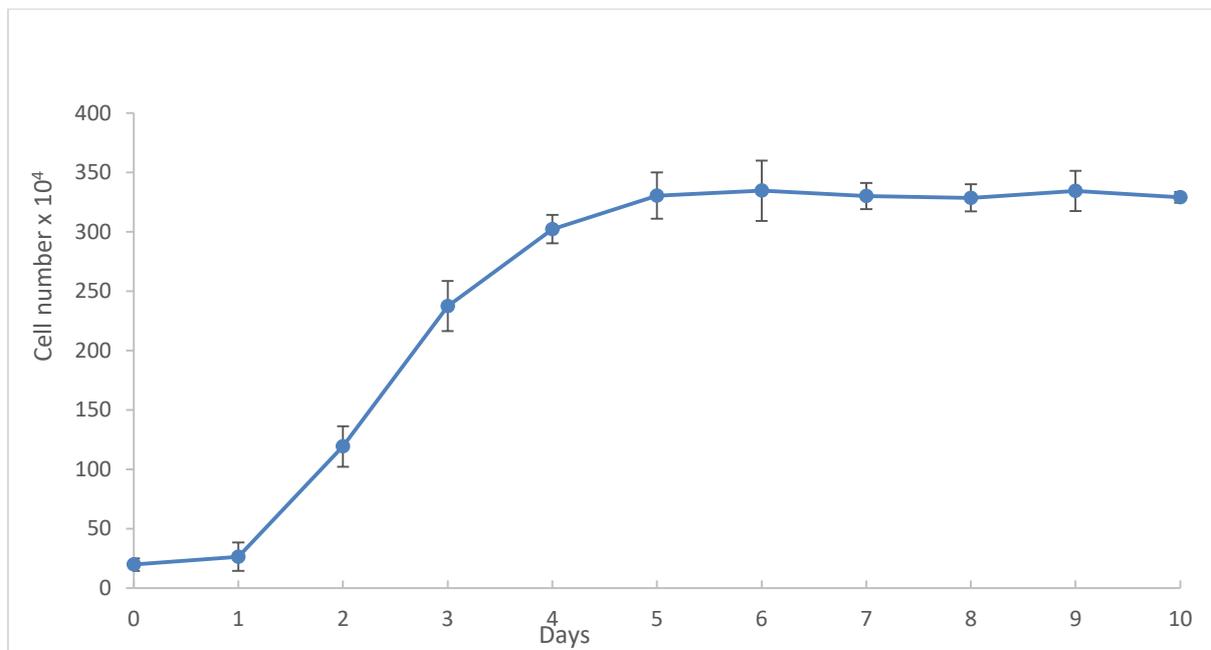
Figure 3-3: Growth Kinetics of AC10 cells *in vitro* determined by manual cell counting.

Cell number per 25cm^2 flask over time following a seeding density of 2×10^5 cells/ 25cm^2 flask. Data is a mean of three independent experiments with values expressed ± SEM.
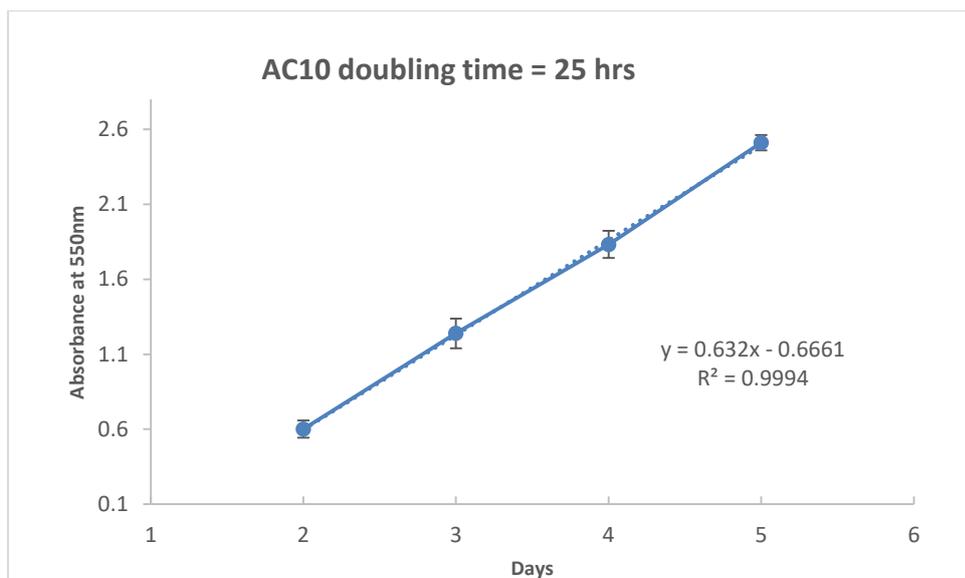
Figure 3-4: Determination of exponential doubling rate for AC10 cells measured by MTT assay.

Time against absorbance at 550nm for a seeding density of 2000 cells/well. Data points show average values ±SEM.

3.4.3 Qualification of MTT assay for evaluation of growth kinetics of AC10 cell line

To validate the MTT assay as a reliable method for quantifying viable cell number, a relationship between cell number, determined manually, and MTT conversion via quantification of absorbance at 550nm was conducted. Figure 3-5 shows a linear relationship between AC10 cell number and absorbance, exemplified by an R^2 value of 0.993.
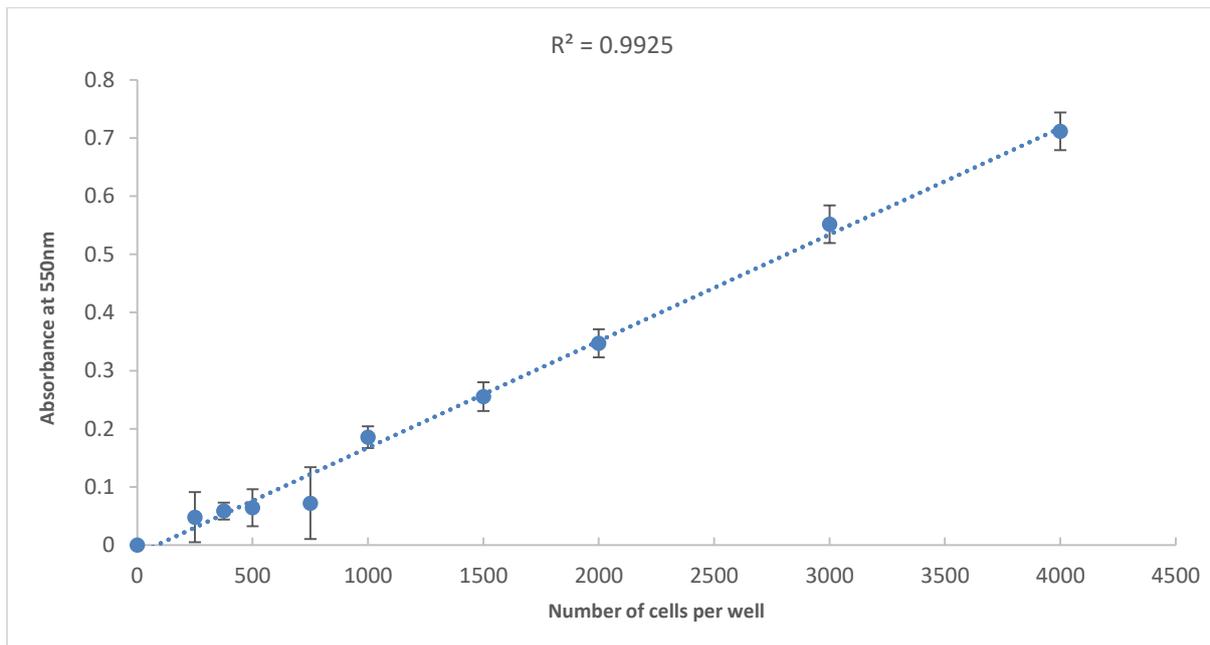
Figure 3-5: Qualification of MTT assay for determination of viable cell number.

Cell number versus absorbance at 550nm of AC10 cells at different densities determined 24 hrs post-seeding. Data is a mean of three independent experiments and values ± SEM; R^2= 0.99

3.4.4 Measurement of growth kinetics of AC10 cells using the MTT assay.

The MTT assay was used to determine growth kinetics of the AC10 cell line. The MTT based growth curve analyses for AC10 cells were conducted across a five-day period at a range of cell densities (1000, 2000, 10,000 and 20,000 cells/well), with the increase in cell number for each seeding density was calculated using the MTT assay (described in section 2.8). Growth curves were constructed to identify cell growth kinetics and optimal seeding densities for subsequent studies.

Over the time course of five days, the lowest concentration of 1000 cells per well demonstrated a slow growth rate and an extended lag phase. Conversely, the highest concentration of 10,000 and 20,000 cells/well showed a much greater rate of proliferation devoid of a lag phase of cell growth, with cells reaching a plateau growth phase at approximately 72 hrs. In contrast, cells seeded at an initial density of 2,000 cells/well demonstrated a defined short lag phase, with exponential growth beginning after 1 day and continuing across the five-day assessment period (Figure 3-6). Subsequently, a seeding density of 2000 cells/well (equating to 6.4×10^3 cells/cm^2) was chosen for cellular studies utilising the MTT assay for assessment of effects upon cells in the exponential growth phase. Further supplementary data are provided in appendix 4.

To determine the optimal seeding density for AC10 cells to achieve in entry into the plateau growth phase within 24 hrs, as determined by MTT assay, cells were initially seeded at densities between 10,000 and 60,000 cells/well. Analysis of the resultant absorbance of the MTT assay revealed this to be relatively stable within 24 hrs at cell densities ≥30,000 cells (Figure 3-7)A seeding density of 40,000 cells/well (equating to 12.5×10^3 cell/cm^2) was therefore identified as optimal for obtaining cells within the plateau growth phase by 24 hrs.
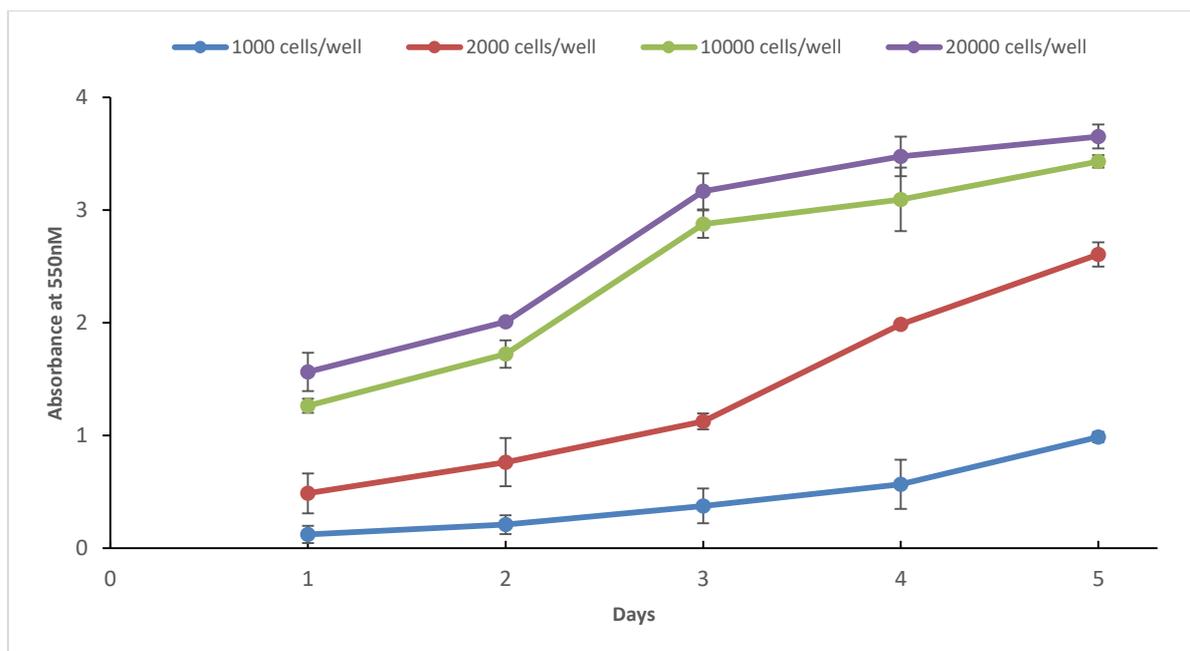
Figure 3-6: Optimisation of AC10 seeding density for MTT studies in exponential growth phase.

Cells plated at different densities and monitored over a period of five days. Experiment performed in triplicate and values are mean ± SEM.
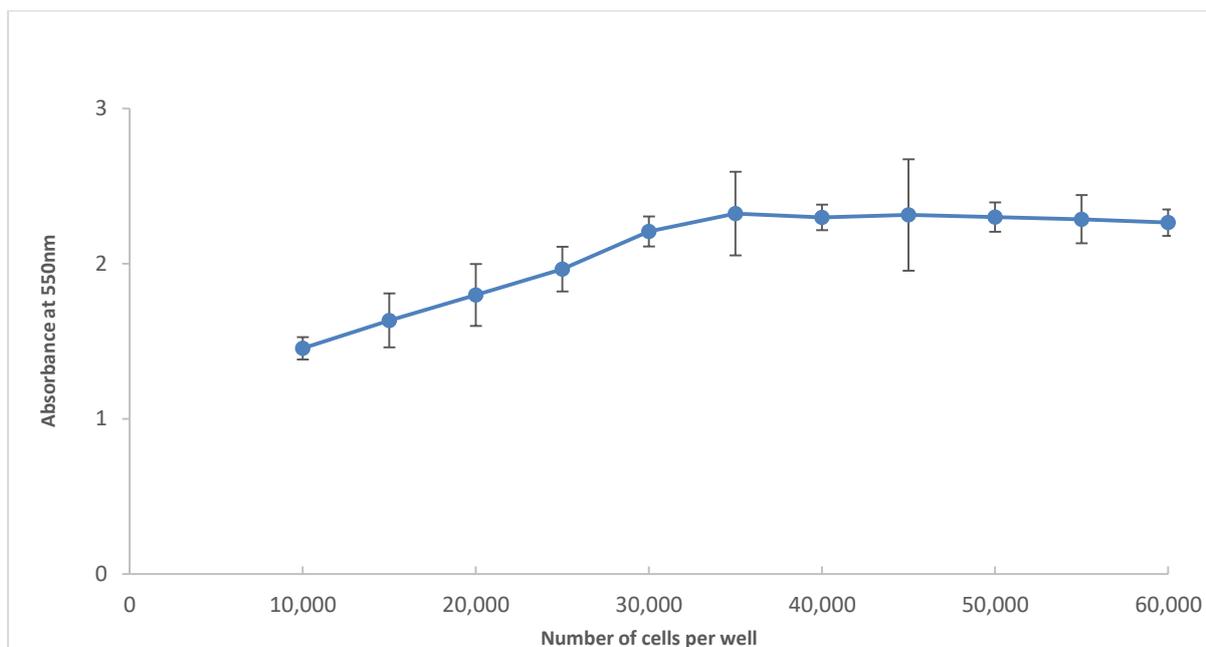
Figure 3-7: Optimisation of AC10 cell seeding density to evaluate cells in the plateau phase of growth measured by MTT assay.

AC10 cell number against absorbance at 550nm for various initial plating densities. Data points show mean values ± SEM.

3.4.5 Measurement of cellular growth and behaviour using the xCELLigence real time cell analyser.

The xCELLigence RTCA was used to assess the proliferation and behaviour of AC10 cells in real-time. This methodology has the benefit of determining both a more specific time-period for drug exposure and monitoring cellular response in real-time. Therefore, defining the appropriate plating cell density for xCELLigence assessment for optimal experimental evaluation was required.

The AC10 cells are strongly adherent proliferative cells, and thus suitable for this assay. Cells were plated and analysed using the methodology as described, using 2-fold serial dilutions to produce cell densities from $6.25x10^2$-$4x10^4$ cells/well (equating to $3.1x10^3$ to $2x10^5$ cells/cm^2) and their growth rate monitored using the xCELLigence RTCA DP Instrument. Cellular growth was determined by plotting corrected cell index against time. Cells plated at the lowest density of 625 cells /well showed a long lag time, requiring almost 60 hrs to reach exponential phase of growth. The highest densities of $\geq5x10^3$ cells/well either did not exhibit lag phase of growth or exhibited a very short lag phase and therefore were unacceptable for drug studies due to the fact that insufficient time for cell adherence would be possible prior to drug exposure. The optimal plating density of AC10 for studies during exponential growth phase was identified as $1.25x10^3$ ($6.25x10^3$ cells/cm^2) to $2.5x10^3$ cells/well ($12.5x10^3$ cells/cm^2) of E-plate. Therefore the approximate average density of $2x10^3$ cells/well ($1x10^4$ cells/cm^2) thus was chosen with a steady exponential growth phase, plateauing at around 120 hrs after seeding (Figure 3-8). Plating at this density allows a 24hr incubation period prior to drug addition, to facilitate cellular adherence and entry of cells into a proliferative state. For studies focused on AC10 cells in the plateau phase of growth, cells were seeded at $1 x10^4$ cell/well ($5x10^4$ cells/cm^2) and incubated for 72 hrs to attach and reach confluence within the well.
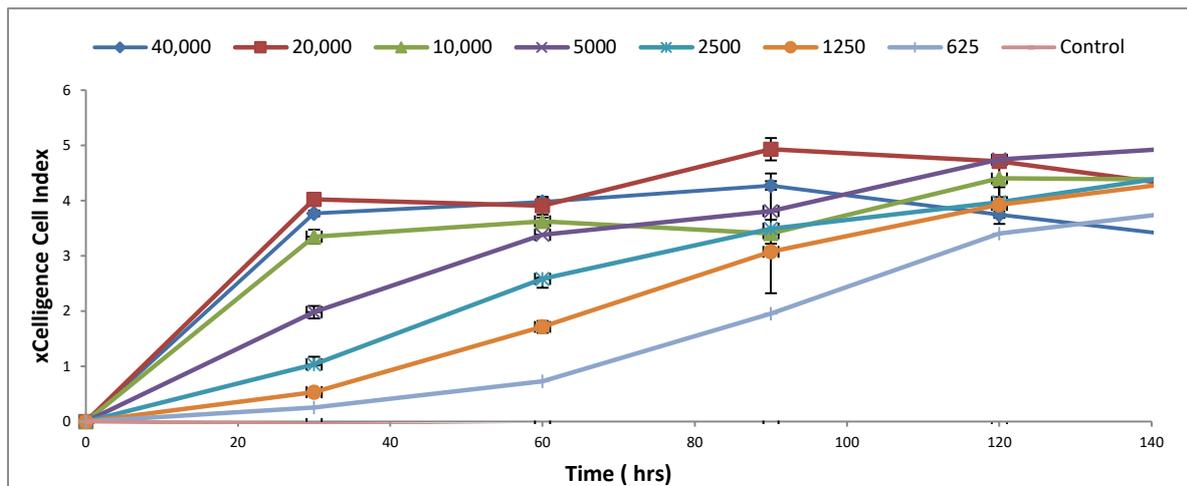
Figure 3-8: AC10 growth kinetics measured by xCELLigence RTCA system.

Traces showing time (hrs) versus xCELLigence cell index for AC10 cells plated at a range of densities. The values penned in the legends are representing the number of cells/well. Data represents the mean cell index values from three different experiments ± SEM.

3.4.6 Evaluation of cytotoxicity of VDAs in the AC10 cardiac cell line.

The effects of Colchicine and CA4P were evaluated using the MTT viability assay. Cells were continually exposed to the drugs for either 24 or 96 hrs prior to evaluation of cellular viability and survival. The drug response curves and values of IC_{50} after treating exponential or plateaued AC10 cell lines with Colchicine and CA4P either continuously for 96 hrs, or for 24 hrs followed by 48 hr 'recovery' are shown below. The viability of AC10 was evaluated to Colchicine (Figure 3-9) and CA4 (Figure 3-10) in both exponential and plateau phase. The value of IC_{50} was lower when cells were in exponential phase of growth, indicating that proliferative AC10 were more sensitive to VDAs than AC10 in plateau phase (Table 3-1).

Toxicity of VDAs was increased in response to prolonged exposure (96 hrs) of AC10 to treatment in both exponential and plateau phases of growth, indicative of a relationship between exposure and detrimental effects. In exponential phase growth, the IC_{50} values at 24 hr (plus 48 hr recovery) and 96- hrs exposure, respectively are 45.8 ± 2.9 nM and 31.5 ± 1.2 nM for Colchicine treated cells, and 7.5 ± 0.7 nM and 4.5 ± 1 nM for CA4 treated cells. In comparison, IC_{50} values at 24- and 96- hrs exposure, respectively for AC10 at plateau phase of growth are 53.5 ± 3.5 nM and 41.6 ± 1.9 nM for Colchicine treated cells, and 20.5 ± 0.9 nM and 12.8 ± 0.9 nM for CA4 treated cells (Table 3-1).
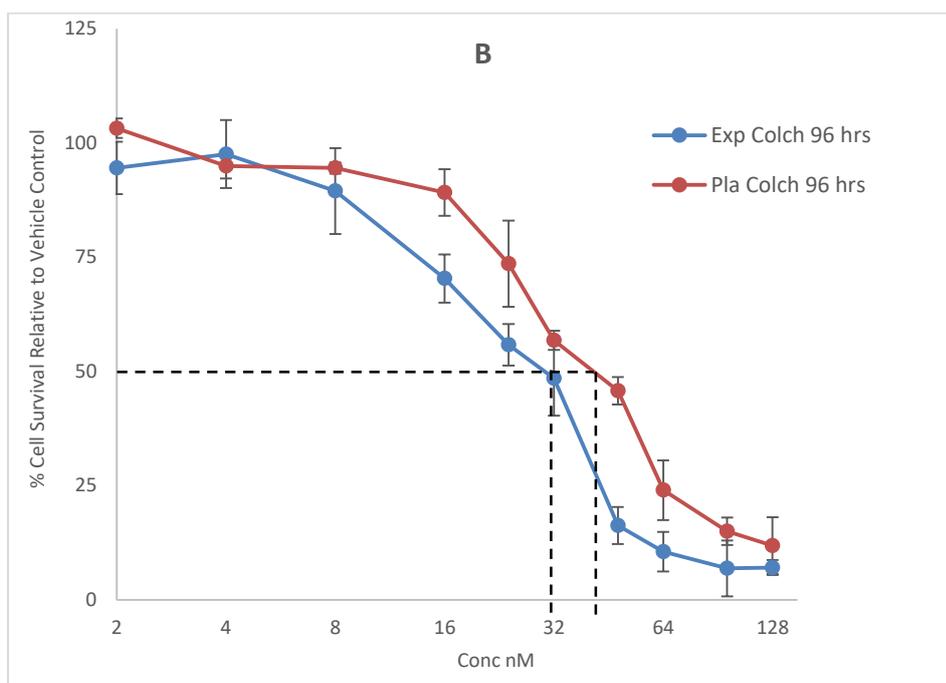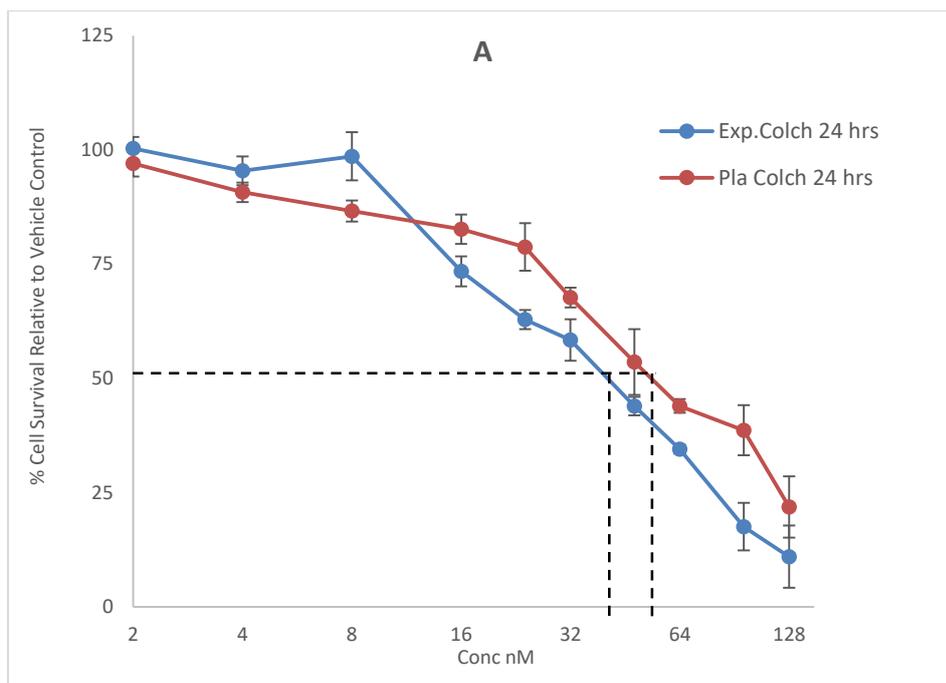
Figure 3-9: Effect of Colchicine on viability of AC10.

Dose response curves showing the effects of Colchicine on viability of AC10 in both exponential and plateau phase of growth after 24 hrs with 48 hr recovery (A) and 96- hr continuous exposure (B). Data are expressed as % cell survival relative to vehicle control, data is representative of n=3 ± SEM.
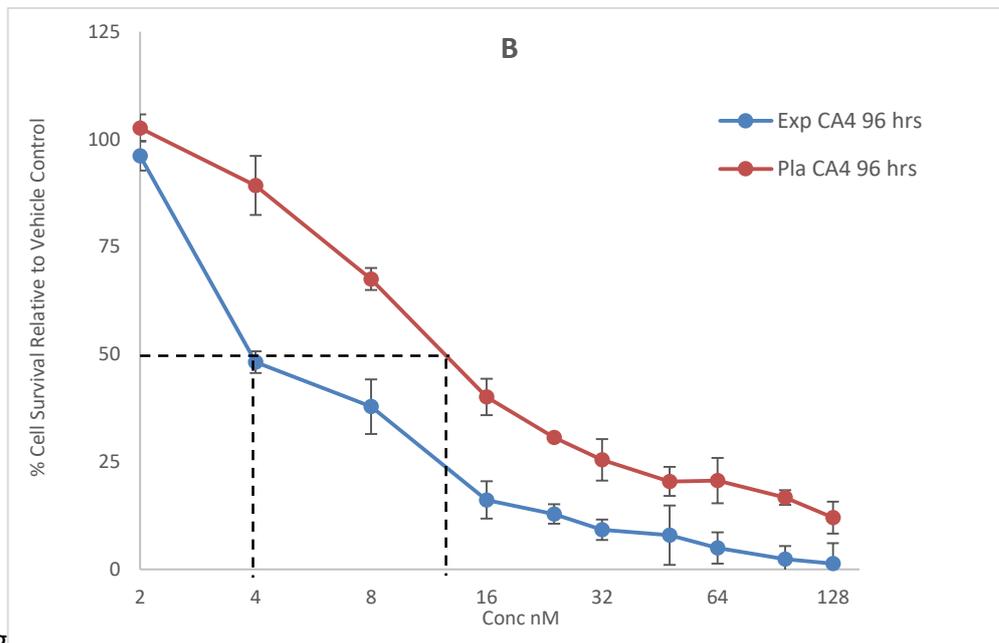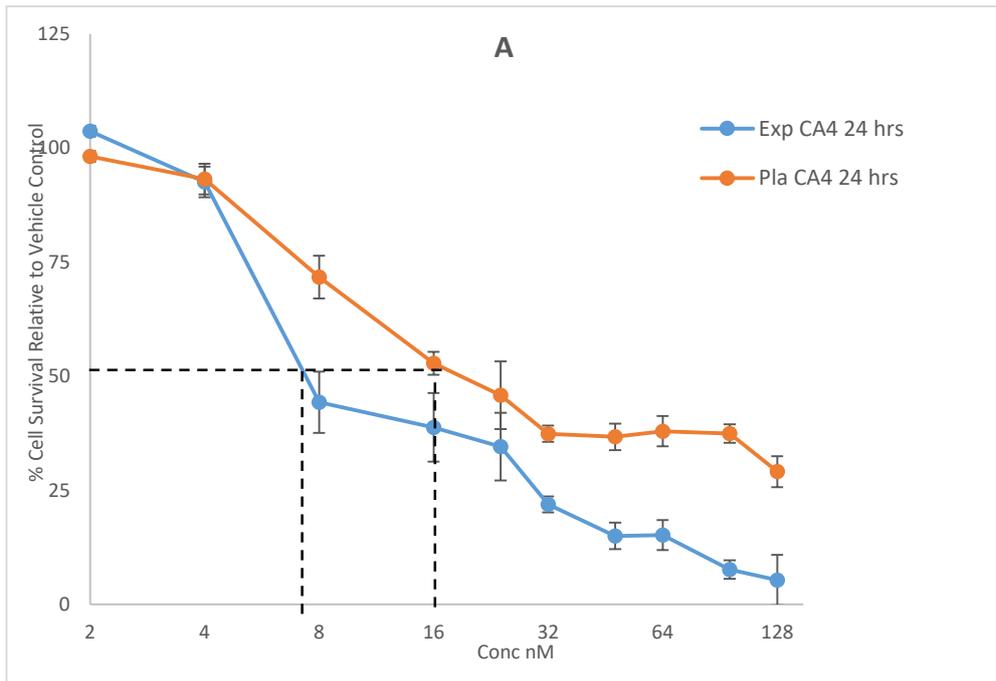
ggg

Figure 3-10: Effect of CA4 on viability of AC10.

Effects of CA4 on viability of AC10 in both exponential and plateau phase of growth after24 hr with 48 hr recovery (A) and 96- hr continuous exposure (B). Data are expressed as % cell survival relative to vehicle control, data is representative of n=3 ± SEM.

IC$_{50}$ (nM)	Exponential AC10		Plateau AC10	
Exposure time	24 hrs	96 hrs	24 hrs	96 hrs
Colchicine	45.8 ± 2.9	31.5 ± 1.2	53.5 ± 3.5	41.6 ± 1.9
CA4	7.5 ± 0.7	4.5 ± 1	20.5± 0.9	12.8 ± 0.9

Table 3-1: IC$_{50}$ values 24 hr (plus 48 hrs recovery) and 96 hrs continuous exposure after treatment of exponential and plateaued AC10 with VDAs. Data is representative of n=3 ± SEM.

3.4.7 Evaluation of cytotoxicity of VDAs against human lung cancer cells.

The effect of VDAs on H460 Lung cancer cells was assessed using MTT assay at exponential

phases of cell growth, as a comparison for assessment of on-target and off-target effects

(Figure 3-11 and Figure 3-12)

In exponential phase growth, the IC$_{50}$ values are 32 ± 6.3 nM and 24.5 ± 3 nM for Colchicine

and 5.4 ± 0.6 nM and 5.0 ± 0.3 nM for CA4, at 24 hr (plus 48 hr recovery) and 96- hrs

continuous exposure, respectively. The results showed no discernible difference of IC$_{50}$ values

between 24 hr or 96 hr treatment with Colchicine or CA4P (Table 3-2).

IC$_{50}$ (nM)	H460	
Exposure time	24 hrs	96 hrs
Colchicine	32 ± 6.3	24.5 ± 3
CA4	5.4 ± 0.6	5.0 ± 0.3

Table 3-2: IC$_{50}$ values 24 hr (plus 48 hrs recovery) and 96 hrs continuous exposure after treatment of H460 with VDAs. Data is representative of n =3 ± SEM
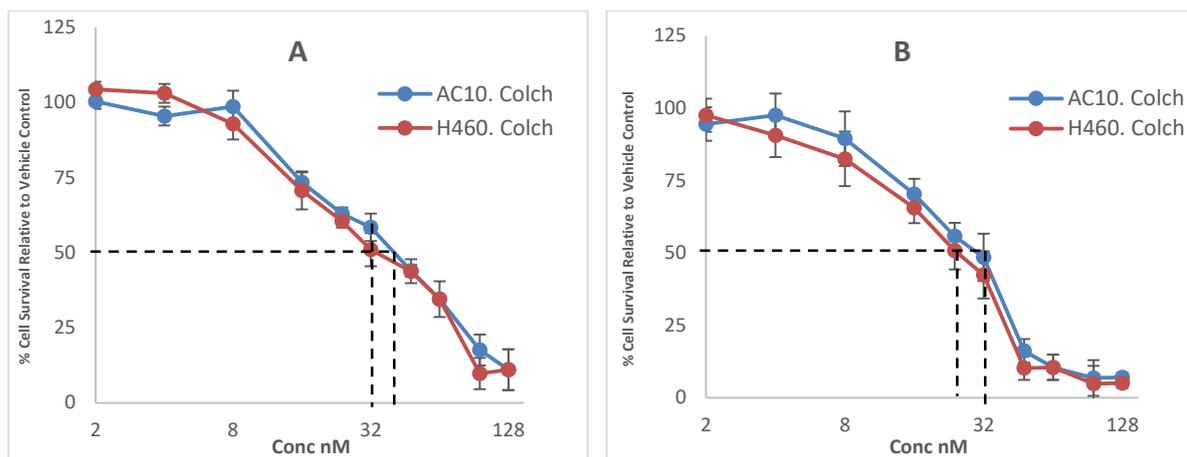
Figure 3-11: Dose response curve showing viability of H460 in exponential growth phase in comparison to AC10 when exposed to Colchicine.

(A) for 24 hrs; (B) for 96 hrs. Experiments performed in triplicate. Data points show average values ± SEM.
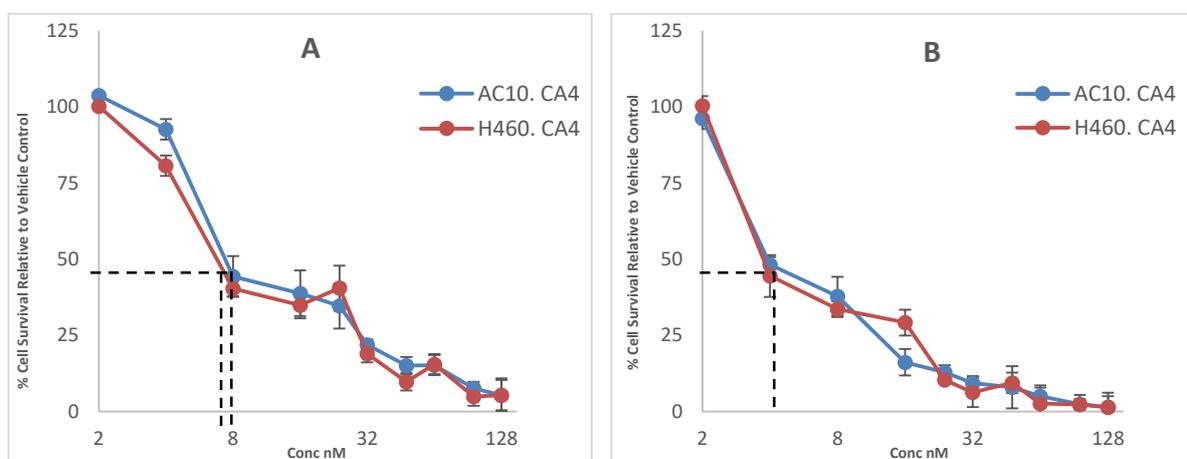
Figure 3-12: Dose response curve showing viability of H460 lung cancer cells in exponential growth phase in comparison to AC10 when exposed to CA4.

(A) for 24 hrs; (B) for 96 hrs. Experiments performed in triplicate. Data points show average values ± SEM.

3.5 Discussion.

Drug-induced cardiotoxicity is a significant issue with many cancer therapies and identification of the potential for causing cardiac effects is thereby required for prediction of clinical risk and mitigation of these effects (Rhoden et al., 1993, Suter and Ewer, 2013, Mann and Krone, 2010, Ewer et al., 2011, Curigliano et al., 2010, Floyd et al., 2005, Albini et al., 2010). Current preclinical methodology for identification of cardiac drug safety is predominantly focused on evaluation of cardiac function effects, especially drug-induced proarrhythmia s. However, methodologies to predict both drug-induced structural toxicities and the mechanistic basis of drug-induced toxicities are currently inadequate. The purpose of this phase of the project was to evaluate the AC10 human ventricular cardiac cell line as a suitable *in vitro* model for such studies and to characterise growth parameters of the cell line using a number of complementary methodologies useful for both mechanistic and molecular studies.

The AC10 cell line is derived from adult human ventricular cardiomyocytes fused with SV40-transformed fibroblasts to produce an immortalised cell line. (Davidson et al., 2005). This study confirmed the cardiac phenotype of the cell line, including a lack of α-smooth muscle actin, a marker of vascular but not cardiac muscle (Figure 3-1). The major confirmatory factor was the expression of troponin I, α-actinin, troponin C and tropomyosin, proteins central to contraction and relaxation of cardiac muscles (Layland et al., 2005) (Figure 3-1). Although positive for these markers, the expression pattern was devoid of a filamentous structure and no evidence of sarcomeric organisation was identified, as would be expected for a mature cardiomyocyte phenotype. Furthermore, this study shows that no expression of myosin light chain 2 (MLC2) or desmin, a muscle-specific type III intermediate filament and marker of

terminal differentiation, was detected (data are not uncluded). Together, this supports the non-contractile capacity of this cell line, as previously reported by the creator of the cell line (Davidson et al., 2005).

Expression of the transcription factor NKX2.5 protein, a key regulatory transcription factor essential for human heart development (Zheng et al., 2006), was detected in the AC10 cell line (Figure 3-1). This transcription factor is known to interact with the GAT4 transcription factor, for which genetic expression had been previously reported in AC10 cells (Davidson et al., 2005). This further evidence the cardiac phenotype of AC10 cells, potentially providing an explanation for the myogenesis developmental phenotype and precontractile nature of the cell line.

A major advantage of AC10 cells being immortalised is their potential for proliferation and expansion, a capability confirmed by expression of peri-centriolar material 1 protein PCM1 and Ki67 (Positive immunostaining of AC10 cell line for proliferative markers.).

In contrast to these confirmatory expression profiles of a cardiac phenotype for AC10 cells, the expression of vimentin, albeit at low levels, was not supportive of a full cardiac phenotype being more characteristic of a fibroblast lineage (Figure 3-1). This might be explained by the fact that the AC10 is a fusion between a cardiomyocyte and an immortalised fibroblast. Similarly, contrary to previous reports, bone morphogenetic protein 2(BMP 2) was also detected in AC10 cells in this study. This protein is reportedly only expressed after silencing the SV40 (Davidson et al., 2005) , but in this study was detected in AC10 without SV40 silencing (Figure 3-1)This may be due to a degree of cellular differentiation following prolonged *in vitro* culture and passaging or a consequence of genetic versus protein detection methodologies.

In addition to the cardiac expression phenotype confirmed in this study, another positive feature of these cells, although not confirmed herein, is their ability to form functional gap junctions (Davidson et al., 2005). Therefore, despite an inability to spontaneously contract, the AC10 cell line is therefore suitable for studies into structural cardiotoxicity and underpinning molecular mechanisms in the assessment of drug-induced toxicity.

In humans, as well as other mammals, cardiomyocytes have a very limited capability for regeneration and are essentially terminally differentiated. Therefore, it is important to model this and simultaneously evaluate effects in quiescent cardiac cells, as opposed to cells actively growing which is the 'conventional' *in vitro* approach for toxicity studies. Seeding densities to investigate the exponential and plateaued AC10 response to addition of cardiotoxicants were identified for cells analysed by manual assessment in tissue flasks, by response to mitochondrial-mediated MTT metabolism, and using the xCELLigence RTCA technologies. In all methodologies the cellular densities required were similar based on cell density/cm^2.

In contrast to both manual cells counting and the MTT assay, which are endpoint and thus destructive methodologies, the xCELLigence RTCA is a real-time non-invasive or destructive methodology to investigate the viability and structural changes induced by cardiotoxicants. Decreases to cell index may represent cytotoxicity or change in cellular morphology, whereas increases to cell index represent increased proliferation or cellular hypertrophy. Along with MTT studies and imaging, xCELLigence findings would provide a thorough integrated analysis of the cellular status at specific time and allow the identification of structural cardiotoxicity.

Once characterised and shown to be a suitable model for evaluation of detrimental drug effects (section 3.4.1), the AC10 cell model was employed to evaluate the cytotoxicity of the VDAs Colchicine and Combretastatin A4 (CA4).

The MTT viability assay, wherein the concentration of the metabolised formazan product is proportional to the number of viable cells present, was performed to evaluate cytotoxicity of VDAs on AC10 cardiac cell. Cells were continually exposed to the drugs for 96 hrs prior to evaluation of cellular viability and survival. The doses used in this study represent the clinical doses as it was between 1-2 μM (Rustin et al., 2003, Jung et al., 2003). The values of drug concentrations that causes a 50% inhibition of cell proliferation (IC_{50}) were calculated. Colchicine was less toxic toward AC10 the cardiac cell line than CA4P (Table 3-1).

In the clinic, VDAs are expected to demonstrate significant cytotoxicity against cancer cells whilst sparing effects against other cell types. The results in this study showed that there was no discernible difference between the AC10 cardiac and H460 cancer cell lines whilst in exponential proliferative cell growth, when treated with Colchicine or CA4P. Colchicine-treated AC10 cells at the exponential phase of growth have IC_{50} values of 45.8 ± 2.9 and 31.5 ± 1.2 nM for exposure time of 24 and 96 hrs, respectively (Table 3-1). In comparison, Colchicine-treated H460 cancer cells at the exponential phase of growth have IC_{50} values of 32 ± 6.3 and 24.5 ± 3 nM for exposure time of 24 and 96 hrs, respectively (Table 3-2). Similarly, with CA4, which was shown to be more potent than Colchicine, AC10 cells in the exponential proliferative phase of growth have IC_{50} values of 7.5 ± 0.7 nM and 4.5 ± 1 nM (Table 3-1) whereas CA4-treated H460 cancer cells have IC_{50} values of 5.4 ± 0.6 nM and 5.0 ± 0.3 nM for exposure time of 24 and 96 hrs (Table 3-2), respectively. This suggesting the drugs are equitoxic to these cell types under the experimental proliferative conditions employed.

Although 'standard' in terms of evaluation of drug-induced cytotoxicity against cells in monolayer culture, the relevance of this approach for evaluation of cells with a low proliferative potential, such as is found in the heart, is somewhat questionable. As such, it is

also crucial to evaluate the effect of compounds upon quiescent cardiac cells, which are a better representative of the adult heart. In monolayer cell studies, this can be recapitulated by evaluation of cells in the plateau phase of cell growth. Therefore, treatment of AC10 cardiomyocytes at plateau phase was performed to rule-out the possible toxicity of the VDAs attributable to the proliferative nature of the AC10, whilst generating a cardiac *in vitro* model mimicking the cardiac cells in adult's human. In comparison, AC10 cardiomyocytes in the exponential growth phase were more sensitive to VDAs treatments (Table 3-1). Furthermore, subsequent to prolonged exposure of 96 hr to VDAs, cardiac cells in the exponential phase of growth were more sensitive compared to exposure time of 24 hrs, with the additional 48 hr recovery period. As expected, the increased exposure increased the toxicity of VDAs in both case of exponential and plateau phases.

In the context of the differential toxicity of VDAs in the clinical situation, wherein VDAs are expected to demonstrate significant cytotoxicity against cancer cells whilst sparing effects against other cell types, a statistically significant difference was found in cytotoxicity when comparing cancer cells in exponential to cardiac cells in plateau phases of growth. Colchicine-treated AC10 cells at the plateau phase of growth demonstrate IC_{50} values of 53.5 ± 3.5 nM and 41.6 ± 1.9 nM for exposure time of 24 (plus 48 hr recovery) and 96 hrs, respectively. In comparison, Colchicine-treated H460 cancer cells at the exponential phase of growth demonstrate IC_{50} values of 32 ± 6.3nM and 24.5 ± 3nM for exposure time of 24 (plus 48 hr recovery) and 96 hrs, respectively. Similarly for CA4-treatment, where plateau phase quiescent AC10 cells have IC_{50} values of 20.5± 0.9 nM and 12.8 ± 0.9 nM and proliferative H460 cells have IC_{50} values of 5.4 ± 0.6 nM and 5.0 ± 0.3 nM for exposure time of 24 and 96 hrs, respectively (Table 3-1 and Table 3-2).

In the context of the examined VDAs in this study, Colchicine and CA4P, there is no clear difference in toxicity between cancer cells and cardiac cells when analysed in exponential growth, due to the proliferative nature of the cells. In contrast, differential effects were observed when compared to plateau phase growth of cardiac cells, representative of the quiescent nature of normal heart cells.

Chapter 4. *In vitro* evaluation of vascular disrupting agent (VDA) induced structural cardiotoxicity and strategies for therapeutic mitigation.

4.1 Structural effects of VDAs in the cardiovascular system.

Drug-induced detrimental effects upon the heart are an inherent problem with many oncology agents, with acute and late-onset drug-induced cardiotoxicity now major issues in cancer therapy (see section 1.8). In preclinical *in vivo* studies, the VDA class of cancer therapeutic have been shown to cause a wide range of detrimental effects upon the cardiovascular system, including structural toxicity effects associated with cardiovascular cell death, vascular constriction and damage, cardiac ischaemia, and haemodynamic changes, and ultimately cardiac remodelling (Gill et al., 2019, Lee and Gewirtz, 2008, Rustin et al., 2010). However, the molecular mechanisms underlying these effects and their significance for clinical use have yet to be elucidated. Understanding the effects of VDAs upon cellular structure and tubulin-driven processes in cardiac cells is therefore essential to appreciating the degree of structural cardiotoxicity and the underlying toxicity mechanism of these agents.

Tubulin is the central cytoskeletal fibre for formation of cellular microtubules, involved in mitotic spindle formation during cell division, maintenance of cell shape, and intracellular transportation (Zhou and Giannakakou, 2005, Jordan et al., 1998). Microtubules are dynamic structures in which there is a requirement for continuous assembly and disassembly of tubulin structures through polymerisation. In the context of the cardiac system, tubulin structured microtubules are also known to be essential for regulation of the contractile phenotype and dynamic movement, cardiomyocyte stiffness and flexibility, as well as correct expression and activity of cardiac ion channels and the electrophysiological response (Robison et al., 2016, Schappi et al., 2014, Hein et al., 2000)

 VDAs disrupt the dynamic instability of the cellular cytoskeleton by binding to the Colchicine binding site of tubulin, inhibiting its depolymerisation and therefore suppressing microtubule

formation (Lu et al., 2012). In endothelial cells associated with tumour angiogenesis, wherein their immaturity means that the cellular infrastructure is reliant on tubulin rather than actin, these VDAs impose a change in their cellular shape and thus a reduction in blood flow and cell permeability which in turn starves the tumour of oxygen and nutrients thereby delivering their therapeutic effects (Chaplin and Dougherty, 1999, Gaya and Rustin, 2005, Gill et al., 2019).

With regards detrimental effects of VDAs upon the cardiovascular system, although the molecular mechanisms responsible for these effects may involve similar effects to that observed in other cell types in relation to direct cytotoxicity, there must also be a degree of diversity and different effects in order to explain the acute structural toxicities, reduced cardiac function, and association with heart failure in the longer-term. The fact that cardiomyocytes by default are non-proliferative and quiescent in the adult heart raises a question regarding the impact of inhibition of mitosis as a major toxicity mechanism in this context. Furthermore, whereas the therapeutic mechanism in terms of vascular disruption is reliant upon the dependency of immature tumour endothelial cells upon tubulin for structure, the cytoskeleton of cardiomyocytes is more robust involving a multitude of cytostructural proteins, suggesting this mechanism may also not be in play with cardiomyocytes. It is however of note that cardiomyocytes isolated from hypertrophic hearts demonstrate loss of compliance, 'stiffness', and potentially restricted sarcomeric movement, reportedly due to increased levels of total tubulin, elevated tubulin polymerisation and increased microtubule stabilisation(Tagawa et al., 1998, Rappaport and Samuel, 1988, Hein et al., 2000) This is suggestive of a central involvement of tubulin in cardiomyocyte structure and function but in a different context to that proposed for endothelial cells.

Development of dilated cardiomyopathy, progressive heart failure and left ventricular dysfunction (LVD) is now known to be a common development and chronic toxicity with several cancer therapies. Although not yet conclusively proven, these effects are believed to be a consequence of initial cardiomyocyte loss from the limited number of cardiomyocytes available in the post-mitotic tissue, alterations in the cellular proportional dynamics of cardiac tissue and putative fibrosis, and resultant cardiomyocyte hypertrophy and subsequent cardiac remodelling. Drug-induced cardiomyopathy is a progressive and multi-factorial process occurring over several months and years, as a compensation reaction to volume and pressure overload in reflection of the cellular hypertrophic response and remodelling process (Curigliano et al., 2012, Herrmann et al., 2016, Touyz et al., 2018, Galluzzi et al., 2015, Gill et al., 2019). If not managed, this pathological cardiac hypertrophic response is often life-threatening (Bevegard and Shepherd, 1967, Raskoff et al., 1976, Weeks and McMullen, 2011).

Identification of the molecular mechanisms and molecular pathways involved and driving changes in cardiomyocyte responses, including morphological, structural and hypertrophic changes, are important for improved understanding of the risk posed by VDAs and management of these effects. However, until recently there was a paucity of human or clinically-relevant models applicable for *in vitro* structural cardiotoxicity studies in this regard, (discussed in chapter 1). One model demonstrating utility in this context is the AC10 cardiomyocyte cell line (AC10), which despite being in a precontractile state, expresses the majority of cardiac specific factors (Davidson et al., 2005). As defined in Chapter 3, the AC10 cell line have a cardiac phenotype and can be used *in vitro* to evaluate drug-induced cardiotoxicity. The analogous AC16 cell line has also been used previously to investigate pathways relating to cellular hypertrophy of cardiomyocytes (Xiao et al., 2017). Consequently,

the AC10 cardiomyocyte cell line has the potential to detect structural drug-induced toxicity of VDAs, contributing to understanding of the cardiotoxicity of these agents.

4.2 Cardioprotective agents to mitigate structural toxicity of cancer chemotherapies

Identification of therapeutic strategies to mitigate or prevent drug-induced cardiotoxicity caused by cancer drugs is a clear goal for successful use of these drugs in the clinic. Therapeutics targeted at interruption of the angiotensin system, such as angiotensin converting enzyme inhibitors (ACEi) or Angiotensin receptor blockers (ARB) are commonly used for treating hypertensive patients and have recently been proposed as a potential prophylactic strategy to mitigate cardiovascular toxicities caused by cancer therapeutics (Gould et al., 2007, Cardinale et al., 2013, Cardinale et al., 2010).

With regards VDAs, although not yet approved for clinical use, several preclinical studies and clinical trials have been completed or are underway (Chapter 1). Despite being tolerated better than other VDAs, exposure to CA4P is still accompanied by a range of cardiac adverse effects (see Chapter 1). In terms of clinical management of CA4P-induced cardiac effects, a treatment algorithm was devised for use in the phase II FOCUS trial (CA4P in combination with the anti-angiogenic agent bevacizumab and cytotoxic chemotherapy) involving differential strategies for patients presenting with hypertension and decreased cardiac function (Monk et al., 2016). Administration of ACEi or other hypertensive medications, alongside frequent monitoring of blood pressure, was deemed essential to mitigate the acute CA4P-induced cardiac complications (Monk et al., 2016, Grisham et al., 2018). In the case of the Colchicine analogue ZD6126, pre-administration of the Ca^{2+} channel-blocker nifedipine and the β-adrenoceptor blocker atenolol to ZD6126-treated rats resulted in reversal of

hypertension and tachycardia, respectively (Gould et al., 2007). Based on these encouraging observations, preclinical studies are thereby required to evaluate potential for therapeutic-mediated mitigation of VDA-induced cardiac effects, with mechanistic insights and the importance of sequence of cardioprotectants versus VDA administration.

4.3 Aims and Objectives

Cardiotoxicity of VDAs is associated with induction of structural changes leading to multiple detrimental outcomes upon the cardiovascular system in the clinic. The aim of this chapter is to interrogate VDA-induced cellular morphological and structural changes, to better understand the mechanisms of VDA-induced cardiotoxicity.

The objectives are as follows:

1) Evaluate the effects of the VDAs upon microtubule organisation in AC10 cardiomyocytes

2) Characterise the effects of VDAs upon cell cycle distribution in AC10-CMs during the proliferative and quiescent growth phases *in vitro*

3) Evaluate changes in cellular morphology in AC10-CMs following exposure to VDAs

4) Assess the ability of cardioprotective drug therapy to prevent VDA-induced structural changes in AC10-CMs.

4.4 Results

4.4.1 VDAs causes disturbance in the organisation of the microtubules network in AC10 cardiomyocyte cells.

Colchicine and CA4 both target the Colchicine-binding site of β-tubulin, inhibit tubulin polymerisation, and as such destabilise microtubules, potentially causing a wide array of subsequent effects (Hill et al., 1993, Bibby et al., 1989, Baguley et al., 1996, Cai, 2007) following exposure to 3, 30 and 300 µM Colchicine and CA4 for 24 hrs, tubulin disruption was shown in AC10 cells (Figure 4-1).

4.4.2 VDAs induce G2/M cell cycle arrest in proliferative AC10 cells.

AC10 cardiomyocyte cells treated with either Colchicine or CA4 whilst in their exponential growth phase resulted in a perturbation of their cell cycle distribution, in agreement with the inhibition of the mitotic spindle dynamics (Table 4-1 and 4-2). Colchicine at 30nM and 300nM resulted in a significant 3-fold higher accumulation of cells in G2/M phase of the cell cycle relative to drug vehicle alone following 24 hr, and 6-fold higher accumulation following 96 hr exposure (Table 4-3). However, low dose Colchicine (3 nM) did not significantly affect cell cycle distribution (Table 4-1). The response of AC10 cells to CA4 was similar to that observed with Colchicine, with 300nM and 30nM inducing a significant G2/M phase arrest at both exposure periods, whilst the lower 3nM concentration did not significantly affect cell cycle distribution (Table 4-2).
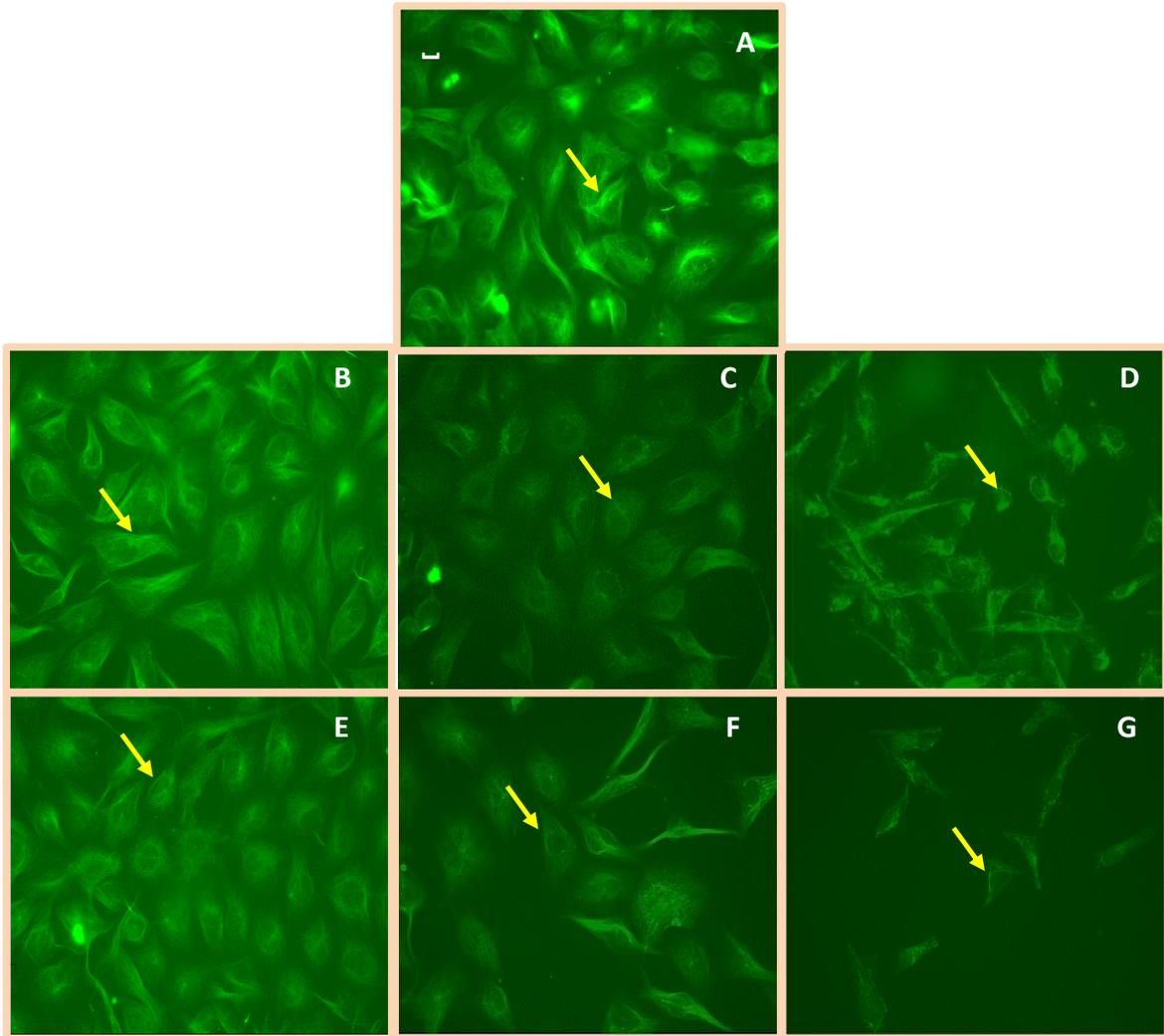
Figure 4-1: Disruption of microtubule network in AC10 cells following exposure to VDAs.

AC10 cells treated for 24 hrs with (A) Control; (B) 3nM Colchicine; (C) 30nM Colchicine; (D) 300nM Colchicine; (E) 3nM CA4; (F) 30nM CA4; (G) 300nM CA4. Tubulin was stained with Tubulin Tracker™ Green and visualised by fluorescence microscopy at 488nm. Images are representative of three independent studies. Scale bar = 50μm.

	Cell cycle phase (% ± SD)			
24 hr exposure	**G1**	**S**	**G2/M**	Sub-G1
Drug vehicle	53 ± 3	26 ± 5	13 ± 3	8 ± 3
3 nM Colchicine	47 ± 3*	25 ± 3	19 ± 3	9 ± 2
30 nM Colchicine	13 ± 2**	11 ± 1*	43 ± 4*	34 ± 3*
300 nM Colchicine	16 ± 2**	9 ± 1*	38. ± 4*	37 ± 4*

96 hr exposure

Drug vehicle	53 ± 2	30 ± 3	9 ± 1.3	8 ± 3
3 nM Colchicine	49 ± 5	25 ± 3	11 ± 3	14 ± 1
30 nM Colchicine	20 ± 1**	13 ± 4**	43 ± 4**	24 ± 2**
300 nM Colchicine	6 ± 2**	9 ± 2**	55 ± 5**	30 ± 6**

Table 4-1: The effect of Colchicine on cell cycle of AC10 in the exponential growth phase. *Cell cycle distribution of AC10 cells in the proliferative growth phase when exposed to Colchicine for 24 or 96 hrs. Values are expressed as a mean percentage of three independent replicates ±SD Statistically significant values relative to vehicle control are indicated by asterisks (∗p<0.05 or ∗∗p<0.01). Statistical analysis used is student t-test.*

24 hr exposure	Cell cycle phase (% ± SD)			
	G1	S	G2/M	Sub-G1
Drug vehicle	53 ± 3	26 ± 5	13 ± 3	8 ± 3
3 nM CA4	50 ± 4	23 ± 5	16 ± 2	11 ± 3
30 nM CA4	16 ± 4**	14 ± 2*	40 ± 2**	31 ± 6*
300 nM CA4	10 ± 1**	9 ± 1**	42 ± 2**	39 ± 3**

96 hr exposure

Drug vehicle	53 ± 2	30 ± 3	9 ± 1.3	8 ± 3
3 nM CA4	51 ± 6	24 ± 3	15 ± 5	10 ± 1
30 nM CA4	16 ± 4**	13 ± 2*	38 ± 2**	33 ± 2**
300 nM CA4	3 ± 1 **	8 ± 2*	51 ± 4**	38 ± 4**

Table 4-2*:* **The effect of CA4 on cell cycle of AC10 in the exponential growth phase.**

Cell cycle distribution of AC10 cells in the proliferative growth phase when exposed to CA4 for 24 or 96 hrs. Values are expressed as a mean percentage of three independent replicates ±SD. Statistically significant values relative to vehicle control are indicated by asterisks (∗p<0.05 or ∗∗p<0.01). Statistical analysis used is student t-test.

4.4.3 VDAs induce G2/M cell cycle arrest in quiescent AC10 cells.

AC10 cardiomyocyte cells in the plateau/quiescent growth phase, representative of cardiomyocytes in cardiac tissue, exhibited 2-fold more cells arrested in G2/M of the cell cycle relative to exponential growth (Table 4-3), a factor supportive of the fact that cardiomyocytes are in a pre-mitotic rather than post-mitotic and that despite being quiescent, a low-level degree of cellular turnover is present to balance cell death.

24 hr post-plating	Cell cycle phase (% ± SD)			
	G1	S	G2/M	Sub-G1
Exponential	53 ± 3	26 ± 5	13 ± 3*	8 ± 3
Plateau	49 ± 4	19 ± 2*	19 ± 3**	14 ± 2
96 hr post-plating				
Exponential	53 ± 2	30 ± 3	9 ± 1.3	8 ± 3
Plateau	53 ± 6	15 ± 3**	20 ± 3**	13 ± 2

Table 4-3: Comparison of cell cycle distribution of AC10 cells whilst in exponential and plateau growth phases.

Cells in plateau phase demonstrate significant reduction of cells in S-phase and accumulation in G2/M phases, indicating reduced proliferative capacity. Values are mean percentage of three independent replicates ±SD. Statistically significant difference of plateau relative to exponential phase are indicated by asterisks (∗p<0.05 or ∗∗p<0.01). Statistical analysis used is student t-test.

Treatment of this quiescent population of AC10 cells with either Colchicine or CA4 for 24 and 96 hrs resulted in further accumulation of cells in G2/M of the cell cycle. Both Colchicine (Table 4-4) and CA4 (Table 4-5) at 30nM and 300nM resulted in a significant doubling of cells in G2/M phase of the cell cycle relative to drug vehicle alone (Table 4-3) following both 24 hr and 96 hr exposure. However, low dose (3nM) did not significantly affect cell cycle distribution.

	Cell cycle phase (% ± SD)			
24 hr exposure	**G1**	**S**	**G2/M**	Sub-G1
Drug vehicle	49 ± 4	19 ± 2	19 ± 3	14 ± 2
3 nM Colchicine	46 ± 3	19 ± 5	17 ± 4	17 ± 3
30 nM Colchicine	30 ± 4*	15 ± 5	37 ± 6**	19 ± 5
300 nM Colchicine	24 ± 5**	19 ± 3	38 ± 5**	20 ± 6

96 hr exposure

Drug vehicle	53 ± 6	15 ± 3	20 ± 3	13 ± 2
3 nM Colchicine	50 ± 3	13 ± 2	22 ± 4	16 ± 3
30 nM Colchicine	23 ± 5**	9 ± 1*	47 ± 5*	20 ± 3**
300 nM Colchicine	12 ± 2*	9 ± 3*	55 ± 5**	23 ± 4*

Table 4-4: The effect of Colchicine on cell cycle of AC10 in the plateau growth phase. *Cell cycle distribution of AC10 cells in the plateau growth phase when exposed to Colchicine for 24 or 96 hrss. Values are expressed as a mean percentage of three independent replicates ±SD Statistically significant values relative to vehicle control are indicated by asterisks (∗p<0.05 or ∗∗p<0.01). Statistical analysis used is student t-test.).*

	Cell cycle phase (% ± SD)			
24 hr exposure	**G1**	**S**	**G2/M**	**Sub-G1**
Drug vehicle	49 ± 4	19 ± 2	19 ± 3	14 ± 2
3 nM CA4	48 ± 5	20 ± 2	17 ± 3	15 ± 3
30 nM CA4	28 ± 4*	17 ± 6	38 ± 2**	17 ± 2*
300 nM CA4	12 ± 3*	15 ± 5	47 ± 5**	26 ± 5*

96 hr exposure

Drug vehicle	53 ± 6	15 ± 3	20 ± 3	13 ± 2
3 nM CA4	48 ± 5	19 ± 3	21 ± 3	13 ± 3
30 nM CA4	25 ± 3*	15 ± 3	38 ± 5*	20 ± 2*
300 nM CA4	4 ± 2*	11 ± 2	49 ± 5**	36 ± 4*

Table 4-5*: **The effect of CA4 on cell cycle of AC10 in the plateau growth phase.**

Cell cycle distribution of AC10 cells in the plateau growth phase when exposed to CA4 for 24 or 96 hrss. Values are expressed as a mean percentage of three independent replicates ±SD Statistically significant values relative to vehicle control are indicated by asterisks (∗p<0.05 or ∗∗p<0.01). Statistical analysis used is student t-test.

4.4.4 Exposure to VDAs causes an increase in size of AC10 cells.

Determination of flow cytometric forward scatter was used as an indicator of the size of AC10 cells and used as an indicator for drug-induced cellular hypertrophy. Exposure of AC10 cells to either Colchicine or CA4 whilst actively proliferating resulted in a significant increase in cell size at cytotoxic concentrations of 300nM and high exposure concentrations of 30nM after both 24 and 96 hr periods. The effects of CA4 being marginally greater than those of Colchicine. No significant change in cell size was observed in response to low sub-therapeutic concentrations of 3nM (Table 4-6).

Cells in the quiescent growth phase, representative of cardiomyocytes in the body, also demonstrated an increase in cell size when exposed to Colchicine and CA4 (Table 4-6). As was observed with proliferative cells, CA4 induced a greater increase in cell size than Colchicine. Interestingly, the effects of CA4 were more striking after 24 hrs than 96 hrs, with a significant effect also observed with low concentrations (3nM), suggesting the effects as being an immediate response rather than an accumulated response (Table 4-6).

To confirm that these changes determined by means of flow cytometric forward scatter variations were indeed a consequence of an increase in cell size, the effects of CA4 was also determined by visualisation of AC10 cells and manual determination of their size (Figure 4-2 and 4-3). Following 24hr treatment with CA4, an obvious change in cell size and shape was observed at all concentrations (Figure 4-2). Calculation of the size of these cells reflected the result obtained by flow cytometry, with a progressive increase in cell size with increasing CA4 concentration (Figure 4-3).

24 hr exposure	Relative Cell size			
	Proliferative growth phase		Quiescent growth phase	
	Colchicine	CA4	Colchicine	CA4
Drug vehicle	1	1	1	1
3 nM	1.05 ± 0.01	1.07 ± 0.02	1.07 ± 0.06	1.12 ± 0.04*
30 nM	1.09 ± 0.03*	1.14 ± 0.05*	1.11 ± 0.03*	1.20 ± 0.01**
300 nM	1.15 ± 0.06*	1.19 ± 0.07**	1.14 ± 0.03*	1.23 ± 0.04**

96 hr exposure

Drug vehicle	1	1	1	1
3 nM	1.07 ± 0.01	1.09 ± 0.02	1.04 ±0.03	1.05 ± 0.01
30 nM	1.11 ± 0.02*	1.14 ± 0.03*	1.10 ± 0.03*	1.10 ± 0.02*
300 nM	1.18 ± 0.07**	1.20 ± 0.03**	1.15 ± 0.04*	1.18 ± 0.02**

Table 4-6: The effect of VDAs on relative size of AC10 cells, in the proliferative and plateau phases of growth, as determined by flow cytometry.

Values of cell size of AC10 as recorded by forward scatter of flow cytometry, expressed relative to drug vehicle treated (control) cells. Data are mean of three independent replicates ± SD. Statistically significant values relative to control, (∗p<0.05 or ∗∗p<0.01). Statistical analysis used is student t-test.
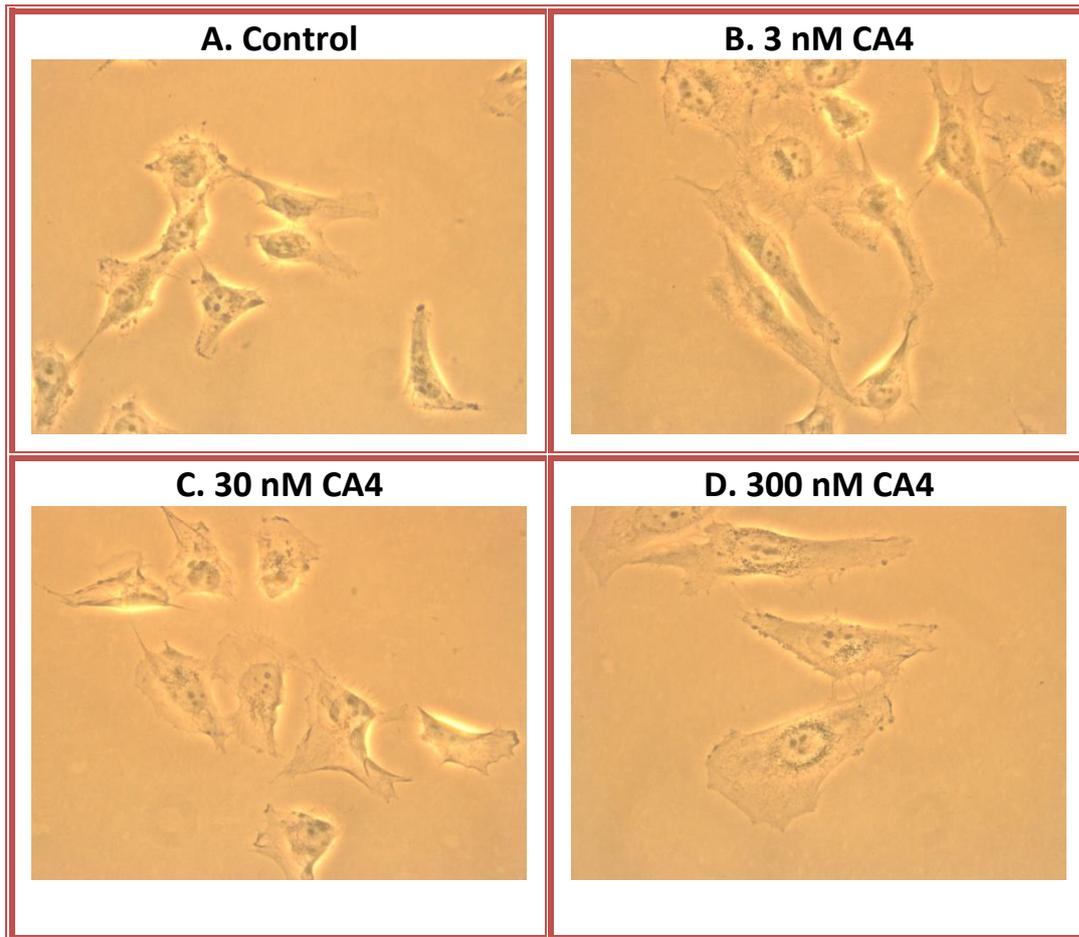
Figure 4-2: Images of AC10 cells exposed to CA4 or drug vehicle.*Images were captured at 40x magnification following 24 hrs exposure to CA4. (A) Control; (B) 3 nM CA4; (C) 30 nM CA4 and (D) 300 nM CA4.*
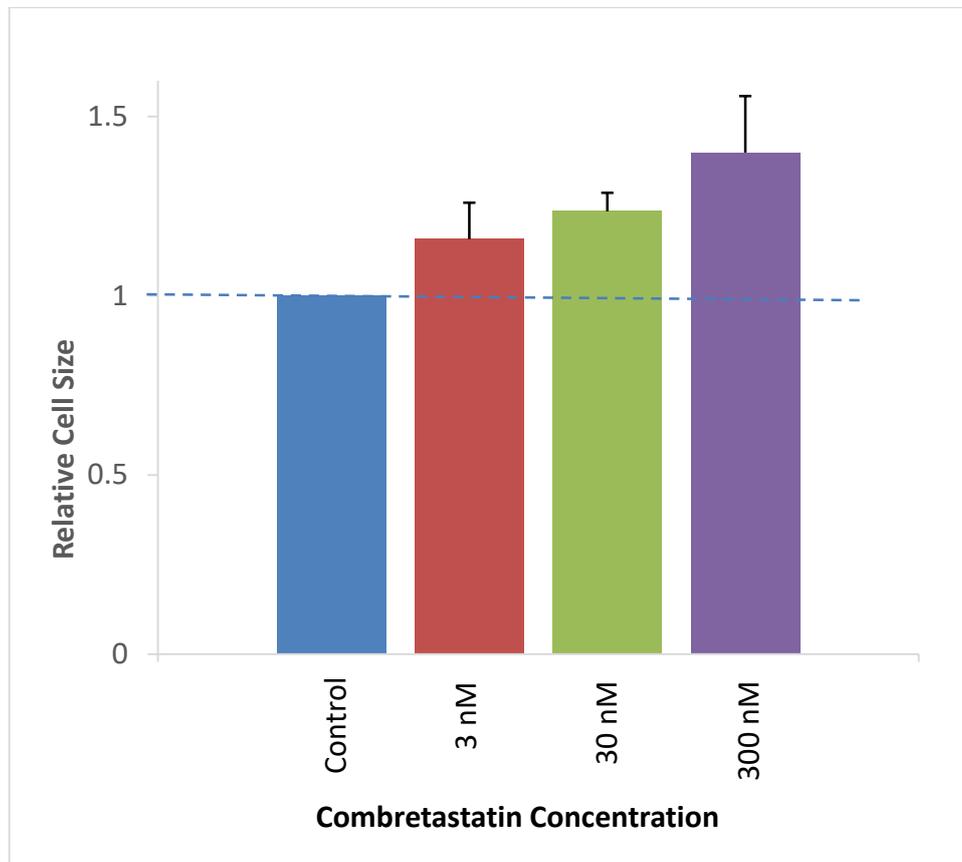
Figure 4-3: Effect of CA4 on size of AC10 cells, determined by manual measurement. *Relative cell size, based on number of comparative cell area, of proliferative AC10 cardiomyocytes following exposure to CA4 for 24 hrs. Values are expressed as a mean percentage of three independent replicates ±SD.*

4.4.5 Exposure to VDAs induces cellular hypertrophy of AC10 cells

The cardiac tissue response to drug-induced cardiotoxicity commonly involves an increase in cell size (hypertrophy) of the 'surviving' cardiomyocytes to compensate for the loss of cells by direct cytotoxicity. To address this potential mechanism, the cellular response to CA4 was monitored in real time by xCELLigence RTCA in combination with determination of cellular viability using the MTT assay, manual quantification of viable cell numbers, and finally the determination of cell size in parallel.

Following 24 hr exposure of exponential growing AC10 cells to CA4, comparable results for cellular loss or reduced cell viability were observed when detected by xCELLigence, MTT assay or manual cell counting (Figure 4-4 A,B & C). Using all three methodologies, dose dependent effects were identified, with minimal effects observed with 3nM or 30nM CA4, and significant loss of cell number and/or viability with the higher 300nM concentration Conversely, an indirectly proportional dose dependent increase in cell size was observed (Figure 4-4 D). This overall result is supportive of VDA-induced cell hypertrophy as a compensatory consequence of loss of viable cell mass.
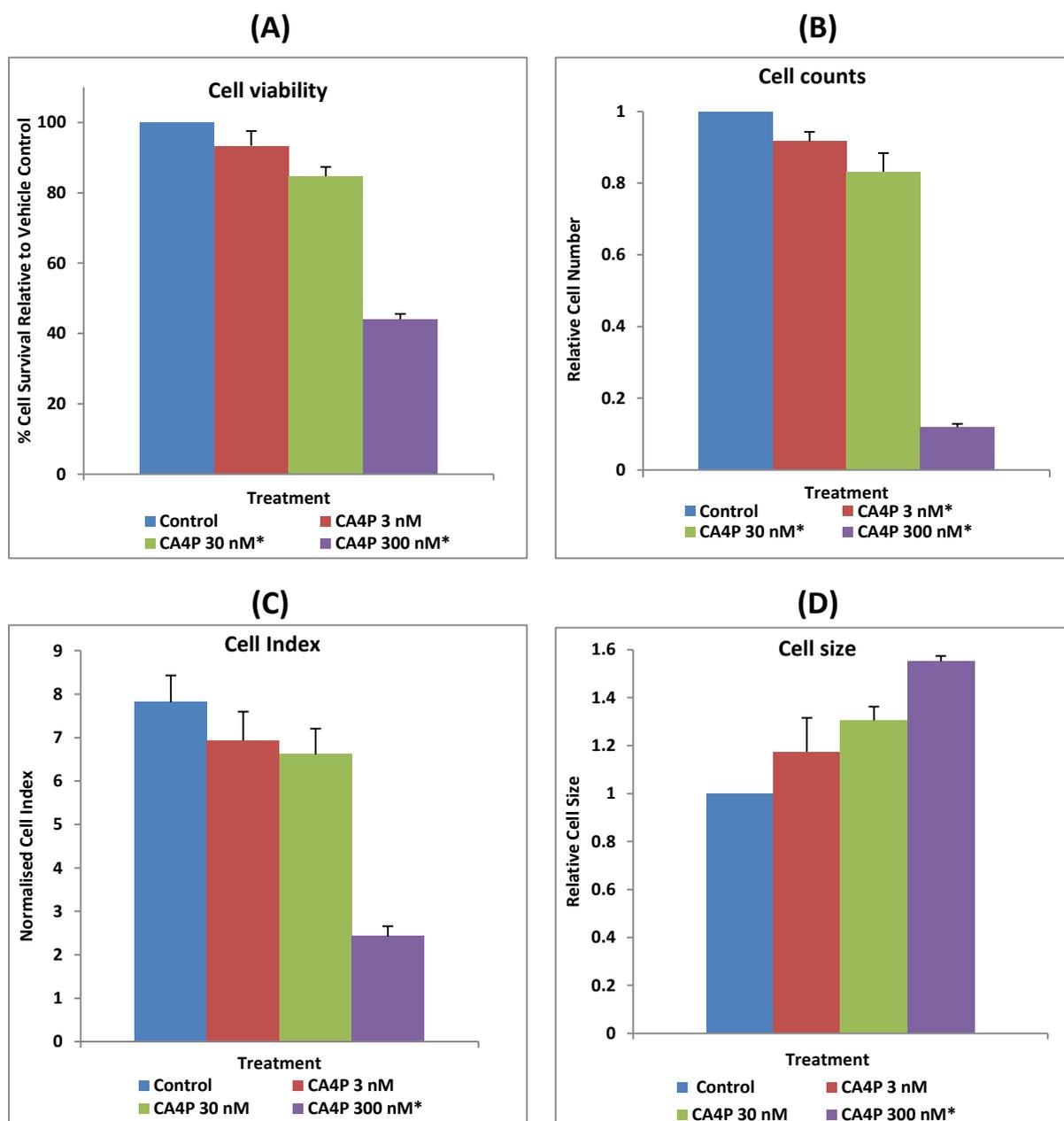
Figure 4-4: Dose dependent inverse relationship between cell viability and cell size in AC10

cells exposed to CA4.*Following 24 hr exposure of AC10 cells to 3, 30 or 300 nM CA4 or vehicle control (DMSO); (A) cell viability was determined by MTT assay, (B) cell number calculated by manual haemocytometer, (C) xCELLigence cell index recorded, and (D) cell size determined by manual measurement (D). Data is the mean of three independent experiments ± SEM.*

4.4.6 Mitigation of VDA-induced toxicity by co-administration of cardioprotective drugs

In consideration of the cardiotoxicity of VDAs, the benefit of either prophylactic, simultaneous, or post-exposure, addition of the cardioprotective beta adrenoceptor antagonists or inhibitors of angiotensin receptor signalling pathway were evaluated.

Initially, any cytotoxicity of the cardioprotectant was determined. A lack of significant cytotoxicity was identified against AC10 cells for 0.1pM-10 μM of either the beta-adrenoceptor blocker carvedilol, the angiotensin receptor blocker telmisartan, the angiotensin- converting enzyme (ACE) inhibitor enalapril or its activated species enalaprilat (Figure 4-5). A similar lack of direct toxicity of these drugs was also detected for the H460 NSCLC cell line (Figure 4-6).

4.4.7 Cytotoxicity of VDAs Against AC10 Cells is Reduced by Combination with the Angiotensin Converting Enzyme Inhibitor (ACEi) Enalapril or its active metabolite Enalaprilat.

The response of AC10 cardiomyocytes to combined treatment of VDAs with Enalapril and Enalaprilat was investigated in both exponential and plateau growth phases after both 24 and 96 hr exposure periods.

Administration of enalapril or enalaprilat 24 hrs prior to exposure of exponentially growing AC10 cells to either Colchicine or CA4 for 24hrs, followed by 48 hr recovery in the presence of enalapril/enalaprilat, resulted in a significant improvement in cell viability (Table 4-7).
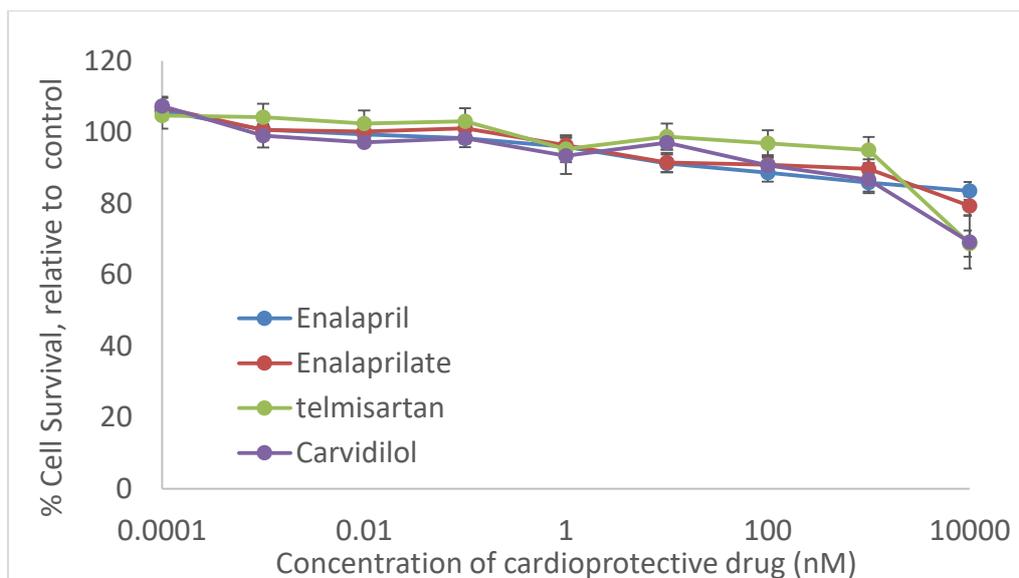
Figure 4-5: Effect of cardioprotectants on viability of AC10 Cardiomyocytes. *Exponentially growing AC10 cells exposed for 96 hrs to 0.1 pM-10 µM Enalapril, Enalaprilat, Telmisartan and Carvedilol. Cell viability determined by MTT assay. Data is representative of n=3 ± SEM.*
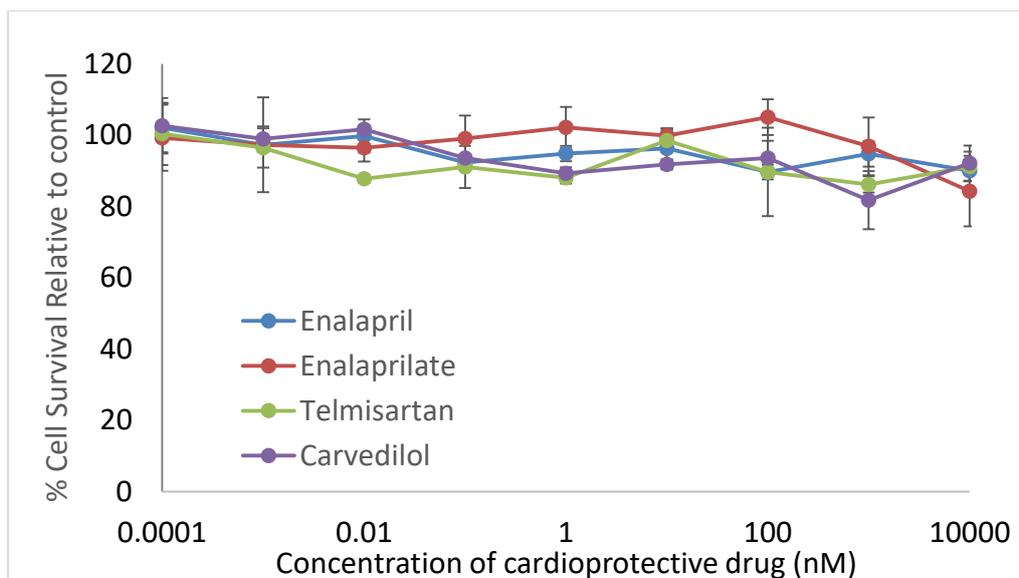
Figure 4-6: Effect of cardioprotectants on viability of H460 NSCLC cells. *Exponentially growing H460 cells exposed for 96 hrs to 0.1 pM-10 µM Enalapril, Enalaprilat, Telmisartan and Carvedilol. Cell viability determined by MTT assay. Data is representative of n=3 ± SEM.*

24 hr exposure		Colchicine	CA4
First drug addition	Second drug addition	IC$_{50}$ value (nM)	IC$_{50}$ value (nM)
VDA	-	45 ± 5.8	7.5 ± 0.7
Enalapril (1µM)	VDA	60.9 ± 0.8 *	31.7 ± 2.9 *
VDA	Enalapril (1µM)	46.1 ± 4.6	11.1 ± 0.9*
Enalaprilat (1µM)	VDA	65.5 ± 2.7*	15.5 ± 2.4*
VDA	Enalaprilat (1µM)	50.2 ± 3.4	11.5 ± 2.4

96 hr exposure

VDA	-	31.3 ± 1.1	4.4 ± 0.6
Enalapril (1µM)	VDA	45.5 ± 2*	7.7 ± 0.9*
VDA	Enalapril (1µM)	30 ± 3.2	5.4 ± 0.7
Enalaprilat (1µM)	VDA	57.9 ± 2.6*	9.4 ± 0.7*
VDA	Enalaprilat (1µM)	35.2 ± 2.3	5.3 ± 0.3

Table 4-7: Effect of combination therapy of Enalapril or Enalaprilat and VDAs on proliferative AC10. *Cells in the exponential phase of growth were administered enalapril or enalaprilat either 24hrs before or after exposure to Colchicine or CA4 with the effect on VDA-induced cytotoxicity determined (indicated by IC$_{50}$ value). Cells were either in the presence of VDAs for 24hrs, with a subsequent 48 hr VDA-free period, or continuously for 96 hrs. Cytotoxicity was determined by MTT assay. Data are mean of three independent replicates ± SEM. Statistically significant values relative to control, (∗p<0.05 or ∗∗p<0.01). Statistical analysis used is student t-test.*

When Colchicine or CA4 was administered to proliferative AC10 cells continually for 96 hrs, with the cells primed with enalapril or enalaprilat for 24 hrs, a smaller but yet significant reduction in cytotoxicity was observed (Table 4-7). Reversal of drug addition, with enalapril/enalaprilat added 24 hrs after VDA had no effect on 96 hr exposure to either Colchicine or CA4 or 24 hr exposure to Colchicine (Table 4-7). However, a reduced but significant effect was observed when enalapril was added 24hr after exposure of AC10 cells to CA4 for 24hrs (Table 4-7).

A similar response was also observed when VDAs in the presence of enalapril or enalaprilat were administered to AC10 cells in the plateau growth phase, representative of the *in vivo* situation. Administration of enalapril or enalaprilat 24 hrs prior to exposure of quiescent AC10 cells to VDAs caused a 25-50% reduction in the cytotoxicity observed, for both 24 and 96 hr VDA exposure periods (Table 4-8). As was observed with proliferative AC10 cells, no protective effects were observed when enalapril or enalaprilat were administered after exposure to either VDA for 96 hrs or 24 hr exposure to Colchicine (Table 4-8). However, a reduced but significant effect was observed when enalapril was added 24hr after exposure of quiescent AC10 cells to CA4 for 24hrs (Table 4-8).

4.4.8 Cytotoxicity of VDAs Against AC10 Cells is Reduced by Combination with the Angiotensin Receptor Blocker (ARB) Telmisartan.

The response of cardiomyocytes to combined treatment of VDAs with Telmisartan was investigated in both exponential and plateau phase of growth with both 24 and 96 hrs VDA exposure periods.

Administration of the angiotensin receptor blocker (ARB) telmisartan 24 hrs prior to exposure of exponentially growing AC10 cells to a 24-hr exposure to either Colchicine or CA4 resulted

in a significant improvement in cell viability (Table 4-9). Similarly, 96 hr continuous exposure of both VDAs, with the cells primed with telmisartan for 24 hrs, also resulted in a significant reduction in cytotoxicity (Table 4-9). Alternatively, if the converse schedule was applied and telmisartan was added after the addition of VDAs, a significant inhibition of cytotoxicity was observed with 96 hr continuous exposure of either Colchicine or CA4, but only with CA4 in the case of 24 hr VDA exposure (Table 4-9).

In agreement with studies of proliferative AC10 cells, in quiescent AC10 cells administration of telmisartan prior to VDA treatment also retarded the cytotoxic effects of these drugs with both 24 and 96 hr exposure durations (Table 4-10). However, although an effect was observed with addition of telmisartan after CA4 addition, no such protective effects were observed in the case of Colchicine (Table 4-10).

4.4.9 Cytotoxicity of VDAs Against AC10 Cells is Reduced by Combination with the Beta-Adrenoreceptor Inhibitor Carvedilol.

The response of cardiomyocytes to combined treatment of VDAs in the presence of the beta-adrenoceptor blocker Carvedilol was investigated in both exponential and plateau phase of growth with both 24 and 96 hrs VDA exposures. Addition of carvedilol, either before or after Colchicine or CA4 administration, to exponentially growing AC10 cells was shown to significantly reduce cytotoxicity following both 24 hr and 96 hr treatment regimens of the VDAs (Table 4-11).

24 hr exposure		Colchicine	CA4
First drug addition	**Second drug addition**	**IC$_{50}$ value (nM)**	**IC$_{50}$ value (nM)**
VDA	-	53.3 ± 5.7	20.0 ± 1.5
Enalapril (1μM)	VDA	106 ± 2.2 *	39.2± 1.1 *
VDA	Enalapril (1μM)	45.6 ± 2.7	25.7 ± 1.4*
Enalaprilat (1μM)	VDA	64.8 ± 4.2*	26.3 ± 0.9*
VDA	Enalaprilat (1μM)	44.3 ± 1.3	21.5 ± 1.1

96 hr exposure

VDA	-	41.3 ± 6.7	12.7 ± 1.3
Enalapril (1μM)	VDA	62.4± 1.5*	20.6± 1.4*
VDA	Enalapril (1μM)	40.8± 1.7	15.2 ± 1.5
Enalaprilat (1μM)	VDA	59.4 ± 1.0*	19.6 ± 3.8*
VDA	Enalaprilat (1μM)	40.9 ± 2.9	13.3 ± 2.8

Table 4-8: Effect of combination therapy of Enalapril/Enalaprilat and VDAs on quiescent AC10 cells.*Cells in the plateau phase of growth were administered enalapril or enalaprilat either 24hrs before or after exposure to Colchicine or CA4 with the effect on VDA-induced cytotoxicity determined (indicated by IC$_{50}$ value). Cells were either in the presence of VDAs for 24hrs, with a subsequent 48 hr VDA-free period, or continuously for 96 hrs. Cytotoxicity was determined by MTT assay. Data are mean of three independent replicates ± SEM. Statistically significant values relative to control, (∗p<0.05 or ∗∗p<0.01). Statistical analysis used is student t-test.*

24 hr exposure		Colchicine	CA4
First drug addition	**Second drug addition**	**IC$_{50}$ value (nM)**	**IC$_{50}$ value (nM)**
VDA	-	45 ± 5.8	7.5 ± 0.7
Telmisartan (200nM)	VDA	64.8 ± 1.2*	15.4 ± 1.9*
VDA	Telmisartan (200nM)	44.6 ± 2.6	16.2 ± 1.8*

96 hr exposure

VDA	-	31.3 ± 1.1	4.4 ± 0.6
Telmisartan (200nM)	VDA	50.7 ± 2.9*	12.6 ± 1.8*
VDA	Telmisartan (200nM)	52.4 ± 3.5**	11.3 ± 1.1*

Table 4-9: Effect of combination therapy of Angiotensin Receptor blocker, Telmisartan, and VDAs on proliferative AC10. *Cells in the exponential phase of growth were administered telmisartan either 24hrs before or after exposure to Colchicine or CA4 with the effect on VDA-induced cytotoxicity determined (indicated by IC$_{50}$ value). Cells were either in the presence of VDAs for 24hrs, with a subsequent 48 hr VDA-free period, or continuously for 96 hrs. Cytotoxicity was determined by MTT assay. Data are mean of three independent replicates ± SEM. Statistically significant values relative to control, (∗p<0.05 or ∗∗p<0.01). Statistical analysis used is student t-test.*

24 hr exposure		Colchicine	CA4
First drug addition	**Second drug addition**	**IC$_{50}$ value (nM)**	**IC$_{50}$ value (nM)**
VDA	-	53.3 ± 5.7	20.0 ± 1.5
Telmisartan (200nM)	VDA	120.6 ± 1.3*	61.9 ± 4.3**
VDA	Telmisartan (200nM)	65.6 ± 1.2	42.7 ± 3.4*

96 hr exposure

VDA	-	41.3 ± 6.7	12.7 ± 1.3
Telmisartan (200nM)	VDA	87.5 ± 3.1*	35.7 ± 4.0*
VDA	Telmisartan (200nM)	40.7 ± 0.9	18.7 ± 0.4*

Table 4-10: Effect of combination therapy of Angiotensin Receptor blocker, Telmisartan, and VDAs on quiescent AC10 cells. *Cells in the plateau phase of growth were administered telmisartan either 24hrs before or after exposure to Colchicine or CA4 with the effect on VDA-induced cytotoxicity determined (indicated by IC$_{50}$ value). Cells were either in the presence of VDAs for 24hrs, with a subsequent 48 hr VDA-free period, or continuously for 96 hrs. Cytotoxicity was determined by MTT assay. Data are mean of three independent replicates ± SEM. Statistically significant values relative to control, (∗p<0.05 or ∗∗p<0.01). Statistical analysis used is student t-test.*

24 hr exposure		Colchicine	CA4
First drug addition	**Second drug addition**	**IC$_{50}$ value (nM)**	**IC$_{50}$ value (nM)**
VDA	-	45 ± 5.8	7.5 ± 0.7
Carvedilol (200nM)	VDA	87.3 ± 2.8*	31.8 ± 3.2*
VDA	Carvedilol (200nM)	60.5 ± 3.3*	17.6 ± 0.8*

96 hr exposure

VDA	-	31.3 ± 1.1	4.4 ± 0.6
Carvedilol (200nM)	VDA	65.5 ± 3.2*	17.9 ± 1.7*
VDA	Carvedilol (200nM)	45.7 ± 1.0*	12.4 ± 1.4*

Table 4-11: Effect of combination therapy of Carvedilol and VDAs on proliferative AC10.

Cells in the exponential phase of growth were administered carvedilol either 24hrs before or after exposure to Colchicine or CA4 with the effect on VDA-induced cytotoxicity determined (indicated by IC$_{50}$ value). Cells were either in the presence of VDAs for 24hrs, with a subsequent 48 hr VDA-free period, or continuously for 96 hrs. Cytotoxicity was determined by MTT assay. Data are mean of three independent replicates ± SEM. Statistically significant values relative to control, (∗p<0.05 or ∗∗p<0.01). Statistical analysis used is student t-test.

Administration of carvedilol and VDAs to AC10 cells in the plateau growth phase demonstrated a mixed response dependent on the timing of carvedilol addition and specific VDA (Table 4-12). When added 24 hrs prior to exposure of quiescent AC10 cells, a 50% reduction in the cytotoxicity of both Colchicine and CA4 was detected for 24 hr exposure to the VDAs (Table 4-12). Prior-exposure to carvedilol was only able to reduce the cytotoxicity of CA4, but not Colchicine, with continuous 96 hr exposure to VDAs (Table 4-12). In contrast to proliferative AC10 cells, with quiescent AC10 cells, no protective effects were observed when the VDA was added before carvedilol and the exposure was continuous throughout the 96 hr period (Table 4-12). However, a protective effect was observed when carvedilol was added after exposure of quiescent AC10 cells to CA4, but not Colchicine, and the exposure of VDA was limited to 24hrs (Table 4-12).

24 hr exposure		Colchicine	CA4
First drug addition	**Second drug addition**	**IC$_{50}$ value (nM)**	**IC$_{50}$ value (nM)**
VDA	-	53.3 ± 5.7	20.0 ± 1.5
Carvedilol (200nM)	VDA	100.2 ± 0.6*	41.3 ± 3.1*
VDA	Carvedilol (200nM)	61.5 ± 1.1	42.7 ± 3.2*

96 hr exposure

VDA	-	41.3 ± 6.7	12.7 ± 1.3
Carvedilol (200nM)	VDA	41.3 ± 3.1	29.3 ± 1.2*
VDA	Carvedilol (200nM)	42.7 ± 3.2	14.3 ± 0.7

Table 4-12: Effect of combination therapy of Carvedilol and VDAs on quiescent AC10

cells. *Cells in the plateau phase of growth were administered carvedilol either 24hrs before or after exposure to Colchicine or CA4 with the effect on VDA-induced cytotoxicity determined (indicated by IC$_{50}$ value). Cells were either in the presence of VDAs for 24hrs, with a subsequent 48 hr VDA-free period, or continuously for 96 hrs. Cytotoxicity was determined by MTT assay. Data are mean of three independent replicates ± SEM. Statistically significant values relative to control, (∗p<0.05 or ∗∗p<0.01). Statistical analysis used is student t-test.*

4.5 Discussion

Despite showing significant promise as cancer therapeutics, through their ability to destroy the vascular networks of tumours and cause widespread tumour necrosis, in preclinical studies these drugs were shown to have potential adverse effects upon the cardiovascular system (Gill et al., 2019, Tochinai et al., 2016, Rustin et al., 2010, Nathan et al., 2012, Zweifel et al., 2011). In many cases, drug-induced adverse effects upon the cardiovascular system are associated with direct cytotoxicity and cellular loss coupled with compensatory cardiac remodelling, morphological alteration of cardiac cells and subsequent reduced activity and functionality, perturbation of cardiac cellular dynamics, and acute electrophysiological disturbances leading to dysrhythmias and disrupted cardiac function (Albini et al., 2010, Dolci et al., 2008, Pai and Nahata, 2000). In essence these effects can be categorised as either functional or structural cardiotoxicity, with the former often linked to dysregulation of ion channel function and coordination, a risk screened for during preclinical studies with the hERG assay or CiPA initiative (Cavero and Holzgrefe, 2014, Gintant et al., 2016, Friedrichs et al., 2005). In contrast, the latter, drug-induced structural cardiotoxicity, is less well characterised preclinically, especially during *in vitro* studies.

Important considerations for analysis of drug-induced cardiotoxicity, or similar processes, *in vitro* is the use of an appropriate model. One such criterion is the degree of proliferative capacity in the model and the relationship to cardiac tissue. Whereas neonatal cardiomyocytes have been used for *in vitro* studies, they have a relatively high proliferative potential and this does not extrapolate directly to adult cardiomyocytes where cellular proliferation is believed to be much lower or in some cases negligible (Siddiqi and Sussman, 2014). Consequently, it is not yet possible to fully recapitulate the *in vivo* contextual

environment *in vitro*. Therefore, an awareness of the limitations of a model is warranted. In this study, AC10 cells in the plateau phase of growth *in vitro* were utilised as a model for the *in vivo* cardiac situation. In this model, a 50% reduction in cells in S-phase and a concomitant 50% increase in cells in G_0/G_1 or G_2/M of the cell cycle compared to proliferative cells was observed. This lack of a complete cell cycle arrest or withdrawal in this cell model does therefore not align with the implication of adult cardiac tissue being post-mitotic and non-proliferative (Rumyantsev, 1977, Soonpaa et al., 1996, Karsner et al., 1925). This dogma has however now been questioned, with inaccuracies identified in terms of the cardiomyocyte context (Siddiqi and Sussman, 2014). Several studies have now proven contrary to initial hypotheses, adult mammalian heart undergoes a low grade of cardiomyocyte turnover (Siddiqi and Sussman, 2014, Karra and Poss, 2017). Furthermore, conventionally the cell cycle is purely assigned to events culminating in cell duplication and generation of daughter cells, but this fails to encompass seamlessly with the role of the cell cycle in hypertrophy and physiological multinucleation, both common phenomena in cardiac cells (Siddiqi and Sussman, 2014). In adult cardiac tissue, although proliferation and cellular turnover are low, cardiomyocytes continue to demonstrate hypertrophic expansion, a process which requires cell cycle activity but does not culminate in cytokinesis and a daughter cell (Siddiqi and Sussman, 2014, Zebrowski and Engel, 2013). Therefore, based on these insights and findings, it is now widely proposed that cardiomyocytes reside in a pre-mitotic rather than post-mitotic state, with a low rather than non-existent capacity for proliferation, and a capacity for cell cycle and microtubular activity. Based on this, the model used in this study whereby AC10 cells are evaluated within the plateau phase of growth, exhibits the appropriate phenotype for studies of cardiotoxicity of VDAs.

The induction of intracellular and structural cellular changes by VDAs and consequent potential for induction of structural cardiotoxicity is central to appraising the risk these drugs pose for clinical use. Colchicine and CA4 bind to tubulin via the Colchicine-binding site and inhibit its polymerisation (Hill et al., 1993, Bibby et al., 1989, Baguley et al., 1996, Cai, 2007). These effects to disrupt tubulin dynamics result in a panoply of potential effects in the cells, most notably suppression of microtubule formation and subsequent disturbance of mitosis, alterations in cellular shape, and disruption of cellular signalling pathways (Lu et al., 2012). In the context of cardiac cells, in this study, both Colchicine and CA4 interacted with intracellular tubulin at clinically relevant concentrations, supporting both cellular entry and target interactions in this cell line. This interaction with tubulin was also shown to cause arrest of proliferative AC10 cardiomyocytes in G2/M of the cell cycle, an effect proportional to increase in both dose and exposure time. Similarly, exposure of AC10 cells in their plateau phase of growth, representative of cardiomyocytes in cardiac tissue, to both short-term and continuous presence of VDAs also caused a further accumulation of cells in G2/M of the cell cycle. These observations support the conventional mechanism of action of both Colchicine and CA4 in these cells, through direct interaction and disruption of cellular microtubules. These results also highlight the potential risk of VDAs towards cardiomyocytes with low proliferative potential, such as predicted in the adult heart.

The role of microtubules in cardiac cells was for many years overlooked due to the belief at that stage that cardiomyocytes were completely terminally differentiated and had no capacity for cellular division (Kerfant et al., 2001). This changed upon elucidation of a role wider than mitotic control for tubulin in cellular dynamics, such as intracellular regulation of organelles and expression and control of cell surface receptors and ion channels (Schappi et al., 2014,

Song et al., 2014, Sasaki et al., 2014, Joseph et al., 2014, Wolff, 2009). The observation that microtubule content was increased in pressure-overload cardiac hypertrophy and that the increased microtubule network impacted the rigidity of failing cardiomyocytes further highlighted the central role for tubulin in cardiomyocyte structure and function (Kerfant et al., 2001, Tagawa et al., 1997). Cardiac hypertrophy can be defined as the ventricular enlargement occurring as a consequence of either volume or pressure overload, in an effort to maintain cardiac output (Sano et al., 2007, Cantor et al., 2005, Shimizu and Minamino, 2016). In addition to physiologically-driven hypertrophy, such as with pregnancy and exercise, the heart can also undergo pathological hypertrophy associated with abnormal haemodynamic stresses, pressure-overload, cardiac necrosis, and drug-induced toxicities (Shimizu and Minamino, 2016). Unlike physiological hypertrophy wherein the response is adaptive and focused on enhanced cardiac function, pathological cardiac hypertrophy is often associated with loss of cardiac cells, fibrosis and progressive loss of cardiac function (Shimizu and Minamino, 2016).

Many cytotoxic cancer chemotherapeutics are associated with development of overt cardiac remodelling and late-stage heart failure, through cardiac remodelling and inherent cardiomyocyte hypertrophy as a compensatory mechanism for the chemotherapy-induced loss of cardiac cells (Du et al., 2017, Geisberg and Sawyer, 2010, Sawyer et al., 2010, Tagawa et al., 1997, Schmidinger et al., 2008). The AC16 cardiomyocyte cell model and more recently AC10 cardiomyocyte cell model, used in this study, have previously been used to assess drug-induced hypertrophy and to investigate pathways relating to cellular hypertrophy of cardiomyocytes (Xiao et al., 2017, Rockley and Gill, 2017). To address whether such a response also associates with VDAs, AC10 cells were exposed to Colchicine and CA4 in both

the proliferative and quiescent growth phases, which indicated a significant increase in cell size measured by flow cytometry. To confirm that this increase in size was a consequence of hypertrophy rather than an artefact of cell detachment and flow cytometric analyses, cells exposed to CA4 were imaged and cell sizes determined manually, which confirmed the response. Furthermore, to ascertain the potential for hypertrophy occurring alongside loss of cardiomyocyte mass, the expected situation in the clinic, parallel studies calculating loss of cell viability, cell number and changes in cell morphology concurrent with changes in cell size were performed. AC10 cells exposed to CA4 confirmed dose-dependent decreases in cell viability and increases in cell size, indicating the realistic potential for compensatory cellular hypertrophy and a change in morphology concurrent with cellular loss. This observation supported the rodent study of CA4DP, wherein cardiac ischaemia and cardiac cell hypertrophy was proposed as an underlying cause of contractile disturbances detected by ECG (Tochinai et al., 2018).

The hypertrophic response of AC10 cardiac cells to a cytotoxic agent, such as Colchicine and CA4, is an expected response based on studies of several other cytotoxic cancer chemotherapies (Du et al., 2017, Geisberg and Sawyer, 2010, Sawyer et al., 2010, Tagawa et al., 1997, Rockley and Gill, 2017, Schmidinger et al., 2008). However, the involvement of tubulin and microtubules in the action of these drugs adds a further dimension to the hypertrophic response, one which may further complicate the cardiotoxicity profile of these drugs. An increase in microtubule content is reported in pathological hypertrophy, with implications for contractility of cardiomyocytes and subsequent cardiac function (Kerfant et al., 2001, Tagawa et al., 1997). In this context, VDAs may well have a secondary activity exacerbated in the continued presence of pathological hypertrophy through effects on this

imbalance in cellular microtubule levels. Microtubule disruption, including exposure to Colchicine and other tubulin-binding agents, has previously been shown to modulate cardiomyocyte contractility, cardiomyocyte electrophysiology, and β-adrenergic responses (Lampidis et al., 1986, Palmer et al., 1998, Webster and Patrick, 2000, Kerfant et al., 2001). Worth to mention that observed hypertrophy could also indicate possibility of senescence. However, senescence was not measured in this study, please refer to section 7.3 in regard to future work recommended for assessment whether cells were senescent. It remains to be determined whether VDA-induced hypertrophy does indeed lead to an increase in intracellular microtubules and a continuum of detrimental effects in this context. Although it was not measured in this study, microtubule dynamics is usually assessed by the determination of the four parameters of dynamic instability: growth speed, shrinkage speed, catastrophe frequency, and rescue frequency. Development of cardiac liabilities following cancer chemotherapy is well established clinically, particularly with the anthracycline class of drug (Gill et al., 2019). In an attempt to manage or circumvent these toxicities, co-administration of cardioprotective agents such as β-adrenoceptor blockers, the iron chelator dexrazoxane, and agents targeting the renin-angiotensin signalling pathway have been evaluated clinically (Gould et al., 2007, Cardinale et al., 2013, Cardinale et al., 2010, Kalam and Marwick, 2013, Wiseman and Spencer, 1998). Based on the promising outcomes achieved through co-administration of cardioprotective agents with other cancer chemotherapeutics, the potential to apply the same concepts to mitigate VDA-induced cardiotoxicity is an attractive approach for the clinic (Ke et al., 2015, Ke et al., 2009, Busk et al., 2011).

In preclinical rodent studies of the Colchicine-derivative VDA, ZD6126, pre-administration of atenolol, a β_1-adrenoceptor selective blocker, was shown to reverse the hypertension and

associated tachycardia associated with this agent (Gould et al., 2007). Despite these effects being monitored at the systemic level, the molecular action of these drugs is to target the β_1-adrenoceptor subtype located primarily on cardiomyocytes, which results in functional effects such as decreased heart rate and contractility alongside structural effects such as cardiomyocyte relaxation (Wallukat, 2002). Atenolol has negligible effects upon the vasculature due to its selectivity for β_1-adrenoceptors, as opposed to β_2-adrenoceptors which are expressed in vascular smooth muscle and have a very limited effect on vascular tone (Conti et al., 2013, Bylund, 2007, Oshima et al., 2014). This thereby supports the protective effects against ZD6126 induced cardiotoxicity been mediated through cardiomyocyte regulation, which consequently reduces cardiac output and hypertension. Additionally, Colchicine has been shown to exacerbate β-adrenergic signalling in cardiac hypertrophy, further supporting the benefit of β_1-adrenoceptor blocker administration for mitigation of detrimental VDA-induced cardiac effects (Palmer et al., 1998, Kerfant et al., 2001). In the current study the β-adrenoceptor blocker carvedilol demonstrated negligible inherent toxicity itself but acted to augment the sensitivity of AC10s to both Colchicine and CA4 cytotoxicity. In the case of proliferative AC10 cells, the sequence of addition of carvedilol, either 24hrs before or after the VDA, did not influence its ability to reduce either short-term (24hr) or long term (96hr) exposure VDA cytotoxicity. However, when administered to AC10 cells in the plateau growth case, purported to recapitulate the clinical cardiac situation, the β-adrenoceptor blocker only reduced cytotoxicity of Colchicine when administered for a short-period and when administered prior to the VDA. With CA4, the β-adrenoceptor blocker could also reduce cytotoxicity of long exposure to the VDA and short-term CA4 exposure when the cardioprotective agent was administered after the VDA, implying a reduced effect of CA4 on

tubulin activities associated with the β-adrenoceptor signalling relative to Colchicine, for which the mechanism is not yet known. Alternatively, the differences in response between Colchicine and CA4 may well be due to the differential dynamic of binding to tubulin, as Colchicine has a very long residence time and slow disassociation rate relative to CA4, with implications for interference with signalling pathways (McLoughlin and O'Boyle, 2020, La Sala et al., 2019).

The rationale for inhibition of the angiotensin signalling pathway is the role it plays in cardiovascular remodelling, with this pathway implicated in both cardiomyocyte growth and left ventricular hypertrophy (Azevedo et al., 2016, Higuchi et al., 2007, Erhardt, 2005). In the current study the ACEi enalapril, its active form enalaprilat, and the angiotensin receptor blocker telmisartan all were effective in reducing the cytotoxicity of both Colchicine and CA4. As was observed with β-adrenoceptor blockade, effects against CA4 were more pronounced than that of Colchicine, possibly reflecting the faster dissociation of CA4 over Colchicine for tubulin (La Sala et al., 2019). Addition of telmisartan compared to enalapril/enalaprilat was shown to produce an improved effect, most likely due to the blockade of angiotensin signalling directly on the cell rather than modulation of the signalling molecule itself. Subsequently, telmisartan exhibited effects when administered after the VDA, whereas such effects were not as evident with the ACEi enalapril/enalaprilat. In this context, a surprising observation was the presence of a response from enalapril versus enalaprilat, as the former is a prodrug of the latter and thus requires metabolic activation. In the human body, angiotensin converting enzyme (ACE) is required to convert angiotensin I to angiotensin II, so enalaprilat, which is the active metabolite of the ACEi enalapril, reduces production of angiotensin II (Miller and Arnold, 2019). Although angiotensin I is thought to primarily

originate from the kidney, recent evidence points toward the existence of a local angiotensin-system in the myocardium to produces the necessary elements to create angiotensin II, although this is still believed to be incomplete with factors required earlier in the pathway, such as renin, being only present in the circulatory system and thus not in this current cellular model (Danser et al., 1999, Dostal and Baker, 1999, Schmermund et al., 1999). Despite this, the evidence for presence of angiotensin II in the cell model, potentially produced paracrine from the cardiac cells, is stronger and supports the response obtained with telmisartan. However, despite this, even if a local angiotensin system was active in the current AC10 model, this still does not explain the unexpected response obtained with enalapril, as the pathway for its activation is not believed to be found in the *in vitro* culture system. Therefore, the fact that a response was obtained with both enalapril and enalaprilat, in conjunction with weak evidence for a local renin-angiotensin pathway, raises questions about the mechanism underlying these effects. It is highly plausible, based on their very close structures, that enalapril and enalaprilat may be causing these effects by an off-target mechanism. For instance, the ACEi moexipril, the prodrug of moexiprilat, has been shown to exhibit activity against phosphodiesterase 4 (PDE4), a protein known to be involved in cardiac hypertrophy structure (La Sala et al., 2019, Abi-Gerges et al., 2021). It remains to be addressed whether such a mechanism could be responsible for the actions of enalapril.

Chapter 5. Evaluation of effects of VDA exposure upon cardiomyocyte function and cellular contraction.

5.1 Drug-induced functional cardiotoxicity

Myocardial cell contractility is the major essential element of heart function, facilitating synchronised cardiac contraction and maintenance of blood circulation. Consequently, drug-induced interference of the contractile properties of cardiomyocytes and synchronicity of cardiac electrophysiology would be significantly detrimental for cardiac function (Louch et al., 2011, Dorn and Molkentin, 2004). Based on this major issue, all drugs prior to entering the clinic must be evaluated for potential adverse effects upon the cardiovascular system (ICH, 2005a, ICH, 2009, ICH, 2005b). Conventionally this involved the *in vitro* assessment of a drugs ability to inhibit the hERG potassium channel in a genetically engineered cell line coupled to a preclinical *in vivo* cardiac study in mammals (Friedrichs et al., 2005), as described in section 1.3.2. However, more recently, the screening paradigm has undergone significant improvement through development of the CiPA initiative, involving *in silico* prediction studies alongside evaluation of drugs against stem-cell derived cardiomyocytes *in vitro* and more robust *in vivo* evaluations, see section 1.3.3 (Cavero and Holzgrefe, 2014, Dorn and Molkentin, 2004, Louch et al., 2011).

In the field of drug safety assessment, cardiomyocytes derived from stem cells have many advantages over the non-cardiac cell hERG assay and immortalised cardiac cell models, not least the ability to evaluate drug effects upon cardiomyocyte electrophysiology and contractile function (Chi, 2013, Scott et al., 2013, Seiler et al., 2011). Although exhibiting limitations associated with their immature phenotype, stem-cell derived cardiomyocytes (especially human induced pluripotent stem cell derived cardiomyocytes, hiPSC-CMs) are currently considered the most applicable *in-vitro* model for assessment of acute drug-induced functional effects studies, specifically drug-induced dysrhythmias (Blinova et al., 2018). The

use of these cell models alongside technologies to measure cardiac electrophysiology, such as microelectrode arrays (section 1.6.5), ion channel activity (section 1.6.4), or cardiac contractility, such as the xCELLigence RTCA (section 1.6.2), permit such assessments to be undertaken *in vitro* with ease and often in real-time.

Understanding the mechanism of drug-induced cardiotoxicity of these classes of therapeutic is therefore important in both determining the risk-benefit balance for drug administration and the subsequent management of cardiotoxic effects.

In preclinical *in vivo* studies, the VDA class of cancer therapeutic have been shown to cause a wide range of detrimental effects upon the cardiovascular system, including structural toxicity effects associated with cardiovascular cell death, vascular constriction and damage such as cardiac ischaemia, haemodynamic changes and hypo-/hypertension (Gill et al., 2019). Additionally, VDAs have also been suggested to induce perturbations in cardiac electrophysiology during preclinical studies, including disruption of ventricular repolarisation, drug induced inotropic and chronotropic effects, and atrial fibrillation (Subbiah et al., 2011, Dowlati et al., 2002b, Garon et al., 2016, Garon et al., 2010). In clinical trials, VDA administration was associated with drug-induced tachycardia and contradictory bradycardia; typically characterised by bradycardia within the first hour post-infusion followed by tachycardia around 3-4 hrs later, and a return to baseline by 24 hrs (Grisham et al., 2018, Rustin et al., 2003, Zweifel et al., 2011). Together this suggest that in addition to effects upon the vasculature system and potentially causing structural cardiotoxicity, as indicated in chapter 3, VDAs may also cause functional cardiotoxicity. However, the underlying mechanism, the duration of effects and degree of reversibility remain to be determined.

5.1.1 In vitro technologies for determination of cardiomyocyte cell contraction and functional response

There are many *in vitro* studies utilise embryonic stem cells (ESC) and induced pluripotent stem cell (iPSC) derived cardiomyocytes from both human and mouse to evaluate drug induced toxicity toward cardiac cells electrophysiology and contractility (Kho et al., 2015, Ali et al., 2004, Pouton and Haynes, 2007, GmbH, Takahashi and Yamanaka, 2006, Abassi et al., 2012, Dick et al., 2010, Ma et al., 2011, Nguemo et al., 2012). The main available *in vitro* technologies in this context are manual patch clamping by which the action potential duration (APD) is measured (Caspi et al., 2009, Verkerk et al., 2017), impedance measurements of cardiac cell contractility (Xi et al., 2011b, Abassi et al., 2012, Xi et al., 2011a) and the assessment of extracellular field potential (FP) by multi-electrode array (MEA) (Goineau and Castagné, 2018, Jans et al., 2017, Asai et al., 2010, Braam et al., 2010). These techniques were discussed in detail in chapter 1.

This study utilised the xCELLigence cellular impedance technology (described in section 2.12) to provides real-time, label-free non-invasive monitoring for viability and contractility of *in vitro* cardiac cell models. This methodology in combination with contractile cardiac cells, such as SC-CMs, provides sensitive and robust monitoring of both functional and structural drug induced cardiotoxicity (Xi et al., 2011a).

5.1.2 Stem-cell derived murine cardiomyocytes (Cor.At)

The use of murine embryonic stem (ES) cells and their derivation into functional cardiomyocytes (ES-CM) made a significant impact on cardiac drug safety assessments (Chi, 2013, Scott et al., 2013, Seiler et al., 2011). The possibility of obtaining beating cardiomyocytes from mouse embryonic stem (ES) cells by differentiation of embryoid bodies (EB) within the

stem cell was first reported over thirty years ago (Doetschman et al., 1985). However, these initial studies comprised a mixture of different cell types inside the EB, with cardiomyocytes comprise less than 5% of the total content (Kolossov et al., 2005). In order to produce a pure population of ES-CM, mouse ES cells (mES) were engineered to express resistance to the puromycin antibiotic, under control of the cardiac specific α-myosin heavy chain (α-MHC) promoter (Kolossov et al., 2005, Kolossov et al., 2006)

Cor.At® mESC-CM cells (Axiogenesis, Cologne, Germany) are a commercially available model with defined reproducibility and full characterisation. In addition to their quick development of contractile fibres and gap junctions, this cell model expresses cardiac-specific connexin-43 and excitation-contraction coupling, forms a functional syncytium, amenable to drug analysis after 72 hrs culture and demonstrates stable contractility over a period of time and is. They can be measured for up to three months. However, their stability is good over 2 weeks reliably. Like primary cell lines, Cor.At cells have highly aligned striated myofibrils arranged parallelly to each other on the long axis of the cardiomyocytes (Aratyn-Schaus et al., 2016). These cells also demonstrate normal electrophysiological cardiac activity in patch clamp, impedance assay and multielectrode array recording (Abassi et al., 2012). When compared to primary cardiac cells, neonatal cardiac cells, and immortalised cardiac cell lines, the Cor.At cell model exhibits several advantages, including a fully functional cardiac phenotype, expressing all ion channels related to cardiac contractility and cardiac action potentials (I_K, I_{Ca}, and I_{Na}) and cellular purity without fibroblast contamination (Kolossov et al., 2005, Sunesen et al., 2012). However, these cell models demonstrate both ventricular-like and atrial-like action potentials, offering a limitation in terms of drug effects upon specific cardiomyocyte sub-types (Sheehy et al., 2014). Taken together, the utility and cardiac representative nature

of the Cor-At® cell model coupled with the impedance-based xCELLigence Cardio RTCA offers a comprehensive in vitro approach for analyses of functional drug-induced changes in contractile structure and function (Aratyn-Schaus et al., 2016).

5.2 Aims and Objectives.

The aim of this chapter is to evaluate the effects of the VDA class of drug upon cardiomyocyte contractility *in vitro*, specifically cardiomyocyte beat-rate and morphological change. This was achieved using stem-cell derived murine cardiomyocytes (Cor.At®) assessed using the xCELLigence Cardio RTCA technology. The objectives are as follows:

1) Appraisal of the Cor.At® stem-cell derived cardiomyocytes against a panel of known cardioactive compounds using the xCELLigence Cardio RTCA system to optimise the methodology and ascertain response signatures.

2) Assessment of functional response of Cor.At stem-cell derived cardiomyocytes to clinically-viable concentrations of VDAs to ascertain degree, extent and mechanisms of VDA-induced functional cardiotoxicities.

5.3 Results

5.3.1 Confirmation of drug-induced perturbations in cardiomyocyte contractile function in response to known cardioactive drugs.

The Cor.AT® cells were applied to the xCELLigence Cardio system to confirm whether this impedance-based system could be used for reproducible evaluation of the effects of drugs upon both cellular survival and cardiac cell contractility, an indicator for drug-induced functional cardiotoxicity. These cells were seeded at 40,000 cells/well with the cells fully confluent at approximately 72 hrs. Throughout the initial growth period the contractility of the cells was monitored at regular intervals to confirm growth, establishment of a confluent syncytium and initiation of contractility. Although contractility became evident in some wells after approximately 40 hrs, this was inconsistent and erratic. Stability of the contractile phenotype of Cor.At® cells was observed from 72 hrs post-plating.

Exposure of the stably contractile Cor.At cells to E-4031, which blocks the hERG K^+ channel, or isoproterenol, a non-selective β-adrenoceptor agonist, were used to confirm characteristic response of the cells to cardioactive drugs. (Figure 5-1 and Figure 5-5) shows stable baseline beating at the point of addition of E4031 and isoproterenol, respectively. No measurable differences in beat-rate or beat amplitude were observed between the two studies.

Exposure of the cells to E4031 (500nM, 250nM and 50nM) led to both a dose and time dependent decrease in beat-rate (Figure 5-2, Figure 5-3 and Figure 5-4).

(A)
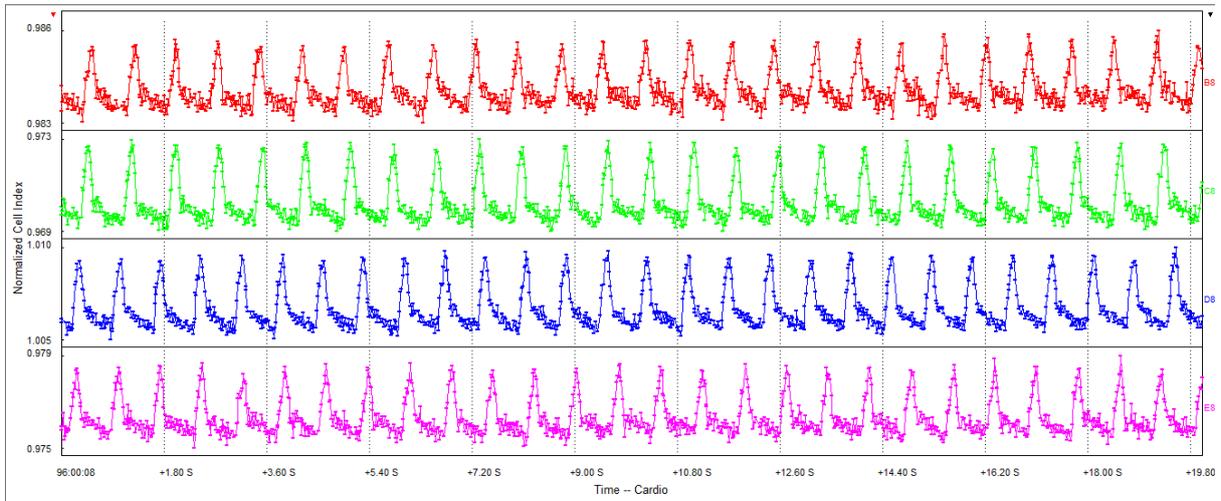
Control — 500 nM — 250 nM — 50 nM
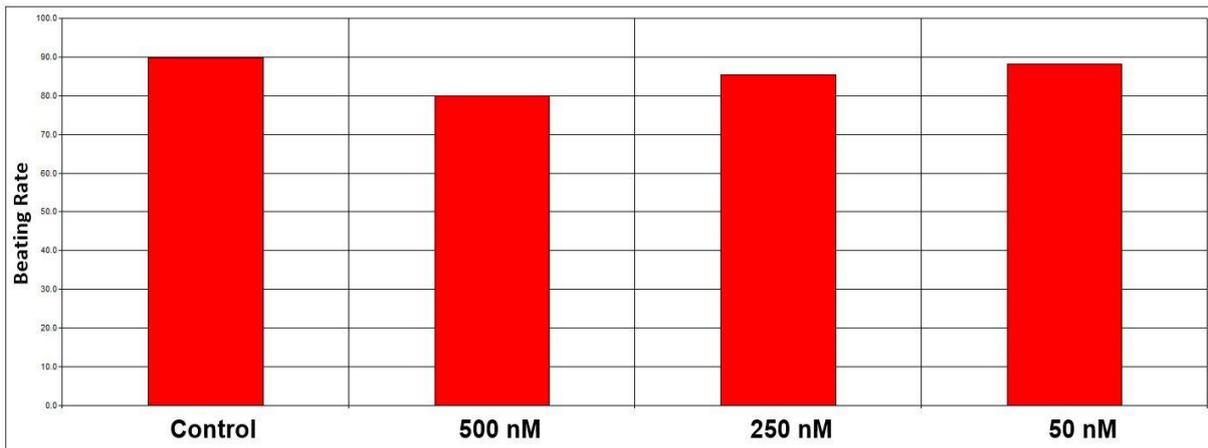
(B)

Figure 5-1: Effect of E4031 on Cor.At cardiomyocytes 0 hours after administration .

The effect of hERG K+ channel Blocker E4031 on (A) Contractility and (B) Beating rate of Cor.At cardiomyocytes 0 hrs after administration. Measurements are obtained from one well for each condition.

(A)

| | Control | 500 nM | 250 nM | 50 nM |
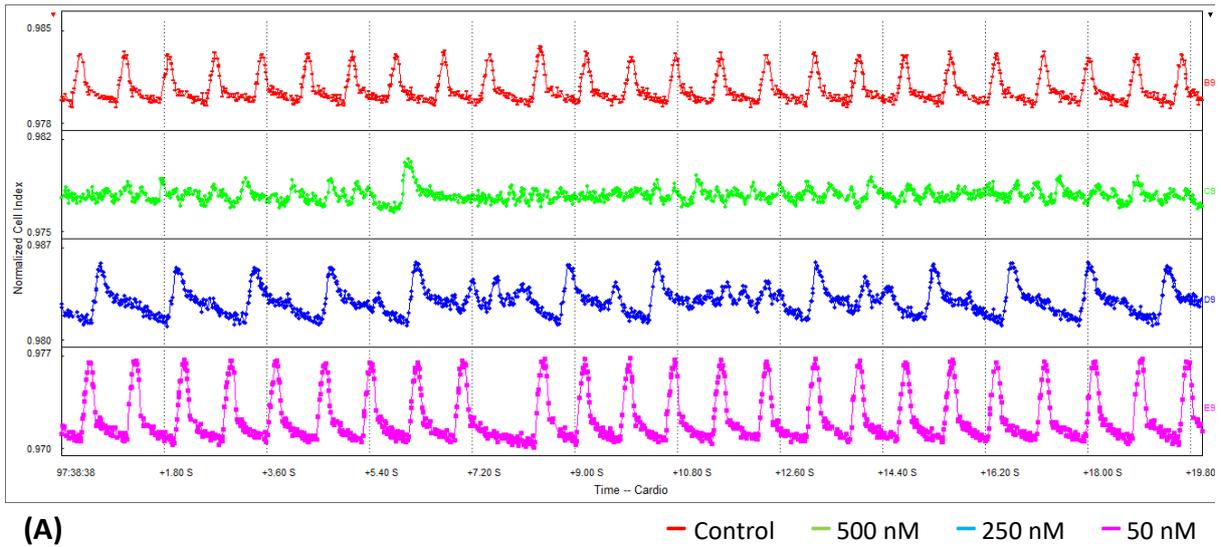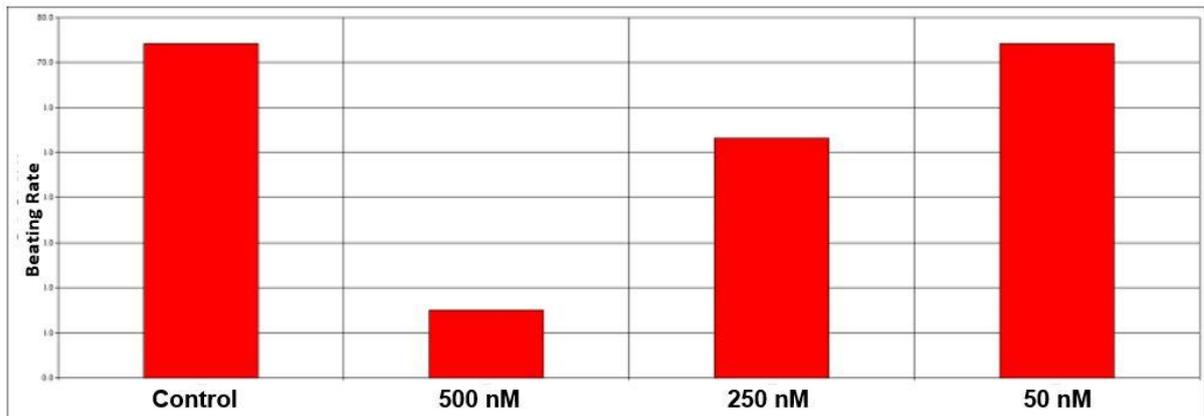
(B)

Figure 5-2: : Effect of E4031 on Cor.At cardiomyocytes 2 hours after administration.

Effect of hERG K+ channel Blocker E4031 on (A) Contractility and (B) Beating rate of Cor.At cardiomyocytes 2 hrs after administration. Measurements are obtained from one well for each condition.

(A)
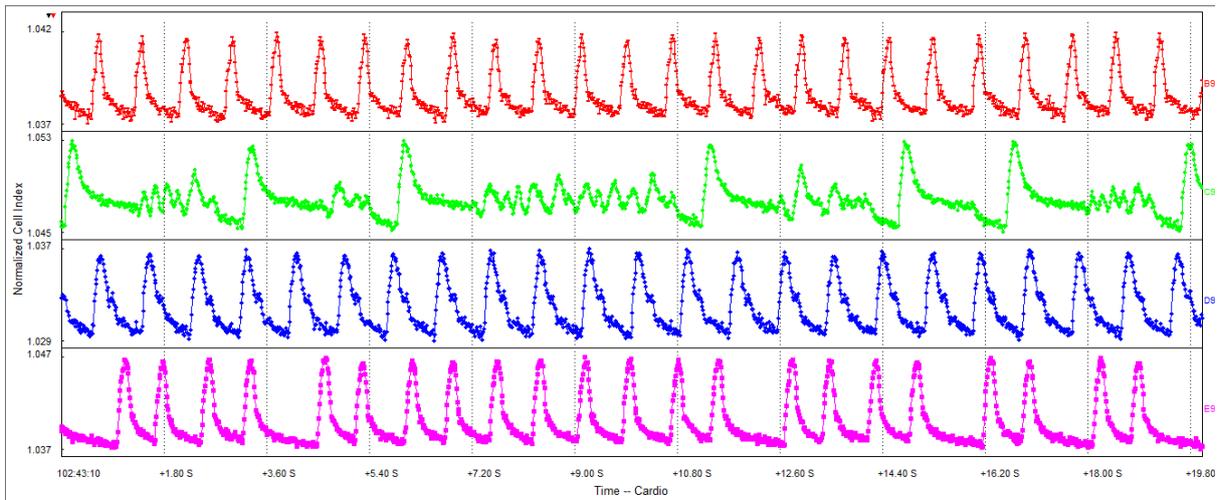
— Control   — 500 nM   — 250 nM   — 50 nM
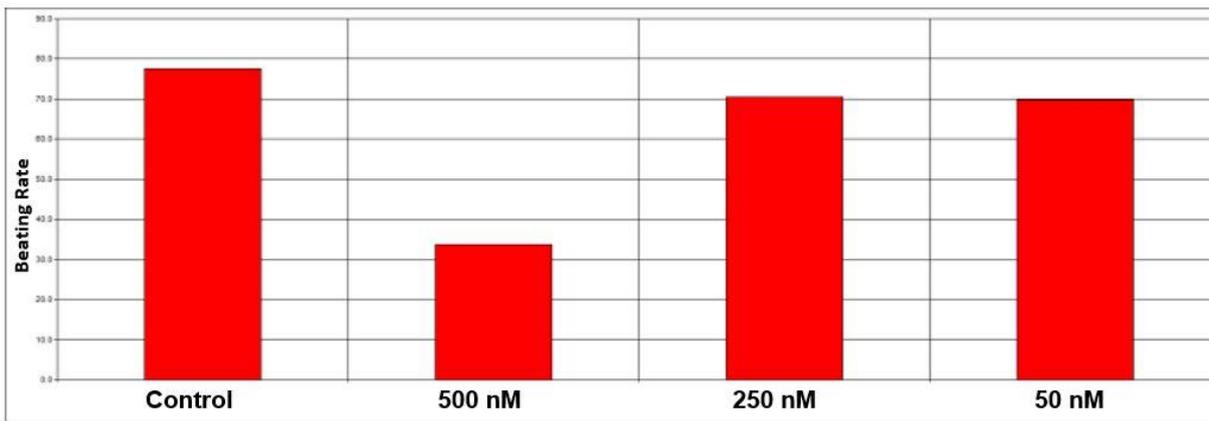
(B)

Figure 5-3: Effect of E4031 on Cor.At cardiomyocytes 6 hours after administration.

Effect of hERG K+ channel Blocker E4031 on (A) Contractility and (B) Beating rate of Cor.At cardiomyocytes 6 hrs after administration. Measurements are obtained from one well for each condition.

(A)
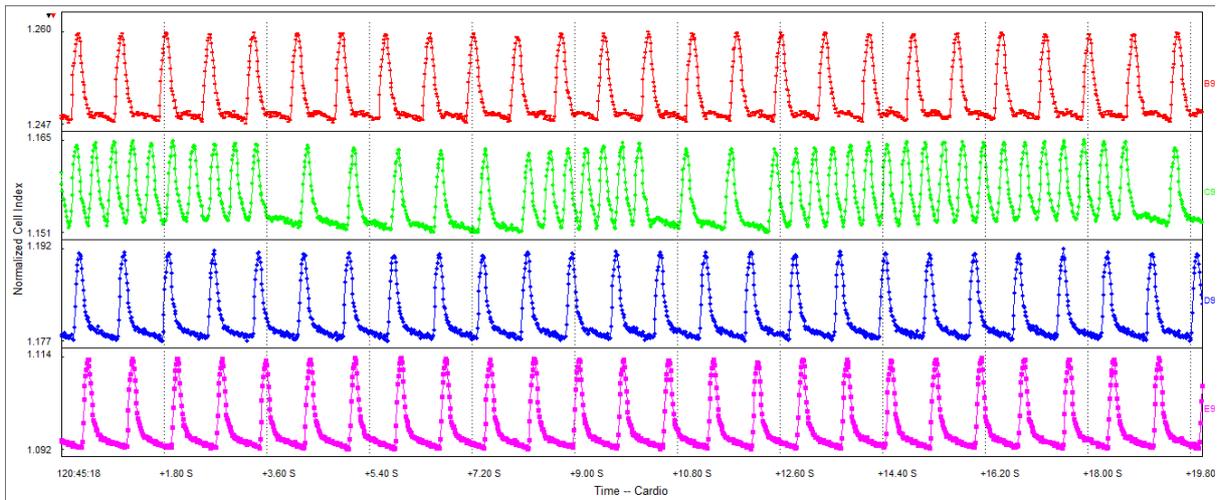
| | Control | 500 nM | 250 nM | 50 nM |
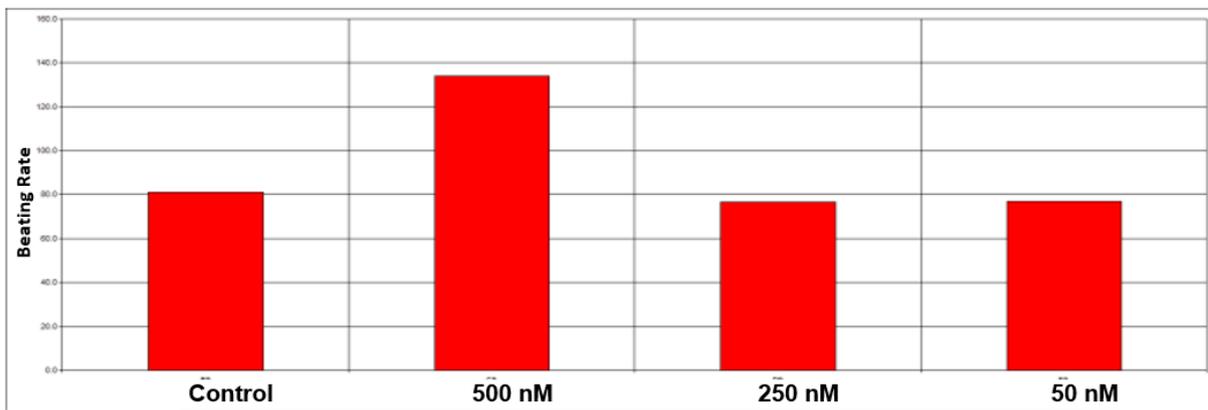
(B)

Figure 5-4: Effect of E4031 on Cor.At cardiomyocytes 24 hours after administration .

Effect of hERG K+ channel Blocker E4031 on (A) Contractility and (B) Beating rate of Cor.At cardiomyocytes 24 hrs after administration. Measurements are obtained from one well for each condition.

(A)
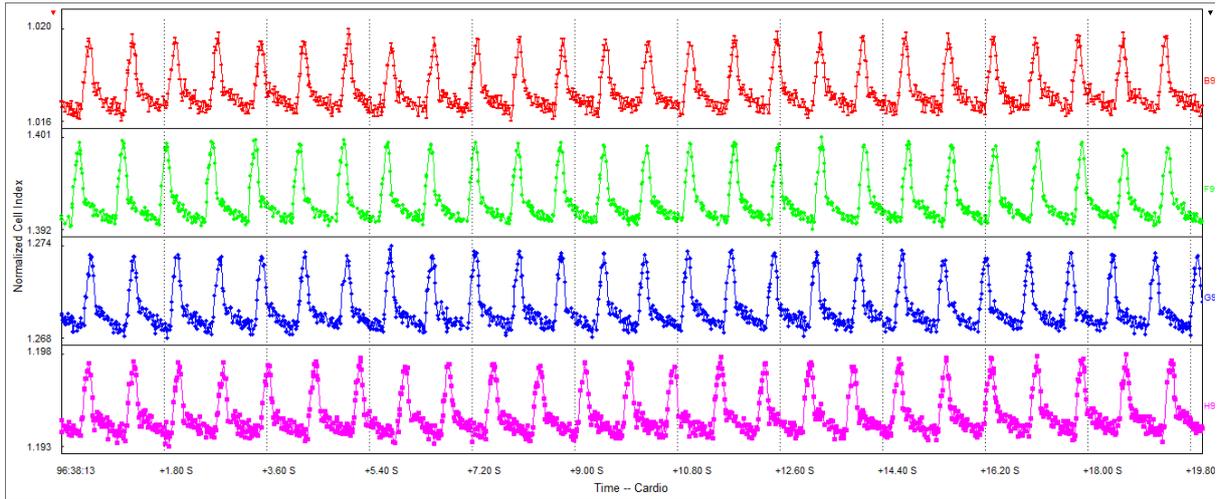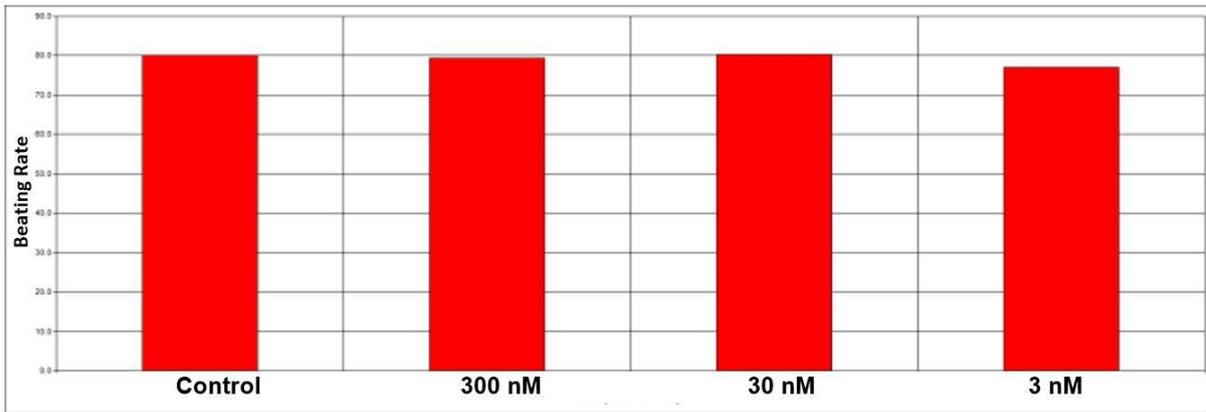
(B)

Figure 5-5: Effect of isoproterenol on Cor.At cardiomyocytes 0 hours after administration.

Effect of β-Blocker isoproterenol on (A) Contractility and (B) Beating rate of Cor.At cardiomyocytes 0 hrs after administration. Measurements are obtained from one well for each condition.

(A)

(B)
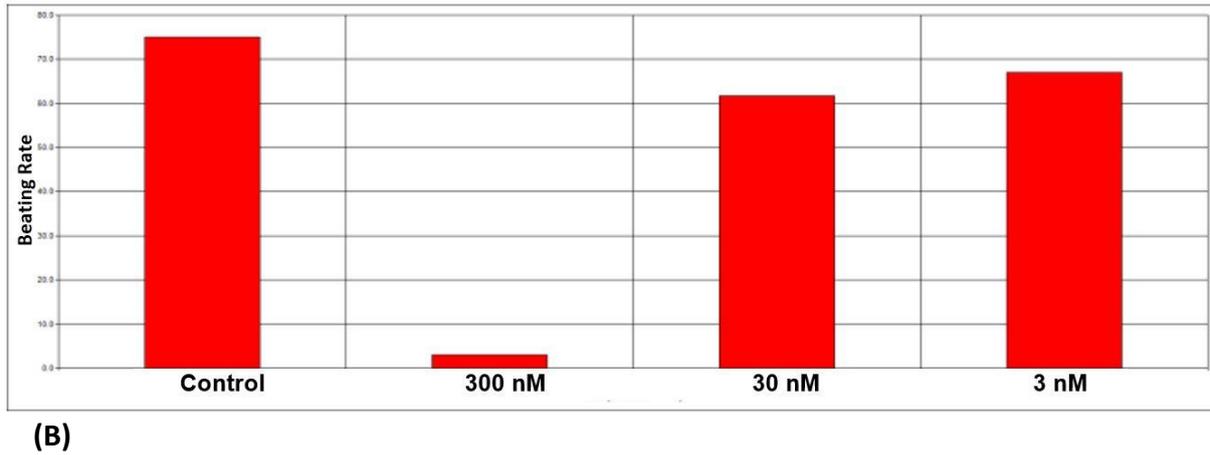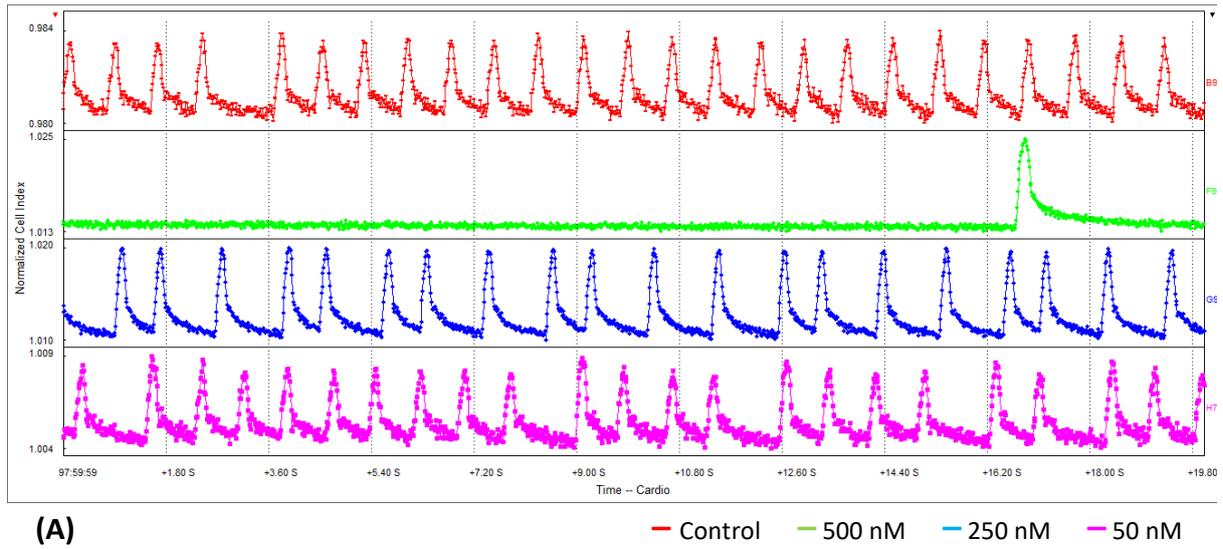
Figure 5-6: Effect of isoproterenol on Cor.At cardiomyocytes 2 hours after administration.

Effect of β-Blocker isoproterenol on (A) Contractility and (B) Beating rate of Cor.At cardiomyocytes 2 hrs after administration. Measurements are obtained from one well for each condition.

(A)
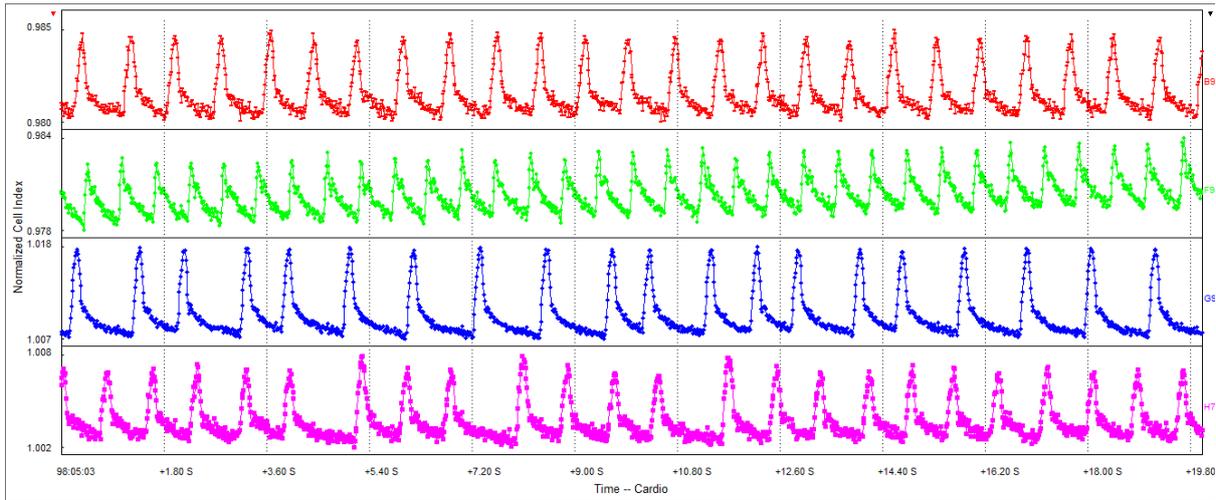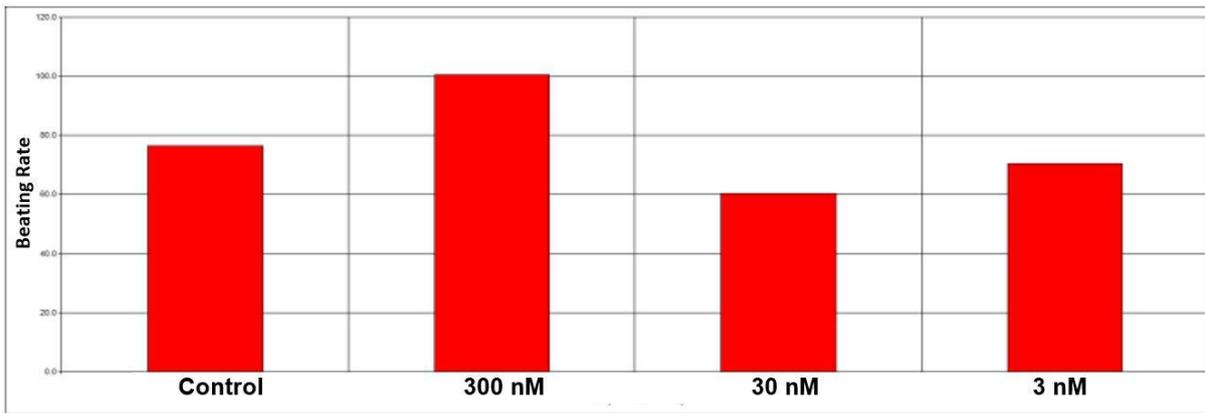
(B)

Figure 5-7: Effect of isoproterenol on Cor.At cardiomyocytes 24 hours after administration.

Effect of β-Blocker isoproterenol on (A) Contractility and (B) Beating rate of Cor.At cardiomyocytes 24 hours after administration. Measurements are obtained from one well for each condition.

There was a dose-dependent response of Cor.At® cells at 2 hrs post treatment with E-4031, with a defined arrhythmia observed at the highest concentration of 500nM (Figure 5-2).

(A)
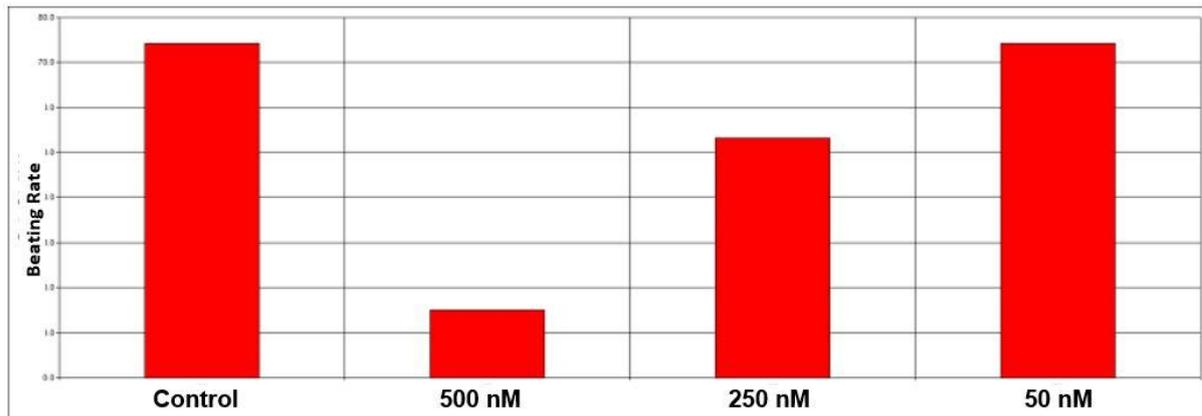
(B)

At 6 hrs after treatment (Figure 5-3), disruption of cardiac contractility was clearly observed with 500nM E-4031 and contraction at the highest dose remained significantly reduced with a fibrillatory appearance. By 24 hrs post-treatment (Figure 5-4) despite the cells recovering and a normal contractile phenotype being observed with lower doses (50nM and 250nM), exposure to the highest dose (500nM) resulted in a compensatory increased beat-rate indicative of reflex tachycardia. These responses are in agreement with the expected response of cardiomyocytes to E-4031.

Exposure of Cor.At® cells to isoproterenol only caused an effect at the highest concentration evaluated (300nM). An apparent cessation of contractility was observed at 2 hrs (Figure 5-6) representative of either a reflex blockade of cellular contraction or an overstimulation of contraction of these cells. However, the expected increase in contractility was observed with 300nM at 24 hrs post drug-addition (Figure 5-7). With lower concentrations (3nM and 30nM) no increase in contractility was observed at any of the timepoints evaluated. However, a

modest decline in contractility was observed with 30nM at 24 hrs after drug addition, indicative of either a reflex response to a modest drug-induced tachycardia or partial agonistic response to a sub-therapeutic concentration of isoproterenol in this cell type.

5.3.2 VDAs induce structural disturbances in stem-cell derived cardiomyocytes.

Cor.At cells were evaluated using the xCELLigence cardio RTCA system to assess the effect of the VDAs, Colchicine and CA4 on their morphology and viability over time. Exposure of Cor.At cells to VDAs induced a decrease in the cell index within 1 hr of drug-addition at all evaluated concentrations, when normalised to the point of drug-addition (Figure 5-8). This decline in cell index was observable with both Colchicine (100nM and 1µM) and CA4 (100nM) over the 8- hr period post drug exposure. In the case of 100nM drug concentrations this decline halted at 8 hrs with the cell index plateauing and then slowly rising by 24 hrs, suggesting that in this case the drugs were causing a change in cellular morphology rather than a cytotoxic response (Figure 5-8). In contrast, despite 1µM Colchicine presenting similar to 100nM Colchicine over the initial 8- hr exposure period, at this concentration the cell index did not plateau but rather continued to gradually decline and eventually 'flat-lined', implying cytotoxicity (Figure 5-8).

5.3.3 VDAs induce functional disturbances in stem-cell derived cardiomyocytes.

Exposure to VDAs caused both time and dose dependent effects on Cor.At cell contractility, affecting both the rate of contractility and the degree of cellular contraction, defined by the number and amplitude of contractions, respectively (Figure 5-10).

The effects of both Colchicine and CA4 upon the beating rate of Cor.At® cells was not observed to be significant over the first 4 hrs post-exposure (Figure 5-9 A,B &C).

However, although the xCELLigence trace for 100nM Colchicine was unremarkable relative to control, the traces for both 100nM CA4 and 1µM Colchicine were indicative of a perturbation of uniform cellular contraction and exhibited an intracontraction fibrillation or 'twitching' response, albeit not changing the overall contraction rate (Figure 5-9).
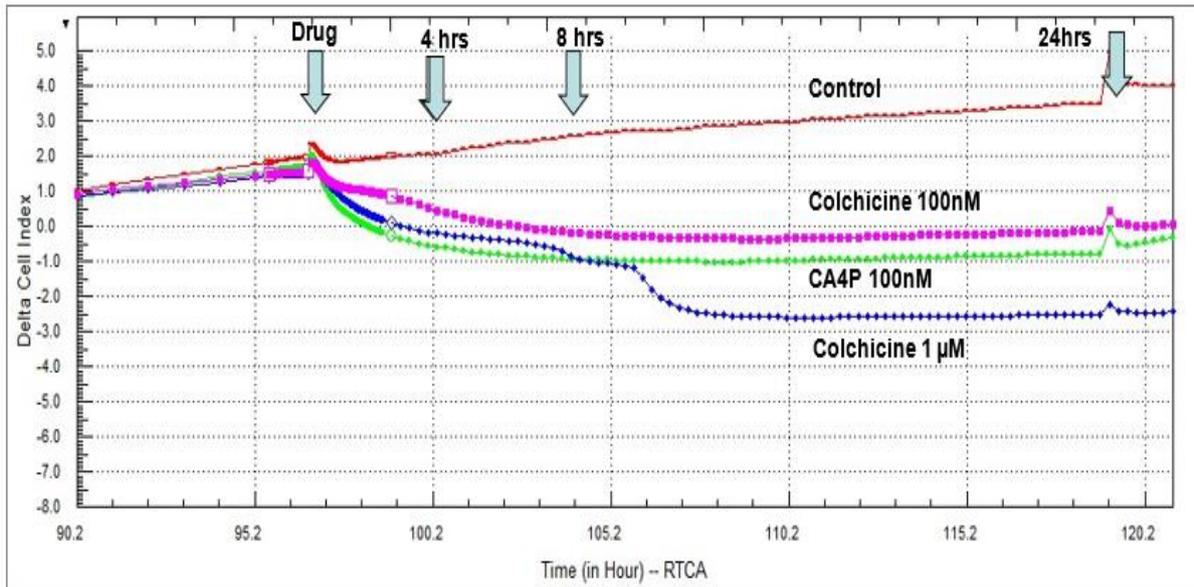
Figure 5-8: Effect of VDAs on morphology of Cor.At cardiomyocytes.

xCELLigence trace showing time (hrs) vs normalised cell index of Cor.At cells exposed to Colchicine (100nM 1uM) and CA4 (100nM) with points of addition (arrows) and exposure time indicated, data points shown are average of at least three wells.

By 8 hrs post-exposure, both 100nM CA4 and 1μM Colchicine appeared to cause a moderate increase in the contractile rate of Cor.At® cells, although this effect may not be a 'true' tachycardic response and may be artefactual based on the limited physical contraction of the cells at this time (Figure 5-9 C&D). Exposure to 100 nM Colchicine for 8 hrs was shown to cause a slight increase in contractile rate, with a trace appearance reflective of that observed with both 100nM CA4 and 1μM Colchicine after 4 hrs drug exposure (Figure 5-9). After 24 hrs drug exposure, the beat-rate of Cor.At® cells was reduced relative to control with both drugs at 100nM. However, in the case of 1μM Colchicine, there was a complete cessation of cellular contraction (Figure 5-9 D).

In contrast to the negligible effects upon Cor.At® beat-rate, both drugs induced a significant effect upon beat amplitude, representative of effects upon the physical mechanics of cellular contraction. A reduction in beat amplitude is indicative of a drugs interaction with the contractile machinery of the cell, the subsequent retardation of morphological change and degree of cellular 'stretch'. All VDAs and concentrations evaluated caused a time dependent decrease in beat amplitude, with effects evident by 4 hrs after drug exposure (Figure 5-10 B). By 8 hrs, the degree of cellular contractile morphological change was noticeably restricted in all cases. After 24 hrs, no contractions were observed with 1μM Colchicine reflecting either loss of cell viability or disruption of the syncytium (Figure 5-9 D). However, at this timepoint and with both 100nM CA4 and 100nM Colchicine, negligible cellular contraction was observed (Figure 5-9 D). These drug-induced effects upon the physical contractile mechanism of Cor.At®, without a concomitant change in contractile rate, are thus indicative of a drug effect upon the cells ability to rapidly reorganise its cytoskeleton structure coupled to limitation of the maximal 'stretch' response of the cell
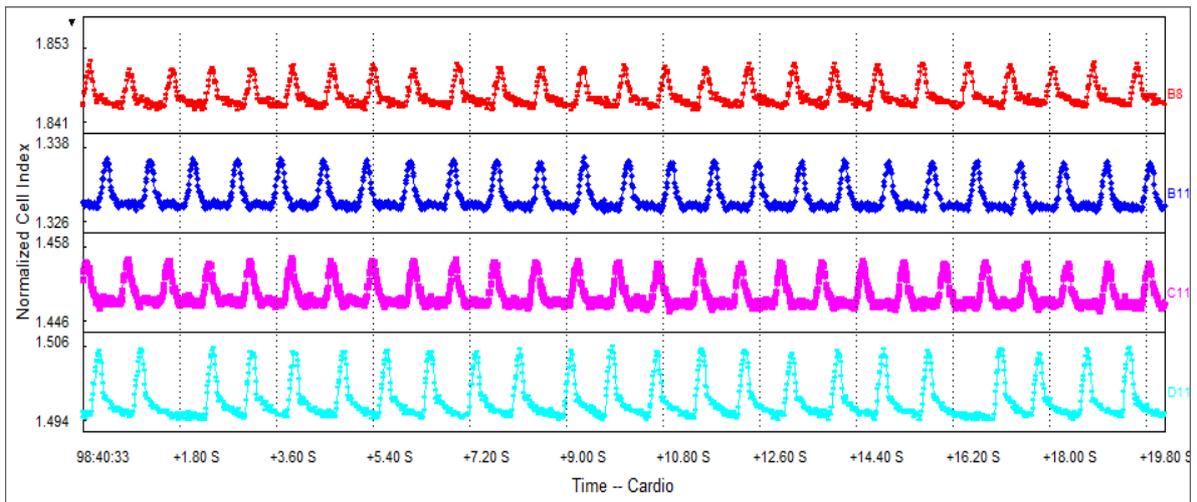
(A) Control — CA4 100 nM — Colchicine 1μM — Colchicine 100 nM

(B) Control — CA4 100 nM — Colchicine 1μM — Colchicine 100 nM

173

(C)

━ Control   ━ CA4 100 nM   ━ Colchicine 1μM   ━ Colchicine 100 nM

(D)
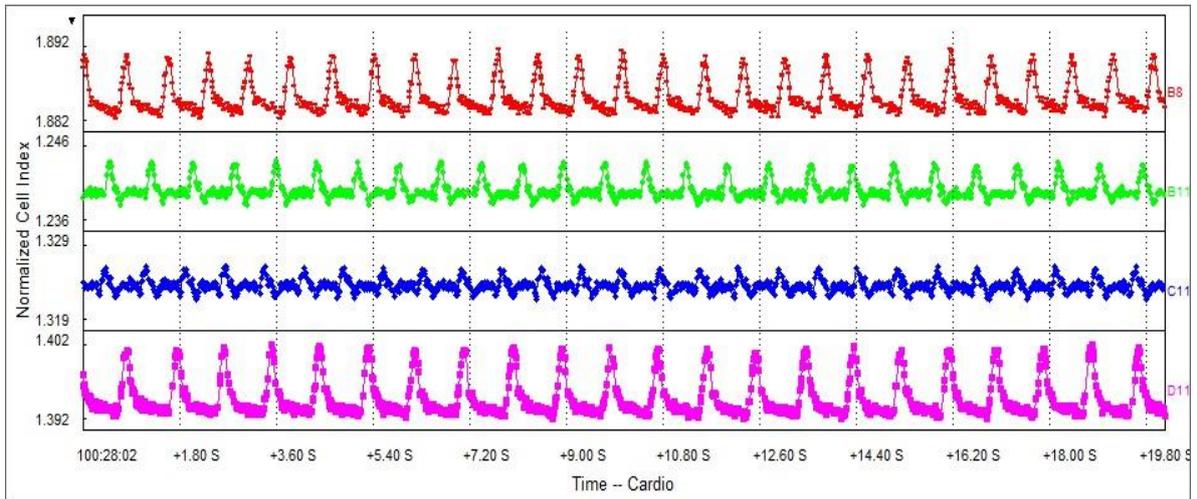
━ Control   ━ CA4 100 nM   ━ Colchicine 1μM   ━ Colchicine 100 nM
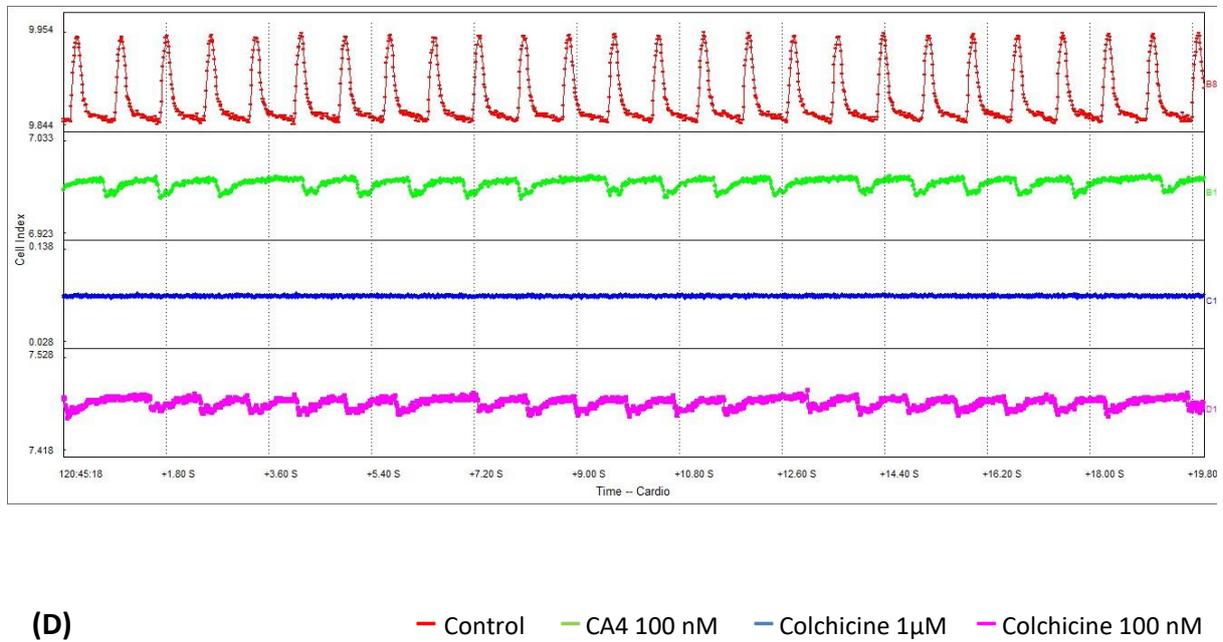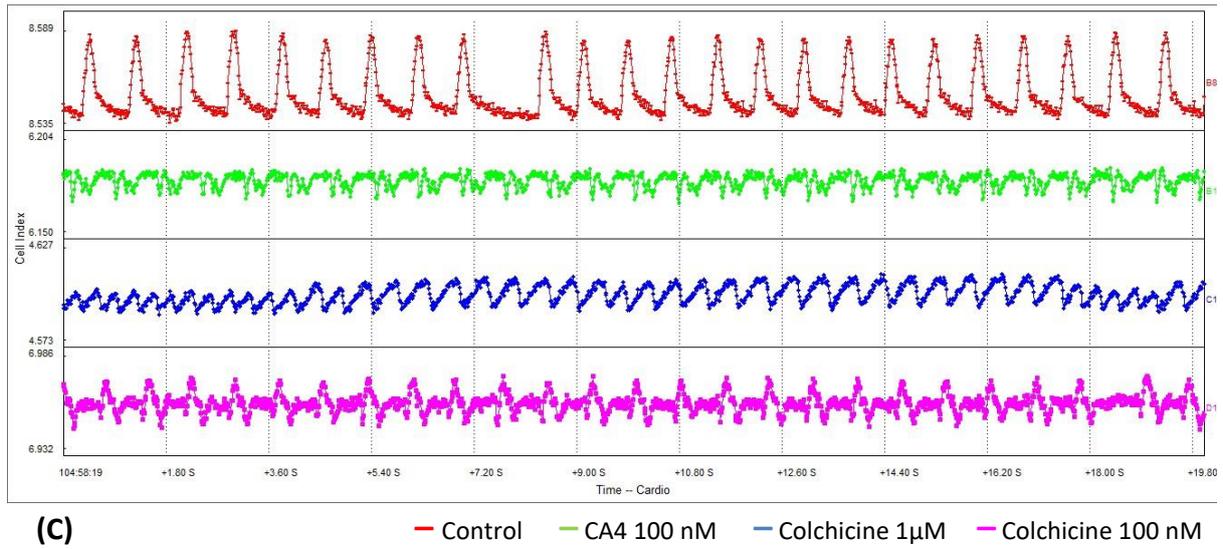
Figure 5-9: Effect of VDAs on contractility and beating rate of Cor.At cardiomyocytes.

Effects of exposure to Colchicine 100nM, Colchicine 1uM and CA4 100nM (A) 0 hrs, (B) 4 hrs, and (C) 8 hrs and (D) 24 hrs after administration.
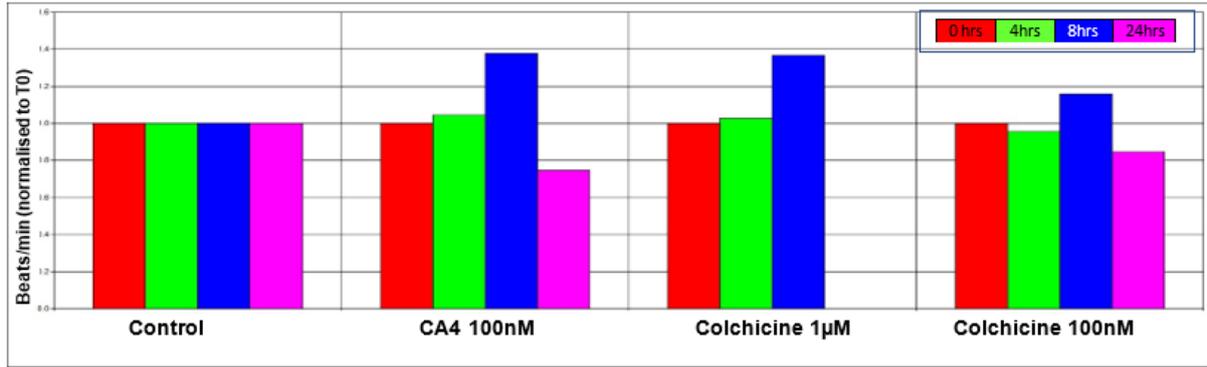
(A)
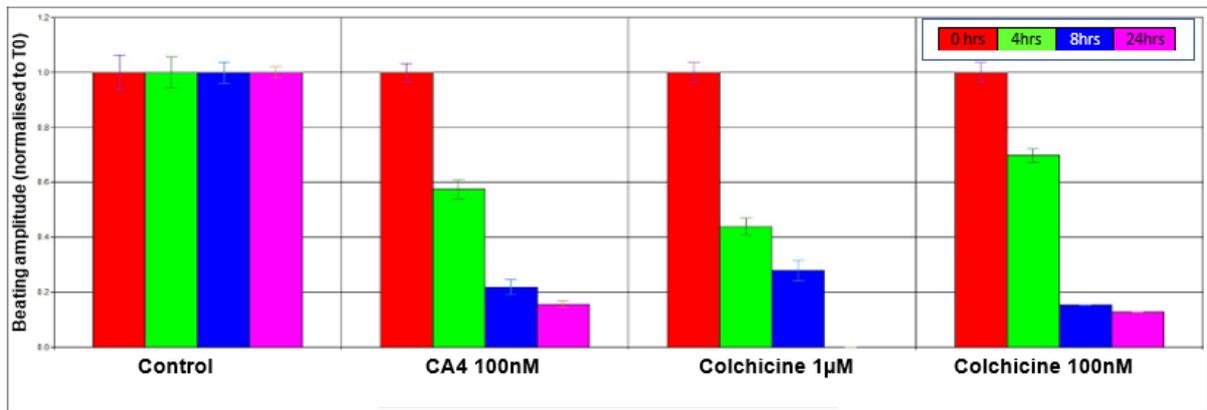
(B)

Figure 5-10: Effect of VDAs on beating rate and beat amplitude of Cor.At cardiomyocytes.

Effects of exposure to Colchicine 100nM, Colchicine 1uM and Combretastatin A4 100nM upon (A) beating rate and (B) beat amplitude over time.

5.4 Discussion

Drug-induced cardiotoxicity is now becoming a major issue for the successful use of many cancer therapies, either causing acute problems within days of treatment or delayed adverse effects many years after cessation of treatment (Lindenfeld and Kelly, 2010, Moslehi and Deininger, 2015, Mercurio et al., 2016). Vascular disrupting agents (VDAs) offer a new dimension to the treatment of solid tumours through their distinct pharmacological mechanism of action. However, progression into the clinic is limited because of potential effects upon the cardiovascular system, with preclinical studies and numerous clinical trials reporting a range of clinical adverse events (Gill et al., 2019). Therefore, in order for this drug class to have utility in the clinic and for any cardiovascular risks to be mitigated, and thus an understanding of the mechanism(s) underpinning their cardiotoxicity is warranted. In this project *in vitro* cardiac cell studies have demonstrated effects of these drugs upon cardiomyocyte morphology (Section 4.4.5), supporting many of the effects observed in clinical studies such as hypo- hypertension, cardiac hypertrophy and reduced left ventricular ejection fraction (LVEF) (Tochinai et al., 2016, Rustin et al., 2010, Nathan et al., 2012, Zweifel et al., 2011). However, effects upon cardiomyocyte function, contractility and subsequent comparison to clinically observed effects have yet to be determined. The purpose of this phase of the project was to evaluate the suitability of stem-cell derived cardiomyocytes, specifically Cor.At®, for detection of drug-induced cardiotoxicity and thus to use this qualified model for the identification of effects of VDAs upon cardiomyocyte contractility.

The growth and contractility of Cor.At® cells was monitored using the xCELLigence cardio system. Upon establishment of a functional syncytium and a stable beating pattern, Cor.At® cells were exposed to the β-adrenergic agonist isoproterenol and the hERG potassium

channel blocker E-4031. Isoproterenol exhibits both positive inotropy and chronotropy, meaning that clinically it causes an increase in both the force and rate of contraction. Analysis of contractility after the addition of isoproterenol showed an increased rate of contraction, but only at the highest concentration evaluated and 24 hrs after exposure, a result in line with previous studies of Cor.At® using the xCELLigence Cardio system (Xi et al., 2011a). The apparent cessation of contraction, rather than a positive chronotropic effect, observed at 2 hrs with high concentration (300nM) isoproterenol is likely a response to positive chronotropy coupled with excessive positive inotropy at these early stages. The fact that contraction resumed and exhibited positive chronotropy later supports this hypothesis and the qualification of Cor.At cells as an appropriate *in vitro* cardiomyocyte model in this context.

The K^+ ion channel blocker E-4031 which retards the hERG-driven rapid delayed rectifier outward potassium current (IKR) functions to delay ventricular repolarisation, thereby prolonging the duration of cardiomyocyte contraction. Clinical inhibition of the hERG K^+ channel by drugs and other chemical entities is commonly associated with arrhythmogenesis, which can lead to the fatal condition Torsades de pointes (TdP) (Haverkamp et al., 2000, Joshi et al., 2004, Finlayson et al., 2004, Bass et al., 2005, Hoffmann and Warner, 2006). Consequently, all new drugs prior to regulatory approval have to be screened for their effects on the hERG and other cardiac ion channels to assess potential for cardiac liabilities (Friedrichs et al., 2005, Cavero and Holzgrefe, 2014) . Exposure of Cor.At® cells to E-4031 resulted in the expected decrease in cardiomyocyte beat-rate and production of a characteristic dysrhythmia phenotypic appearance.

This study has thus demonstrated that Cor.At® cells are responsive to positive chronotropic (isoproterenol) and negative chronotropic (E-4031) agents and that such effects can be

monitored in real-time and reliably on the xCELLigence cardio system, thereby confirming this as a suitable platform for the assessment of drug-induced perturbations in cardiomyocyte contractility.

VDAs have been reported in *in vivo* studies and clinical trials to cause acute functional cardiovascular effects, including arrythmias and cardiac fibrillations (Grisham et al., 2018, Rustin et al., 2003, Zweifel et al., 2011). Furthermore, QT prolongation and changes in cardiac contractility have been reported in clinical trials for CA4P, albeit transient and moderate (Cooney et al., 2004). However, the mechanisms responsible for this and their mode of action have yet to be resolved. Evaluation of the effects of the VDAs, Colchicine and CA4, on Cor.At® cardiomyocytes were assessed in real-time and at different exposure concentrations using the xCELLigence Cardio system. In both cases drug concentrations were clinically relevant, being below the maximum tolerated dose defined during preclinical development and C_{max} values determined in clinical trials (He et al., 2011). It is worth to mention that the experiment was initially performed with lower concentrations (in line with the concentration used for AC10 cardiomyocytes) but they had no effect on Cor.At® cardiomyocytes (data are not included).

Exposure of Cor.At® cells to either Colchicine or CA4P resulted in a measurable decline in cell index within 30 minutes of drug-addition. This decline in cell index is indicative of either loss of cell viability and subsequent cell death or a change in cellular morphology, predominantly hypotrophy or reduction in cell size. The discriminator between the two outcomes is the degree to which the cell index is reduced and the timescale over which this occurs, with a gradual but continuous reduction attributed to a loss of cell number and thus cytotoxicity in comparison to a rapid but defined decline in cell index representative of a change in cellular

morphology (Denelavas et al., 2011). Therefore, the rapid but contained reduction in the cell index with drugs at 100nM concentrations supported a change in cellular morphology rather than overt cytotoxicity. Such a morphological change is reflective of the mechanistic basis of VDAs in their ability to bind tubulin and inhibit microtubule polymerisation and consequently alter cellular structure and morphology. These effects are reflective of those reported in endothelial cells with both Colchicine and CA4P, wherein disruption of microtubule aggregation, disturbance of microtubule polymerisation, and morphological deformation of the cells is reported (Galbraith et al., 2001)

Although exposure of Cor.At® cells to 1µM colchicine also caused a reduction in cell index indicative of morphological change, in agreement with the lower colchicine concentration of 100nM100, this response appeared to be biphasic with an initial drop over the first 8 hrs and then a second continuous decline across the 24- hr period. This decline in cell index was indicative of a loss of cellular viability or significant disruption of the syncytium. However, although the cell index significantly declined it did not completely drop to zero levels representative of total cell loss. This suggests the response is more likely a reflection of altered cell morphology, cell motility, cellular interactions and subsequently disjunction of the required syncytium for contractility. A lack of contractility, whilst maintaining a detectable cell index, is in support of this response. Unfortunately, confirmation of this hypothesis was not possible due to the lack of capacity for viewing Cor.At® cells within the xCELLigence plate and the inability for cellular detachment to ascertain degree of cellular viability.

The rapid decline in cell index, plateau and subsequent detectable increase in cell index after approximately 24- hrs with Colchicine and CA4 at a 100nM concentration is suggestive of potential for the Cor.At® cells to overcome the effects of the drugs over time. This recovery

response from VDAs has been previously reported in endothelial cells wherein a drug-induced change in cell shape was reported following a short 30-minute exposure to both Colchicine and CA4P (Galbraith et al., 2001, Deng et al., 2020) . However, despite recovery of endothelial cell shape by 24- hrs after the short exposure to CA4P, no recovery of cell shape was observed for Colchicine (Galbraith et al., 2001). It is unclear whether such a response is also observed with Cor.At® cells as cellular drug exposure was continuous over the duration of the study due to technical limitations, in contrast to the endothelial cell study where drug exposure was restricted to 30-minutes. Furthermore, due to the longevity of the functionality of Cor.At® cells being restricted to 72- hrs once contracting, coupled to the concurrent evaluation period on the xCELLigence RTCA system being limited, longer-term recovery of Cor.At® cells was unattainable. Further studies are therefore required with shorter drug exposure durations and potentially drug wash-out inclusions, within the constraints of the evaluation period of Cor.At® cells on the xCELLigence system, to determine the recovery effect and differences between Colchicine and CA4.

The effects of Colchicine and CA4 on the contractile rate of Cor.At® cells was found to be minimal across the duration of the study, with contractile rates largely unaffected relative to control. This is in agreement with a previous study evaluating the effects of Colchicine upon rat neonatal cardiomyocytes using the xCELLigence RTCA system (Lamore et al., 2013). At 8-hrs post-exposure the beat-rate did appear to moderately increase with both drugs and concentrations, reflecting previous studies wherein Colchicine treatment related to an increase in contractile rate in rat primary cardiomyocytes, determined visually over a short-incubation period (Klein, 1983). However, inspection of the actual xCELLigence trace confirmed that this response was more likely a reflection of changes in cell morphology and

perturbation of the normal contractile function of the cells, indicated by the reduced beat amplitude and presence of additional 'fibrillations' within many of the contractile peaks, a mechanism would not have been detectable in visual monitoring of cardiomyocyte contractility. The lack of effects upon cellular contractility over this period was suggestive that neither of these drugs have a direct impact upon cardiomyocyte electrophysiology or ion channel functionality. Furthermore, often beat-rate increases to higher variable rates alongside a reduction in amplitude of contraction, before reversing and beat cessation, as observed with several microtubule-interactive agents (Lamore et al., 2013). Therefore, the response of VDAs upon the contractile rate of Cor.At® was unlikely to be 'true' tachycardia and reflects previous studies using rat neonatal cardiomyocytes on the xCELLigence system. (Lamore et al., 2013).

The lack of effect upon contractility of Cor.At® cells would appear to contradict the response of combretastatin VDAs upon contraction of human induced pluripotent stem-cell derived cardiomyocytes (hiPS-CMs), with these drugs reported to steadily increase beat-rate by 20% over a 24- hr assessment period (Tochinai et al., 2016). The concentrations used in this published study were in excess of those used in this project and were significantly higher than the reported clinical C_{max} for these drugs (He et al., 2011), ranging from 100nM (used herein) up to 10 µM, with increases in cardiomyocyte beat-rate being associated with higher concentrations. In agreement with the study herein, no significant change in beat-rate was observed with 100nM CA4P at earlier timepoints, with a noticeable but non-significant increase evident after several hours in both Cor.At® and hiPSC-CM cell models. A more striking relevant point in this published study is a biphasic drop in the xCELLigence cell index upon exposure of hiPSC-CMs to combretastatins, with a rapid decrease observed within one hour

followed by a progressive decline over the 36- hr study period. Although the initial decline was reflective of the morphological changes identified with Cor.At® cells, the lack of a cell index plateau and further cell index decline was indicative of cell loss (Tochinai et al., 2016), as reported in this study with 1µM Colchicine. It is therefore questionable, due to the continual loss of cells, whether the reported increase in contractility in hiPSC-CMs with combretastatins is indeed real or is a consequence of retardation of beat amplitude and false-positive intrapeak contractions, as observed with Cor.At® cells. The lack of reported data for beat amplitude or presentation of xCELLigence traces for the hiPSC-CM study inhibits resolution of this discrepancy. Alternatively, this maybe a consequence of species difference in contractile mechanisms or differential involvement of microtubules in the contractile mechanism between cell models (Webster and Patrick, 2000). This is somewhat unlikely as both cell models respond comparably to other drugs and cardioactive agents.

The most noticeable and significant effect imparted on Cor.At® cells by both Colchicine and CA4P was a time-dependent reduction in the beat-amplitude, representative of a reduction in cellular ability to contract, relax and stretch. This response to tubulin-interactive agents is in agreement with a published study evaluating their effects upon primary neonatal rat cardiomyocytes assessed using the xCELLigence system, wherein the decrease in beat amplitude was also not attributable to a drug-induced decrease in cell viability (Lamore et al., 2013). The rationale for the effects of VDAs upon cardiomyocytes is fairly straightforward in that inhibition of microtubule dynamics by tubulin-binding agents restricts motility of the cellular cytoskeleton and subsequently contractility. Microtubules are central to mechanosignalling, contractility, and myocyte stiffness (Robison et al., 2016, Schappi et al., 2014, Hein et al., 2000). Within the cardiomyocyte cytoskeleton, microtubules are repeatedly

recycled through polymerization and depolymerization to assist with contraction and at any time only approximately 30% of microtubules are polymerised (Hein et al., 2000, Rappaport and Samuel, 1988). Therefore, depolymerisation of cardiomyocyte microtubules upon exposure to Colchicine-binding site interactive agents, such as Colchicine and CA4P, acts to impede cardiomyocyte functioning at multiple levels (Hein et al., 2000).

This limitation of cardiomyocyte contractility observed in this and other *in vitro* studies is however at odds and contradictory with studies of cardiac hypertrophy in which administration of Colchicine improves cardiac contractility and reduces in cardiomyocyte stiffness (Hein et al., 2000). In hypertrophy, cardiomyocytes demonstrate loss of compliance and significant contractile dysfunction. In terms of tubulin, hypertrophic cardiomyocytes have increased levels of total tubulin and elevated polymerisation, contributing to the observed cytoskeletal stiffness and potentially restricted sarcomeric movement (Hein et al., 2000, Rappaport and Samuel, 1988, Tagawa et al., 1998). As opposed to 'normal' cardiomyocytes, wherein approximately 30% of tubulin is polymerised, hypertrophic cardiomyocytes and those from heart failure are also reported to demonstrate a reversal of this polymerised to non-polymerised tubulin ratio (Sato et al., 1997). It was thereby hypothesised that augmentation of tubulin coupled with increased microtubule stabilisation and the consequent effects upon the cardiomyocyte cytoskeleton were responsible for the restricted contractility and stiffness of hypertrophic and failing hearts (Hein et al., 2000, Tagawa et al., 1996). Based on these observations, exposure to Colchicine was proposed as a strategy for mitigation of cardiomyocyte stiffness and reengagement of normal contractility, due to the reduction of rate of tubulin polymerisation towards 'normal' levels(Hein et al., 2000.). In hypertrophic cardiac tissue, treatment with Colchicine, albeit low concentrations, causes a

reduction in microtubule hyper-polymerisation, reversal of cardiomyocyte stiffness and resumption of normalised contractility, supporting the therapeutic hypothesis (D'Amario et al., 2021, Nidorf et al., 2013, Nidorf et al., 2019, Nidorf et al., 2020). It is however worth highlighting that many of these studies were *in vivo* or *ex vivo* rather than *in vitro* cellular studies, wherein stress load upon the cardiac system is a factor. Nevertheless, further support for the importance of the degree of tubulin polymerisation in regulation of cardiomyocyte contraction is provided by studies evaluating the taxane class of drug which bind to tubulin and function to enhance and stabilise microtubule polymerisation, as opposed to inhibition of polymerisation with Colchicine and CA4P. Exposure to these drugs results in reduced contractility and slowing of cardiac conduction, due to an effect of increased tubulin polymerisation inhibiting correct expression of the Nav1.5 sodium channel and subsequently reducing Na^+ currents (Casini et al., 2010). Furthermore, drugs targeting microtubule-associated kinases, which exhibit dose-limiting cardiovascular toxicities in the clinic, exhibited cessation of contractility *in vitro* when evaluated using the xCELLigence system (Lamore et al., 2013). Therefore, the observation of reduced contractility of Cor.At® cells in the presence of Colchicine and CA4P, observed in this study, aligns rather than contrasts the effects observed in hypertrophic cardiac tissue, as in both cases the drugs reduce microtubule stabilisation.

A limitation of the current study is the use of murine-derived cardiomyocytes and their applicability to the clinical scenario, with known species, maturity, and electrophysiological differences reported (Freund and Mummery, 2009, Mandenius et al., 2011). To address this issue, future studies may need to use either hiPSC-derived CMs or primary human cardiomyocytes should be conducted. However, it must be noted that the results obtained

using murine Cor.At® cells have reflected the clinical effects of VDAs and have responded to cardioactive agents in a manner representative of hiPSC-derived cardiomyocytes.

Due to time aspect it was not possible to repeat this experiment. Obtained results from three wells were generally comparable, however shown results are from only one well and not an average.

In summary, the combination of the xCELLigence Cardio RTCA for monitoring the beating function of Cor.At® SC-derived cardiomyocytes provides an excellent *in vitro* methodology to evaluate drug-induced functional and structural cardiotoxicities. In this case, an effect of VDAs upon cardiomyocyte function was observed at clinically relevant concentrations. The lack of an effect upon rate of contractility but rather an effect upon degree of contractility is a pertinent finding, aligning with the pharmacological mechanism of VDAs upon perturbation of microtubule dynamics. Translation of this observation to the clinic would explain a relative lack of acute drug-induced dysrhythmias but support modulations of cardiac function by VDAs. Such an effect would thus highlight a potential for VDAs to affect cardiac contractility and potential cardiac 'stiffening' within the clinical environment, a response which would exacerbate the established haemodynamic changes associated with VDA treatment (Gill et al., 2019). As was observed in this *in vitro* study, CA4P therapy in the clinic is also associated with transient delayed tachycardia, reinforcing the validity of this study (Grisham et al., 2018, Rustin et al., 2003, Zweifel et al., 2011). Clinical trials of CA4P also reported the presence of premature ventricular contractions following presentations of drug-induced sinus bradycardia and subsequent tachycardia (He et al., 2011), a response also observed in this study with intrapeak fibrillations. Although changes in Q-T interval, representative of cardiomyocyte repolarisation, have been reported for CA4P and other tubulin-interactive

VDAs in clinical trial, the underlying mechanism is now being questioned. It is now hypothesised that this transient electrophysiological disturbance may not be a consequence of drug-induced myocardial repolarization but rather a factor of modulation and variability of haemodynamic factors (He et al., 2011, Cooney et al., 2004). However, it is not inconceivable to suggest that the detected unstable modulations in cardiac repolarisation maybe a consequence of VDA-induced restrictions of cardiac contraction, which in themselves would affect cardiomyocyte function transiently and potentially in a heterogeneous fashion across the myocardium. Further studies are thereby warranted to further interrogate this mechanism.

Chapter 6. Preliminary investigation of *in Vivo* Molecular Changes in Cardiac Gene Expression Induced by Exposure to VDAs.

6.1 Molecular genetic changes of drug-induced cardiotoxicity

The induction of cardiotoxicity by drugs is associated with perturbation, activation and inhibition of a number of signalling pathways within the cardiomyocyte. These signalling pathways lead to modification of both cardiomyocyte cell structure and contractile function (Lamore et al., 2013, Audebrand et al., 2020, Lamore et al., 2020, Force et al., 2007). The consequence of these drug-induced changes at the cellular level is the alteration of overall cardiac structure and function, resulting in cardiac remodelling, acute effects such as induction of arrhythmias, and chronic and delayed-effects leading to cardiac failure (Peterson, 2002, Kemp and Conte, 2012). However, it is important to remember that these drug-induced responses are initiated at the molecular level, through alteration of gene transcription or post-translational modification of proteins . Understanding these molecular changes is central to identification of the cellular and tissue changes and to the severity and extent of any such drug-induced effects.

6.1.1 Molecular responses to Colchicine and mechanisms of Colchicine toxicity

Colchicine and its derivatives, including the combretastatins, have a clearly defined toxicity at the cellular level due to their action in binding to tubulin and stabilising cellular microtubules (Ravelli et al., 2004, Sève and Dumontet, 2008, Stengel et al., 2010, Lippert III, 2007). This disruption of the cellular cytoskeleton can lead to a panoply of effects including induction of cell cycle arrest, retardation of cellular motility, alterations in activity of cellular organelles and cellular communication and ultimately cell death. At the tissue level these changes impart physiological, morphological and functional disturbances. (Rustin et al., 2010, Cooney et al., 2006, Garon et al., 2016, Sosa et al., 2011)

Overdose and toxicity of Colchicine is associated with multi-organ dysfunction, including the cardiovascular system. Acute Colchicine poisoning manifests itself in three phases. The initial gastrointestinal stage, after oral ingestion, reflects mucosal damage. The second phase is characterised by effects on several organs and associated metabolic derangements. The last phase is observed in individuals who have not succumbed to the effects of multi-organ failure, characterised by reversal of bone marrow depression, rebound leukocytosis, resolution of organ failure, and in some cases full recovery. In instances where Colchicine toxicity is too severe, death occurs most commonly within 48 hrs as a result of drug-induced dysrhythmias and haemodynamic collapse (Finkelstein et al., 2010, Sauder et al., 1983, Hood, 1994, Mullins et al., 2000, Klintschar et al., 1999).

In the clinic, Colchicine is used at low doses for management of gout and other inflammatory conditions (Dalbeth et al., 2014, Lange et al., 2001, Lange et al., 2002a, Lange et al., 2002b). The use of Colchicine and its analogues as VDAs requires much higher doses to be administered than would be used for gout and inflammatory conditions, although as acute rather than chronic treatment protocols. Clinical studies of VDAs have identified a number of cardiovascular adverse effects in the clinic, notably hyper/hypotension, atrial fibrillation and reduced cardiac outputs (Tochinai et al., 2016, Rustin et al., 2010, Nathan et al., 2012, Zweifel et al., 2011). In this preclinical study, we have demonstrated using *in vitro* approaches that VDAs, specifically Colchicine and CA4, cause structural effects upon cardiomyocytes and impair their contractility at clinically relevant concentrations. These effects have been shown largely to be a direct consequence of VDAs upon tubulin and microtubules within the cardiomyocytes. However, the overall effect of VDAs upon the cardiovascular system and identification of molecular pathways underlying these effects has not been appraised,

principally due to the fact that such studies are not easily achievable using *in vitro* or cell-based methodologies. Understanding the molecular pathways altered by VDAs in the cardiac system is therefore important and requires *in vivo* and *ex vivo* analyses.

From a therapeutic perspective, low dose Colchicine has been evaluated as a strategy for prevention of postoperative atrial fibrillation, with promising outcomes (Imazio et al., 2011, Van Wagoner David, 2011). The mechanism for these effects is proposed to involve attenuation of neutrophil activation and subsequent endothelial cell adhesion rather than disruption of cardiomyocyte microtubule activity and regulation of adrenergic receptors or modulation of calcium signalling pathways (Van Wagoner David, 2011, Malan et al., 2003). In an attempt to elucidate the mechanisms responsible for reducing post-operative atrial fibrillation a transcriptomic approach was applied using left atrial tissue from rats exposed to low dose (0.8 mg/kg) Colchicine (Yue et al., 2019). These gene analyses indicated a central involvement of the IL-17 signalling pathway, which is known to be involved in stimulation of pro-inflammatory cytokines associated with myocardial remodelling, cardiac fibrosis and potentially atrial fibrillation (Zhou et al., 2014). Furthermore, exposure to Colchicine was also reported to reduce the risk of atrial fibrillation through dysregulation of genes associated with the renin-angiotensin-aldosterone pathway axis, a central player in blood pressure homeostasis (Yue et al., 2019). However, although the intention of this study was the evaluation of Colchicine-mediated management of post-operative atrial fibrillation, drug-induced gene perturbations are multifactorial processes and thus it is conceivable that these molecular pathways may also have a major role in the mechanism of cardiotoxicity of VDAs.

One study evaluating toxicity of tubulin-binding agents has shown that alongside effects upon cardiomyocytes within the heart, these drugs have a defined affect upon endothelial cells

within the myocardium (Mikaelian et al., 2010). Analyses of cardiac tissue following administration of high dose (2 mg/kg) Colchicine supported cell cycle arrest predominantly in interstitial cells relative to cardiomyocytes (Mikaelian et al., 2010). Using transcriptomic profiling many of these interstitial cells were confirmed as endothelial cells due to upregulation of genes associated with vascular damage and downregulation of endothelial cell specific molecule 1 and apelin (Mikaelian et al., 2010) . This effect of Colchicine upon endothelial cells is obviously in agreement with the mode of action of these agents as VDAs in cancer, albeit affecting neovasculature rather than established vasculature (Gill et al., 2019). The effects of these agents on cardiac endothelium relative to endothelium of other tissues was postulated to be due to a higher proliferative index of cardiac endothelial cells relative to other tissues, although this has not been proven (Mikaelian et al., 2010). It is however noteworthy that rapid regeneration of cardiac endothelial cells has been demonstrated following cardiac injury, including ischaemia associated with reduced blood flow, offering a cell population susceptible to the effects of VDAs (Karra et al., 2017). A contributory effect on cardiac vasculature would thereby support the association of VDAs with haemodynamic effects and due to effects on cardiac coronary vasculature subsequent myocardial infarctions. This however would not explain the direct effects of VDAs upon cardiomyocytes as evidenced in this study. Further studies are thereby warranted to gain a better understanding of molecular pathways associated with Colchicine-exposure in the heart.

6.2 Aims and Objectives.

Preliminary identification of molecular pathways dysregulated by exposure of the cardiovascular system to VDAs *in vivo* is the aim of this chapter. This was achieved by assessment of gene expression changes in cardiac tissue excised from mice treated with Colchicine.

The objective is to evaluate gene expression differences between cardiac tissue exposed to high dose Colchicine (1.5 mg/kg) relative to drug-vehicle alone (10% DMSO/Saline). This was achieved using the mouse cardiotoxicity RT² Profiler™ quantitative PCR (qPCR) array, which includes key genes and genetic markers associated with cardiac injury. Pathway analysis of the differentially expressed genes being utilised to indicate signalling pathways potentially involved in Colchicine-induced cardiovascular toxicity.

6.3 Results

6.3.1 Confirming the quality of cDNA

In advance of the qRT-PCR gene arrays analysis, pre-array verification of cDNA quality is required. The cDNA quality was determined by examining gene expression of a house-keeping gene (GAPDH) in the control and treated samples using reverse transcriptase PCR (RT-PCR. Figure 5-8 shows that GAPDH was detected in comparably equal levels in cDNA generated from control and Colchicine treated murine cardiac tissue. This suggests suitability of obtained cDNA for use in gene array experiments.
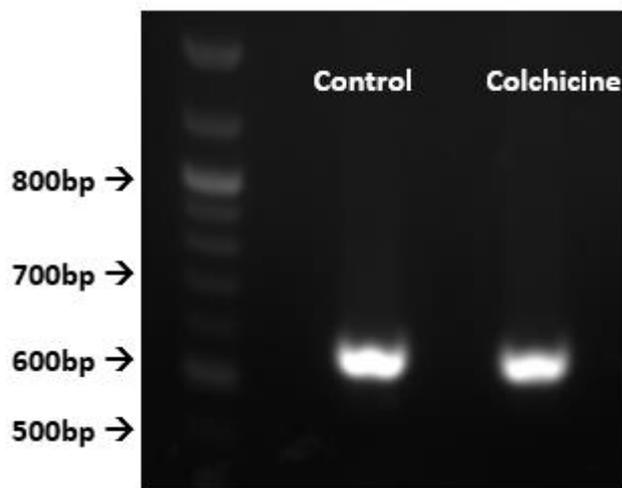
Figure 6-1: GAPDH was detected at equal levels in cDNA generated from mouse hearts exposed to drug vehicle (control) or Colchicine.

Reverse-transcriptase PCR showing expression of GAPDH, expected band size 598bp. Molecular markers for determination of product size shown on the left.

6.3.2 Colchicine alters expression of genes associated with cardiotoxicity in murine cardiac tissue following in vivo drug exposure.

In comparison to mice treated with drug vehicle alone (10% DMSO/saline) heart tissue from mice treated with high dose Colchicine for 24 hrs demonstrated a number of upregulated (red) and down-regulated (green) genes.

Many known genetic markers of cardiac toxicity were dysregulated in the myocardium of mice medicated with Colchicine. Out of 84 genes in the array, 23 genes were up-regulated, and 23 were down-regulated, by at least two-fold in Colchicine treated cardiac tissue relative to normal tissue (Table 6-1, Figure 6-2, appendix 4 and appendix 5).

6.3.3 Molecular pathways dysregulated in Colchicine treated murine cardiac tissue.

Analyses of genes dysregulated in cardiac tissue following exposure to high dose Colchicine demonstrates a number of common molecular pathways associated with cardiotoxicity (Table 6-2 and Table 6-3)

	1	2	3	4	5	6	7	8	9	10	11	12
A	Abhd2 -2.2835	Abra -6.6413	Acta1 2.7392	Adra2a	Aifm1 -4.3357	Ak3	Ash1l 4.7858	Atp5j	Bcat1 2.1343	Bgn -5.487	Bsn 2.134	Btg2 -8.7619
B	Ccl7	Ccr1	Cd14	Cfd 2.1343	Ch25h	Ckm 45.7674	Col15a1 -4.3658	Col3a1	Crem -2.6322	Csnk2a2 -9.2615	Dusp8 -2.8506	Egr1
C	Fcgr2b -2.7535	Fhl1 -28.6656	Fosl1	Gja1 -11.052	Gpm6a 3.847	Hamp 2.1343	Hspa2	Hsph1	Ift20 -16.751	Igfbp5 2.4263	Il6	Itpr2 4.2391
D	Klhl41 8.6563	Klhl40 3.1684	Kcnj12	Mcm6	Mt1 -13.512	Nexn	Nfib	Pdk4 -24.868	Pkn2 2.3114	Pla2g4a	Plau	Pln
E	Plunc (Bpifa1) 22.5296	Postn	Ppbp 2.7015	Ppp1r14c	Prkab2 10.2585	Psma2	Psmd7 -2.4988	Pum2 3.3607	Pvr -2.1981	Rbm3 -9.3908	Reg3b	Rnd1 3.3259
F	Rps6kb1 -3.6332	S1pr2 15.3349	Serpine1	Sik1	Slc4a3 -3.2631	Sox4	Spp1 23.4863	Tcf4	Tgfb2	Thrap3	Tiam1 13.1205	Timp1
G	Tubb6 2.7203	Txnip	Uba5 16.9563	Ubxn2a 3.4913	Uck2	Ucp1	Vcan	Vegfa -7.2917	Vim	Wipi1 -6.3478	Zfp148	Zfp612

Table 6-1: Genetic expression profile of genes related to cardiotoxicity in murine hearts exposed to Colchicine.

Fold change increases in gene expression (green highlighted genes), decreases in gene expression (red highlighted) and unchanged genes(white) recorded following 24-hr in vivo exposure to high dose 1.5 mg/kg Colchicine. Numbers shown in this table represents the fold changes in gene expression, positive numbers indicating upregulation while negative numbers indicating down regulation.
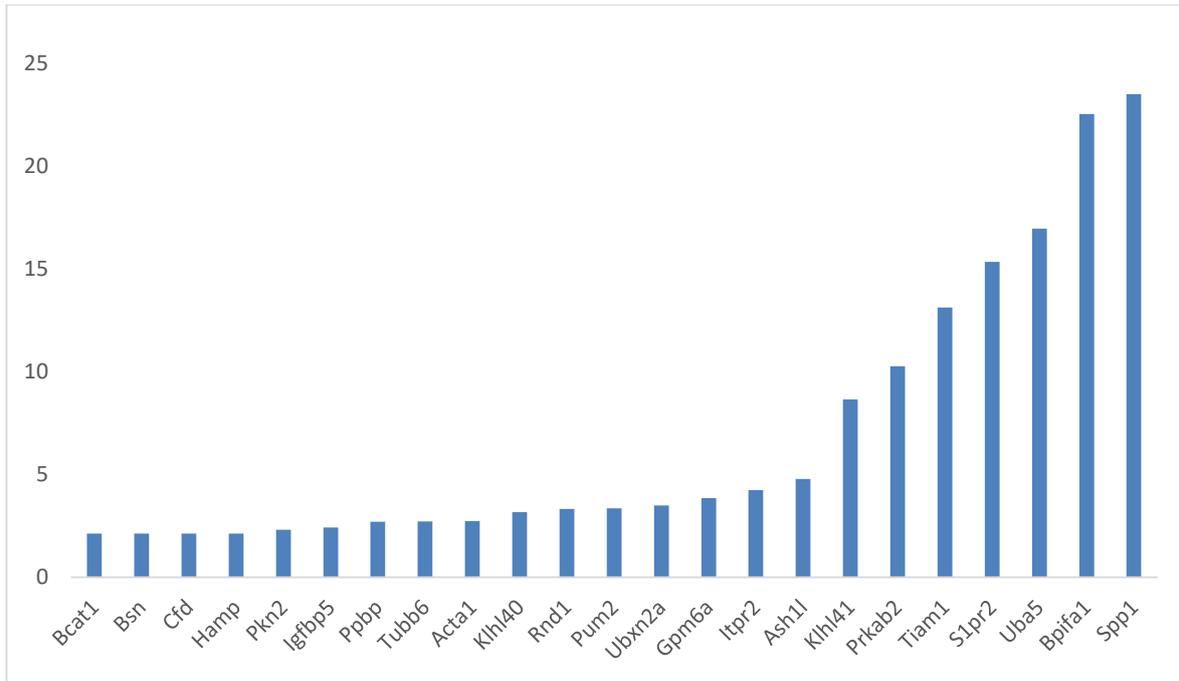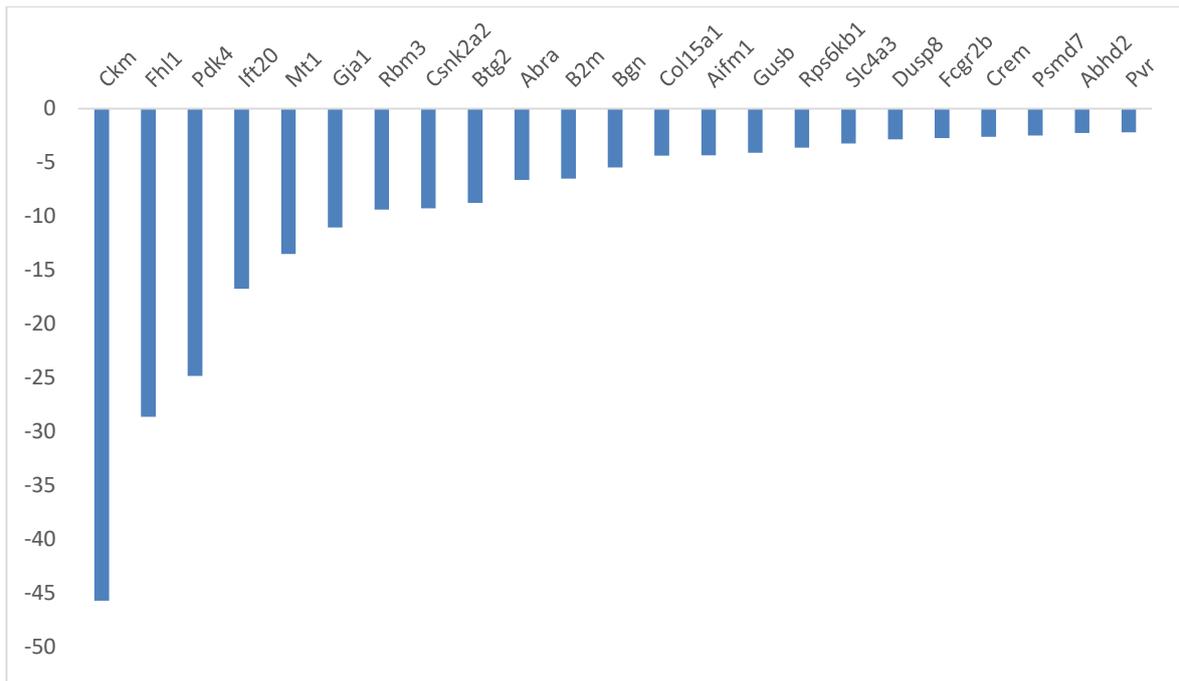
Figure 6-2: Colchicine induces changes in expression of genes related to cardiotoxicity in murine cardiac tissue. *Clustered graph showing genes with more than 2-fold change in gene expression. (A) shows the upregulated genes and (B) shows the down regulated genes.*

Up-regulated genes		Klhl41	Il6	Serpine1	Rnd1	Tiam1	Bact1	Fosl1	Hspa2	Spp1	Timp1	Ucp1	Pla2g4a	Pum2	Ppbp	Cfd	Hamp	Klhl40	Bpifa1	Reg3b	Tubb6
1	Apoptotic Pathways in Synovial Fibroblasts		■								■				■						
2	PEDF Induced Signalling		■																		
3	GPCR Pathway		■								■				■						
4	TGF-Beta Pathway		■																		
5	ERK Signalling		■							■	■				■						
6	Semaphorin interactions				■																
7	Developmental Biology				■	■															
8	Axon guidance				■																
9	Development Slit-Robo signalling				■																■
10	EPH-Ephrin signalling				■	■															
11	p75 NTR receptor-mediated signalling					■															
12	Signalling by GPCR					■															
13	Signalling by Rho GTPases		■			■															
14	Valine, leucine and isoleucine degradation						■														
15	Metabolism						■					■	■	■							
16	Carbon metabolism						■														
17	Sulfur amino acid metabolism						■														
18	Viral mRNA Translation						■														

#	Up-regulated genes	Klhl41	Il6	Serpine1	Rnd1	Tiam1	Bact1	Fosl1	Hspa2	Spp1	Timp1	Ucp1	Pla2g4a	Pum2	Ppbp	Cfd	Hamp	Klhl40	Bpifa1	Reg3b	Tubb6
19	Toll-like receptor signalling pathway							■		■											
20	Wnt Signalling Pathway							■													
21	Calcineurin-regulated NFAT-dependent transcription in lymphocytes							■													
22	Immune response IL-2 activation and signalling pathway							■													
23	IL-17 Family Signalling Pathways							■													
24	Cellular response to heat stress								■												
25	Influenza A								■												
26	Mechanisms of CFTR activation by S-nitrosoglutathione								■												
27	HSF1-dependent transactivation								■												
28	Parkin-Ubiquitin Proteasomal System pathway								■												
29	Integrin Pathway									■											
30	Degradation of the extracellular matrix									■											
31	Phospholipase-C Pathway									■											
32	Platelet activation, signalling and aggregation										■				■	■					
33	Cellular response to hypoxia										■										
34	Respiratory electron transport, ATP synthesis by chemiosmotic coupling, and heat production by uncoupling proteins											■									
35	Mitochondrial Uncoupling Proteins											■									
36	PPAR signalling pathway											■			■						

Up-regulated genes		Klhl41	Il6	Serpine1	Rnd1	Tiam1	Bact1	Fosl1	Hspa2	Spp1	Timp1	Ucp1	Pla2g4a	Pum2	Ppbp	Cfd	Hamp	Klhl40	Bpifa1	Reg3b	Tubb6
37	Mesenchymal Stem Cell Differentiation Pathways and Lineage-specific Markers											■									
38	Glycerophospholipid biosynthesis												■								
39	DAG and IP3 signalling												■								
40	Acyl chain remodelling of PC												■								
41	Immune response Fc epsilon RI pathway												■								
42	Peptide ligand-binding receptors														■						
43	Immune response Lectin induced complement pathway															■					
44	Creation of C4 and C2 activators															■					
45	Immune System															■					
46	Complement and coagulation cascades															■					
47	Iron metabolism in placenta																■				
48	Cooperation of Prefoldin and TriC/CCT in actin and tubulin folding																				■
49	Cytoskeleton remodeling Neurofilaments																				■
50	Chaperonin-mediated protein folding																				■
51	Regulation of CFTR activity (norm and CF)																				■

Table 6-2: Up-regulated genes and affected pathways.

Down-regulated genes		Gja1	Rps6kb1	Col15a1	Vegfa	Aifm1	Dusp8	Csnk2a2	Psmd7	Pln	Atp5j	Ift20	Slc4a3	Wipi1
1	Gap junction trafficking	■												
2	Microtubule-dependent trafficking of connexons from Golgi to the plasma membrane	■												
3	Blood-Brain Barrier and Immune Cell Transmigration: Pathways Overview	■												
4	Myometrial Relaxation and Contraction Pathways	■												
5	Signalling in Gap Junctions	■												
6	Translation Insulin regulation of translation		■				■							
7	IL-7 Signalling Pathways		■											
8	Interleukin-3, 5 and GM-CSF signalling		■		■				■					
9	mTOR signalling		■											■
10	Development IGF-1 receptor signalling		■											
11	Integrin_Pathway			■										
12	ERK Signalling			■										
13	Collagen biosynthesis and modifying enzymes			■										
14	Degradation of the extracellular matrix			■										
15	Phospholipase-C Pathway			■										
16	Platelet activation, signalling and aggregation				■									
17	Cellular response to hypoxia				■									
18	VEGF Pathway				■									
19	Development VEGF signalling via VEGFR2 - generic cascades				■									

Down-regulated genes		Gja1	Rps6kb1	Col15a1	Vegfa	Aifm1	Dusp8	Csnk2a2	Psmd7	Pln	Atp5j	Ift20	Slc4a3	Wipi1
20	Spinal Cord Injury					■								
21	Signalling by Wnt						■							
22	Signalling by ERBB2						■							
23	Signalling by GPCR						■							
24	Endocytosis						■							
25	Cell Cycle, Mitotic							■						
26	Regulation of TP53 Activity							■						
27	Gene Expression							■						
28	Developmental Biology							■						
29	Chaperonin-mediated protein folding							■						
30	CDK-mediated phosphorylation and removal of Cdc6								■					
31	Chks in Checkpoint Regulation								■					
32	Infectious disease								■					
33	Immune System								■					
34	Cardiac conduction (Muscle contraction and cardiac conduction									■				
35	Activation of cAMP-Dependent PKA									■				
36	cGMP-PKG signalling pathway									■				
37	DAG and IP3 signalling									■				
38	Transport of glucose, sugars, bile salts, organic acids, metal ions and amine compounds									■			■	

Down-regulated genes		Gja1	Rps6kb1	Col15a1	Vegfa	Aifm1	Dusp8	Csnk2a2	Psmd7	Pln	Atp5j	Ift20	Slc4a3	Wipi1
39	Respiratory electron transport, ATP synthesis by chemiosmotic coupling										■			
40	Metabolism										■			
41	Alzheimers disease										■			
42	FOXA1 transcription factor network										■			
43	Organelle biogenesis and maintenance											■		
44	Intraflagellar transport											■		
45	Hepatic ABC Transporters												■	
46	Unfolded Protein Response (UPR)													■
47	Transport to the Golgi and subsequent modification													■
48	Cellular Senescence													■
49	Regulation of autophagy													■

Table 6-3: Down-regulated genes and affected pathways.

6.4 Discussion

The objective of this phase of the project was to preliminary evaluate genetic changes induced in cardiac tissue following *in vivo* exposure to VDAs, assessed using the mouse cardiotoxicity RT² Profiler™ PCR array. Changes in gene expression of 84 genes involved in drug induced or chemical cardiotoxicity were assessed following administration of high dose (1.5 mg/kg) Colchicine, of which 46 genes showed greater than 2-fold changes to gene expression. For the purposes of this project, genes were attributed to molecular pathways and appraised with respect to their potential involvement in Colchicine-induced cardiotoxicity. There are common genetic pathways which appear to be affected as a result of Colchicine treatment, with roles in cell survival, inflammation, and cellular signalling pathways amongst others.

Induction of apoptosis and cell death is demonstrated by genetic up-regulation of IL-6, Timp1 and Ppbp, supporting cytotoxicity of Colchicine as observed in *in vitro* studies in this project. Although these effects are likely to be related to induction of vascular damage, as previously reported (Mikaelian et al., 2010) and in agreement with the mode-of-action for VDAs, the gene array used in this study did not include analyses of endothelial-specific genes such as endothelial cell specific molecule 1 and apelin.

Downregulation of genes related to insulin regulation of translation (Rps6kb1 and Dusp8) as well as those involved in transport of glucose and sugars (Slc4a3 and Pln) suggests that Colchicine also modifies vascular tonicity, in agreement with modification of this signalling pathway observed with several pathological conditions including type-2 diabetes, myocardial ischaemia, and cardiac hypertrophy (Bertrand et al., 2008).

Several signalling pathways are indicated to be activated by Colchicine in cardiac tissue, including extracellular-signal-regulated kinase (ERK) pathways (IL6, Timp1, Ppbp, Spp1 and Tiam1), Toll-like receptor signalling (Fosl1 and Spp1) and the intracellular peroxisome proliferator activated receptor (PPAR) pathway (Ucp1 and Ppbp). In pathological hypertrophy, ERK and mitogen-activated protein kinase (MAPK) signalling is involved in controlling cardiac hypertrophy and remodelling (Liu et al., 2016). Upregulation of ERK and MAPK cascades was shown in cardiac tissue exposed to Colchicine, supporting activation of signalling pathways driving cell division, differentiation, apoptosis and stress responses (Keshet and Seger, 2010, Sabio and Davis, Plotnikov et al., 2011).

Elevated expression of genes involved with platelet activation and aggregation (Timp, Ppbp and Cfd), a mechanism that supports vascular damage in cardiac tissue, was also noted following Colchicine treatment. However, despite a rationale for associations between vascular damage and increased thrombus formation, *in vitro* studies have shown Colchicine reduces platelet aggregation by modulating cytoskeleton rearrangement (Cimmino et al., 2018, Cirillo et al., 2020). The reason for this discrepancy is as yet unclear and it can not be taken as a fact because the results are preliminary and this experiment was performed only once. However, a plausible explanation is the fact that previous studies have focused on low-dose Colchicine rather than the high-dose required for VDA therapy herein. Therefore, former studies are unlikely to induce significant vascular damage or be associated with more severe toxicities, as evidenced when comparing low and high dose Colchicine (Cirillo et al., 2020).

The upregulation of pro-inflammatory interleukin-6 (IL-6) is in agreement with previous studies evaluating genetic changes associated with Colchicine as a therapeutic strategy for management of post-operative atrial fibrillation, wherein upregulation of pro-inflammatory IL-

17 signalling was detected (Yue et al., 2019). IL-17 is known to stimulate expression and release of pro-inflammatory factors, including IL-6, involved in myocardial remodelling and cardiac fibrosis (Yue et al., 2019, Onishi and Gaffen, 2010). Furthermore, in this study a downregulation of anti-inflammatory IL-5 expression was also reported, an observation in agreement with cardiotoxicity induced by the anticancer drug doxorubicin (Xiao et al., 2020). Together this strongly supports induction of an inflammatory response in the heart following exposure to Colchicine, with a defined risk for subsequent development of cardiac fibrosis and cardiac hypertrophy.

Although some of the changes in gene expression are more difficult to assign to a specific pathway, the results in this section provide preliminary evidence that treatment with Colchicine causes changes in gene expression that indicates a clear risk of cardiotoxicity for clinical use. Although further work is needed to verify and add to the changes in gene expression discussed, the work described herein implicates VDAs as having a direct effect on the cardiovascular system and potentiating the pathogenesis of drug-induced cardiotoxicity.

Chapter 7. General discussion and conclusion

7.1 General discussion

During the last few decades, significant improvements have been made in the therapy of cancer (Jemal et al., 2011, Miller et al., 2019, Miller et al., 2016), particularly through the development of therapies targeting defining features of malignancy such as angiogenesis and establishment of their own vascular system. However, despite significant improvements in cancer treatment and patient survival, it is now clear that the increasing success of cancer chemotherapy is counterbalanced by adverse toxic effects, particularly upon the cardiovascular system (Lindenfeld and Kelly, 2010, Moslehi and Deininger, 2015, Mercurio et al., 2016). This is even more so because the prolonged patient survival allows the patient to live long enough to encounter the long-term detrimental effects of the therapeutic. A situation then arises in which cardiovascular toxicity can be the main determinant of quality of life and potentially be responsible for premature death, as opposed to cancer (Oeffinger et al., 2006,(Hanrahan et al., 2007, Mann and Krone, 2010). Consequently, challenges exist with respect to identifying, managing or at least monitoring the cardiovascular toxicity associated with cancer-therapy, to provide the most beneficial cancer treatment, and ultimately improve patient outcomes and longer-term healthcare (Rhoden et al., 1993, Suter and Ewer, 2013, Mann and Krone, 2010, Ewer et al., 2011, Curigliano et al., 2010, Floyd et al., 2005, Albini et al., 2010, Force et al., 2007, Curigliano et al., 2012, Schmidinger et al., 2008).

Vascular disrupting agents (VDAs) offer a new dimension to the treatment of solid tumours through their distinct pharmacological mechanism of action. However, progression into the clinic is limited because of potential effects upon the cardiovascular system, with preclinical studies and numerous clinical trials reporting a range of clinical adverse events (Gill et al., 2019). There are many VDAs currently in preclinical

development or late-stage clinical trial (Ji et al., 2015; Mason et al., 2011, Gill et al., 2019). Therefore, in order for this drug class to have utility in the clinic and for any cardiovascular risks to be mitigated, an understanding of the mechanism(s) underpinning their cardiotoxicity is warranted. This was a central aim of this project.

An initial study aim was to qualify the *in vitro* AC10 cardiomyocyte model for use in *in vitro* screening to detect structural and functional cardiotoxicity. The AC10 cell line is derived from adult human ventricular cardiomyocytes fused with SV40-transformed fibroblasts to produce an immortalised cell line (Davidson et al., 2005). The cardiac phenotype of the cell line was confirmed. The major factors being the expression of troponin I, α-actinin, troponin C and tropomyosin, proteins central to contraction and relaxation of cardiac muscles (Layland et al., 2005). This was coupled with a lack of α-smooth muscle actin, a marker of vascular but not cardiac muscle. The cell line was reported as being precontractile (Davidson et al., 2005), a state supported by expression of the transcription factor NKX2.5 protein, a key regulatory transcription factor essential for human heart development (Zheng et al., 2006), and a lack of detectable contractile activity *in vitro*.

In humans, as well as other mammals, cardiomyocytes have a very limited capability for regeneration, with low or negligible proliferative capacity, being in a pre-mitotic arrested state (Siddiqi and Sussman, 2014). Therefore, it is important to model this and simultaneously evaluate effects in quiescent cardiac cells, because it is crucial to evaluate the effect of compounds upon cardiac cells which are a better representation of the adult heart. This low proliferative rate and cellular quiescence was aligned to AC10 cells in the plateau phase of growth in this project. Therefore, alongside 'conventional' assessment of drug effects upon proliferative cells *in vitro,* the treatment of AC10 cardiomyocytes in

the plateau growth phase was also performed to overcome effects attributed to the proliferative nature of the AC10 rather than those aligned to the clinical status of cardiomyocytes. In this context, responses of highly proliferative AC10 cells were demonstrated to be more sensitive to treatment with VDAs than cells in the plateau growth phase, with low proliferative capacities. Similarly, although no discernible difference in cytotoxicity of VDAs were observed between cancer cells and proliferative AC10 cells, a significant difference was detected when the sensitivity of cancer cells to VDAs was evaluated against AC10 cells in the plateau phase of growth, representative of the clinic. This supports the potential for a viable therapeutic index for VDAs in the clinic. Furthermore, toxicity of VDAs was increased in response to prolonged exposure of cells to these agents, indicative of a relationship between exposure and detrimental effects. The results obtained in this phase of the project were in agreement with clinical findings indicative of dose-limiting adverse effects with VDA monotherapy, related to direct cytotoxicity (Subbiah et al., 2011, Rustin et al., 2003, Dowlati et al., 2002a, Nathan et al., 2012).

Although VDAs demonstrate a degree of direct cytotoxicity against cardiac cells, this does not completely explain their reported clinic cardiotoxicity profile wherein longer-term effects are evidenced. As such, further to an initial cytotoxic insult to cardiac cells, other toxicity mechanisms must also be at play, especially in the case of exposure to sub-cytotoxic VDA concentrations related to pharmacokinetics of VDAs during prolonged exposures. As would be expected, both Colchicine and CA4 bound to tubulin causing microtubules stabilisation in the AC10 cell model (Hill et al., 1993, Bibby et al., 1989, Baguley et al., 1996, Cai, 2007). Additionally, both VDAs also resulted in accumulation of AC10 cells in G2/M of the cell cycle, an effect proportional to increase in both dose and

exposure time of the VDAs. Importantly, although AC10 cells in the plateau phase of growth demonstrated twice as many cells resident in G2/M than proliferative cells, exposure to VDAs caused further accumulation of these cells in this phase at the detriment of those cells in S-phase at the time of exposure. Although this supports the pre-mitotic phenotype of cardiomyocytes, it highlights the potential 'hidden' effect these agents may have on the cardiac system through retardation of a potential for cell cycle re-entry and responsive proliferation to the toxicological insult in the quiescent cell population. Further studies are thereby warranted using *in vivo* models or clinical studies to confirm this potential effect.

Alongside direct loss of cardiomyocytes through cytotoxic effects, a common reactionary and compensatory cardiac tissue response to drug-induced cardiotoxicity is an increase in cell size (hypertrophy) of the 'surviving' cardiomyocytes to compensate for the loss of cells by direct cytotoxicity. This is the case with a number of cancer chemotherapies, with cytotoxicity alongside cardiac hypertrophy reported (Du et al., 2017, Schmidinger et al., 2008, Geisberg and Sawyer, 2010, Sawyer et al., 2010, Tagawa et al., 1997). Confirmed through several parallel methodologies in this study, exposure of AC10 cells to either Colchicine or CA4 resulted in a significant dose and time dependent increase in cell size. This cellular response being observed with both proliferative and quiescent AC10 cells, with the effects of CA4 being marginally greater than those of Colchicine. Interestingly, these effects of CA4 were more striking after short-exposure as opposed to continuous exposure, with a significant effect also observed with low concentrations. This is suggestive of these effects being an immediate response rather than an accumulated response to VDA exposure. Similar effects associated with cardiac remodelling and changes in LVEF had previously been observed clinically (Grisham et al., 2018, Rustin et al., 2003, Zweifel et al., 2011). Furthermore, *In vivo* rodent studies had also revealed

changes in cardiac functions following CA4DP-treatment, an observation linked to ischemia and cardiac cells hypertrophy (Tochinai et al., 2018). The fact that the *in vitro* studies herein also showed this hypertrophic response further supports this toxicological mechanism of action for VDAs against cardiomyocytes.

Due to the high potential to mitigate VDA-induced cardiotoxicity, attention is placed toward prevention and mitigation rather than treatment and management of VDA-induced cardiotoxicity (Ke et al., 2015, Ke et al., 2009, Busk et al., 2011). In this context, this study also investigated the response of AC10 cardiomyocytes to combined treatment of VDAs with cardioprotectants, to appraise potential strategies for clinical mitigation. Administration of drugs inhibiting the renin-angiotensin pathway resulted in a reduction in cytotoxic potential for VDAs, albeit only when administered prior to the VDA. A cardioprotective differential effect was observed between Colchicine and CA4, reflecting the differential dynamics of drug-target interaction for these drugs. Treatment of AC10 cells with the β-blocker carvedilol also mitigated the cytotoxicity of both Colchicine and CA4. However, in contrast to proliferative AC10 cells, no protective effects were observed with quiescent AC10 cells when the VDA was added before carvedilol and the exposure period was continuous. Additionally, a protective effect was observed when carvedilol was added after exposure of quiescent AC10 cells to short-duration exposure of CA4, but not Colchicine. This again relates to the drug-target dynamics of Colchicine versus CA4, suggesting a one-size-fits-all approach may not be appropriate for drug-induced mitigation of VDA-induced cardiotoxic effects.

VDAs have been reported in *in vivo* studies and clinical trials to cause QT prolongation, changes in cardiac contractility, acute functional cardiovascular effects, including arrythmias and cardiac fibrillations (Cooney et al., 2004, Grisham et al., 2018, Rustin et

al., 2003, Zweifel et al., 2011). Therefore, an angle addressed in this project focused on the effect of VDAs upon cardiomyocyte function and contractility. This was evaluated through determination of the contractility of VDA-treated Cor.At® stem-cell derived cardiomyocytes monitored using the xCELLigence cardio system. Exposure of Cor.At® cells to either Colchicine or CA4P resulted in a measurable decline in cell index within 30 minutes of drug-addition, supporting a tubulin-mediated change in cellular morphology rather than overt cytotoxicity. The effects of Colchicine and CA4 on the contractile rate of Cor.At® cells was found to be minimal across the duration of the study, in agreement with a previous study evaluating the effects of Colchicine upon rat neonatal cardiomyocytes using the xCELLigence RTCA system (Lamore et al., 2013). The most noticeable and significant effect upon cardiomyocyte contractile function was a time-dependent reduction in the beat-amplitude, representative of a reduction in cellular ability to contract, relax and stretch. This response is again in agreement with the published effects of Colchicine upon primary neonatal rat cardiomyocytes, wherein the decrease in beat amplitude was also not attributable to a drug-induced decrease in cell viability (Lamore et al., 2013). The lack of an effect upon rate of contractility but rather an effect upon degree of contractility is a pertinent finding, aligning with the pharmacological mechanism of VDAs upon perturbation of microtubule dynamics. Translation of this observation to the clinic would explain a relative lack of acute drug-induced dysrhythmias but support modulations of cardiac function by VDAs. Such an effect would thus highlight a potential for VDAs to affect cardiac contractility and potential cardiac 'stiffening' within the clinical environment, a response which would exacerbate the established haemodynamic changes associated with VDA treatment (Gill et al., 2019).

Assessment of genetic changes induced in cardiac tissue following *in vivo* exposure to Colchicine indicated activation or perturbation of several common genetic pathways, including cell survival, inflammation, and cellular signalling amongst others. Induction of cell death pathways was indicative of both cardiac cell death and induction of vascular damage, as previously reported (Mikaelian et al., 2010). Downregulation of genes related to insulin signalling and glucose transport supported Colchicine-mediated effects on vascular tonicity (Bertrand et al., 2008). Drug-induced hypertrophy, reflecting the *in vitro* studies in this project, was indicated by activation of ERK and mitogen-activated protein kinase (MAPK) signalling pathways involved in control of cardiac hypertrophy and cardiac remodelling (Liu et al., 2016). The activation of pro-inflammatory and downregulation of anti-inflammatory signalling pathways following exposure to Colchicine was also detected in this study, genetic factors commonly associated with myocardial remodelling and fibrosis (Yue et al., 2019, Onishi and Gaffen, 2010) (Xiao et al., 2020). Together the genetic changes induced by Colchicine *in vivo* were strongly supportive of direct cytotoxicity, morphological alteration and development of cardiac fibrosis and cardiac hypertrophy. These changes detected *in vivo* were therefore reflective of the effects of VDAs identified in the *in vitro* methodologies, substantiating the breadth of findings in this study.

Taken together, these data identify direct effect of VDAs on cardiomyocytes as a primary cause of the VDA-induced cardiotoxicity and identify direct cytotoxicity, cell growth arrest and cellular hypertrophy as contributory mechanisms of structural toxicity for VDAs. An effect on functionality of cardiomyocytes through restriction of their contractility, rather than an effect upon rate of contraction, in alignment with their effects on intracellular cytoskeleton proteins further adds to putative cardiotoxicity of VDAs in the clinic. Despite this, a potential for mitigation of cardiotoxicity through prophylactic administration of

drugs targeting the angiotensin signalling pathway or inhibiting β-adrenergic signalling is provided.

7.2 Limitations of the study

Like any other research, this study had number of limitations. The aim of this section to identify and acknowledge these limitations.

The AC10 cell line, although derived from human adult cardiomyocytes, is a fusion with a fibroblast cell line. Despite demonstrating a cardiac phenotype and responding appropriately to known cardiac active agents, this cell line is non-contractile and the results obtained from this cell line should always be appraised with an element of caution because of the fusion status and limited degree of functional attributes demonstrated., However, the observation of comparable results from the stem-cell derived cardiomyocyte cell model does somewhat negate some of these concerns.

The Cor.AT cardiomyocyte stem cell model, although demonstrating defined reproducibility, good characterisation and stable contractility over an extended period of time, it must be borne in mind that these cells are murine and to some extent cannot truly recapitulate full cardiac human physiology. This can be mitigated through the parallel use of hiPSC cardiomyocytes in confirmatory investigations. Full validation of results would also require future experiments to determine the effect of VDAs on cardiac functions to be repeated at least three times.

All cardiac cell studies in this project were conducted in two-dimensional in vitro assays. Consequently, the involvement of other cell types within the heart and three-dimensional cellular interactions was not assessed. To further confirm the findings of this project, such three-dimensional multicellular studies should also be conducted.

The mouse cardiotoxicity RT² Profiler™ quantitative PCR (qPCR) array, which utilised in vivo cardiac tissue, due to time constraints was only performed once, although these results do still demonstrate value as they were obtained from pooling of multiple samples and multiple internal gene expression repeat evaluations. Further investigation into the obtained preliminary finding on the effect of VDAs upon specific genetic pathways within cardiomyocytes would require confirmatory qPCR studies.

7.3 Future Directions

An important direction for future studies would be to appraise and confirm the outcome of the studies with AC10 cardiomyocytes and Cor.At® cardiomyocytes in other cell systems, such as hiPSC-CMs and primary cardiomyocytes, to ensure robust characterisation of VDA cytotoxicities. This should thereafter be evaluated in either three-dimensional cardiac models incorporating cells of different lineages, *in vivo* studies and ideally clinical biopsies or through use of clinical imaging technologies. An example of a 3D cardiac model that would be used in future work could be by co-culturing human embryonic stem cell derived cardiomyocytes (hESC-CMs) in spheroid microtissue format as this was already examined by Ravenscroft et al in 2016 (Ravenscroft et al., 2016).

The induction of cardiomyocyte hypertrophy by VDAs is suggested as a major underpinning mechanism of toxicity, supporting the observations and outcomes from *in vivo* studies. Monitoring of this in the clinic, through either systemic biomarkers or imaging technologies, would thus be warranted to confirm translational of the *in vitro* findings from this study. However, further studies are also necessary to elaborate the specific mechanisms responsible for VDA-induced hypertrophy, to ascertain whether this is exclusively associated with tubulin disruption or whether other factors such as mitochondrial dysregulation or biochemical changes also have a contributory role.

Although it was not assessed, hypertrophy of AC10 might be attributed to senescence. Senescence could be by detected the staining of β-Galactosidase, a known characteristic enzyme of senescent cells which hydrolyse of β-galactosides into monosaccharides only in senescent cells. Another biomarker of cellular senescence is P16 Ink4A.

Although the mitigation of VDA-induced cytotoxicity was demonstrated by both enalapril and enalaprilat, these effects were unanticipated due to their action upon extracellular production of angiotensin II, factors not believed to be present in the *in vitro* system. As such, further studies are required to either confirm the presence of this signalling system within the cell model, or to identify the off-target mechanism by which these drugs cause these effects. Furthermore, analysis of the dynamics of drug-target interactions of both Colchicine and CA4 should be investigated to gain greater understanding of the differences in response to cardioprotection of these agents.

Ultimately, comparative studies should be incorporated into future clinical trials of VDAs to assess the outcomes from this project and their relevance and translational applicability to the clinical progression of VDAs.

References:

ABAS, L., BOGOYEVITCH, M. A. & GUPPY, M. 2000. Mitochondrial ATP production is necessary for activation of the extracellular-signal-regulated kinases during ischaemia/reperfusion in rat myocyte-derived H9c2 cells. *Biochemical Journal,* 349**,** 119-126.

ABASSI, Y. A., XI, B., LI, N., OUYANG, W., SEILER, A., WATZELE, M., KETTENHOFEN, R., BOHLEN, H., EHLICH, A., KOLOSSOV, E., WANG, X. & XU, X. 2012. Dynamic monitoring of beating periodicity of stem cell-derived cardiomyocytes as a predictive tool for preclinical safety assessment. *Br J Pharmacol,* 165**,** 1424-41.

ABI-GERGES, A., CASTRO, L., LEROY, J., DOMERGUE, V., FISCHMEISTER, R. & VANDECASTEELE, G. 2021. Selective changes in cytosolic β-adrenergic cAMP signals and L-type Calcium Channel regulation by Phosphodiesterases during cardiac hypertrophy. *Journal of Molecular and Cellular Cardiology,* 150**,** 109-121.

ABRAHAM, W. T., CHIN, F. M. H., FELDMAN, A. M., FRANCIS, F. G. S., GANIATS, F. T. G., MANCINI, D. M. & MICHL, K. 2009. 2009 Focused update incorporated into the ACC/AHA 2005 Guidelines for the Diagnosis and Management of Heart Failure in Adults. *Journal of the American College of Cardiology,* 53**,** e1-90.

AGGARWAL, S. 2010. Targeted cancer therapies. *Nature Reviews Drug Discovery,* 9**,** 427-428.

AIRD, W. C. 2007. Phenotypic heterogeneity of the endothelium: II. Representative vascular beds. *Circulation research,* 100**,** 174-190.

AIREY, C. L., DODWELL, D. J., JOFFE, J. K. & JONES, W. G. 1995. Etoposide-related myocardial infarction. *Clinical Oncology,* 7**,** 135.

ALAMEDDINE, R. S., YAKAN, A. S., SKOURI, H., MUKHERJI, D., TEMRAZ, S. & SHAMSEDDINE, A. 2015. Cardiac and vascular toxicities of angiogenesis inhibitors: The other side of the coin. *Critical Reviews in Oncology/Hematology,* 96**,** 195-205.

ALBINI, A., PENNESI, G., DONATELLI, F., CAMMAROTA, R., DE FLORA, S. & NOONAN, D. M. 2010. Cardiotoxicity of anticancer drugs: the need for cardio-oncology and cardio-oncological prevention. *J Natl Cancer Inst.* United States.

ALI, N. N., XU, X., BRITO-MARTINS, M., POOLE-WILSON, P. A., HARDING, S. E. & FULLER, S. J. 2004. Beta-adrenoceptor subtype dependence of chronotropy in mouse embryonic stem cell-derived cardiomyocytes. *Basic Res Cardiol,* 99**,** 382-91.

ANAND, A. J. 1994. Fluorouracil cardiotoxicity. *Ann Pharmacother,* 28**,** 374-8.

ANDERSON, B. & SAWYER, D. B. 2008. Predicting and preventing the cardiotoxicity of cancer therapy. *Expert review of cardiovascular therapy,* 6**,** 1023-1033.

ANDERSON, H. L., YAP, J. T., MILLER, M. P., ROBBINS, A., JONES, T. & PRICE, P. M. 2003. Assessment of pharmacodynamic vascular response in a phase I trial of combretastatin A4 phosphate. *Journal of Clinical Oncology,* 21**,** 2823-2830.

ANVERSA, P., OLIVETTI, G., MELISSARI, M. & LOUD, A. V. 1980. Stereological measurement of cellular and subcellular hypertrophy and hyperplasia in the papillary muscle of adult rat. *J Mol Cell Cardiol,* 12**,** 781-95.

ARATYN-SCHAUS, Y., PASQUALINI, F. S., YUAN, H., MCCAIN, M. L., YE, G. J. C., SHEEHY, S. P., CAMPBELL, P. H. & PARKER, K. K. 2016. Coupling primary and stem cell-derived cardiomyocytes in an in vitro model of cardiac cell therapy. *The Journal of cell biology,* 212**,** 389-397.

ARMULIK, A., ABRAMSSON, A. & BETSHOLTZ, C. 2005. Endothelial/pericyte interactions. *Circulation research,* 97**,** 512-523.

ARNOLD, M. R., MARK J; BARDOT, AUDE; FERLAY, JACQUES; ANDERSSON, THERESE M-L; MYKLEBUST, TOR ÅGE; TERVONEN, HANNA; THURSFIELD, VICKY; RANSOM, DAVID; SHACK, LORRAINE; WOODS, RYAN R; TURNER, DONNA; LEONFELLNER, SUZANNE; RYAN, SUSAN; SAINT-JACQUES, NATHALIE; DE, PRITHWISH; MCCLURE, CAROL; RAMANAKUMAR, AGNIHOTRAM V; STUART-PANKO, HEATHER; ENGHOLM, GERDA; WALSH, PAUL M; JACKSON, CHRISTOPHER; VERNON, SALLY; MORGAN, EILEEN; GAVIN, ANNA; MORRISON, DAVID S; HUWS, DYFED W; PORTER, GEOFF; BUTLER, JOHN; BRYANT, HEATHER; CURROW, DAVID C; HIOM, SARA; PARKIN, D MAX; SASIENI, PETER; LAMBERT, PAUL C; MØLLER, BJØRN; SOERJOMATARAM, ISABELLE; BRAY, FREDDIE 2019. Progress in cancer survival, mortality, and incidence in seven high-income countries 1995–2014 (ICBP SURVMARK-2): a population-based study. *The Lancet Oncology,* 20**,** 12.

ASAI, Y., TADA, M., G OTSUJI, T. & NAKATSUJI, N. 2010. Combination of functional cardiomyocytes derived from human stem cells and a highly-efficient microelectrode array system: an ideal hybrid model assay for drug development. *Current stem cell research & therapy,* 5**,** 227-232.

ATKINSON, J. M., FALCONER, R. A., EDWARDS, D. R., PENNINGTON, C. J., SILLER, C. S., SHNYDER, S. D., BIBBY, M. C., PATTERSON, L. H., LOADMAN, P. M. & GILL, J. H. 2010. Development of a novel tumor-targeted vascular disrupting agent activated by membrane-type matrix metalloproteinases. *Cancer research,* 70**,** 6902-6912.

AUDEBRAND, A., DÉSAUBRY, L. & NEBIGIL, C. G. 2020. Targeting GPCRs Against Cardiotoxicity Induced by Anticancer Treatments. *Frontiers in cardiovascular medicine,* 6**,** 194-194.

AVOLIO, E., RODRIGUEZ-ARABAOLAZA, I., SPENCER, H. L., RIU, F., MANGIALARDI, G., SLATER, S. C., ROWLINSON, J., ALVINO, V. V., IDOWU, O. O. & SOYOMBO, S. 2015. Expansion and characterization of neonatal cardiac pericytes provides a novel cellular option for tissue engineering in congenital heart disease. *Journal of the American Heart Association,* 4**,** e002043.

AZEVEDO, P. S., POLEGATO, B. F., MINICUCCI, M. F., PAIVA, S. A. & ZORNOFF, L. A. 2016. Cardiac Remodeling: Concepts, Clinical Impact, Pathophysiological Mechanisms and Pharmacologic Treatment. *Arq Bras Cardiol,* 106**,** 62-9.

BACAC, M. & STAMENKOVIC, I. 2008. Metastatic cancer cell. *Annu. Rev. Pathol. Mech. Dis.,* 3**,** 221-247.

BAGULEY, B. C., ZHUANG, L. & KESTELL, P. 1996. Increased plasma serotonin following treatment with flavone-8-acetic acid, 5, 6-dimethylxanthenone-4-acetic acid, vinblastine, and colchicine: relation to vascular effects. *Oncology research,* 9**,** 55-60.

BALDWIN, H. S., JENSEN, K. L. & SOLURSH, M. 1991. Myogenic cytodifferentiation of the precardiac mesoderm in the rat. *Differentiation,* 47**,** 163-72.

BALUK, P., HASHIZUME, H. & MCDONALD, D. M. 2005. Cellular abnormalities of blood vessels as targets in cancer. *Curr Opin Genet Dev,* 15**,** 102-11.

BANKS-SCHLEGEL, S. P., GAZDAR, A. F. & HARRIS, C. C. 1985. Intermediate filament and cross-linked envelope expression in human lung tumor cell lines. *Cancer Res,* 45**,** 1187-97.

BARLOW, K. D., SANDERS, A. M., SOKER, S., ERGUN, S. & METHENY-BARLOW, L. J. 2013. Pericytes on the tumor vasculature: jekyll or hyde? *Cancer microenvironment : official journal of the International Cancer Microenvironment Society,* 6**,** 1-17.

BASS, A. S., TOMASELLI, G., BULLINGHAM III, R. & KINTER, L. B. 2005. Drugs effects on ventricular repolarization: a critical evaluation of the strengths and weaknesses of current methodologies and regulatory practices. *Journal of pharmacological and toxicological methods,* 52**,** 12-21.

BEEREPOOT, L. V., RADEMA, S. A., WITTEVEEN, E. O., THOMAS, T., WHEELER, C., KEMPIN, S. & VOEST, E. E. 2006. Phase I clinical evaluation of weekly administration of the novel vascular-targeting agent, ZD6126, in patients with solid tumors. *J Clin Oncol,* 24**,** 1491-8.

BERARDI, R., CARAMANTI, M., SAVINI, A., CHIORRINI, S., PIERANTONI, C., ONOFRI, A., BALLATORE, Z., DE LISA, M., MAZZANTI, P. & CASCINU, S. 2013. State of the art for cardiotoxicity due to chemotherapy and to targeted therapies: a literature review. *Crit Rev Oncol Hematol,* 88**,** 75-86.

BERGERS, G. & SONG, S. 2005. The role of pericytes in blood-vessel formation and maintenance. *Neuro-Oncology,* 7**,** 452-464.

BERS, D. M. 2002. Cardiac excitation–contraction coupling. *Nature,* 415**,** 198-205.

BERTRAND, L., HORMAN, S., BEAULOYE, C. & VANOVERSCHELDE, J.-L. 2008. Insulin signalling in the heart. *Cardiovascular Research,* 79**,** 238-248.

BEVEGARD, B. S. & SHEPHERD, J. T. 1967. Regulation of the circulation during exercise in man. *Physiol Rev,* 47**,** 178-213.

BHULLAR, K. S., LAGARÓN, N. O., MCGOWAN, E. M., PARMAR, I., JHA, A., HUBBARD, B. P. & RUPASINGHE, H. P. V. 2018. Kinase-targeted cancer therapies: progress, challenges and future directions. *Molecular Cancer,* 17**,** 48.

BIBBY, M. C., DOUBLE, J. A., LOADMAN, P. M. & DUKE, C. V. 1989. Reduction of Tumor Blood Flow by Flavone Acetic Acid: A Possible Component of Therapy. *Journal of the National Cancer Institute,* 81**,** 216-220.

BLAKEY, D. C., ASHTON, S. E., WESTWOOD, F. R., WALKER, M. & RYAN, A. J. 2002. ZD6126: A novel small molecule vascular targeting agent. *International Journal of Radiation Oncology*Biology*Physics,* 54**,** 1497-1502.

BLINOVA, K., DANG, Q., MILLARD, D., SMITH, G., PIERSON, J., GUO, L., BROCK, M., LU, H. R., KRAUSHAAR, U., ZENG, H., SHI, H., ZHANG, X., SAWADA, K., OSADA, T., KANDA, Y., SEKINO, Y., PANG, L., FEASTER, T. K., KETTENHOFEN, R., STOCKBRIDGE, N., STRAUSS, D. G. & GINTANT, G. 2018. International Multisite Study of Human-Induced Pluripotent Stem Cell-Derived Cardiomyocytes for Drug Proarrhythmic Potential Assessment. *Cell Rep,* 24**,** 3582-3592.

BLINOVA, K., STOHLMAN, J., VICENTE, J., CHAN, D., JOHANNESEN, L., HORTIGON-VINAGRE, M. P., ZAMORA, V., SMITH, G., CRUMB, W. J. & PANG, L. 2017. Comprehensive translational assessment of human-induced pluripotent stem cell derived cardiomyocytes for evaluating drug-induced arrhythmias. *Toxicological Sciences,* 155**,** 234-247.

BORISOV, A. B. & CLAYCOMB, W. C. 1995. Proliferative potential and differentiated characteristics of cultured cardiac muscle cells expressing the SV40 T oncogene. *Ann N Y Acad Sci,* 752**,** 80-91.

BRAAM, S. R., TERTOOLEN, L., VAN DE STOLPE, A., MEYER, T., PASSIER, R. & MUMMERY, C. L. 2010. Prediction of drug-induced cardiotoxicity using human embryonic stem cell-derived cardiomyocytes. *Stem Cell Res,* 4**,** 107-16.

BRANA, I. & TABERNERO, J. 2010. Cardiotoxicity. *Annals of Oncology,* 21**,** vii173-vii179.

BRANCO, A. F., PEREIRA, S. P., GONZALEZ, S., GUSEV, O., RIZVANOV, A. A. & OLIVEIRA, P. J. 2015. Gene Expression Profiling of H9c2 Myoblast Differentiation towards a Cardiac-Like Phenotype. *PloS one,* 10**,** e0129303-e0129303.

BROOKS, P. C. 1996. Cell adhesion molecules in angiogenesis. *Cancer Metastasis Rev,* 15**,** 187-94.

BRUNSKILL, E. W., WITTE, D. P., YUTZEY, K. E. & POTTER, S. S. 2001. Novel cell lines promote the discovery of genes involved in early heart development. *Developmental biology,* 235**,** 507-520.

BURTON, K. P. 1994. Effects of 21-aminosteroids in neonatal rat cardiac myocyte cell cultures exposed to free radicals. *Cardiovasc Res,* 28**,** 1500-6.

BUSK, M., BOHN, A. B., SKALS, M., WANG, T. & HORSMAN, M. R. 2011. Combretastatin-induced hypertension and the consequences for its combination with other therapies. *Vascul Pharmacol,* 54**,** 13-7.

BYLUND, D. B. 2007. Beta-2 Adrenoceptor*. *In:* ENNA, S. J. & BYLUND, D. B. (eds.) *xPharm: The Comprehensive Pharmacology Reference.* New York: Elsevier.

CAI, S. X. 2007. Small molecule vascular disrupting agents: potential new drugs for cancer treatment. *Recent patents on anti-cancer drug discovery,* 2**,** 79-101.

CAMELLITI, P., BORG, T. K. & KOHL, P. 2005. Structural and functional characterisation of cardiac fibroblasts. *Cardiovascular research,* 65**,** 40-51.

CAMERON, A. C., TOUYZ, R. M. & LANG, N. N. 2016. Vascular Complications of Cancer Chemotherapy. *Canadian Journal of Cardiology,* 32**,** 852-862.

CANTOR, E. J., BABICK, A. P., VASANJI, Z., DHALLA, N. S. & NETTICADAN, T. 2005. A comparative serial echocardiographic analysis of cardiac structure and function in rats subjected to pressure or volume overload. *J Mol Cell Cardiol,* 38**,** 777-86.

CAPPETTA, D., DE ANGELIS, A., SAPIO, L., PREZIOSO, L., ILLIANO, M., QUAINI, F., ROSSI, F., BERRINO, L., NAVIGLIO, S. & URBANEK, K. 2017. Oxidative stress and cellular response to doxorubicin: A common factor in the complex milieu of anthracycline cardiotoxicity. *Oxidative Medicine and Cellular Longevity,* 2017.

CAPPETTA, D., ROSSI, F., PIEGARI, E., QUAINI, F., BERRINO, L., URBANEK, K. & DE ANGELIS, A. 2018. Doxorubicin targets multiple players: A new view of an old problem. *Pharmacological Research,* 127**,** 4-14.

CARDINALE, D., BACCHIANI, G., BEGGIATO, M., COLOMBO, A. & CIPOLLA, C. M. 2013. Strategies to prevent and treat cardiovascular risk in cancer patients. *Semin Oncol,* 40**,** 186-98.

CARDINALE, D., BIASILLO, G. & CIPOLLA, C. M. 2016. Curing Cancer, Saving the Heart: A Challenge That Cardioncology Should Not Miss. *Current Cardiology Reports,* 18.

CARDINALE, D., COLOMBO, A., LAMANTIA, G., COLOMBO, N., CIVELLI, M., DE GIACOMI, G., RUBINO, M., VEGLIA, F., FIORENTINI, C. & CIPOLLA, C. M. 2010. Anthracycline-induced cardiomyopathy: clinical relevance and response to pharmacologic therapy. *J Am Coll Cardiol,* 55**,** 213-20.

CASINI, S., TAN, H. L., DEMIRAYAK, I., REMME, C. A., AMIN, A. S., SCICLUNA, B. P., CHATYAN, H., RUIJTER, J. M., BEZZINA, C. R., VAN GINNEKEN, A. C. G. & VELDKAMP, M. W. 2010. Tubulin polymerization modifies cardiac sodium channel expression and gating. *Cardiovascular Research,* 85**,** 691-700.

CASPI, O., ITZHAKI, I., KEHAT, I., GEPSTEIN, A., ARBEL, G., HUBER, I., SATIN, J. & GEPSTEIN, L. 2009. In vitro electrophysiological drug testing using human embryonic stem cell derived cardiomyocytes. *Stem Cells Dev,* 18**,** 161-72.

CAVANAUGH, P. F., MOSKWA, P. S., DONISH, W. H., PERA, P. J., RICHARDSON, D. & ANDRESE, A. P. 1990. A semi-automated neutral red based chemosensitivity assay for drug screening. *Investigational new drugs,* 8**,** 347-354.

CAVERO, I. & HOLZGREFE, H. 2014. Comprehensive in vitro Proarrhythmia Assay, a novel in vitro/in silico paradigm to detect ventricular proarrhythmic liability: a visionary 21st century initiative. *Expert Opin Drug Saf,* 13**,** 745-58.

CHAFFER, C. L. & WEINBERG, R. A. 2011. A perspective on cancer cell metastasis. *Science,* 331**,** 1559-64.

CHAMBERS, A. F., GROOM, A. C. & MACDONALD, I. C. 2002. Dissemination and growth of cancer cells in metastatic sites. *Nature Reviews Cancer,* 2**,** 563-572.

CHAPLIN, D. & DOUGHERTY, G. 1999. Tumour vasculature as a target for cancer therapy. *British journal of cancer,* 80**,** 57-64.

CHASE, D. M., CHAPLIN, D. J. & MONK, B. J. 2017. The development and use of vascular targeted therapy in ovarian cancer. *Gynecol Oncol,* 145**,** 393-406.

CHEN, M., LEI, X., SHI, C., HUANG, M., LI, X., WU, B., LI, Z., HAN, W., DU, B. & HU, J. 2017. Pericyte-targeting prodrug overcomes tumor resistance to vascular disrupting agents. *The Journal of clinical investigation,* 127**,** 3689-3701.

CHI, K. R. 2013. Revolution dawning in cardiotoxicity testing. *Nat Rev Drug Discov,* 12**,** 565-7.

CHIU, R. C.-J., ZIBAITIS, A. & KAO, R. L. 1995. Cellular cardiomyoplasty: myocardial regeneration with satellite cell implantation. *The Annals of thoracic surgery,* 60**,** 12-18.

CHO, M.-H., NILES, A., HUANG, R., INGLESE, J., AUSTIN, C. P., RISS, T. & XIA, M. 2008. A bioluminescent cytotoxicity assay for assessment of membrane integrity using a proteolytic biomarker. *Toxicology in vitro,* 22**,** 1099-1106.

CHU, T. F., RUPNICK, M. A., KERKELA, R., DALLABRIDA, S. M., ZURAKOWSKI, D., NGUYEN, L., WOULFE, K., PRAVDA, E., CASSIOLA, F., DESAI, J., GEORGE, S., HARRIS, D. M., ISMAIL, N. S., CHEN, J.-H., SCHOEN, F. J., VAN DEN ABBEELE, A. D., DEMETRI, G. D., FORCE, T., CHEN, M. H. & MORGAN, J. A. 2007. Cardiotoxicity associated with tyrosine kinase inhibitor sunitinib. *The Lancet,* 370**,** 2011-2019.

CIMMINO, G., TARALLO, R., CONTE, S., MORELLO, A., PELLEGRINO, G., LOFFREDO, F. S., CALÌ, G., DE LUCA, N., GOLINO, P., TRIMARCO, B. & CIRILLO, P. 2018. Colchicine reduces platelet aggregation by modulating cytoskeleton rearrangement via inhibition of cofilin and LIM domain kinase 1. *Vascular Pharmacology,* 111**,** 62-70.

CIRILLO, P., TAGLIALATELA, V., PELLEGRINO, G., MORELLO, A., CONTE, S., DI SERAFINO, L. & CIMMINO, G. 2020. Effects of colchicine on platelet aggregation in patients on dual antiplatelet therapy with aspirin and clopidogrel. *Journal of Thrombosis and Thrombolysis,* 50**,** 468-472.

CLAIRE ROBERTSON, S. 2013. Maturation phases of human pluripotent stem cellderived cardiomyocytes. *Stem Cells,* 31**,** 1e17.

CLAYCOMB, W. C., LANSON, N. A., JR., STALLWORTH, B. S., EGELAND, D. B., DELCARPIO, J. B., BAHINSKI, A. & IZZO, N. J., JR. 1998. HL-1 cells: a cardiac muscle cell line that contracts and retains phenotypic characteristics of the adult cardiomyocyte. *Proc Natl Acad Sci U S A,* 95**,** 2979-84.

CLAYCOMB, W. C. & PALAZZO, M. C. 1980. Culture of the terminally differentiated adult cardiac muscle cell: a light and scanning electron microscope study. *Developmental biology,* 80**,** 466-482.

COLATSKY, T., FERMINI, B., GINTANT, G., PIERSON, J. B., SAGER, P., SEKINO, Y., STRAUSS, D. G. & STOCKBRIDGE, N. 2016. The Comprehensive in Vitro Proarrhythmia Assay (CiPA) initiative — Update on progress. *Journal of Pharmacological and Toxicological Methods,* 81**,** 15-20.

COLLIER, J., WHITE, S., WILLIAM, C. & SCOTT, S. 2002. Insulin represses and chronic hyperglycemia stimulates adrenomedullin gene expression in HL-1 cultured cardiac myocytes. *Diabetes,* 51.

CONTI, V., RUSSOMANNO, G., CORBI, G., IZZO, V., VECCHIONE, C. & FILIPPELLI, A. 2013. Adrenoreceptors and nitric oxide in the cardiovascular system. *Frontiers in physiology,* 4**,** 321-321.

COONEY, M., SAVVIDES, P., AGARWALA, S., WANG, D., FLICK, S., BERGANT, S., BHAKTA, S., LAVERTU, P., ORTIZ, J. & REMICK, S. 2006. Phase II study of combretastatin A4 phosphate (CA4P) in patients with advanced anaplastic thyroid carcinoma (ATC). *Journal of Clinical Oncology,* 24**,** 5580-5580.

COONEY, M. M., RADIVOYEVITCH, T., DOWLATI, A., OVERMOYER, B., LEVITAN, N., ROBERTSON, K., LEVINE, S. L., DECARO, K., BUCHTER, C., TAYLOR, A., STAMBLER, B. S. & REMICK, S. C. 2004. Cardiovascular safety profile of combretastatin a4 phosphate in a single-dose phase I study in patients with advanced cancer. *Clin Cancer Res,* 10**,** 96-100.

COSMAI, L., GALLIENI, M. & PORTA, C. 2015. Renal toxicity of anticancer agents targeting HER2 and EGFR. *Journal of Nephrology,* 28**,** 647-657.

CROSS, M. J. & CLAESSON-WELSH, L. 2001. FGF and VEGF function in angiogenesis: signalling pathways, biological responses and therapeutic inhibition. *Trends Pharmacol Sci,* 22**,** 201-7.

CROUCH, S., KOZLOWSKI, R., SLATER, K. & FLETCHER, J. 1993. The use of ATP bioluminescence as a measure of cell proliferation and cytotoxicity. *Journal of immunological methods,* 160**,** 81-88.

CSAPO, M. & LAZAR, L. 2014. Chemotherapy-Induced Cardiotoxicity: Pathophysiology and Prevention. *Clujul Med,* 87**,** 135-42.

CURIGLIANO, G., CARDINALE, D., DENT, S., CRISCITIELLO, C., ASEYEV, O., LENIHAN, D. & CIPOLLA, C. M. 2016. Cardiotoxicity of anticancer treatments: epidemiology, detection, and management. *CA: a cancer journal for clinicians,* 66**,** 309-325.

CURIGLIANO, G., CARDINALE, D., SUTER, T., PLATANIOTIS, G., DE AZAMBUJA, E., SANDRI, M. T., CRISCITIELLO, C., GOLDHIRSCH, A., CIPOLLA, C., ROILA, F. & GROUP, O. B. O. T. E. G. W. 2012. Cardiovascular toxicity induced by chemotherapy, targeted agents and radiotherapy: ESMO Clinical Practice Guidelines. *Annals of Oncology,* 23**,** vii155-vii166.

CURIGLIANO, G., MAYER, E. L., BURSTEIN, H. J., WINER, E. P. & GOLDHIRSCH, A. 2010. Cardiac toxicity from systemic cancer therapy: a comprehensive review. *Prog Cardiovasc Dis,* 53**,** 94-104.

D'AMARIO, D., CAPPETTA, D., CAPPANNOLI, L., PRINCI, G., MIGLIARO, S., DIANA, G., CHOUCHANE, K., BOROVAC, J. A., RESTIVO, A., ARCUDI, A., DE ANGELIS, A., VERGALLO, R., MONTONE, R. A., GALLI, M., LIUZZO, G. & CREA, F. 2021. Colchicine in ischemic heart disease: the good, the bad and the ugly. *Clinical Research in Cardiology*.

DAILY, N. J., SANTOS, R., VECCHI, J., KEMANLI, P. & WAKATSUKI, T. 2017. Calcium Transient Assays for Compound Screening with Human iPSC-derived Cardiomyocytes: Evaluating New Tools. *Journal of evolving stem cell research,* 1**,** 1-11.

DALBETH, N., LAUTERIO, T. J. & WOLFE, H. R. 2014. Mechanism of Action of Colchicine in the Treatment of Gout. *Clinical Therapeutics,* 36**,** 1465-1479.

DANSER, A. H. J., SARIS, J. J., SCHUIJT, M. P. & VAN KATS, J. P. 1999. Is there a local renin—angiotensin system in the heart? *Cardiovascular Research,* 44**,** 252-265.

DAVIDSON, M. M., NESTI, C., PALENZUELA, L., WALKER, W. F., HERNANDEZ, E., PROTAS, L., HIRANO, M. & ISAAC, N. D. 2005. Novel cell lines derived from adult human ventricular cardiomyocytes. *J Mol Cell Cardiol,* 39**,** 133-47.

DELCARPIO, J. B., LANSON, N. A., JR., FIELD, L. J. & CLAYCOMB, W. C. 1991. Morphological characterization of cardiomyocytes isolated from a transplantable cardiac tumor derived from transgenic mouse atria (AT-1 cells). *Circ Res,* 69**,** 1591-600.

DELGADO, J. L., HSIEH, C. M., CHAN, N. L. & HIASA, H. 2018. Topoisomerases as anticancer targets. *Biochemical Journal,* 475**,** 373-398.

DENELAVAS, A., WEIBEL, F., PRUMMER, M., IMBACH, A., CLERC, R. G., APFEL, C. M. & HERTEL, C. 2011. Real-time cellular impedance measurements detect Ca(2+) channel-dependent oscillations of morphology in human H295R adrenoma cells. *Biochim Biophys Acta,* 1813**,** 754-62.

DENG, C., ZHAO, J., ZHOU, S., DONG, J., CAO, J., GAO, J., BAI, Y. & DENG, H. 2020. The Vascular Disrupting Agent CA4P Improves the Antitumor Efficacy of CAR-T Cells in Preclinical Models of Solid Human Tumors. *Molecular Therapy,* 28**,** 75-88.

DERYUGINA, E. I. & QUIGLEY, J. P. 2015. Tumor angiogenesis: MMP-mediated induction of intravasation- and metastasis-sustaining neovasculature. *Matrix Biol,* 44-46**,** 94-112.

DI LORENZO, G., AUTORINO, R., BRUNI, G., CARTENÌ, G., RICEVUTO, E., TUDINI, M., FICORELLA, C., ROMANO, C., AIETA, M., GIORDANO, A., GIULIANO, M., GONNELLA, A., DE NUNZIO, C., RIZZO, M., MONTESARCHIO, V., EWER, M. & DE PLACIDO, S. 2009. Cardiovascular toxicity following sunitinib therapy in metastatic renal cell carcinoma: a multicenter analysis. *Annals of Oncology,* 20**,** 1535-1542.

DICK, E., RAJAMOHAN, D., RONKSLEY, J. & DENNING, C. 2010. Evaluating the utility of cardiomyocytes from human pluripotent stem cells for drug screening. *Biochem Soc Trans,* 38**,** 1037-45.

DOETSCHMAN, T. C., EISTETTER, H., KATZ, M., SCHMIDT, W. & KEMLER, R. 1985. The in vitro development of blastocyst-derived embryonic stem cell lines: formation of visceral yolk sac, blood islands and myocardium. *J Embryol Exp Morphol,* 87**,** 27-45.

DOHERTY, K. R., TALBERT, D. R., TRUSK, P. B., MORAN, D. M., SHELL, S. A. & BACUS, S. 2015. Structural and functional screening in human induced-pluripotent stem cell-derived cardiomyocytes accurately identifies cardiotoxicity of multiple drug types. *Toxicol Appl Pharmacol,* 285**,** 51-60.

DOLCI, A., DOMINICI, R., CARDINALE, D., SANDRI, M. T. & PANTEGHINI, M. 2008. Biochemical markers for prediction of chemotherapy-induced cardiotoxicity: systematic review of the literature and recommendations for use. *Am J Clin Pathol,* 130**,** 688-95.

DORN, G. W. & MOLKENTIN, J. D. 2004. Manipulating cardiac contractility in heart failure: data from mice and men. *Circulation,* 109**,** 150-158.

DOSTAL, D. E. & BAKER, K. M. 1999. The cardiac renin-angiotensin system: conceptual, or a regulator of cardiac function? *Circ Res,* 85**,** 643-50.

DOWLATI, A., ROBERTSON, K., COONEY, M., PETROS, W. P., STRATFORD, M., JESBERGER, J., RAFIE, N., OVERMOYER, B., MAKKAR, V. & STAMBLER, B. 2002a. A phase I pharmacokinetic and translational study of the novel vascular targeting agent combretastatin a-4 phosphate on a single-dose intravenous schedule in patients with advanced cancer. *Cancer research,* 62**,** 3408-3416.

DOWLATI, A., ROBERTSON, K., COONEY, M., PETROS, W. P., STRATFORD, M., JESBERGER, J., RAFIE, N., OVERMOYER, B., MAKKAR, V., STAMBLER, B., TAYLOR, A., WAAS, J., LEWIN, J. S., MCCRAE, K. R. & REMICK, S. C. 2002b. A phase I pharmacokinetic and translational study of the novel vascular targeting agent combretastatin a-4 phosphate on a single-dose intravenous schedule in patients with advanced cancer. *Cancer Res,* 62**,** 3408-16.

DU PRÉ, B. C., DIERICKX, P., CRNKO, S., DOEVENDANS, P. A., VOS, M. A., GEIJSEN, N., NEUTEL, D., VAN VEEN, T. A. B. & VAN LAAKE, L. W. 2017. Neonatal rat

cardiomyocytes as an in vitro model for circadian rhythms in the heart. *Journal of Molecular and Cellular Cardiology,* 112**,** 58-63.

DU, Q., ZHU, B., ZHAI, Q. & YU, B. 2017. Sirt3 attenuates doxorubicin-induced cardiac hypertrophy and mitochondrial dysfunction via suppression of Bnip3. *Am J Transl Res,* 9**,** 3360-3373.

DUONG, M. N., GENESTE, A., FALLONE, F., LI, X., DUMONTET, C. & MULLER, C. 2017. The fat and the bad: Mature adipocytes, key actors in tumor progression and resistance. *Oncotarget,* 8**,** 57622.

EISNER, D. A., CALDWELL, J. L., KISTAMÁS, K. & TRAFFORD, A. W. 2017. Calcium and excitation-contraction coupling in the heart. *Circulation research,* 121**,** 181-195.

ERHARDT, L. R. 2005. A review of the current evidence for the use of angiotensin-receptor blockers in chronic heart failure. *International Journal of Clinical Practice,* 59**,** 571-578.

ESCOTO, H., RINGEWALD, J. & KALPATTHI, R. 2010. Etoposide-related cardiotoxicity in a child with haemophagocytic lymphohistiocytosis. *Cardiology in the Young,* 20**,** 105-107.

ESTEVEZ, M. D., WOLF, A. & SCHRAMM, U. 2000. Effect of PSC 833, verapamil and amiodarone on adriamycin toxicity in cultured rat cardiomyocytes. *Toxicol In Vitro,* 14**,** 17-23.

EWER, M. S. & EWER, S. M. 2010. Cardiotoxicity of anticancer treatments: what the cardiologist needs to know. *Nature Reviews Cardiology,* 7**,** 564.

EWER, M. S., SWAIN, S. M., CARDINALE, D., FADOL, A. & SUTER, T. M. 2011. Cardiac dysfunction after cancer treatment. *Tex Heart Inst J,* 38**,** 248-52.

EWER, M. S. & YEH, E. T. H. 2013. *Cancer and the Heart*, PMPH-USA.

FABIATO, A. 1983. Calcium-induced release of calcium from the cardiac sarcoplasmic reticulum. *Am J Physiol,* 245**,** C1-14.

FABIATO, A. & FABIATO, F. 1975. Contractions induced by a calcium-triggered release of calcium from the sarcoplasmic reticulum of single skinned cardiac cells. *The Journal of physiology,* 249**,** 469-495.

FANG, J., SHING, Y., WIEDERSCHAIN, D., YAN, L., BUTTERFIELD, C., JACKSON, G., HARPER, J., TAMVAKOPOULOS, G. & MOSES, M. A. 2000. Matrix metalloproteinase-2 is required for the switch to the angiogenic phenotype in a tumor model. *Proc Natl Acad Sci U S A,* 97**,** 3884-9.

FARES, J., FARES, M. Y., KHACHFE, H. H., SALHAB, H. A. & FARES, Y. 2020. Molecular principles of metastasis: a hallmark of cancer revisited. *Signal Transduction and Targeted Therapy,* 5**,** 28.

FARUQUE, L. I., LIN, M., BATTISTELLA, M., WIEBE, N., REIMAN, T., HEMMELGARN, B., THOMAS, C. & TONELLI, M. 2014. Systematic review of the risk of adverse

outcomes associated with vascular endothelial growth factor inhibitors for the treatment of cancer. *PLoS ONE,* 9.

FERRI, N., SIEGL, P., CORSINI, A., HERRMANN, J., LERMAN, A. & BENGHOZI, R. 2013. Drug attrition during pre-clinical and clinical development: understanding and managing drug-induced cardiotoxicity. *Pharmacol Ther,* 138**,** 470-84.

FIELD, L. J. 1988. Atrial natriuretic factor-SV40 T antigen transgenes produce tumors and cardiac arrhythmias in mice. *Science,* 239**,** 1029-33.

FILIGHEDDU, N., FUBINI, A., BALDANZI, G., CUTRUPI, S., GHÈ, C., CATAPANO, F., BROGLIO, F., BOSIA, A., PAPOTTI, M. & MUCCIOLI, G. 2001. Hexarelin protects H9c2 cardiomyocytes from doxorubicin-induced cell death. *Endocrine,* 14**,** 113-119.

FINKELSTEIN, Y., AKS, S. E., HUTSON, J. R., JUURLINK, D. N., NGUYEN, P., DUBNOV-RAZ, G., POLLAK, U., KOREN, G. & BENTUR, Y. 2010. Colchicine poisoning: the dark side of an ancient drug. *Clinical Toxicology,* 48**,** 407-414.

FINLAYSON, K., WITCHEL, H. J., MCCULLOCH, J. & SHARKEY, J. 2004. Acquired QT interval prolongation and HERG: implications for drug discovery and development. *European journal of pharmacology,* 500**,** 129-142.

FLOYD, J. D., NGUYEN, D. T., LOBINS, R. L., BASHIR, Q., DOLL, D. C. & PERRY, M. C. 2005. Cardiotoxicity of cancer therapy. *J Clin Oncol,* 23**,** 7685-96.

FLUCHER, B. E. 1992. Structural analysis of muscle development: transverse tubules, sarcoplasmic reticulum, and the triad. *Dev Biol,* 154**,** 245-60.

FOLKMAN, J. 1971. Tumor angiogenesis: therapeutic implications. *N Engl J Med,* 285**,** 1182-6.

FORCE, T., KRAUSE, D. S. & VAN ETTEN, R. A. 2007. Molecular mechanisms of cardiotoxicity of tyrosine kinase inhibition. *Nature Reviews Cancer,* 7**,** 332-344.

FORMICA, V., MORELLI, C., RIONDINO, S., RENZI, N., NITTI, D., DI DANIELE, N., ROSELLI, M. & TESAURO, M. 2020. Obesity and common pathways of cancer and cardiovascular disease. *Endocrine and Metabolic Science,* 1**,** 100065.

FREUND, C. & MUMMERY, C. L. 2009. Prospects for pluripotent stem cell-derived cardiomyocytes in cardiac cell therapy and as disease models. *J Cell Biochem,* 107**,** 592-9.

FRIEDRICHS, G. S., PATMORE, L. & BASS, A. 2005. Non-clinical evaluation of ventricular repolarization (ICH S7B): results of an interim survey of international pharmaceutical companies. *J Pharmacol Toxicol Methods,* 52**,** 6-11.

FÜRST, R. & VOLLMAR, A. M. 2013. A new perspective on old drugs: non-mitotic actions of tubulin-binding drugs play a major role in cancer treatment. *Pharmazie,* 68**,** 478-83.

GALBRAITH, S. M., CHAPLIN, D. J., LEE, F., STRATFORD, M. R., LOCKE, R. J., VOJNOVIC, B. & TOZER, G. M. 2001. Effects of combretastatin A4 phosphate on endothelial cell

morphology in vitro and relationship to tumour vascular targeting activity in vivo. *Anticancer Res,* 21**,** 93-102.

GALLUZZI, L., BUQUÉ, A., KEPP, O., ZITVOGEL, L. & KROEMER, G. 2015. Immunological Effects of Conventional Chemotherapy and Targeted Anticancer Agents. *Cancer Cell,* 28**,** 690-714.

GARG, P., GARG, V., SHRESTHA, R., SANGUINETTI, M. C., KAMP, T. J. & WU, J. C. 2018. Human Induced Pluripotent Stem Cell-Derived Cardiomyocytes as Models for Cardiac Channelopathies: A Primer for Non-Electrophysiologists. *Circulation research,* 123**,** 224-243.

GARON, E. B., KABBINAVAR, F. F., NEIDHART, J. A., NEIDHART, J. D., GABRAIL, N. Y., OLIVEIRA, M. R., LU, S. P. & BALKISSOON, J. 2010. Randomized phase II trial of a tumor vascular disrupting agent fosbretabulin tromethamine (CA4P) with carboplatin (C), paclitaxel (P), and bevacizumab (B) in stage IIIb/IV nonsquamous non-small cell lung cancer (NSCLC): The FALCON trial. *Journal of Clinical Oncology,* 28**,** 7587-7587.

GARON, E. B., NEIDHART, J. D., GABRAIL, N. Y., DE OLIVEIRA, M. R., BALKISSOON, J. & KABBINAVAR, F. 2016. A randomized Phase II trial of the tumor vascular disrupting agent CA4P (fosbretabulin tromethamine) with carboplatin, paclitaxel, and bevacizumab in advanced nonsquamous non-small-cell lung cancer. *OncoTargets and therapy,* 9**,** 7275.

GAYA, A. M. & RUSTIN, G. J. S. 2005. Vascular disrupting agents: a new class of drug in cancer therapy. *Clinical Oncology,* 17**,** 277-290.

GEISBERG, C. A. & SAWYER, D. B. 2010. Mechanisms of anthracycline cardiotoxicity and strategies to decrease cardiac damage. *Current hypertension reports,* 12**,** 404-410.

GILL, J. H., LOADMAN, P. M., SHNYDER, S. D., COOPER, P., ATKINSON, J. M., RIBEIRO MORAIS, G., PATTERSON, L. H. & FALCONER, R. A. 2014. Tumor-targeted prodrug ICT2588 demonstrates therapeutic activity against solid tumors and reduced potential for cardiovascular toxicity. *Molecular Pharmaceutics,* 11**,** 1294-1300.

GILL, J. H., ROCKLEY, K. L., DE SANTIS, C. & MOHAMED, A. K. 2019. Vascular Disrupting Agents in cancer treatment: Cardiovascular toxicity and implications for co-administration with other cancer chemotherapeutics. *Pharmacology and Therapeutics,* 202**,** 18-31.

GINTANT, G. 2011. An evaluation of hERG current assay performance: Translating preclinical safety studies to clinical QT prolongation. *Pharmacol Ther,* 129**,** 109-19.

GINTANT, G., SAGER, P. T. & STOCKBRIDGE, N. 2016. Evolution of strategies to improve preclinical cardiac safety testing. *Nat Rev Drug Discov,* 15**,** 457-71.

GMBH, N. T. Recordings of Action Potentials in Mouse ES Cell-Derived Cor.At® Cardiomyocytes on Nanion's Patchliner®.

GOINEAU, S. & CASTAGNÉ, V. 2018. Electrophysiological characteristics and pharmacological sensitivity of two lines of human induced pluripotent stem cell derived cardiomyocytes coming from two different suppliers. *Journal of Pharmacological and Toxicological Methods,* 90**,** 58-66.

GOMEZ, J. P., POTREAU, D., BRANKA, J. E. & RAYMOND, G. 1994. Developmental changes in Ca2+ currents from newborn rat cardiomyocytes in primary culture. *Pflügers Archiv,* 428**,** 241-249.

GORDON, A., HOMSHER, E. & REGNIER, M. 2000. Regulation of contraction in striated muscle. *Physiological reviews,* 80**,** 853-924.

GOTWALS, P., CAMERON, S., CIPOLLETTA, D., CREMASCO, V., CRYSTAL, A., HEWES, B., MUELLER, B., QUARATINO, S., SABATOS-PEYTON, C., PETRUZZELLI, L., ENGELMAN, J. A. & DRANOFF, G. 2017. Prospects for combining targeted and conventional cancer therapy with immunotherapy. *Nature Reviews Cancer,* 17**,** 286-301.

GOULD, S., WESTWOOD, F. R., CURWEN, J. O., ASHTON, S. E., ROBERTS, D. W., LOVICK, S. C. & RYAN, A. J. 2007. Effect of pretreatment with atenolol and nifedipine on ZD6126-induced cardiac toxicity in rats. *J Natl Cancer Inst,* 99**,** 1724-8.

GRISHAM, R., KY, B., TEWARI, K. S., CHAPLIN, D. J. & WALKER, J. 2018. Clinical trial experience with CA4P anticancer therapy: focus on efficacy, cardiovascular adverse events, and hypertension management. *Gynecologic oncology research and practice,* 5**,** 1-1.

GROSIOS, K., HOLWELL, S. E., MCGOWN, A. T., PETTIT, G. R. & BIBBY, M. C. 1999. In vivo and in vitro evaluation of combretastatin A-4 and its sodium phosphate prodrug. *British journal of cancer,* 81**,** 1318-1327.

GUO, L., ABRAMS, R. M., BABIARZ, J. E., COHEN, J. D., KAMEOKA, S., SANDERS, M. J., CHIAO, E. & KOLAJA, K. L. 2011. Estimating the risk of drug-induced proarrhythmia using human induced pluripotent stem cell–derived cardiomyocytes. *Toxicological Sciences,* 123**,** 281-289.

HANAHAN, D. & WEINBERG, R. A. 2011. Hallmarks of cancer: the next generation. *Cell,* 144**,** 646-74.

HANRAHAN, E. O., GONZALEZ-ANGULO, A. M., GIORDANO, S. H., ROUZIER, R., BROGLIO, K. R., HORTOBAGYI, G. N. & VALERO, V. 2007. Overall survival and cause-specific mortality of patients with stage T1a,bN0M0 breast carcinoma. *J Clin Oncol,* 25**,** 4952-60.

HAVERKAMP, W., BREITHARDT, G., CAMM, A. J., JANSE, M. J., ROSEN, M. R., ANTZELEVITCH, C., ESCANDE, D., FRANZ, M., MALIK, M. & MOSS, A. 2000. The potential for QT prolongation and pro-arrhythmia by non-anti-arrhythmic drugs: clinical and regulatory implications: report on a Policy Conference of the European Society of Cardiology. *Cardiovascular research,* 47**,** 219-233.

HE, X., LI, S., HUANG, H., LI, Z., CHEN, L., YE, S., HUANG, J., ZHAN, J. & LIN, T. 2011. A pharmacokinetic and safety study of single dose intravenous combretastatin A4

phosphate in Chinese patients with refractory solid tumours. *Br J Clin Pharmacol,* 71**,** 860-70.

HEIN, S., KOSTIN, S., HELING, A., MAENO, Y. & SCHAPER, J. 2000. The role of the cytoskeleton in heart failure. *Cardiovascular Research,* 45**,** 273-278.

HERRMANN, J. 2016. Tyrosine Kinase Inhibitors and Vascular Toxicity: Impetus for a Classification System? *Curr Oncol Rep,* 18**,** 33.

HERRMANN, J., YANG, E. H., ILIESCU, C. A., CILINGIROGLU, M., CHARITAKIS, K., HAKEEM, A., TOUTOUZAS, K., LEESAR, M. A., GRINES, C. L. & MARMAGKIOLIS, K. 2016. Vascular Toxicities of Cancer Therapies: The Old and the New--An Evolving Avenue. *Circulation,* 133**,** 1272-89.

HIGGINS, A. Y., O'HALLORAN, T. D. & CHANG, J. D. 2015. Chemotherapy-induced cardiomyopathy. *Heart Fail Rev,* 20**,** 721-30.

HIGUCHI, S., OHTSU, H., SUZUKI, H., SHIRAI, H., FRANK, G. D. & EGUCHI, S. 2007. Angiotensin II signal transduction through the AT1 receptor: novel insights into mechanisms and pathophysiology. *Clin Sci (Lond),* 112**,** 417-28.

HILL, S. A., LONERGAN, S. J., DENEKAMP, J. & CHAPLIN, D. J. 1993. Vinca alkaloids: anti-vascular effects in a murine tumour. *Eur J Cancer,* 29a**,** 1320-4.

HIMMEL, H. M. 2013. Drug-induced functional cardiotoxicity screening in stem cell-derived human and mouse cardiomyocytes: effects of reference compounds. *Journal of pharmacological and toxicological methods,* 68**,** 97-111.

HINNEN, P. & ESKENS, F. A. L. M. 2007. Vascular disrupting agents in clinical development. *British Journal of Cancer,* 96**,** 1159-1165.

HO, Y.-J., WANG, T.-C., FAN, C.-H. & YEH, C.-K. 2017. Current progress in antivascular tumor therapy. *Drug Discovery Today,* 22**,** 1503-1515.

HOFFMANN, P. & WARNER, B. 2006. Are hERG channel inhibition and QT interval prolongation all there is in drug-induced torsadogenesis? A review of emerging trends. *Journal of pharmacological and toxicological methods,* 53**,** 87-105.

HOOD, R. L. 1994. Colchicine poisoning. *The Journal of Emergency Medicine,* 12**,** 171-177.

HURWITZ, H., FEHRENBACHER, L., NOVOTNY, W., CARTWRIGHT, T., HAINSWORTH, J., HEIM, W., BERLIN, J., BARON, A., GRIFFING, S. & HOLMGREN, E. 2004. Bevacizumab plus irinotecan, fluorouracil, and leucovorin for metastatic colorectal cancer. *New England journal of medicine,* 350**,** 2335-2342.

ICH 2005a. The clinical evaluation of QT/QTC interval prolongation and proarrhythmic potential for non-antiarrhythmic drugs. ICH E14. *ICH Harmonised Tripartite Guidline*.

ICH 2005b. The Non-Clinical Evaluation of the Potential for Delayed Ventricular Repolarization (QT Interval Prolongation) by Human Pharmaceuticals S7B. *ICH Harmonised Tripartite Guideline*.

ICH 2009. Non clinical evaluation for anticancer pharmaceuticals S9. *The International Conference on Harmonisation of technical requirements for registration of pharmaceuticals for human use*.

IMAZIO, M., BRUCATO, A., FERRAZZI, P., ROVERE MARIA, E., GANDINO, A., CEMIN, R., FERRUA, S., BELLI, R., MAESTRONI, S., SIMON, C., ZINGARELLI, E., BAROSI, A., SANSONE, F., PATRINI, D., VITALI, E., TRINCHERO, R., SPODICK DAVID, H., ADLER, Y. & NULL, N. 2011. Colchicine Reduces Postoperative Atrial Fibrillation. *Circulation,* 124**,** 2290-2295.

JAFFREDO, T., CHESTIER, A., BACHNOU, N. & DIETERLEN-LIÈVRE, F. 1991. MC29-immortalized clonal avian heart cell lines can partially differentiate in vitro. *Exp Cell Res,* 192**,** 481-91.

JAHN, L., SADOSHIMA, J., GREENE, A., PARKER, C., MORGAN, K. G. & IZUMO, S. 1996. Conditional differentiation of heart- and smooth muscle-derived cells transformed by a temperature-sensitive mutant of SV40 T antigen. *Journal of Cell Science,* 109**,** 397.

JANS, D., CALLEWAERT, G., KRYLYCHKINA, O., HOFFMAN, L., GULLO, F., PRODANOV, D. & BRAEKEN, D. 2017. Action potential-based MEA platform for in vitro screening of drug-induced cardiotoxicity using human iPSCs and rat neonatal myocytes. *Journal of Pharmacological and Toxicological Methods,* 87**,** 48-52.

JAROCH, K., KAROLAK, M., GÓRSKI, P., JAROCH, A., KRAJEWSKI, A., ILNICKA, A., SLODERBACH, A., STEFAŃSKI, T. & SOBIAK, S. 2016. Combretastatins: In vitro structure-activity relationship, mode of action and current clinical status. *Pharmacological Reports,* 68**,** 1266-1275.

JEMAL, A., BRAY, F., CENTER, M. M., FERLAY, J., WARD, E. & FORMAN, D. 2011. Global cancer statistics. *CA: a cancer journal for clinicians,* 61**,** 69-90.

JI, Y. T., LIU, Y. N. & LIU, Z. P. 2015. Tubulin colchicine binding site inhibitors as vascular disrupting agents in clinical developments. *Curr Med Chem,* 22**,** 1348-60.

JORDAN, A., HADFIELD, J. A., LAWRENCE, N. J. & MCGOWN, A. T. 1998. Tubulin as a target for anticancer drugs: agents which interact with the mitotic spindle. *Medicinal research reviews,* 18**,** 259-296.

JORDAN, M. A. 2002. Mechanism of action of antitumor drugs that interact with microtubules and tubulin. *Curr Med Chem Anticancer Agents,* 2**,** 1-17.

JOSEPH, N., REICHER, B. & BARDA-SAAD, M. 2014. The calcium feedback loop and T cell activation: how cytoskeleton networks control intracellular calcium flux. *Biochim Biophys Acta,* 1838**,** 557-68.

JOSEPHSON, M. E. 2008. *Clinical cardiac electrophysiology: techniques and interpretations*, Lippincott Williams & Wilkins.

JOSHI, A., DIMINO, T., VOHRA, Y., CUI, C. & YAN, G.-X. 2004. Preclinical strategies to assess QT liability and torsadogenic potential of new drugs: the role of experimental models. *Journal of electrocardiology,* 37**,** 7-14.

JUNG, Y.-J., ISAACS, J. S., LEE, S., TREPEL, J. & NECKERS, L. 2003. Microtubule Disruption Utilizes an NFκB-dependent Pathway to Stabilize HIF-1α Protein. *Journal of Biological Chemistry,* 278**,** 7445-7452.

KALAM, K. & MARWICK, T. H. 2013. Role of cardioprotective therapy for prevention of cardiotoxicity with chemotherapy: a systematic review and meta-analysis. *Eur J Cancer,* 49**,** 2900-9.

KALRA, K. & TOMAR, P. 2014. Stem cell: basics, classification and applications. *American Journal of Phytomedicine and Clinical Therapeutics,* 2**,** 919-930.

KANTHOU, C. & TOZER, G. M. 2007. Tumour targeting by microtubule-depolymerizing vascular disrupting agents. *Expert Opin Ther Targets,* 11**,** 1443-57.

KARRA, R. & POSS, K. D. 2017. Redirecting cardiac growth mechanisms for therapeutic regeneration. *The Journal of Clinical Investigation,* 127**,** 427-436.

KARRA, R., WALTER, A. O. & WU, S. M. 2017. The relationship between cardiac endothelium and fibroblasts: it's complicated. *The Journal of Clinical Investigation,* 127**,** 2892-2894.

KARSNER, H. T., SAPHIR, O. & TODD, T. W. 1925. The State of the Cardiac Muscle in Hypertrophy and Atrophy. *Am J Pathol,* 1**,** 351-372.1.

KATZ, E., STEINHELPER, M., DELCARPIO, J., DAUD, A., CLAYCOMB, W. & FIELD, L. 1992. Cardiomyocyte proliferation in mice expressing alpha-cardiac myosin heavy chain-SV40 T-antigen transgenes. *American Journal of Physiology-Heart and Circulatory Physiology,* 262**,** H1867-H1876.

KE, N., WANG, X., XU, X. & ABASSI, Y. A. 2011. The xCELLigence system for real-time and label-free monitoring of cell viability. *Mammalian Cell Viability.* Springer.

KE, Q., BODYAK, N., RIGOR, D. L., HURST, N. W., CHAPLIN, D. J. & KANG, P. M. 2009. Pharmacological inhibition of the hypertensive response to combretastatin A-4 phosphate in rats. *Vascul Pharmacol,* 51**,** 337-43.

KE, Q., SAMAD, M. A., BAE, S., CHAPLIN, D. J. & KANG, P. M. 2015. Exaggerated hypertensive response to combretastatin A-4 phosphate in hypertensive rats: Effective pharmacological inhibition by diltiazem. *Vascul Pharmacol,* 74**,** 73-9.

KEMP, C. D. & CONTE, J. V. 2012. The pathophysiology of heart failure. *Cardiovasc Pathol,* 21**,** 365-71.

KERFANT, B. G., VASSORT, G. & GÓMEZ, A. M. 2001. Microtubule Disruption by Colchicine Reversibly Enhances Calcium Signaling in Intact Rat Cardiac Myocytes. *Circulation Research,* 88**,** e59-e65.

KHIATI, S., ROSA, I. D., SOURBIER, C., MA, X., RAO, V. A., NECKERS, L. M., ZHANG, H. & POMMIER, Y. 2014. Mitochondrial topoisomerase i (Top1mt) is a novel limiting factor of doxorubicin cardiotoxicity. *Clinical Cancer Research,* 20**,** 4873-4881.

KHO, D., MACDONALD, C., JOHNSON, R., UNSWORTH, C., #039, CARROLL, S., MEZ, E., ANGEL, C. & GRAHAM, E. 2015. Application of xCELLigence RTCA Biosensor Technology for Revealing the Profile and Window of Drug Responsiveness in Real Time. *Biosensors,* 5**,** 199.

KHOSHMANESH, K., NAHAVANDI, S., BARATCHI, S., MITCHELL, A. & KALANTAR-ZADEH, K. 2011. Dielectrophoretic platforms for bio-microfluidic systems. *Biosensors and Bioelectronics,* 26**,** 1800-1814.

KHOSRAVI SHAHI, P. & FERNÁNDEZ PINEDA, I. 2008. Tumoral angiogenesis: review of the literature. *Cancer Invest,* 26**,** 104-8.

KILLEEN, M. J. 2012. *Cardiac Drug Safety: A Bench to Bedside Approach*, World Scientific.

KIMES, B. W. & BRANDT, B. L. 1976. Properties of a clonal muscle cell line from rat heart. *Experimental Cell Research,* 98**,** 367-381.

KLEIN, I. 1983. Colchicine stimulates the rate of contraction of heart cells in culture. *Cardiovascular Research,* 17**,** 459-465.

KLINTSCHAR, M., BEHAM-SCHMIDT, C., RADNER, H., HENNING, G. & ROLL, P. 1999. Colchicine poisoning by accidental ingestion of meadow saffron (Colchicum autumnale): pathological and medicolegal aspects. *Forensic Science International,* 106**,** 191-200.

KNOLLMANN, B. C. 2013. Controversies in Cardiovascular Research: Induced pluripotent stem cell-derived cardiomyocytes – boutique science or valuable arrhythmia model? *Circulation research,* 112**,** 969-976.

KOENE, R. J., PRIZMENT, A. E., BLAES, A. & KONETY, S. H. 2016. Shared Risk Factors in Cardiovascular Disease and Cancer. *Circulation,* 133**,** 1104-1114.

KOLOSSOV, E., BOSTANI, T., ROELL, W., BREITBACH, M., PILLEKAMP, F., NYGREN, J. M., SASSE, P., RUBENCHIK, O., FRIES, J. W., WENZEL, D., GEISEN, C., XIA, Y., LU, Z., DUAN, Y., KETTENHOFEN, R., JOVINGE, S., BLOCH, W., BOHLEN, H., WELZ, A., HESCHELER, J., JACOBSEN, S. E. & FLEISCHMANN, B. K. 2006. Engraftment of engineered ES cell-derived cardiomyocytes but not BM cells restores contractile function to the infarcted myocardium. *J Exp Med,* 203**,** 2315-27.

KOLOSSOV, E., LU, Z., DROBINSKAYA, I., GASSANOV, N., DUAN, Y., SAUER, H., MANZKE, O., BLOCH, W., BOHLEN, H., HESCHELER, J. & FLEISCHMANN, B. K. 2005. Identification and characterization of embryonic stem cell-derived pacemaker and atrial cardiomyocytes. *Faseb j,* 19**,** 577-9.

KWON, O., HONG, S.-M., SUTTON, T. A. & TEMM, C. J. 2008. Preservation of peritubular capillary endothelial integrity and increasing pericytes may be critical to recovery

from postischemic acute kidney injury. *American Journal of Physiology-Renal Physiology,* 295**,** F351-F359.

KY, B., VEJPONGSA, P., YEH, E. T., FORCE, T. & MOSLEHI, J. J. 2013. Emerging paradigms in cardiomyopathies associated with cancer therapies. *Circ Res,* 113**,** 754-64.

L'ECUYER, T., HORENSTEIN, M. S., THOMAS, R. & VANDER HEIDE, R. 2001. Anthracycline-induced cardiac injury using a cardiac cell line: potential for gene therapy studies. *Molecular genetics and metabolism,* 74**,** 370-379.

LA SALA, G., OLIERIC, N., SHARMA, A., VITI, F., DE ASIS BALAGUER PEREZ, F., HUANG, L., TONRA, J. R., LLOYD, G. K., DECHERCHI, S., DÍAZ, J. F., STEINMETZ, M. O. & CAVALLI, A. 2019. Structure, Thermodynamics, and Kinetics of Plinabulin Binding to Two Tubulin Isotypes. *Chem,* 5**,** 2969-2986.

LABIANCA, R., BERETTA, G., CLERICI, M., FRASCHINI, P. & LUPORINI, G. 1982. Cardiac toxicity of 5-fluorouracil: a study on 1083 patients. *Tumori,* 68**,** 505-10.

LAFLAMME, M. A., CHEN, K. Y., NAUMOVA, A. V., MUSKHELI, V., FUGATE, J. A., DUPRAS, S. K., REINECKE, H., XU, C., HASSANIPOUR, M. & POLICE, S. 2007. Cardiomyocytes derived from human embryonic stem cells in pro-survival factors enhance function of infarcted rat hearts. *Nature biotechnology,* 25**,** 1015-1024.

LAMORE, S. D., KAMENDI, H. W., SCOTT, C. W., DRAGAN, Y. P. & PETERS, M. F. 2013. Cellular Impedance Assays for Predictive Preclinical Drug Screening of Kinase Inhibitor Cardiovascular Toxicity. *Toxicological Sciences,* 135**,** 402-413.

LAMORE, S. D., KOHNKEN, R. A., PETERS, M. F. & KOLAJA, K. L. 2020. Cardiovascular Toxicity Induced by Kinase Inhibitors: Mechanisms and Preclinical Approaches. *Chemical Research in Toxicology,* 33**,** 125-136.

LAMORE SD, S. C., PETERS MF 2015. Cardiomyocyte Impedance Assays Assay Guidance Manual. *Assay Guidance Manual [Internet]: Eli Lilly & Company and the National Center for Advancing Translational Sciences*.

LAMPIDIS, T. J., TREVORROW, K. W. & RUBIN, R. W. 1986. Effects of colchicine on cardiac cell function indicate possible role for membrane surface tubulin. *Experimental Cell Research,* 164**,** 463-470.

LAND, H., CHEN, A. C., MORGENSTERN, J. P., PARADA, L. F. & WEINBERG, R. A. 1986. Behavior of myc and ras oncogenes in transformation of rat embryo fibroblasts. *Molecular and cellular biology,* 6**,** 1917-1925.

LANGE, U., SCHUMANN, C. & SCHMIDT, K. L. 2001. Current aspects of colchicine therapy -- classical indications and new therapeutic uses. *European journal of medical research,* 6**,** 150-160.

LANGE, U., SCHUMANN, C. & SCHMIDT, K. L. 2002a. [Aspects of colchicine therapy. 1: Pharmacology, toxicology, classic indications]. *Zeitschrift fur arztliche Fortbildung und Qualitatssicherung,* 96**,** 59-63.

LANGE, U., SCHUMANN, C. & SCHMIDT, K. L. 2002b. [Aspects of colchicine therapy. 2. Additional classical indications and new therapeutic aspects]. *Zeitschrift fur arztliche Fortbildung und Qualitatssicherung,* 96**,** 115-119.

LASSER, K. E., ALLEN, P. D., WOOLHANDLER, S. J., HIMMELSTEIN, D. U., WOLFE, S. M. & BOR, D. H. 2002. Timing of new black box warnings and withdrawals for prescription medications. *Jama,* 287**,** 2215-2220.

LAVERTY, H., BENSON, C., CARTWRIGHT, E., CROSS, M., GARLAND, C., HAMMOND, T., HOLLOWAY, C., MCMAHON, N., MILLIGAN, J., PARK, B., PIRMOHAMED, M., POLLARD, C., RADFORD, J., ROOME, N., SAGER, P., SINGH, S., SUTER, T., SUTER, W., TRAFFORD, A., VOLDERS, P., WALLIS, R., WEAVER, R., YORK, M. & VALENTIN, J. 2011. How can we improve our understanding of cardiovascular safety liabilities to develop safer medicines? *Br J Pharmacol,* 163**,** 675-93.

LAYLAND, J., SOLARO, R. J. & SHAH, A. M. 2005. Regulation of cardiac contractile function by troponin I phosphorylation. *Cardiovasc Res,* 66**,** 12-21.

LEE, L. L. & CHINTALGATTU, V. 2019. Pericytes in the heart. *Pericyte Biology in Different Organs.* Springer.

LEE, R. M. & GEWIRTZ, D. A. 2008. Colchicine site inhibitors of microtubule integrity as vascular disrupting agents. *Drug Development Research,* 69**,** 352-358.

LENIHAN, D. J., HARTLAGE, G., DECARA, J., BLAES, A., FINET, J. E., LYON, A. R., CORNELL, R. F., MOSLEHI, J., OLIVEIRA, G. H., MURTAGH, G., FISCH, M., ZEEVI, G., IAKOBISHVILI, Z., WITTELES, R., PATEL, A., HARRISON, E., FRADLEY, M., CURIGLIANO, G., LENNEMAN, C. G., MAGALHAES, A., KRONE, R., PORTER, C., PARASHER, S., DENT, S., DOUGLAS, P. & CARVER, J. 2016. Cardio-Oncology Training: A Proposal From the International Cardioncology Society and Canadian Cardiac Oncology Network for a New Multidisciplinary Specialty. *Journal of Cardiac Failure,* 22**,** 465-471.

LI, R.-K., MICKLE, D. A. G., WEISEL, R. D., CARSON, S., OMAR, S. A., TUMIATI, L. C., WILSON, G. J. & WILLIAMS, W. G. 1996. Human pediatric and adult ventricular cardiomyocytes in culture: assessment of phenotypic changes with passaging. *Cardiovascular research,* 32**,** 362-373.

LI, X., ZHANG, R., ZHAO, B., LOSSIN, C. & CAO, Z. 2016. Cardiotoxicity screening: a review of rapid-throughput in vitro approaches. *Archives of Toxicology,* 90**,** 1803-1816.

LIMAME, R., WOUTERS, A., PAUWELS, B., FRANSEN, E., PEETERS, M., LARDON, F., DE WEVER, O. & PAUWELS, P. 2012. Comparative analysis of dynamic cell viability, migration and invasion assessments by novel real-time technology and classic endpoint assays. *PloS one,* 7**,** e46536.

LINDENFELD, J. & KELLY, P. A. 2010. Developing a cardiology-oncology clinical practice guideline. *Prog Cardiovasc Dis,* 53**,** 173-9.

LIPPERT III, J. W. 2007. Vascular disrupting agents. *Bioorganic & medicinal chemistry,* 15**,** 605-615.

LIPPERT, J. W., 3RD 2007. Vascular disrupting agents. *Bioorg Med Chem,* 15**,** 605-15.

LIPSHULTZ, S. E., COCHRAN, T. R., FRANCO, V. I. & MILLER, T. L. 2013. Treatment-related cardiotoxicity in survivors of childhood cancer. *Nature Reviews Clinical Oncology,* 10**,** 697-710.

LORUSSO, P., YEE, L., PAPADOPOULOS, K., TOLCHER, A., ROMERO, O., WANG, D., HEATH, E., LLOYD, G., LONGENECKER, A. & NEUTEBOOM, S. 2007. Phase 1 clinical trials of NPI-2358 (a novel vascular disrupting agent) in patients with solid tumors and lymphomas. AACR.

LOTRIONTE, M., BIONDI-ZOCCAI, G., ABBATE, A., LANZETTA, G., D'ASCENZO, F., MALAVASI, V., PERUZZI, M., FRATI, G. & PALAZZONI, G. 2013. Review and meta-analysis of incidence and clinical predictors of anthracycline cardiotoxicity. *American Journal of Cardiology,* 112**,** 1980-1984.

LOUCH, W. E., SHEEHAN, K. A. & WOLSKA, B. M. 2011. Methods in cardiomyocyte isolation, culture, and gene transfer. *Journal of molecular and cellular cardiology,* 51**,** 288-298.

LU, Y., CHEN, J., XIAO, M., LI, W. & MILLER, D. D. 2012. An Overview of Tubulin Inhibitors That Interact with the Colchicine Binding Site. *Pharmaceutical Research,* 29**,** 2943-2971.

LUNDY, S. D., ZHU, W.-Z., REGNIER, M. & LAFLAMME, M. A. 2013. Structural and functional maturation of cardiomyocytes derived from human pluripotent stem cells. *Stem cells and development,* 22**,** 1991-2002.

MA, J., GUO, L., FIENE, S. J., ANSON, B. D., THOMSON, J. A., KAMP, T. J., KOLAJA, K. L., SWANSON, B. J. & JANUARY, C. T. 2011. High purity human-induced pluripotent stem cell-derived cardiomyocytes: electrophysiological properties of action potentials and ionic currents. *Am J Physiol Heart Circ Physiol,* 301**,** H2006-17.

MA, J. & WAXMAN, D. J. 2008. Combination of antiangiogenesis with chemotherapy for more effective cancer treatment. *Molecular Cancer Therapeutics,* 7**,** 3670.

MADDAMS, J., UTLEY, M. & MØLLER, H. 2012. Projections of cancer prevalence in the United Kingdom, 2010–2040. *British journal of cancer,* 107**,** 1195-1202.

MAGDY, T., SCHULDT, A. J. T., WU, J. C., BERNSTEIN, D. & BURRIDGE, P. W. 2018. Human Induced Pluripotent Stem Cell (hiPSC)-Derived Cells to Assess Drug Cardiotoxicity: Opportunities and Problems. *Annual Review of Pharmacology and Toxicology,* 58**,** 83-103.

MAHAL, K., BIERSACK, B., CAYSA, H., SCHOBERT, R. & MUELLER, T. 2015. Combretastatin A-4 derived imidazoles show cytotoxic, antivascular, and antimetastatic effects based on cytoskeletal reorganisation. *Investigational new drugs,* 33**,** 541-554.

MAITLAND, M. L., BAKRIS, G. L., BLACK, H. R., CHEN, H. X., DURAND, J.-B., ELLIOTT, W. J., IVY, S. P., LEIER, C. V., LINDENFELD, J. & LIU, G. 2010. Initial assessment, surveillance, and management of blood pressure in patients receiving vascular

endothelial growth factor signaling pathway inhibitors. *Journal of the National Cancer Institute,* 102**,** 596-604.

MALAN, D., GALLO, M. P., BEDENDI, I., BIASIN, C., LEVI, R. C. & ALLOATTI, G. 2003. Microtubules mobility affects the modulation of L-type ICa by muscarinic and β-adrenergic agonists in guinea-pig cardiac myocytes. *Journal of Molecular and Cellular Cardiology,* 35**,** 195-206.

MANDEL, E., LEWINSKI, U. & DJALDETTI, M. 2010. Vincristine-induced myocardial infarction. *Cancer,* 36**,** 1979-82.

MANDENIUS, C. F., STEEL, D., NOOR, F., MEYER, T., HEINZLE, E., ASP, J., ARAIN, S., KRAUSHAAR, U., BREMER, S., CLASS, R. & SARTIPY, P. 2011. Cardiotoxicity testing using pluripotent stem cell-derived human cardiomyocytes and state-of-the-art bioanalytics: a review. *J Appl Toxicol,* 31**,** 191-205.

MANN, D. L. & KRONE, R. J. 2010. Cardiac disease in cancer patients: an overview. *Prog Cardiovasc Dis,* 53**,** 80-7.

MARTIN TA, Y. L., SANDERS AJ, ET AL. 2000. Cancer Invasion and Metastasis: Molecular and Cellular Perspective. *Madame Curie Bioscience Database [Internet],* Austin (TX): Landes Bioscience;.

MARTINELLI, M., BONEZZI, K., RICCARDI, E., KUHN, E., FRAPOLLI, R., ZUCCHETTI, M., RYAN, A. J., TARABOLETTI, G. & GIAVAZZI, R. 2007. Sequence dependent antitumour efficacy of the vascular disrupting agent ZD6126 in combination with paclitaxel. *British Journal of Cancer,* 97**,** 888-894.

MASON, R. P., ZHAO, D., LIU, L., TRAWICK, M. L. & PINNEY, K. G. 2011. A perspective on vascular disrupting agents that interact with tubulin: preclinical tumor imaging and biological assessment. *Integrative biology : quantitative biosciences from nano to macro,* 3**,** 375-387.

MCLOUGHLIN, E. C. & O'BOYLE, N. M. 2020. Colchicine-Binding Site Inhibitors from Chemistry to Clinic: A Review. *Pharmaceuticals,* 13.

MCWHINNEY, C. D., HANSEN, C. & ROBISHAW, J. D. 2000. Alpha-1 adrenergic signaling in a cardiac murine atrial myocyte (HL-1) cell line. *Molecular and cellular biochemistry,* 214**,** 111-119.

MENSAH, G. A., WEI, G. S., SORLIE, P. D., FINE, L. J., ROSENBERG, Y., KAUFMANN, P. G., MUSSOLINO, M. E., HSU, L. L., ADDOU, E., ENGELGAU, M. M. & GORDON, D. 2017. Decline in Cardiovascular Mortality: Possible Causes and Implications. *Circulation research,* 120**,** 366-380.

MERCURIO, V., PIROZZI, F., LAZZARINI, E., MARONE, G., RIZZO, P., AGNETTI, G., TOCCHETTI, C. G., GHIGO, A. & AMERI, P. 2016. Models of heart failure based on the cardiotoxicity of anticancer drugs. *Journal of cardiac failure,* 22**,** 449-458.

MICHEL, L., RASSAF, T. & TOTZECK, M. 2019. Cardiotoxicity from immune checkpoint inhibitors. *Int J Cardiol Heart Vasc,* 25**,** 100420.

MIKAELIAN, I., BUNESS, A., DE VERA-MUDRY, M.-C., KANWAL, C., COLUCCIO, D., RASMUSSEN, E., CHAR, H. W., CARVAJAL, V., HILTON, H., FUNK, J., HOFLACK, J.-C., FIELDEN, M., HERTING, F., DUNN, M. & SUTER-DICK, L. 2010. Primary Endothelial Damage Is the Mechanism of Cardiotoxicity of Tubulin-Binding Drugs. *Toxicological Sciences,* 117**,** 144-151.

MILLER, A. J. & ARNOLD, A. C. 2019. The renin-angiotensin system in cardiovascular autonomic control: recent developments and clinical implications. *Clin Auton Res,* 29**,** 231-243.

MILLER, K. D., NOGUEIRA, L., MARIOTTO, A. B., ROWLAND, J. H., YABROFF, K. R., ALFANO, C. M., JEMAL, A., KRAMER, J. L. & SIEGEL, R. L. 2019. Cancer treatment and survivorship statistics, 2019. *CA: A Cancer Journal for Clinicians,* 69**,** 363-385.

MILLER, K. D., SIEGEL, R. L., LIN, C. C., MARIOTTO, A. B., KRAMER, J. L., ROWLAND, J. H., STEIN, K. D., ALTERI, R. & JEMAL, A. 2016. Cancer treatment and survivorship statistics, 2016. *CA: a cancer journal for clinicians,* 66**,** 271-289.

MINAMI, T. & AIRD, W. C. 2005. Endothelial cell gene regulation. *Trends in cardiovascular medicine,* 15**,** 174. e1-174. e24.

MINCHINTON, A. I. & TANNOCK, I. F. 2006. Drug penetration in solid tumours. *Nature Reviews Cancer,* 6**,** 583-592.

MITA, M. M., SARGSYAN, L., MITA, A. C. & SPEAR, M. 2013. Vascular-disrupting agents in oncology. *Expert Opin Investig Drugs,* 22**,** 317-28.

MONIRI, M. R., YOUNG, A., REINHEIMER, K., RAYAT, J., DAI, L.-J. & WARNOCK, G. L. 2015. Dynamic assessment of cell viability, proliferation and migration using real time cell analyzer system (RTCA). *Cytotechnology,* 67**,** 379-386.

MONK, B. J., HERZOG, T., ALVAREZ, R., CHAN, J., CHASE, D., COUCHENOUR, R., CRAM, C. & BOOKMAN, M. Focus study: Physician's choice chemotherapy (PCC) plus bevacizumab and CA4P versus PCC plus bevacizumab and placebo in platinum-resistant ovarian cancer. 2016 2016. LIPPINCOTT WILLIAMS & WILKINS TWO COMMERCE SQ, 2001 MARKET ST, PHILADELPHIA …, 878-879.

MOSLEHI, J. J. & DEININGER, M. 2015. Tyrosine kinase inhibitor–associated cardiovascular toxicity in chronic myeloid leukemia. *Journal of clinical oncology,* 33**,** 4210.

MOSMANN, T. 1983. Rapid colorimetric assay for cellular growth and survival: application to proliferation and cytotoxicity assays. *J Immunol Methods,* 65**,** 55-63.

MULLINS, M. E., MULLINS, M., CARRICO, E. A. & HOROWITZ, B. Z. 2000. Fatal Cardiovascular Collapse Following Acute Colchicine Ingestion. *Journal of Toxicology: Clinical Toxicology,* 38**,** 51-54.

MULROONEY, D. A., YEAZEL, M. W., KAWASHIMA, T., MERTENS, A. C., MITBY, P., STOVALL, M., DONALDSON, S. S., GREEN, D. M., SKLAR, C. A. & ROBISON, L. L. 2009. Cardiac outcomes in a cohort of adult survivors of childhood and adolescent cancer: retrospective analysis of the Childhood Cancer Survivor Study cohort. *Bmj,* 339.

MURRY, C. E., WISEMAN, R. W., SCHWARTZ, S. M. & HAUSCHKA, S. D. 1996. Skeletal myoblast transplantation for repair of myocardial necrosis. *The Journal of clinical investigation,* 98**,** 2512-2523.

MUTHUKKARUPPAN, V. R., KUBAI, L. & AUERBACH, R. 1982. Tumor-induced neovascularization in the mouse eye. *J Natl Cancer Inst,* 69**,** 699-708.

NATHAN, P., ZWEIFEL, M., PADHANI, A. R., KOH, D. M., NG, M., COLLINS, D. J., HARRIS, A., CARDEN, C., SMYTHE, J., FISHER, N., TAYLOR, N. J., STIRLING, J. J., LU, S. P., LEACH, M. O., RUSTIN, G. J. & JUDSON, I. 2012. Phase I trial of combretastatin A4 phosphate (CA4P) in combination with bevacizumab in patients with advanced cancer. *Clin Cancer Res,* 18**,** 3428-39.

NEGISHI, Y., KUDO, A., OBINATA, A., KAWASHIMA, K., HIRANO, H., YANAI, N., OBINATA, M. & ENDO, H. 2000. Multipotency of a bone marrow stromal cell line, TBR31-2, established from ts-SV40 T antigen gene transgenic mice. *Biochemical and biophysical research communications,* 268**,** 450-455.

NGUEMO, F., SARIC, T., PFANNKUCHE, K., WATZELE, M., REPPEL, M. & HESCHELER, J. 2012. In vitro model for assessing arrhythmogenic properties of drugs based on high-resolution impedance measurements. *Cell Physiol Biochem,* 29**,** 819-32.

NIDORF, S. M., EIKELBOOM, J. W., BUDGEON, C. A. & THOMPSON, P. L. 2013. Low-Dose Colchicine for Secondary Prevention of Cardiovascular Disease. *Journal of the American College of Cardiology,* 61**,** 404-410.

NIDORF, S. M., FIOLET, A. T. L., EIKELBOOM, J. W., SCHUT, A., OPSTAL, T. S. J., BAX, W. A., BUDGEON, C. A., TIJSSEN, J. G. P., MOSTERD, A., CORNEL, J. H. & THOMPSON, P. L. 2019. The effect of low-dose colchicine in patients with stable coronary artery disease: The LoDoCo2 trial rationale, design, and baseline characteristics. *Am Heart J,* 218**,** 46-56.

NIDORF, S. M., FIOLET, A. T. L., MOSTERD, A., EIKELBOOM, J. W., SCHUT, A., OPSTAL, T. S. J., THE, S. H. K., XU, X. F., IRELAND, M. A., LENDERINK, T., LATCHEM, D., HOOGSLAG, P., JERZEWSKI, A., NIEROP, P., WHELAN, A., HENDRIKS, R., SWART, H., SCHAAP, J., KUIJPER, A. F. M., VAN HESSEN, M. W. J., SAKLANI, P., TAN, I., THOMPSON, A. G., MORTON, A., JUDKINS, C., BAX, W. A., DIRKSEN, M., ALINGS, M., HANKEY, G. J., BUDGEON, C. A., TIJSSEN, J. G. P., CORNEL, J. H. & THOMPSON, P. L. 2020. Colchicine in Patients with Chronic Coronary Disease. *N Engl J Med,* 383**,** 1838-1847.

NITISS, J. L. 2009. Targeting DNA topoisomerase II in cancer chemotherapy. *Nature Reviews Cancer,* 9**,** 338-350.

NUSS, H. B. & MARBAN, E. 1994. Electrophysiological properties of neonatal mouse cardiac myocytes in primary culture. *The Journal of physiology,* 479 (Pt 2)**,** 265-279.

OCTAVIA, Y., TOCCHETTI, C. G., GABRIELSON, K. L., JANSSENS, S., CRIJNS, H. J. & MOENS, A. L. 2012. Doxorubicin-induced cardiomyopathy: From molecular mechanisms to

therapeutic strategies. *Journal of Molecular and Cellular Cardiology,* 52**,** 1213-1225.

OEFFINGER, K. C., MERTENS, A. C., SKLAR, C. A., KAWASHIMA, T., HUDSON, M. M., MEADOWS, A. T., FRIEDMAN, D. L., MARINA, N., HOBBIE, W., KADAN-LOTTICK, N. S., SCHWARTZ, C. L., LEISENRING, W. & ROBISON, L. L. 2006. Chronic health conditions in adult survivors of childhood cancer. *N Engl J Med,* 355**,** 1572-82.

OGDEN, D. & STANFIELD, P. Patch clamp techniques for single channel and whole-cell recording. Microelectrode techniques: the Plymouth workshop handbook, 1994. Company of Biologists Cambridge, 53-78.

ONISHI, R. M. & GAFFEN, S. L. 2010. Interleukin-17 and its target genes: mechanisms of interleukin-17 function in disease. *Immunology,* 129**,** 311-321.

ORONSKY, B. T., REID, T., KNOX, S. J. & SCICINSKI, J. J. 2012. The Scarlet Letter of Alkylation: A Mini Review of Selective Alkylating Agents. *Translational Oncology,* 5**,** 226-229.

OSHIMA, N., ONIMARU, H., YAMAMOTO, K., TAKECHI, H., NISHIDA, Y., ODA, T. & KUMAGAI, H. 2014. Expression and functions of β1- and β2-adrenergic receptors on the bulbospinal neurons in the rostral ventrolateral medulla. *Hypertension Research,* 37**,** 976-983.

PAI, V. B. & NAHATA, M. C. 2000. Cardiotoxicity of chemotherapeutic agents: incidence, treatment and prevention. *Drug Saf,* 22**,** 263-302.

PALMER, B. M., VALENT, S., HOLDER, E. L., WEINBERGER, H. D. & BIES, R. D. 1998. Microtubules modulate cardiomyocyte β-adrenergic response in cardiac hypertrophy. *American Journal of Physiology-Heart and Circulatory Physiology,* 275**,** H1707-H1716.

PARK, S., JOHNSON, D. K., ISHIZAWA, C. I., PARILLA, P. A. & DAVIS, M. F. 2009. Measuring the crystallinity index of cellulose by solid state 13 C nuclear magnetic resonance. *Cellulose,* 16**,** 641-647.

PECORINO, L. 2016. *Molecular biology of cancer: mechanisms, targets, and therapeutics*, Oxford University Press, USA.

PETERS, G. J., VAN DER WILT, C. L., VAN MOORSEL, C. J. A., KROEP, J. R., BERGMAN, A. M. & ACKLAND, S. P. 2000. Basis for effective combination cancer chemotherapy with antimetabolites. *Pharmacology & Therapeutics,* 87**,** 227-253.

PETERSON, K. L. 2002. Pressure overload hypertrophy and congestive heart failure. Where is the "Achilles' heel"? *J Am Coll Cardiol,* 39**,** 672-5.

PIEGARI, E., DE ANGELIS, A., CAPPETTA, D., RUSSO, R., ESPOSITO, G., COSTANTINO, S., GRAIANI, G., FRATI, C., PREZIOSO, L., BERRINO, L., URBANEK, K., QUAINI, F. & ROSSI, F. 2013. Doxorubicin induces senescence and impairs function of human cardiac progenitor cells. *Basic Research in Cardiology,* 108.

POINTON, A., ABI-GERGES, N., CROSS, M. J. & SIDAWAY, J. E. 2013. Phenotypic profiling of structural cardiotoxins in vitro reveals dependency on multiple mechanisms of toxicity. *Toxicol Sci,* 132**,** 317-26.

POLK, A., VISTISEN, K., VAAGE-NILSEN, M. & NIELSEN, D. L. 2014. A systematic review of the pathophysiology of 5-fluorouracil-induced cardiotoxicity. *BMC Pharmacology and Toxicology,* 15**,** 47.

POLUZZI, E., RASCHI, E., DIEMBERGER, I. & DE PONTI, F. 2017. Drug-Induced Arrhythmia: Bridging the Gap Between Pathophysiological Knowledge and Clinical Practice. *Drug Safety,* 40**,** 461-464.

POMMIER, Y. 2013. Drugging topoisomerases: Lessons and Challenges. *ACS Chemical Biology,* 8**,** 82-95.

POPRACH, A., PETRÁKOVÁ, K., VYSKOCIL, J., LAKOMÝ, R., NEMECEK, R., KOCÁK, I., KOCÁKOVÁ, I. & VYZULA, R. 2008. [Cardiotoxicity of drugs used in oncology]. *Klin Onkol,* 21**,** 288-93.

POUTON, C. W. & HAYNES, J. M. 2007. Embryonic stem cells as a source of models for drug discovery. *Nature Reviews Drug Discovery,* 6**,** 605-616.

QIAGEN. 2011. RT2 PreAMP cDNA Synthesis Handbook.

QIAGEN. 2014. RT2 Profiler PCR Array Handbook.

QUARESMA, M., COLEMAN, M. P. & RACHET, B. 2015. 40-year trends in an index of survival for all cancers combined and survival adjusted for age and sex for each cancer in England and Wales, 1971–2011: a population-based study. *The lancet,* 385**,** 1206-1218.

RAPPAPORT, L. & SAMUEL, J. L. 1988. Microtubules in Cardiac Myocytes. *In:* JEON, K. W. & FRIEDLANDER, M. (eds.) *International Review of Cytology.* Academic Press.

RASKOFF, W. J., GOLDMAN, S. & COHN, K. 1976. The "athletic heart". Prevalence and physiological significance of left ventricular enlargement in distance runners. *Jama,* 236**,** 158-62.

RAULF, A., HORDER, H., TARNAWSKI, L., GEISEN, C., OTTERSBACH, A., RÖLL, W., JOVINGE, S., FLEISCHMANN, B. K. & HESSE, M. 2015. Transgenic systems for unequivocal identification of cardiac myocyte nuclei and analysis of cardiomyocyte cell cycle status. *Basic Research in Cardiology,* 110**,** 33.

RAVELLI, R. B., GIGANT, B., CURMI, P. A., JOURDAIN, I., LACHKAR, S., SOBEL, A. & KNOSSOW, M. 2004. Insight into tubulin regulation from a complex with colchicine and a stathmin-like domain. *Nature,* 428**,** 198-202.

RAVENSCROFT, S. M., POINTON, A., WILLIAMS, A. W., CROSS, M. J. & SIDAWAY, J. E. 2016. Cardiac Non-myocyte Cells Show Enhanced Pharmacological Function Suggestive of Contractile Maturity in Stem Cell Derived Cardiomyocyte Microtissues. *Toxicological Sciences,* 152**,** 99-112.

REDFERN, W., EWART, L., HAMMOND, T., BIALECKI, R., KINTER, L., LINDGREN, S., POLLARD, C., ROBERTS, R., ROLF, M. & VALENTIN, J. 2010. Impact and frequency of different toxicities throughout the pharmaceutical life cycle. *The Toxicologist,* 114**,** 1081.

RENU, K., V.G, A., P.B, T. P. & ARUNACHALAM, S. 2018. Molecular mechanism of doxorubicin-induced cardiomyopathy – An update. *European Journal of Pharmacology,* 818**,** 241-253.

RHEA, I. B. & OLIVEIRA, G. H. 2018. Cardiotoxicity of Novel Targeted Chemotherapeutic Agents. *Current Treatment Options in Cardiovascular Medicine,* 20.

RHODEN, W., HASLETON, P. & BROOKS, N. 1993. Anthracyclines and the heart. *British Heart Journal,* 70**,** 499-502.

ROBISON, P., CAPORIZZO, M. A., AHMADZADEH, H., BOGUSH, A. I., CHEN, C. Y., MARGULIES, K. B., SHENOY, V. B. & PROSSER, B. L. 2016. Detyrosinated microtubules buckle and bear load in contracting cardiomyocytes. *Science,* 352.

ROCKLEY, K. & GILL, J. 2017. Characterisation of Novel Molecular Mechanisms Involved in Anthracycline-Induced Cardiotoxicity. *Journal of Pharmacological and Toxicological Methods,* 88**,** 202.

ROHDE, D., BUSCH, M., VOLKERT, A., RITTERHOFF, J., KATUS, H. A., PEPPEL, K. & MOST, P. 2015. Cardiomyocytes, endothelial cells and cardiac fibroblasts: S100A1's triple action in cardiovascular pathophysiology. *Future cardiology,* 11**,** 309-321.

ROSIAK, J. & SADOWSKI, L. 2005. Hypertension associated with bevacizumab. *Clinical journal of oncology nursing,* 9**,** 407.

RUMYANTSEV, P. P. 1977. Interrelations of the proliferation and differentiation processes during cardiact myogenesis and regeneration. *Int Rev Cytol,* 51**,** 186-273.

RUSTIN, G. J., GALBRAITH, S. M., ANDERSON, H., STRATFORD, M., FOLKES, L. K., SENA, L., GUMBRELL, L. & PRICE, P. M. 2003. Phase I clinical trial of weekly combretastatin A4 phosphate: clinical and pharmacokinetic results. *Journal of clinical oncology,* 21**,** 2815-2822.

RUSTIN, G. J., SHREEVES, G., NATHAN, P. D., GAYA, A., GANESAN, T. S., WANG, D., BOXALL, J., POUPARD, L., CHAPLIN, D. J., STRATFORD, M. R., BALKISSOON, J. & ZWEIFEL, M. 2010. A Phase Ib trial of CA4P (combretastatin A-4 phosphate), carboplatin, and paclitaxel in patients with advanced cancer. *Br J Cancer,* 102**,** 1355-60.

SAGER, P. 2008. Key clinical considerations for demonstrating the utility of preclinical models to predict clinical drug-induced torsades de pointes. *British journal of pharmacology,* 154**,** 1544-1549.

SAGER, P. T., GINTANT, G., TURNER, J. R., PETTIT, S. & STOCKBRIDGE, N. 2014. Rechanneling the cardiac proarrhythmia safety paradigm: A meeting report from the Cardiac Safety Research Consortium. *American Heart Journal,* 167**,** 292-300.

SALVATORELLI, E., MENNA, P., CANTALUPO, E., CHELLO, M., COVINO, E., WOLF, F. I. & MINOTTI, G. 2015. The concomitant management of cancer therapy and cardiac therapy. *Biochimica et Biophysica Acta - Biomembranes,* 1848**,** 2727-2737.

SANO, M., MINAMINO, T., TOKO, H., MIYAUCHI, H., ORIMO, M., QIN, Y., AKAZAWA, H., TATENO, K., KAYAMA, Y., HARADA, M., SHIMIZU, I., ASAHARA, T., HAMADA, H., TOMITA, S., MOLKENTIN, J. D., ZOU, Y. & KOMURO, I. 2007. p53-induced inhibition of Hif-1 causes cardiac dysfunction during pressure overload. *Nature,* 446**,** 444-448.

SASAKI, S., YUI, N. & NODA, Y. 2014. Actin directly interacts with different membrane channel proteins and influences channel activities: AQP2 as a model. *Biochim Biophys Acta,* 1838**,** 514-20.

SATO, H., NAGAI, T., KUPPUSWAMY, D., NARISHIGE, T., KOIDE, M., MENICK, D. R. & COOPER, G. T. 1997. Microtubule stabilization in pressure overload cardiac hypertrophy. *J Cell Biol,* 139**,** 963-73.

SAUDER, P., KOPFERSCHMITT, J., JAEGER, A. & MANTZ, J. M. 1983. Haemodynamic Studies in Eight Cases of Acute Colchicine Poisoning. *Human Toxicology,* 2**,** 169-173.

SAWYER, D. B., PENG, X., CHEN, B., PENTASSUGLIA, L. & LIM, C. C. 2010. Mechanisms of anthracycline cardiac injury: can we identify strategies for cardioprotection? *Progress in cardiovascular diseases,* 53**,** 105-113.

SCHAPPI, J. M., KRBANJEVIC, A. & RASENICK, M. M. 2014. Tubulin, actin and heterotrimeric G proteins: coordination of signaling and structure. *Biochimica et Biophysica Acta (BBA)-Biomembranes,* 1838**,** 674-681.

SCHMERMUND, A., LERMAN, L. O., RITMAN, E. L. & RUMBERGER, J. A. 1999. Cardiac Production of Angiotensin II and Its Pharmacologic Inhibition: Effects on the Coronary Circulation. *Mayo Clinic Proceedings,* 74**,** 503-513.

SCHMIDINGER, M., ZIELINSKI, C. C., VOGL, U. M., BOJIC, A., BOJIC, M., SCHUKRO, C., RUHSAM, M., HEJNA, M. & SCHMIDINGER, H. 2008. Cardiac Toxicity of Sunitinib and Sorafenib in Patients With Metastatic Renal Cell Carcinoma. *Journal of Clinical Oncology,* 26**,** 5204-5212.

SCHWARTZ, E. L. 2009. Antivascular actions of microtubule-binding drugs. *Clin Cancer Res,* 15**,** 2594-601.

SCHWARZER, S., EBER, B., GREINIX, H. & LIND, P. 1991. Non-Q-wave myocardial infarction associated with bleomycin and etoposide chemotherapy. *European heart journal,* 12**,** 748-750.

SCOTT, C. W., PETERS, M. F. & DRAGAN, Y. P. 2013. Human induced pluripotent stem cells and their use in drug discovery for toxicity testing. *Toxicol Lett,* 219**,** 49-58.

SCOTT, C. W., ZHANG, X., ABI-GERGES, N., LAMORE, S. D., ABASSI, Y. A. & PETERS, M. F. 2014. An impedance-based cellular assay using human iPSC-derived

cardiomyocytes to quantify modulators of cardiac contractility. *Toxicol Sci,* 142**,** 331-8.

SEILER, A., OELGESCHLÄGER, M., LIEBSCH, M., PIROW, R., RIEBELING, C., TRALAU, T. & LUCH, A. 2011. Developmental toxicity testing in the 21st century: the sword of Damocles shattered by embryonic stem cell assays? *Arch Toxicol,* 85**,** 1361-72.

SEN, A., DUNNMON, P., HENDERSON, S. A., GERARD, R. D. & CHIEN, K. R. 1988. Terminally differentiated neonatal rat myocardial cells proliferate and maintain specific differentiated functions following expression of SV40 large T antigen. *Journal of Biological Chemistry,* 263**,** 19132-19136.

SESSA, C. & PAGANI, O. 2001. Docetaxel and epirubicin in advanced breast cancer. *Oncologist,* 6**,** 13-16.

SÈVE, P. & DUMONTET, C. 2008. Is class III β-tubulin a predictive factor in patients receiving tubulin-binding agents? *The lancet oncology,* 9**,** 168-175.

SHAH, R. R. 2006. Can pharmacogenetics help rescue drugs withdrawn from the market?

SHEEHY, SEAN P., PASQUALINI, F., GROSBERG, A., PARK, SUNG J., ARATYN-SCHAUS, Y. & PARKER, KEVIN K. 2014. Quality Metrics for Stem Cell-Derived Cardiac Myocytes. *Stem Cell Reports,* 2**,** 282-294.

SHIMIZU, I. & MINAMINO, T. 2016. Physiological and pathological cardiac hypertrophy. *Journal of Molecular and Cellular Cardiology,* 97**,** 245-262.

SHUKLA, S. J., HUANG, R., AUSTIN, C. P. & XIA, M. 2010. The future of toxicity testing: a focus on in vitro methods using a quantitative high-throughput screening platform. *Drug discovery today,* 15**,** 997-1007.

SIDDIQI, S. & SUSSMAN, M. A. 2014. The Heart: Mostly Postmitotic or Mostly Premitotic? Myocyte Cell Cycle, Senescence, and Quiescence. *Canadian Journal of Cardiology,* 30**,** 1270-1278.

SIEMANN, D. W., CHAPLIN, D. J. & HORSMAN, M. R. 2017. Realizing the Potential of Vascular Targeted Therapy: The Rationale for Combining Vascular Disrupting Agents and Anti-Angiogenic Agents to Treat Cancer. *Cancer Invest,* 35**,** 519-534.

SIEMANN, D. W., CHAPLIN, D. J. & WALICKE, P. A. 2009. A review and update of the current status of the vasculature-disabling agent combretastatin-A4 phosphate (CA4P). *Expert Opin Investig Drugs,* 18**,** 189-97.

SINNATAMBY, C. S. 2011. *Last's Anatomy, International Edition: Regional and Applied*, Elsevier Health Sciences.

SIRAMSHETTY, V. B., NICKEL, J., OMIECZYNSKI, C., GOHLKE, B.-O., DRWAL, M. N. & PREISSNER, R. 2016. WITHDRAWN—a resource for withdrawn and discontinued drugs. *Nucleic acids research,* 44**,** D1080-D1086.

SMITTENAAR, C., PETERSEN, K., STEWART, K. & MOITT, N. 2016. Cancer incidence and mortality projections in the UK until 2035. *British journal of cancer,* 115**,** 1147-1155.

SONG, W., LIU, C. & UPADHYAYA, A. 2014. The pivotal position of the actin cytoskeleton in the initiation and regulation of B cell receptor activation. *Biochim Biophys Acta,* 1838**,** 569-78.

SOONPAA, M. H., KIM, K. K., PAJAK, L., FRANKLIN, M. & FIELD, L. J. 1996. Cardiomyocyte DNA synthesis and binucleation during murine development. *Am J Physiol,* 271**,** H2183-9.

SOORIAKUMARAN, P. 2006. COX-2 inhibitors and the heart: are all coxibs the same? *Postgraduate medical journal,* 82**,** 242-245.

SOSA, J. A., ELISEI, R., JARZAB, B., BAL, C. S., KOUSSIS, H., GRAMZA, A. W., BEN-YOSEF, R., GITLITZ, B. J., HAUGEN, B., KARANDIKAR, S. M., KHURI, F. R., LICITRA, L. F., REMICK, S. C., MARUR, S., LU, C., ONDREY, F. G., LU, S. & BALKISSOON, J. 2011. A randomized phase II/III trial of a tumor vascular disrupting agent fosbretabulin tromethamine (CA4P) with carboplatin (C) and paclitaxel (P) in anaplastic thyroid cancer (ATC): Final survival analysis for the FACT trial. *Journal of Clinical Oncology,* 29**,** 5502-5502.

SPALLAROSSA, P., GARIBALDI, S., ALTIERI, P., FABBI, P., MANCA, V., NASTI, S., ROSSETTIN, P., GHIGLIOTTI, G., BALLESTRERO, A. & PATRONE, F. 2004. Carvedilol prevents doxorubicin-induced free radical release and apoptosis in cardiomyocytes in vitro. *Journal of molecular and cellular cardiology,* 37**,** 837-846.

STEGMEIER, F., WARMUTH, M., SELLERS, W. R. & DORSCH, M. 2010. Targeted Cancer Therapies in the Twenty-First Century: Lessons From Imatinib. *Clinical Pharmacology & Therapeutics,* 87**,** 543-552.

STEINHELPER, M. E., LANSON, N. A., JR., DRESDNER, K. P., DELCARPIO, J. B., WIT, A. L., CLAYCOMB, W. C. & FIELD, L. J. 1990. Proliferation in vivo and in culture of differentiated adult atrial cardiomyocytes from transgenic mice. *Am J Physiol,* 259**,** H1826-34.

STENGEL, C., NEWMAN, S., LEESE, M., POTTER, B., REED, M. & PUROHIT, A. 2010. Class III β-tubulin expression and in vitro resistance to microtubule targeting agents. *British journal of cancer,* 102**,** 316-324.

STIVENS, A. & LOWE, J. 1997. Human histology, 2-nd ed. *London: Mosby*.

SUBBIAH, I. M., LENIHAN, D. J. & TSIMBERIDOU, A. M. 2011. Cardiovascular toxicity profiles of vascular-disrupting agents. *The oncologist,* 16**,** 1120-1130.

SUNESEN, M., SCHRØDER, R. & KETTENHOFEN, R. 2012. Cor.At® cells: Embryonic stem cell derived cardiomyocytes. *Sophion Bioscience,* Application Report.

SUTER, T. M. & EWER, M. S. 2013. Cancer drugs and the heart: importance and management. *Eur Heart J,* 34**,** 1102-11.

SUZUKI, Y. J. 2003. Stress-induced activation of GATA-4 in cardiac muscle cells. *Free Radical Biology and Medicine,* 34**,** 1589-1598.

TAGAWA, H., KOIDE, M., SATO, H. & COOPER, G. T. 1996. Cytoskeletal role in the contractile dysfunction of cardiocytes from hypertrophied and failing right ventricular myocardium. *Proc Assoc Am Physicians,* 108**,** 218-29.

TAGAWA, H., KOIDE, M., SATO, H., ZILE, M. R., CARABELLO, B. A. & COOPER, G. T. 1998. Cytoskeletal role in the transition from compensated to decompensated hypertrophy during adult canine left ventricular pressure overloading. *Circ Res,* 82**,** 751-61.

TAGAWA, H., WANG, N., NARISHIGE, T., INGBER, D. E., ZILE, M. R. & COOPER, G. T. 1997. Cytoskeletal mechanics in pressure-overload cardiac hypertrophy. *Circ Res,* 80**,** 281-9.

TAKAHASHI, K. & YAMANAKA, S. 2006. Induction of pluripotent stem cells from mouse embryonic and adult fibroblast cultures by defined factors. *Cell,* 126**,** 663-76.

TAM, S., GU, W., MAHDAVI, V. & NADAL-GINARD, B. 1995. Cardiac myocyte terminal differentiation. Potential for cardiac regeneration. *Annals of the New York Academy of Sciences,* 752**,** 72.

TANG, S., XIE, M., CAO, N. & DING, S. 2016. Patient-Specific Induced Pluripotent Stem Cells for Disease Modeling and Phenotypic Drug Discovery: Miniperspective. *Journal of medicinal chemistry,* 59**,** 2-15.

TARIN, D. 2008. Comparisons of metastases in different organs: biological and clinical implications. *Clinical Cancer Research,* 14**,** 1923-1925.

THURSTON, D. E. & PYSZ, I. 2021. *Chemistry and Pharmacology of Anticancer Drugs*, CRC Press.

TOCCHETTI, C. G., GALLUCCI, G., COPPOLA, C., PISCOPO, G., CIPRESSO, C., MAUREA, C., GIUDICE, A., IAFFAIOLI, R. V., ARRA, C. & MAUREA, N. 2013. The emerging issue of cardiac dysfunction induced by antineoplastic angiogenesis inhibitors. *European Journal of Heart Failure,* 15**,** 482-489.

TOCHINAI, R., KOMATSU, K., MURAKAMI, J., NAGATA, Y., ANDO, M., HATA, C., SUZUKI, T., KADO, S., KOBAYASHI, T. & KUWAHARA, M. 2018. Histopathological and functional changes in a single-dose model of combretastatin A4 disodium phosphate-induced myocardial damage in rats. *Journal of toxicologic pathology,* 31**,** 307-313.

TOCHINAI, R., NAGATA, Y., ANDO, M., HATA, C., SUZUKI, T., ASAKAWA, N., YOSHIZAWA, K., UCHIDA, K., KADO, S., KOBAYASHI, T., KANEKO, K. & KUWAHARA, M. 2016. Combretastatin A4 disodium phosphate-induced myocardial injury. *Journal of toxicologic pathology,* 29**,** 163-171.

TODARO, M. C., ORETO, L., QAMAR, R., PATERICK, T. E., CARERJ, S. & KHANDHERIA, B. K. 2013. Review: Cardioncology: State of the heart. *International Journal of Cardiology,* 168**,** 680-687.

TOUYZ, R. M., HERRMANN, S. M. S. & HERRMANN, J. 2018. Vascular toxicities with VEGF inhibitor therapies–focus on hypertension and arterial thrombotic events. *Journal of the American Society of Hypertension,* 12**,** 409-425.

TOZER, G. M., AKERMAN, S., CROSS, N. A., BARBER, P. R., BJÖRNDAHL, M. A., GRECO, O., HARRIS, S., HILL, S. A., HONESS, D. J. & IRESON, C. R. 2008. Blood vessel maturation and response to vascular-disrupting therapy in single vascular endothelial growth factor-A isoform–producing tumors. *Cancer research,* 68**,** 2301-2311.

TOZER, G. M., KANTHOU, C. & BAGULEY, B. C. 2005. Disrupting tumour blood vessels. *Nat Rev Cancer,* 5**,** 423-435.

TURNER, N. A., XIA, F., AZHAR, G., ZHANG, X., LIU, L. & WEI, J. Y. 1998. Oxidative stress induces DNA fragmentation and caspase activation via the c-Jun NH2-terminal kinase pathway in H9c2 cardiac muscle cells. *Journal of molecular and cellular cardiology,* 30**,** 1789-1801.

VALASTYAN, S. & WEINBERG, R. A. 2011. Tumor metastasis: molecular insights and evolving paradigms. *Cell,* 147**,** 275-292.

VAN DIJK, C. G., NIEUWEBOER, F. E., PEI, J. Y., XU, Y. J., BURGISSER, P., VAN MULLIGEN, E., EL AZZOUZI, H., DUNCKER, D. J., VERHAAR, M. C. & CHENG, C. 2015. The complex mural cell: pericyte function in health and disease. *Int J Cardiol,* 190**,** 75-89.

VAN WAGONER DAVID, R. 2011. Colchicine for the Prevention of Postoperative Atrial Fibrillation. *Circulation,* 124**,** 2281-2282.

VEJPONGSA, P. & YEH, E. T. H. 2014. Topoisomerase 2β: A promising molecular target for primary prevention of anthracycline-induced cardiotoxicity. *Clinical Pharmacology and Therapeutics,* 95**,** 45-52.

VERKERK, A. O., VEERMAN, C. C., ZEGERS, J. G., MENGARELLI, I., BEZZINA, C. R. & WILDERS, R. 2017. Patch-Clamp Recording from Human Induced Pluripotent Stem Cell-Derived Cardiomyocytes: Improving Action Potential Characteristics through Dynamic Clamp. *International journal of molecular sciences,* 18**,** 1873.

VICENTE, J., ZUSTERZEEL, R., JOHANNESEN, L., MASON, J., SAGER, P., PATEL, V., MATTA, M. K., LI, Z., LIU, J. & GARNETT, C. 2018. Mechanistic model-informed proarrhythmic risk assessment of drugs: review of the "CiPA" initiative and design of a prospective clinical validation study. *Clinical Pharmacology & Therapeutics,* 103**,** 54-66.

VILLANI, F., GUINDANI, A. & PAGNONI, A. 1979. 5-Fuorouracil cardiotoxicity. *Tumori,* 65**,** 487-95.

WALLUKAT, G. 2002. The beta-adrenergic receptors. *Herz,* 27**,** 683-90.

WANG, H., NAGHAVI, M., ALLEN, C., BARBER, R. M., BHUTTA, Z. A., CARTER, A., CASEY, D. C., CHARLSON, F. J., CHEN, A. Z., COATES, M. M., COGGESHALL, M., DANDONA, L., DICKER, D. J., ERSKINE, H. E., FERRARI, A. J., FITZMAURICE, C., FOREMAN, K., FOROUZANFAR, M. H., FRASER, M. S., FULLMAN, N., GETHING, P. W., GOLDBERG,

E. M., GRAETZ, N., HAAGSMA, J. A., HAY, S. I., HUYNH, C., JOHNSON, C. O., KASSEBAUM, N. J., KINFU, Y., KULIKOFF, X. R., KUTZ, M., KYU, H. H., LARSON, H. J., LEUNG, J., LIANG, X., LIM, S. S., LIND, M., LOZANO, R., MARQUEZ, N., MENSAH, G. A., MIKESELL, J., MOKDAD, A. H., MOONEY, M. D., NGUYEN, G., NSOESIE, E., PIGOTT, D. M., PINHO, C., ROTH, G. A., SALOMON, J. A., SANDAR, L., SILPAKIT, N., SLIGAR, A., SORENSEN, R. J. D., STANAWAY, J., STEINER, C., TEEPLE, S., THOMAS, B. A., TROEGER, C., VANDERZANDEN, A., VOLLSET, S. E., WANGA, V., WHITEFORD, H. A., WOLOCK, T., ZOECKLER, L., ABATE, K. H., ABBAFATI, C., ABBAS, K. M., ABD-ALLAH, F., ABERA, S. F., ABREU, D. M. X., ABU-RADDAD, L. J., ABYU, G. Y., ACHOKI, T., ADELEKAN, A. L., ADEMI, Z., ADOU, A. K., ADSUAR, J. C., AFANVI, K. A., AFSHIN, A., AGARDH, E. E., AGARWAL, A., AGRAWAL, A., KIADALIRI, A. A., AJALA, O. N., AKANDA, A. S., AKINYEMI, R. O., AKINYEMIJU, T. F., AKSEER, N., LAMI, F. H. A., ALABED, S., AL-ALY, Z., ALAM, K., ALAM, N. K. M., ALASFOOR, D., ALDHAHRI, S. F., ALDRIDGE, R. W., ALEGRETTI, M. A., ALEMAN, A. V., ALEMU, Z. A., ALEXANDER, L. T., et al. 2016. Global, regional, and national life expectancy, all-cause mortality, and cause-specific mortality for 249 causes of death, 1980–2015: a systematic analysis for the Global Burden of Disease Study 2015. *The Lancet,* 388**,** 1459-1544.

WANG, T. H., WANG, H. S. & SOONG, Y. K. 2000. Paclitaxel-induced cell death: where the cell cycle and apoptosis come together. *Cancer,* 88**,** 2619-28.

WANG, Y.-C., NECKELMANN, N., MAYNE, A., HERSKOWITZ, A., SRINIVASAN, A., SELL, K. W. & AHMED-ANSARI, A. 1991. Establishment of a human fetal cardiac myocyte cell line. *In Vitro Cellular & Developmental Biology-Animal,* 27**,** 63-74.

WATKINS, S. J., BORTHWICK, G. M. & ARTHUR, H. M. 2011. The H9C2 cell line and primary neonatal cardiomyocyte cells show similar hypertrophic responses in vitro. *In Vitro Cell Dev Biol Anim,* 47**,** 125-31.

WEBSTER, D. R. & PATRICK, D. L. 2000. Beating rate of isolated neonatal cardiomyocytes is regulated by the stable microtubule subset. *American Journal of Physiology-Heart and Circulatory Physiology,* 278**,** H1653-H1661.

WEEKS, K. L. & MCMULLEN, J. R. 2011. The athlete's heart vs. the failing heart: can signaling explain the two distinct outcomes? *Physiology (Bethesda),* 26**,** 97-105.

WEIS, S. M. & CHERESH, D. A. 2011. Tumor angiogenesis: molecular pathways and therapeutic targets. *Nat Med,* 17**,** 1359-70.

WELCH, D. R. & HURST, D. R. 2019. Defining the Hallmarks of Metastasis. *Cancer Research,* 79**,** 3011.

WELSER, J. 2015. Primary Cells Versus Cell Lines [Internet]. *ScienCell Research Laboratories*.

WISEMAN, L. R. & SPENCER, C. M. 1998. Dexrazoxane. A review of its use as a cardioprotective agent in patients receiving anthracycline-based chemotherapy. *Drugs,* 56**,** 385-403.

WOLFF, J. 2009. Plasma membrane tubulin. *Biochimica et Biophysica Acta (BBA) - Biomembranes,* 1788**,** 1415-1433.

XI, B., WANG, T., LI, N., OUYANG, W., ZHANG, W., WU, J., XU, X., WANG, X. & ABASSI, Y. A. 2011a. Functional Cardiotoxicity Profiling and Screening Using the xCELLigence RTCA Cardio System. *JALA: Journal of the Association for Laboratory Automation,* 16**,** 415-421.

XI, B., WANG, T., LI, N., OUYANG, W., ZHANG, W., WU, J., XU, X., WANG, X. & ABASSI, Y. A. 2011b. Functional cardiotoxicity profiling and screening using the xCELLigence RTCA Cardio System. *J Lab Autom,* 16**,** 415-21.

XIAO, D., ZHAN, Y., YANG, Z., FAN, C., LIU, L. & LIN, Y. 2020. Anti-interleukin-5-neutralizing antibody attenuates caradiac injury and cadiac dysfunction by aggravating the inflammatory response in doxorubicin-treated mice. *Cell Biology International,* 44**,** 1363-1372.

XIAO, Y., YANG, Z., WU, Q.-Q., JIANG, X.-H., YUAN, Y., CHANG, W., BIAN, Z. Y., ZHU, J. X. & TANG, Q.-Z. 2017. Cucurbitacin B Protects Against Pressure Overload Induced Cardiac Hypertrophy. *Journal of Cellular Biochemistry,* 118**,** 3899-3910.

YANG, L., SOONPAA, M. H., ADLER, E. D., ROEPKE, T. K., KATTMAN, S. J., KENNEDY, M., HENCKAERTS, E., BONHAM, K., ABBOTT, G. W., LINDEN, R. M., FIELD, L. J. & KELLER, G. M. 2008. Human cardiovascular progenitor cells develop from a KDR+ embryonic-stem-cell-derived population. *Nature,* 453**,** 524-8.

YANO, S. & SHIMADA, K. 1996. Vasospastic angina after chemotherapy by with carboplatin and etoposide in a patient with lung cancer. *Japanese Circulation Journal,* 60**,** 185-188.

YEH, E. T. & BICKFORD, C. L. 2009. Cardiovascular complications of cancer therapy: incidence, pathogenesis, diagnosis, and management. *J Am Coll Cardiol,* 53**,** 2231-47.

YEH, E. T., TONG, A. T., LENIHAN, D. J., YUSUF, S. W., SWAFFORD, J., CHAMPION, C., DURAND, J. B., GIBBS, H., ZAFARMAND, A. A. & EWER, M. S. 2004. Cardiovascular complications of cancer therapy: diagnosis, pathogenesis, and management. *Circulation,* 109**,** 3122-31.

YEH, E. T. H. 2006. Cardiotoxicity induced by chemotherapy and antibody therapy. *Annual Review of Medicine.*

YOKOO, N., BABA, S., KAICHI, S., NIWA, A., MIMA, T., DOI, H., YAMANAKA, S., NAKAHATA, T. & HEIKE, T. 2009. The effects of cardioactive drugs on cardiomyocytes derived from human induced pluripotent stem cells. *Biochem Biophys Res Commun,* 387**,** 482-8.

YUE, H., LIANG, W., GU, J., ZHAO, X., ZHANG, T., QIN, X., ZHU, G. & WU, Z. 2019. Comparative transcriptome analysis to elucidate the therapeutic mechanism of colchicine against atrial fibrillation. *Biomedicine & Pharmacotherapy,* 119**,** 109422.

ZAMBELLI, A., DELLA PORTA, M. G., ELEUTERI, E., DE GIULI, L., CATALANO, O., TONDINI, C. & RICCARDI, A. 2011. Predicting and preventing cardiotoxicity in the era of breast cancer targeted therapies. Novel molecular tools for clinical issues. *Breast,* 20**,** 176-83.

ZAMORANO, J. L., LANCELLOTTI, P., RODRIGUEZ MUÑOZ, D., ABOYANS, V., ASTEGGIANO, R., GALDERISI, M., HABIB, G., LENIHAN, D. J., LIP, G. Y. H., LYON, A. R., LOPEZ FERNANDEZ, T., MOHTY, D., PIEPOLI, M. F., TAMARGO, J., TORBICKI, A., SUTER, T. M. & GROUP, E. S. C. S. D. 2016. 2016 ESC Position Paper on cancer treatments and cardiovascular toxicity developed under the auspices of the ESC Committee for Practice Guidelines: The Task Force for cancer treatments and cardiovascular toxicity of the European Society of Cardiology (ESC). *European Heart Journal,* 37**,** 2768-2801.

ZEBROWSKI, D. C. & ENGEL, F. B. 2013. The Cardiomyocyte Cell Cycle in Hypertrophy, Tissue Homeostasis, and Regeneration. *In:* NILIUS, B., AMARA, S. G., GUDERMANN, T., JAHN, R., LILL, R., OFFERMANNS, S. & PETERSEN, O. H. (eds.) *Reviews of Physiology, Biochemistry and Pharmacology, Vol. 165.* Cham: Springer International Publishing.

ZHANG, S., ZHOU, Z., GONG, Q., MAKIELSKI, J. C. & JANUARY, C. T. 1999. Mechanism of block and identification of the verapamil binding domain to HERG potassium channels. *Circulation Research,* 84**,** 989-998.

ZHANG, X., GUO, L., ZENG, H., WHITE, S. L., FURNISS, M., BALASUBRAMANIAN, B., LIS, E., LAGRUTTA, A., SANNAJUST, F., ZHAO, L. L., XI, B., WANG, X., DAVIS, M. & ABASSI, Y. A. 2016. Multi-parametric assessment of cardiomyocyte excitation-contraction coupling using impedance and field potential recording: A tool for cardiac safety assessment. *J Pharmacol Toxicol Methods,* 81**,** 201-16.

ZHENG, B., WEN, J. K. & HAN, M. 2006. hhLIM is involved in cardiomyogenesis of embryonic stem cells. *Biochemistry (Mosc),* 71 Suppl 1**,** S71-6, 6.

ZHOU, J. & GIANNAKAKOU, P. 2005. Targeting microtubules for cancer chemotherapy. *Current Medicinal Chemistry-Anti-Cancer Agents,* 5**,** 65-71.

ZHOU, S.-F., YUAN, J., LIAO, M.-Y., XIA, N., TANG, T.-T., LI, J.-J., JIAO, J., DONG, W.-Y., NIE, S.-F., ZHU, Z.-F., ZHANG, W.-C., LV, B.-J., XIAO, H., WANG, Q., TU, X., LIAO, Y.-H., SHI, G.-P. & CHENG, X. 2014. IL-17A promotes ventricular remodeling after myocardial infarction. *Journal of Molecular Medicine,* 92**,** 1105-1116.

ZWEIFEL, M., JAYSON, G. C., REED, N. S., OSBORNE, R., HASSAN, B., LEDERMANN, J., SHREEVES, G., POUPARD, L., LU, S. P., BALKISSOON, J., CHAPLIN, D. J. & RUSTIN, G. J. 2011. Phase II trial of combretastatin A4 phosphate, carboplatin, and paclitaxel in patients with platinum-resistant ovarian cancer. *Ann Oncol,* 22**,** 2036-41.

Appendix 1

Preparation of paraformaldehyde (PFA).

Concentration of 4% paraformaldehyde (PFA) was prepared by dissolving 4 gm of PFA in 80 ml of 1X PBS at 60 C. to aid in dissolution volume of 1 ml NaOH 7 added to the mix. Once completely dissolved and cooled, the solution was made up to 100 ml and the PH brought up to 7 using 1M HCL (approximately 1 mL).

Appendix 2

Preparation of TubulinTracker™ reagents

Contents:

TubulinTracker™ Green reagent is supplied as a kit containing two vials:

- Component A which is TubulinTracker™ Green reagent: a lyophilized vial weighed 100 µg.
- Component B which is Pluronic F-127 20% solution in DMSO: a volume of 1 mL of solvent to make stock solutions.

Reagents Preparation:

A stock solution of 1 mM TubulinTracker™ Green reagent was prepared by dissolving the contents of Component A in 71 µL of anhydrous DMSO. Stock solution then aliquoted and stored at –20°C. An intermediate stock solution was made to concentration of 500 µM by mixing equal volume of the aliquot of 1mM TubulinTracker™ Green reagent stock (prepared above) to component B. the mounting medium was prepared by dilution of the intermediate stock solution to 250 M using PBS containing calcium and Magnesium. Only freshly made mounting medium at 37˚C is used for staining .
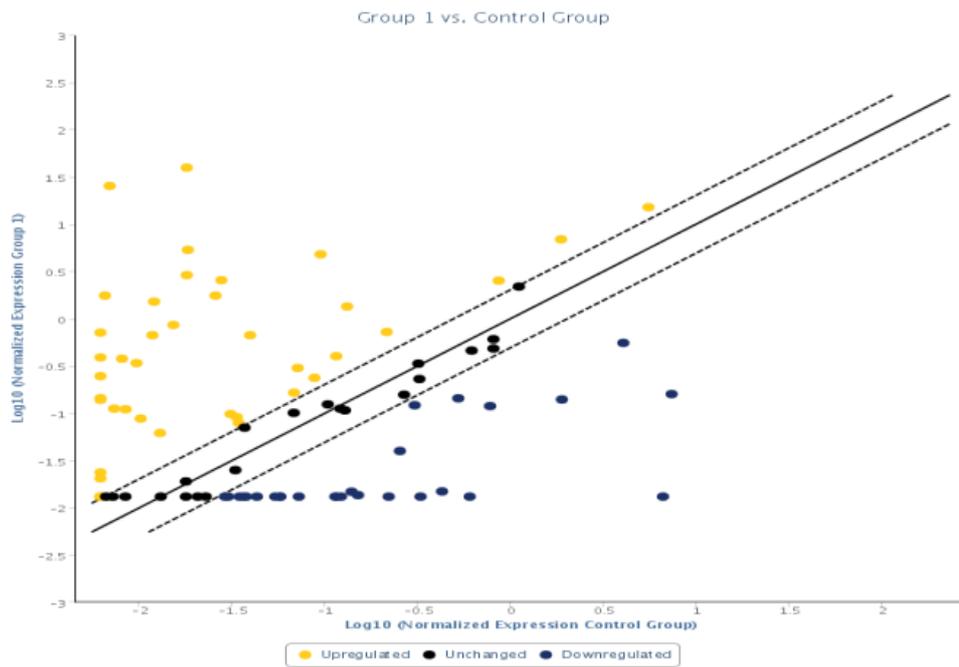
Appendix 3

Supporting data and information

Validation of MTT assay for exponential AC10 cardiomyocytes
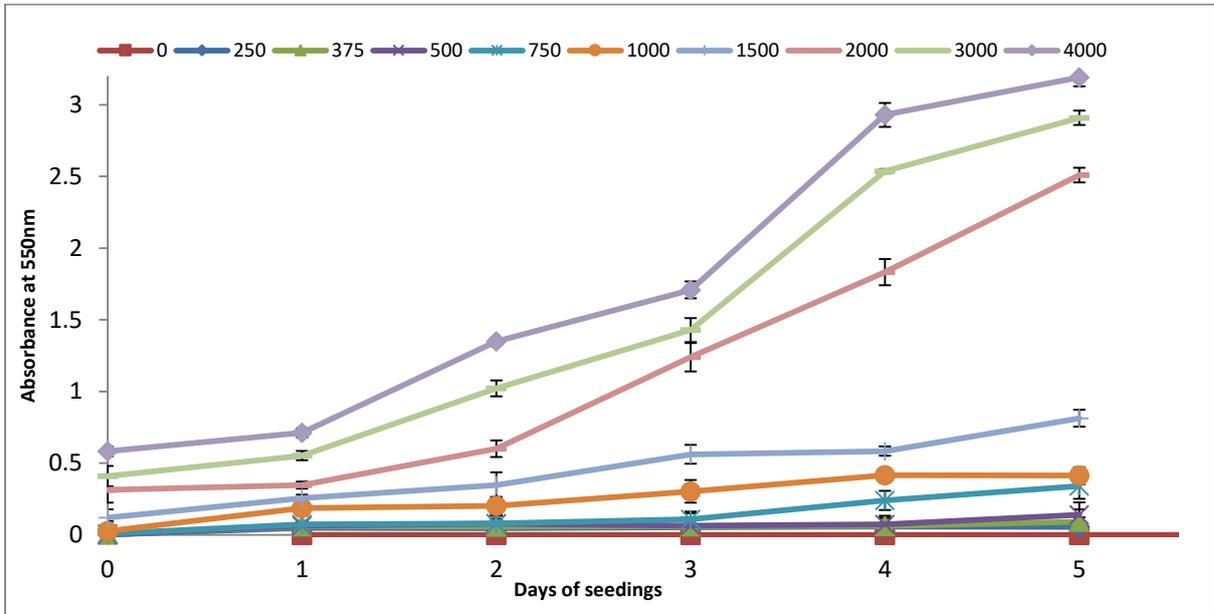
Validation of MTT assay of exponential AC10 cardiomyocytes over a period of five days. Days of seeding against absorbance at 550nm for different AC10 densities. Experiment performed in triplicate and values are representing mean ± SEM.

Scatter plot shows relative change in gene expression in hearts of mice treated with

Colchicine vs control.*The yellow dotes represent upregulated genes, black dotes are for unchanged genes and blue are for down regulated genes. Colchicine treatment was given for 24 hrs at high dose of 1.5 mg/kg.*

Appendix 5

SN	Gene	Name
1	Abhd2	Abhydrolase domain containing 2
2	Abra	Actin-binding Rho activating protein
3	Acta1	Actin, alpha 1, skeletal muscle
4	Aifm1	Apoptosis-inducing factor, mitochondrion-associated 1
5	Ash1l	Ash1 (absent, small, or homeotic)-like (Drosophila)
6	Bcat1	Branched chain aminotransferase 1, cytosolic
7	Bgn	Biglycan
8	Bsn	Bassoon
9	Cfd	Complement factor D (adipsin)
10	Ch25h	Cholesterol 25-hydroxylase
11	Ckm	Creatine kinase, muscle
12	Col15a1	Collagen, type XV, alpha 1
13	Crem	CAMP responsive element modulator
14	Csnk2a2	Casein kinase 2, alpha prime polypeptide
15	Dusp8	Dual specificity phosphatase 8
16	Fcgr2b	Fc receptor, IgG, low affinity IIb
17	Fhl1	Four and a half LIM domains 1
18	Gja1	Gap junction protein, alpha 1
19	Gpm6a	Glycoprotein m6a
20	Hamp	Hepcidin antimicrobial peptide
21	Ift20	Intraflagellar transport 20 homolog (Chlamydomonas)
22	Igfbp5	Insulin-like growth factor binding protein 5
23	Itpr2	Inositol 1,4,5-triphosphate receptor 2
24	Klhl41	Kelch repeat and BTB (POZ) domain containing 10
25	Klhl40	Kelch repeat and BTB (POZ) domain containing 5
26	Mt1	Metallothionein 1
27	Pdk4	Pyruvate dehydrogenase kinase, isoenzyme 4
28	Pkn2	Protein kinase N2
29	Plunc (Bpifa1)	Palate, lung, and nasal epithelium associated
30	Ppbp	Pro-platelet basic protein
31	Prkab2	Protein kinase, AMP-activated, beta 2 non-catalytic subunit
32	Psmd7	Proteasome (prosome, macropain) 26S subunit, non-ATPase, 7
33	Pum2	Pumilio 2 (Drosophila)
34	Pvr	Poliovirus receptor
35	Rbm3	RNA binding motif protein 3
36	Rnd1	Rho family GTPase 1
37	Rps6kb1	Ribosomal protein S6 kinase, polypeptide 1

38	S1pr2	Sphingosine-1-phosphate receptor 2
39	Slc4a3	Solute carrier family 4 (anion exchanger), member 3
40	Spp1	Secreted phosphoprotein 1
41	Tiam1	T-cell lymphoma invasion and metastasis 1
42	Tubb6	Tubulin, beta 6
43	Uba5	Ubiquitin-like modifier activating enzyme 5
44	Ubxn2a	UBX domain protein 2A
45	Vegfa	Vascular endothelial growth factor A
46	Wipi1	WD repeat domain, phosphoinositide interacting 1

Table showing full names of genes with more or less than a 2-fold change in expression in cardiac tissue as a result of high dose in vivo Colchicine treatment.